REFERENCE ONLY

UNIVERSITY OF LONDON THESIS

Degree PhD Year 2006 Name of Author GEERING, Barbara

COPYRIGHT

This is a thesis accepted for a Higher Degree of the University of London. It is an unpublished typescript and the copyright is held by the author. All persons consulting the thesis must read and abide by the Copyright Declaration below.

COPYRIGHT DECLARATION

I recognise that the copyright of the above-described thesis rests with the author and that no quotation from it or information derived from it may be published without the prior written consent of the author.

LOANS

Theses may not be lent to individuals, but the Senate House Library may lend a copy to approved libraries within the United Kingdom, for consultation solely on the premises of those libraries. Application should be made to: Inter-Library Loans, Senate House Library, Senate House, Malet Street, London WC1E 7HU.

REPRODUCTION

University of London theses may not be reproduced without explicit written permission from the Senate House Library. Enquiries should be addressed to the Theses Section of the Library. Regulations concerning reproduction vary according to the date of acceptance of the thesis and are listed below as guidelines.

A. Before 1962. Permission granted only upon the prior written consent of the author. (The Senate House Library will provide addresses where possible).

B. 1962 - 1974. In many cases the author has agreed to permit copying upon completion of a Copyright Declaration.

C. 1975 - 1988. Most theses may be copied upon completion of a Copyright Declaration.

D. 1989 onwards. Most theses may be copied.

This thesis comes within category D.

☐ This copy has been deposited in the Library of UCL

☐ This copy has been deposited in the Senate House Library, Senate House, Malet Street, London WC1E 7HU.

nders 65

REGULATION OF CLASS IA PHOSPHOINOSITIDE 3-KINASE SIGNALLING ENZYMES BY POST-TRANSLATIONAL MODIFICATIONS, PROTEIN INTERACTIONS AND ABSOLUTE PROTEIN EXPRESSION LEVELS

BARBARA GEERING
2006

LUDWIG INSTITUTE FOR CANCER RESEARCH

UNIVERSITY COLLEGE LONDON BRANCH, 91 RIDING HOUSE STREET, LONDON

AND

UNIVERSITY COLLEGE LONDON

DEPARTMENT OF BIOCHEMISTRY AND MOLECULAR BIOLOGY, GOWER STREET, LONDON

This thesis is submitted in fulfilment of the requirements for the degree of Doctor of Philosophy from the University of London

UMI Number: U592828

All rights reserved

INFORMATION TO ALL USERS
The quality of this reproduction is dependent upon the quality of the copy submitted.

In the unlikely event that the author did not send a complete manuscript
and there are missing pages, these will be noted. Also, if material had to be removed,
a note will indicate the deletion.

UMI U592828
Published by ProQuest LLC 2013. Copyright in the Dissertation held by the Author.
Microform Edition © ProQuest LLC.
All rights reserved. This work is protected against
unauthorized copying under Title 17, United States Code.

ProQuest LLC
789 East Eisenhower Parkway
P.O. Box 1346
Ann Arbor, MI 48106-1346

ABSTRACT

Phosphoinositide 3-kinases (PI3Ks) are signal transduction proteins that regulate a wide range of cellular processes. A key subset of PI3Ks are the so-called class IA enzymes consisting of a p85 regulatory and p110 catalytic subunit. While the biological activities of PI3Ks have been investigated in detail, the biochemical mechanism of their regulation is underexplored. We therefore strived to investigate post-translational modifications and absolute protein levels of class IA PI3Ks using electrophoresis and mass spectrometry (MS). We thereby focused on endogenous PI3K subunits and physiological stimulation.

Modifications including amino acid substitutions, phosphorylation and hydroxylation were detected in the regulatory subunit of unstimulated cells. While modifications in p85 were unaltered following cellular stimulation, dynamic changes in the tyrosine phosphorylation of the catalytic subunit p110δ were detected upon B cell stimulation. p110δ tyrosine phosphorylation does not appear to be critical for intrinsic PI3K lipid kinase activity, but might have a role in the interaction of p110δ with known and novel potential PI3K partners identified by MS. However, identification of modified amino acid residues by MS turned out to be challenging, also because p110 proteins could not be resolved by 2D-gel electrophoresis.

An important question in the PI3K field is whether class IA subunits can exist as monomers. It has been reported that p85 is present in excess over p110 and suggested that monomeric p85 has a negative role in the regulation of PI3K activity. Our analysis of class IA PI3K protein expression, amongst other by affinity and ion exchange chromatography, does not support this notion.

In summary, our work has revealed dynamic changes in the post-translational modification of the p110 (but not p85) and their interaction with partners. The ratio of p110 to p85, however, does not seem to be as dynamic, with equal amounts of p85 to p110 under all conditions investigated.

STATEMENT

This thesis is the result of work conducted at the Ludwig Institute for Cancer Research, UCL Branch, London, between September 2002 to June 2006. Except where references are given, this thesis contains my own original work in agreement with the regulations of University College London.
Some of the work presented in this thesis has been published elsewhere:

Cutillas, P.R., Geering, B., Waterfield, M.D. and Vanhaesebroeck, B. (2005) Quantification of gel-separated proteins and their phosphorylation sites by LC-MS using unlabeled internal standards: analysis of phosphoprotein dynamics in a B cell lymphoma cell line. *Mol Cell Proteomics*, **4**, 1038-1051.

Vanhaesebroeck, B., Ali, K., Bilancio, A., Geering, B. and Foukas, L.C. (2005) Signalling by PI3K isoforms: insights from gene-targeted mice. *Trends Biochem Sci*, **30**, 194-204.

Geering, B., Cutilllas, P.R., and Vanhaesebroeck, B. (in press) Negative regulation of insulin signalling by the p85 regulatory subunit of PI3K: is there a role for free p85?

Geering, B., Cutillas, P.R., Gharbi, S., Vanhaesebroeck, B. (In preparation) Class IA phosphoinositide 3-kinase are obligate heterodimers: evidence against the existence of free p85.

ACKNOWLEDGEMENTS

First and most, I would like to thank Bart Vanhaesebroeck for giving me the opportunity to work in an outstanding laboratory. I am very grateful for the support, advice and stimulating discussions he offered. He has been an extremely motivating and creative mentor.

During my PhD, I have had the opportunity to be taught several sophisticated techniques by excellent scientists. The support of Karin Barnouin greatly helped to set up 2-dimensional gel electrophoresis experiments and I would like to thank her for passing on her invaluable knowledge and many tips. I am very thankful to Pedro Cutillas who is a brilliant mass spectrometrist and who was happily sharing his expertise and ideas with me. Furthermore, I owe many acknowledgements to Severine Gharbi, for her support and advice with the Q-TOF. Nick Morrice greatly supported us with his knowledge and instrumentation to investigate phosphorylation sites in p110δ, and I am very grateful for his help.

During my time at the Ludwig Institute I met many excellent scientists. I would especially like to thank Klaus Okkenhaug, Ashreena Salpekar, Heike Rebholz, Mariona Graupera, Lazaros Foukas, and Clotilde Billotet for helpful, interesting and inspiring discussions and debates.

I am grateful for the financial support by Roche Research Foundation, ORS student awards, Uarda Frutiger-Fonds and Janggen Poehn Stiftung.

I want to thank my family for their support in all these years and Daniel for his love.

Barbara

CONTENTS

LIST OF FIGURES

LIST OF TABLES

ABBREVIATIONS

AA	Amino acid
Ab	Antibody
BCR	B cell antigen receptor
BSA	Bovine serum albumin
ECL	Enhanced chemiluminescence
EDTA	Ethylenediaminetetraacetic acid
ESI	Electrospray ionisation
FCS	Fetal calf serum
GPCR	G protein coupled receptor
IMAC	Immobilised metal ion affinity chromatography
IP	Immunoprecipitation
IPG	Immobilised pH gradient
IS	Internal standard
KI	Knock-in
KO	Knock-out
LC	Liquid chromatography
m/z	Mass-to-charge ratio
mAb	Monoclonal antibody
MALDI	Matrix-assisted laser desorption ionisation
MeOH	Methanol
MRM	Multiple reaction monitoring
MS/MS	Tandem mass spectrometry
NCBI	National Center for Biotechnology Information
OA	Okadaic acid
pAb	Polyclonal antibody
PDGF	Platelet-derived growth factor
PH	Pleckstrin Homology
pI	Isoelectric point
PI3K	Phosphoinositide 3-kinase
PTB domain	Phospho-tyrosine binding domain
RP	Reverse-phase
pV	pervanadate
PVDF	Polyvinylidene fluoride
Q-TOF	Quadrupole time-of-flight
RT	Room temperature
SD	Standard deviation
SDS-PAGE	Sodium dodecyl sulfate-polyacrylamide gel electrophoresis
SN	Supernatant
TCL	Total cell lysate, whole cell lysate
TCR	T cell receptor
TIC	Total ion chromatogram
TOF	Time-of-flight
WM	Wortmannin
WT	Wild-type
XIC	Extracted ion chromatogram

1 INTRODUCTION

1.1 Cell signalling

Cell signalling is the communication of a cell with its environment and the transmission of these signals within the cell. Multicellular organisms need to be able to sense changes in the environment and translate these signals into appropriate cellular responses. Signalling cascades have evolved to transmit extracellular signals to the nucleus leading to changes in proliferation, migration and/or differentiation. Two important features of most signalling cascades are the potential for signal amplification and signal modulation. Furthermore, reversibility is critical for the components of the pathway in order to return to the basal state after the signal has passed through the cascade. The major information highways are gated through receptor tyrosine (Tyr) kinases (RTK), G protein coupled receptors (GPCR), ion channels, and intracellular sterol-binding receptors. Signal transduction pathways downstream of these receptors include the Ras-mitogen-activated protein kinase (Ras-MAPK), the Janus kinase (JAK)-Stat, phospholipase C (PLC), and the phosphoinositide 3-kinase (PI3K) pathway (Teaching-Resources, 2005)

The focus of this work is on the PI3K signal transduction pathway which will be therefore described in greater detail.

1.2 Phosphoinositide 3-kinase

Phosphoinositide 3-kinases (PI3Ks) are an evolutionary conserved family of signal transducing enzymes first identified as a phosphoinositide kinase activity associated with polyoma middle T antigen, the Src Tyr kinase and growth factor receptors (Kaplan et al., 1987; Macara et al., 1984; Sugimoto et al., 1984; Whitman et al., 1985). PI3Ks catalyse the transfer of γ-phosphate of ATP to the 3'-OH position of the inositol ring of phosphatidylinositols (PtdIns) and phosphoinositides (PIs) thereby generating 3'-phosphorylated PIs (Traynor-Kaplan et al., 1988; Whitman et al., 1988).

The basal levels of PIs residing in the plasma membrane are low (Funaki et al., 2000). Following cellular stimulation, PI3Ks are activated leading to the transient accumulation of PI3K lipid products in cell membranes. Proteins containing phospholipid-binding domains such as pleckstrin homology (PH) or FYVE domains can interact with PI3K lipid products. Membrane recruitment of these proteins induces their interaction with protein binding partners and activation. A variety of biological responses, such as cell survival, differentiation, proliferation, and growth are controlled by PI3Ks.

Multiple isoforms of PI3Ks exist, which can be divided into 3 classes based on their *in vitro* lipid substrate specificity, primary structure and mode of regulation (Vanhaesebroeck et al., 1997). A fourth group of enzymes named class IV or PI3K-related kinases contain regions homologous to PI3Ks. These proteins do not produce 3-PIs, but have protein kinase activity.

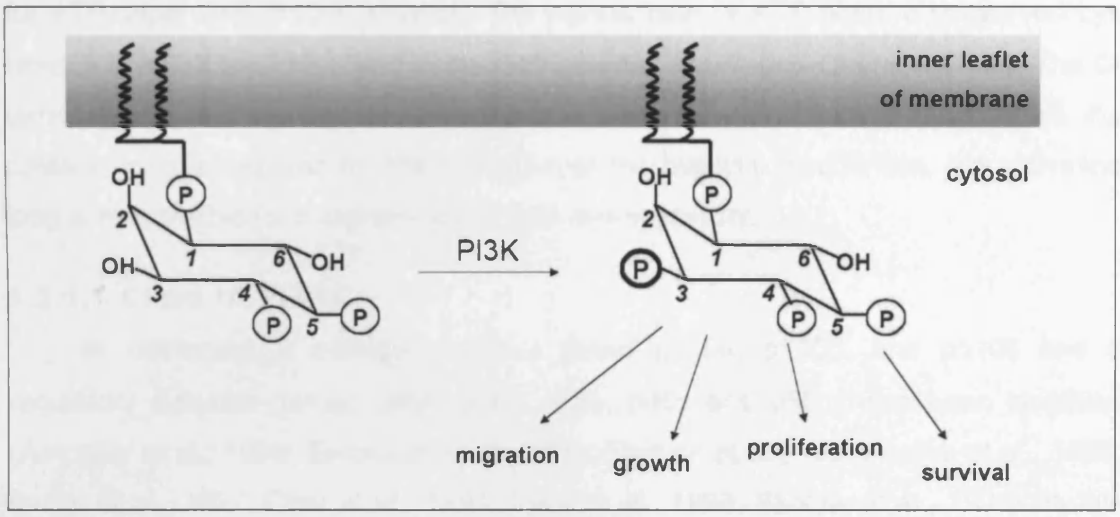

Figure 1.1: PI3Ks catalyse the phosphorylation of phospholipids
PI3Ks by definition catalyse the phosphorylation of the 3'-OH position of PtdIns and PIs to generate 3-phosphorylated PI. In this figure, the reaction performed by class I PI3K is shown whereby PtdIns(4,5)P_2 is phosphorylated to produce PtdIns(3,4,5)P_3, also known as PIP_3.

1.2.1 Class I PI3Ks

Class I PI3Ks are heterodimeric proteins consisting of a catalytic and a regulatory subunit. These enzymes utilise PtdIns, PtdIns(4)P, and PtdIns(4,5)P_2 to generate PIP_3 *in vitro,* however, their preferred substrate *in vivo* appears to be PtdIns(4,5)P_2 (Hawkins et al., 1992). In addition to their lipid kinase activity, class I PI3Ks possess intrinsic protein kinase activity (§ 1.3.3).

Class I PI3Ks are divided into 2 subclasses, called class IA (§ 1.2.1.1) and class IB (§ 1.2.1.2). Class IA PI3Ks are activated by interaction of the regulatory subunit with phosphorylated Tyr residues in activated receptors or adaptor molecules. The single class IB PI3K is activated by interaction with heterotrimeric GPCRs (Stephens et al., 1994). While the primary structure of regulatory subunits of class IA and IB do not share homology (§ 1.2.1.1.2 and § 1.2.1.2), comparison of the primary structure among members of class I PI3K catalytic subunits revealed four homology regions (HR1-4) (Zvelebil et al., 1996). Information obtained from the crystal structure of p110γ has provided the following general model of class I PI3K catalytic subunit conformation (Pacold et al., 2000; Walker et al., 2000; Walker et al., 1999). The N-terminal region,

which provides binding to the regulatory subunit, is followed by a Ras binding domain (RBD), a C2 domain, a helical (PIK) domain and a catalytic domain (Figure 1.2, Figure 1.4). While the RBD binds the GTP-bound small GTPase Ras, the C2 domain mainly interacts with the helical domain and serves as membrane attachment. The helical domain is believed to provide a core scaffold around which the other domains lie. The catalytic domain is made of a small N-terminal lobe and a large C-terminal lobe typical for ATP-dependent protein kinases. The γ-phosphate of ATP binds a conserved Lys residue (Lys833 in p110γ) lying in the cleft between the N- and C-terminal lobe. The C-terminal lobe can be further divided into a catalytic and activation loop. While the catalytic loop is required for the execution of the catalytic mechanism, the activation loop is responsible for substrate recognition and specificity.

1.2.1.1 Class IA PI3Ks

In mammals, 3 catalytic subunits called p110α, p110β, and p110δ and 5 regulatory subunits named p85α, p85β, p55γ, p55α and p50α have been identified (Antonetti et al., 1996; Escobedo et al., 1991; Fruman et al., 1996; Inukai et al., 1996; Inukai et al., 1997; Otsu et al., 1991; Pons et al., 1995; Skolnik et al., 1991). In this work, the catalytic subunits will be referred to as 'p110' and the regulatory subunits as 'p85'.

Class IA PI3K homologues have been identified in *C. elegans* (AGE-1), *D. melanogaster* (Dp110), and *D. discoideum* (PIK1-3) (Leevers et al., 1996; Morris et al., 1996; Zhou et al., 1995). No class IA homologues have been detected in yeast or plant (Vanhaesebroeck et al., 1997). The isoforms identified show a high degree of conservation during evolution.

In all mammalian cell types investigated, at least one class IA PI3K isoform is expressed. In addition, virtually every receptor that induces Tyr kinase activity also leads to PI3K activation (Wymann and Pirola, 1998), emphasising the important role of class IA PI3Ks in cellular function.

1.2.1.1.1 Class IA PI3K catalytic subunits

The three class IA PI3K catalytic subunits p110α, p110β and p110δ are products of 3 separate genes, but share 42-58% amino acid sequence identity (Hiles et al., 1992; Hu et al., 1993; Vanhaesebroeck et al., 1997).

Growing evidence indicates non-redundant functions for class IA catalytic subunits. The catalytic subunits share to the best of our knowledge the same substrate specificity, binding to any of the 5 regulatory subunits, interaction with phosphorylated Tyr residues in receptors or adaptors, and subcellular localisation. However, they differ in their tissue distribution, binding partners, and *in vitro* lipid and protein kinase

activities. Furthermore, differences in the oncogenic potential of class IA isoforms were recently revealed: the p110α gene is selectively amplified in a number of cancer lineages, including ovary, cervix and lung (Kang et al., 2005) and activating mutations in p110α have been identified (Bader et al., 2006; Samuels and Velculescu, 2004; Samuels et al., 2004). No oncogenic mutations have been found in the genes for p110β or p110δ (Cornillet-Lefebvre et al., 2006; Kang et al., 2005), but increased protein expression of p110β and p110δ occurs in some tumours and glioblastoma (Benistant et al., 2000; Knobbe and Reifenberger, 2003).

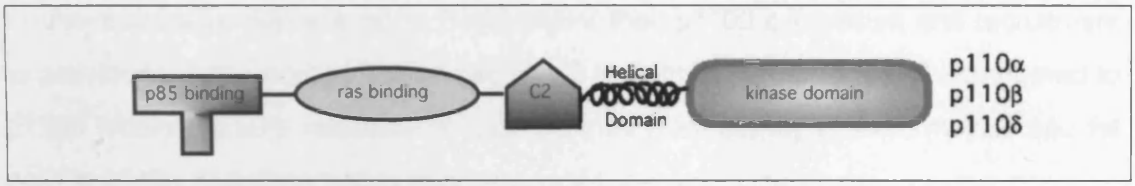

Figure 1.2: Schematic representation of the class IA PI3K catalytic subunit

Class IA PI3Ks consist of p110α, p110β and p110δ catalytic subunits. These enzymes are made of an N-terminal p85 binding domain, followed by a Ras-binding, C2, helical (PIK), and C-terminal kinase domain. More detailed information is provided in § 1.2.1.1.1. Figure adapted from (Deane and Fruman, 2004).

1.2.1.1.1.1 p110α

The *PIK3CA* gene gives rise to a ubiquitously expressed p110α protein. p110α has been implicated in cell growth. Thus, tissue-specific overexpression of membrane-targeted, mammalian p110α, which is constituitively active, leads to increased heart size, whereas overexpression of kinase-dead p110α results in heart reduction (Shioi et al., 2000). Furthermore, p110α seems to have a role in the regulation of cell division. Overexpressed p110α increases mitogenesis in cell culture models, and neutralisation of p110α by Abs blocks mitogenesis following some (PDGF, EGF, insulin, CSF-1), but not all (bombesin, LPA) stimuli (Roche et al., 1998; Vanhaesebroeck et al., 1999). A further role for p110α has been suggested in glucose uptake. Membrane-targeted p110α induces translocation of the glucose transporter Glut4 (Frevert and Kahn, 1997; Tanti et al., 1996). This translocation is abolished by the PI3K inhibitor Wortmannin (WM) (Kanai et al., 1993) and increased by a constitutively active Akt (Kohn et al., 1996).

Not much information was gained by the generation of p110α KO mice. p110α KO embryos die between E9.5 and E10.5 due to severe proliferative defects in many tissues. Importantly, overexpression of the regulatory subunit was observed in p110α KO compared to WT cells (Bi et al., 1999). This finding hampers the analysis of the role of p110α in these mice, since defects could be due to p110α deletion or p85

overexpression. Mice heterozygous for p110α show no obvious defects (Brachmann et al., 2005).

Generation of p110α KI mice have revealed that p110α is a key regulator in metabolic signalling (Foukas et al., 2006), in contrast to previous reports (Asano et al., 2000; Roche et al., 1998). In these p110α KI mice, class IA PI3K subunit expression is unchanged. Homozygous KI embryos die between E10 and E11, but heterozygous KI mice are viable and fertile. These mice are smaller than their WT littermate and display defects in insulin sensitivity and glucose metabolism due to reduced signalling via insulin-receptor substrate proteins. It was shown that p110α protein expression in insulin-responsive tissue is up to 2-fold higher than p110β expression and recruitment to activated insulin receptor substrates was 2 to 8 times higher for p110α compared to p110β leading to 50% reduction in total class IA PI3K activity in liver, muscle and fat cells in p110α KI heterozygous mice.

1.2.1.1.1.2 p110β

As for p110α, p110β is widely expressed. In contrast to p110α and p110δ, p110β was shown to interact with Gβγ subunits of trimeric G proteins (Kurosu et al., 1997; Maier et al., 2000). Stimulation of GPCR by lysophosphatidic acid (LPA) leads to p110β activation (Roche et al., 1998) and this activation can be synergystically enhanced by interaction with phosphorylated Tyr residues in activated receptors or adaptor molecules.

p110β appears to be involved in the mitogenic response induced by certain growth factors. Microinjection of neutralising Abs specific for p110β into fibroblasts inhibits DNA synthesis normally induced by insulin and LPA but hardly affects PDGF receptor signalling (Roche et al., 1998). p110β was further shown to have a role in cytoskeletal organisation (Hooshmand-Rad et al., 2000; Vanhaesebroeck et al., 1999), where p110β is necessary for CSF-induced modulation of actin dynamics. Furthermore, p110β has a role in exocytosis since Glut4 translocation following insulin stimulation in NIH-3T3 is abolished upon microinjection of p110β Abs (Asano et al., 2000). Recently, p110β was also implicated in the regulation of adhesion. Studies using a small molecule inhibitor with selectivity for p110β (detailed in § 1.6.1.2) revealed that this catalytic subunit is involved in integrin activation and platelet aggregation by regulating Ca^{2+} flux and Gβγ-dependent activation of the small GTPase Rap (Jackson et al., 2005).

Murine p110β gene-targeting studies did not offer great insight into potential p110β non-redundant function. Indeed, p110β KO embryos die during implantation and p110β heterozygous mice display no obvious defects (Bi et al., 2002; Brachmann et al.,

2005). Double p110α/p110β KO heterozygous mice are slightly glucose intolerant and exhibited hyperinsulinaemia in the fasting state, attributing a role for p110α and p110β in metabolism. Interestingly, in addition to reduced p110 protein expression, also p85 protein levels are decreased by 50% in these cells, indicating instability of monomeric regulatory subunits (Brachmann et al., 2005).

1.2.1.1.1.3 p110δ

p110δ is primarily expressed in leukocytes, but can also be detected in neurons and cells of melanocytic or breast origin (Sawyer et al., 2003; Vanhaesebroeck et al., 1997). p110δ primary sequence analysis revealed a p110δ unique Src-homology-3 (SH3) domain and a basic-region leucine zipper (bZIP) motif shared with p110β (Vanhaesebroeck et al., 1997). Gene-targeting of p110δ by KO or KI strategies have emphasised the important role of p110δ in leukocyte function and development.

Two research groups (Clayton et al., 2002; Jou et al., 2002) generated murine strains with a deletion in p110δ gene leading to ablation of p110δ protein expression. However, these p110δ KO mice also display reduced expression of the regulatory subunits p85α, p55α and p50α. The mutant mice are viable, but have reduced numbers of mature B cells and subsequently have smaller spleens and lymph nodes. Cellular signalling through the B cell antigen receptor (BCR) is affected with reduced PIP_3 production and reduced phosphorylation of downstream effectors leading to reduced Ca^{2+} flux. *Ex vivo* proliferation of p110δ KO cells is also reduced in response to various stimuli. In contrast to the B cell phenotype, the proportion of $CD4^+$ and $CD8^+$ peripheral T cells of p110δ KO mice is similar to WT mice.

The phenotype of the p110δ KI mice appears to be more severe (Okkenhaug et al., 2002). BCR-induced phosphorylation of the downstream effector Akt is ablated and Ca^{2+} flux in stimulated B cells is greatly reduced (see § 1.7.2). *Ex vivo* proliferation following BCR engagement was abrogated. The effects of p110δ inactivation on B cell signalling detected in KI mice were recently confirmed by p110δ inhibitor studies (Bilancio et al., 2006). p110δ KI mice also display reduced T cell numbers in the spleen. Akt phosphorylation and Ca^{2+} flux is reduced in response to T cell receptor (TCR) stimulation (Okkenhaug et al., 2002). Furthermore, mast cell function is affected in p110δ KI mice. Akt phosphorylation downstream of IL3 and SCF receptor is reduced, leading to reduced DNA synthesis and degranulation of mast cells (Ali et al., 2004). p110δ has also been implicated in the control of neutrophil function (Ptasznik et al., 1996; Sadhu et al., 2003) and was recently shown to be activated following p110γ activation upon neutrophil stimulation (Condliffe et al., 2005).

1.2.1.1.2 Class IA PI3K regulatory subunits

In mammals, 5 regulatory subunits have been identified. p85α, p85β and p55γ are products of separate genes. Whether p55α and p50α are mRNA splice variants of the p85α gene or the result of alternative promoter usage is controversial (Abell et al., 2005).

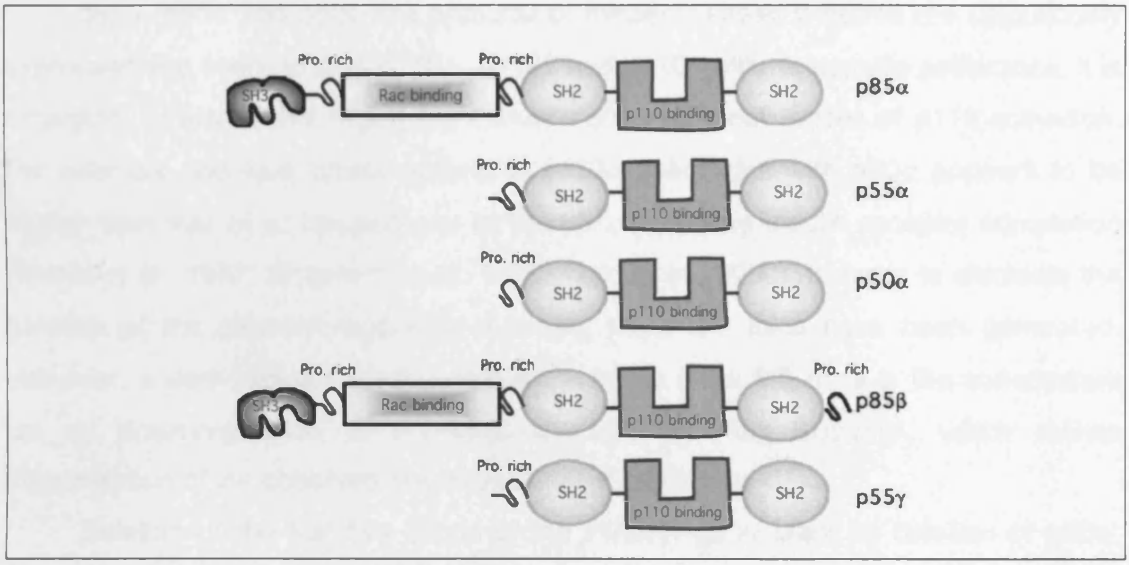

Figure 1.3: Schematic representation of class IA PI3K regulatory subunits

Class IA PI3K regulatory subunits are the products of 3 separate genes (*PIK3R1*, *PIK3R2* and *PIK3R3*) giving rise to p85α, p85β and p55γ. *PIK3R1* gives further rise to p55α and p50α protein either by mRNA splicing or alternative promoter usage. The regulatory subunits contain a variety of protein-interacting domains such as the SH3 domain, which binds to proline rich motifs, and the SH2 domains that interact with phosphorylated Tyr residues in YxxM-motifs. A Rac binding domain has been shown to have binding affinity to small GTPases such as Rac1 and Cdc42 and the p110-binding domain also called interSH2 domain facilitates binding to the catalytic subunit (figure taken from (Deane and Fruman, 2004)).

The regulatory subunits are composed of several protein-protein interaction domains. While the N-termini differ substantially between the different regulatory subunits, the C-termini of the various regulatory subunits are conserved. A proline-rich region (P2), which facilitates interactions with SH3 domain-containing proteins, is followed by two SH2 domains. The SH2 domains allow for binding to phospho-tyrosine (pTyr) residues in the sequence context pYxxM (where pY is phospho-tyrosine, x stands for any amino acid and M is methionine) (Songyang et al., 1993). The domain in-between the two SH2 domains is called interSH2 (iSH2) or p110 binding domain and mediates binding to the p85-binding domain of class IA catalytic subunits (§ 1.3.2.1). In p85α and p85β, an N-terminal SH3 domain is followed by a proline-rich segment (P1) and a Breakpoint Cluster Region Homology (BH) domain, which is also called Rac-binding domain (Otsu et al., 1991; Musacchio et al., 1996). In the shorter versions of

the regulatory subunits, the N-termini are unique and do not have homology to known domains.

In addition to its role in the regulation of p110, p85 was suggested to independently stimulate signalling pathways (reviewed in (Okkenhaug and Vanhaesebroeck, 2001)).

1.2.1.1.2.1 p85α, p55α and p50α

p85α, p55α and p50α are products of *PIK3R1*. These isoforms are ubiquitously expressed and seem to bind p110α, p110β and p110δ with no specific preference. It is emerging, however, that regulatory subunits allow different modes of p110 activation. For example, the lipid kinase activity of p110α associated with p50α appears to be higher than that of p110α-p55α or p110α-p85α following insulin receptor stimulation (Inukai et al., 1997; Shepherd et al., 1997; Ueki et al., 2000). In order to elucidate the function of the different regulatory subunits, p85α KO mice have been generated. However, a very frequent confounding issue in the p85α KO mice is the concomitant up- or down-regulation of non-targeted class IA PI3K subunits, which makes interpretation of the observed phenotypes not straightforward.

Deletion of the last five exons of the *PIK3R1* gene leads to deletion of p85α, p55α and p50α protein (referred to as p85α-full KO). p85β is upregulated in cells of these mice, whereas p110α and p110β are downregulated. Mice containing this mutation die shortly after birth. The animals have reduced numbers of mature B cells and show a defect in B cell function, with reduced *ex vivo* proliferation in response to various stimuli. Furthermore, mast cells of p85α-full KO mice display a defect in SCF responses, but normal IgE-driven signalling (Fruman et al., 1999; Suzuki et al., 1999), while T cell function appears to be normal. The p85α-full KO mice feature necrosis of the liver and brown fat tissue. These mice are hypoglycaemic, contain lower insulin levels, and have increased glucose tolerance due to upregulation of PI3K signalling. These findings are unexpected since PI3Ks have been implicated in *positively* regulating insulin signalling *in vitro* (Fruman et al., 2000). Mice heterozygous for the p85α-full KO also possess improved insulin signalling and glucose homeostasis (Mauvais-Jarvis et al., 2002).

In mice with deletion of the first exon of *PIK3R1*, only the expression of full-length p85α protein is abrogated. Countervailing upregulation of p55α and p50α protein expression is observed. Mice containing this mutation have a similar phenotype to p85α-full KO, but were viable (Suzuki et al., 1999; Terauchi et al., 1999).

Mice containing a mutation in *PIK3R1* gene resulting in p55α and p50α protein deletion show a milder phenotype than the p85α-only KO mice. These mice are viable

and contain normal blood glucose levels, but display lower fasting insulin levels (Chen et al., 2004).

1.2.1.1.2.2 p85β

The regulatory subunit p85β is ubiquitously expressed and seems to occur in minor amounts than p85α in insulin-sensitive cells (Ueki et al., 2002).

p85β KO mice were generated and have normal class IA PI3K isoform expression, but display hypoinsulinaemia, hypoglycaemia, and increased insulin sensitivity (Ueki et al., 2002). Lymphocyte development was normal in p85β KO mice. *Ex vivo* proliferation of p85β KO B cells was similar to WT cells following various stimuli, but proliferation of KO T cells was found to be mildly increased. Following T cell stimulation, a decrease in cell death was observed in p85β KO cells probably due to reduced levels of caspase-6 mRNA and reduced caspase-6 enzyme activity (Deane et al., 2004). These results indicate a T-cell specific function for p85β.

1.2.1.1.2.3 p55γ

p55γ has high homology to p85α in the two SH2 and iSH2 domains but lacks the BH and SH3 domains. p55γ mRNA is expressed early during development and is ubiquitously expressed in adult tissues (Inukai et al., 1996). The p55γ regulatory subunit was isolated by screening expression libraries with Tyr phosphorylated IRS-1. The N-terminal SH2 domain of p55γ was subsequently shown to interact with pYxxM-motif of IRS-1 (Pons et al., 1995). No p55γ KO mice have been generated to date.

1.2.1.2 Class IB PI3K

p110γ, the single class IB catalytic subunit, is coupled to smaller regulatory subunits called p101 and p84/p87^{PIKAP} (Suire et al., 2005; Voigt et al., 2006). p110γ has 36% protein sequence identity to p110α (Stoyanov et al., 1995), whereas p101 was believed to have no functional homology to any known protein (Stephens et al., 1997). However, an 84 kDa protein was recently discovered located beside the p101 locus with 30% sequence identity to p101. This p84 protein was shown to interact with p110γ and Gβγ *in vitro* and *in vivo* (Suire et al., 2005) and appears to be predominantly expressed in the heart (Voigt et al., 2006). Furthermore, p84 was shown to interact with phosphodiesterase-3B (PDE3B).

Binding of p110γ to p101 and to a lesser extent to p84 increases the activation of p110γ by Gβγ subunit of trimeric G proteins, and is therefore believed to be critical for coupling of p110γ to GPCRs. Activation of p110γ by Gβγ subunits does not solely depend on membrane recruitment since either monomeric p110γ or p110γ/p101 heterodimers associate with lipid monolayers *in vitro* irrespectively of the presence of

Gβγ (Krugmann et al., 2002). Therefore, it seems more likely that Gβγ-induced p110γ activation is due to conformational changes induced by this interaction. Similarly, activation of p110γ by Ras does not appear to be due to membrane recruitment. Comparison of the crystal structures of p110γ or p110γ in complex with Ras indicated that a change in p110γ conformation might allosterically increase PI3K activity (Pacold et al., 2000; Walker et al., 1999).

p110γ autophosphorylates Ser1101 located in the C-terminal kinase domain. This modification does not impact on the *in vitro* lipid kinase activity, however, autophosphorylation of Ser1101 is induced by Gβγ subunits (Czupalla et al., 2003). The biological significance of this phosphorylation has not been investigated.

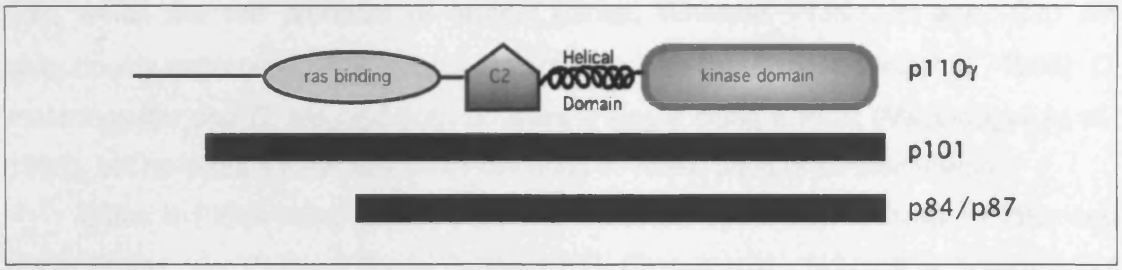

Figure 1.4: Schematic representation of class IB PI3K

Class IB PI3K consists of a 110 kDa catalytic subunit called p110γ coupled to one of two smaller regulatory subunits, p101 or p84. p110γ contains a RBD, C2 domain, helical domain and kinase domain with homology to class IA PI3Ks. The N-terminal region contains a unique binding site for the regulatory subunits. The regulatory subunits have a sequence homology of 30% to each other but no functional homology to any known protein.

Class IB PI3K is expressed mainly in cells of hematopoietic origin. Analyses of p110γ KO and kinase-dead KI mice (Hirsch et al., 2000; Li et al., 2000; Patrucco et al., 2004; Sasaki et al., 2000) which are viable and fertile, have shown that p110γ is an important component of the myeloid cell compartment. This protein seems to be crucial for neutrophil and macrophage migration towards sites of inflammation. Furthermore, a lack of p110γ in mast cells impairs degranulation and p110γ seems to play a role in platelet aggregation (Sasaki et al., 2000), while B cell function is normal in p110γ KO and KI mice. Importantly, KO and KI mice show phenotypic differences: While p110γ has been implicated in the modulation of heart contractility in KO mice, this phenotype is not observed in p110γ KI cells (Crackower et al., 2002). The molecular mechanism underlying the difference between these two types of p110γ mutant mice is proposed to be based on a scaffolding function of p110γ. p110γ has been shown to bind and control PDE3B in a manner independent of its catalytic activity. PDE3B degrades cAMP leading to inactivation of protein kinase A and decreased heart contractility.

Deregulation of PDE3B induces the opposite reaction (reviewed in (Vanhaesebroeck et al., 2004)).

1.2.2 Class II PI3Ks

Class II PI3Ks are large enzymes of 170-210 kDa predominantly associated with the membrane fraction of cells (Arcaro et al., 1998; Prior and Clague, 1999). Their catalytic domain is 45-50% homologous to class I PI3Ks, their large N-terminal region shows no homology to any known protein and the C-terminal region contains homology to C2 domains. This C2 domain can bind to phospholipids in a Ca^{2+}-independent manner *in vitro* (MacDougall et al., 1995).

Mammals have 3 class II PI3K isoforms called PI3K-C2α, PI3K-C2β, and PI3K-C2γ, which are the products of distinct genes. Whereas PI3K-C2α and -C2β are ubiquitously expressed, PI3K-C2γ is restricted to liver tissues (Misawa et al., 1998). *D. melanogaster* and *C. elegans* both possess a single class II PI3K (MacDougall et al., 1995), but no class II PI3K has been identified in yeast, plant or *D. discoideum*.

Class II PI3Ks have different *in vitro* substrate specificity to class I PI3Ks and prefer PtdIns over PtdIns(4)P and PtdIns(4,5)P_2 (Domin et al., 1997). It is, however, not clear which phospholipids are generated by class II PI3Ks *in vivo*. Furthermore, the mode of activation of class II PI3Ks inside cells is not well understood, but it was shown that PI3K-C2β and to a lesser extent -C2α can be activated by several receptor systems (Arcaro et al., 2000; Brown et al., 1999; Turner et al., 1998; Zhang et al., 1998).

1.2.3 Class III PI3K

The single class III PI3K identified in mammalian cells is a homologue to the yeast vesicular protein-sorting protein Vps34p (Herman et al., 1992). Other homologues have been identified in *D. discoideum* and *D. melanogaster* (Linassier et al., 1997; Volinia et al., 1995; Zhou et al., 1995).

Vsp34p was originally identified in a screen for mutants conditionally defective in vacuolar protein sorting (Herman and Emr, 1990). It associates with a Ser/Thr protein kinase, Vsp15p, that is N-terminally myristoylated and targets Vsp34p to membranes (Stack et al., 1993).

Class III PI3K appears not to be activated following cellular stimulation and can only use PtdIns as substrate *in vitro*. This enzyme is thought to be responsible for the production of most cellular PtdIns(3)P, the levels of which remain relatively constant.

Vsp34p also has intrinsic protein kinase activity and has been shown to autophosphorylate on Ser, Thr and Tyr *in vitro* in the absence of lipid substrate (Stack

and Emr, 1994). However, Vsp34p has not been shown to phosphorylate any exogenous protein substrate and autophosphorylation does not affect its lipid kinase activity. Thus, the significance of Vsp34p protein kinase activity remains unclear.

1.2.4 Class IV PI3Ks

Class IV PI3K-related kinases share a catalytic domain with homology to all PI3Ks. The kinase domain of these enzymes possesses Ser/Thr protein kinase activity rather than lipid kinase activity and no lipid substrates for these kinases have been identified (Brown et al., 1995; Jung et al., 1997). Members include gene products that regulate cell cycle progression in response to DNA damage (RAD3, MEC1, TEL1, ATM and ATR) as well as DNA-activated protein kinase (DNA-PK) and TOR/FRAP/RAFT1 members.

1.3 Class IA PI3K activation and regulation

Surprisingly little is understood about the regulation of class IA PI3K activity *in vivo*. This scarce knowledge is due to various factors: First, regulation of class IA PI3K activity most likely occurs on many levels and is therefore *per se* very complex. Second, analysis of PI3K activity has mainly been performed with recombinant protein and in *in vitro* experiments. Third, distinction between different isoforms, which are likely regulated in unique ways, has been impossible or neglected.

We try below to give an overview of the various possibilities to regulate class IA PI3K activity. In Figure 1.5, the *in vitro* mechanisms to regulate the intrinsic lipid kinase activity (described in more detail in § 1.3.1, 1.3.2, 1.3.3, and 1.3.4) are summarised. The *in vitro* lipid kinase activity of PI3Ks after experimental manipulation is compared to non-activated, cytosolic heterodimer yielding positive and negative regulation mechanisms. Briefly, compared to the p85-p110 complex residing in the cytosol, monomeric p110 (A) as well as membrane-targeted PI3K (B) are thought to possess higher lipid kinase activities. Interaction with activated, pYxxM-containing proteins (C) and Ras (D) also increases PI3K activity of all p110 subunits, while p110β was shown to be further activated by interaction with Gβγ subunits of trimeric G proteins (E). The PI3K enhancer PIKE is believed to induce lipid kinase activity of nuclear PI3K (F). In contrast to mechanisms positively regulating PI3K activity, Ser phosphorylation of p110 or p85 (G) likely reduces the intrinsic PI3K lipid kinase activity and interaction of p85 with Ruk (H) was also shown to reduce lipid kinase activity.

In addition to the regulation of intrinsic p110 lipid kinase activity, the net PI3K activity *in vivo* is thought to be further positively and negatively modulated by protein-protein interactions, by subcellular localisation and by expression of monomeric p85.

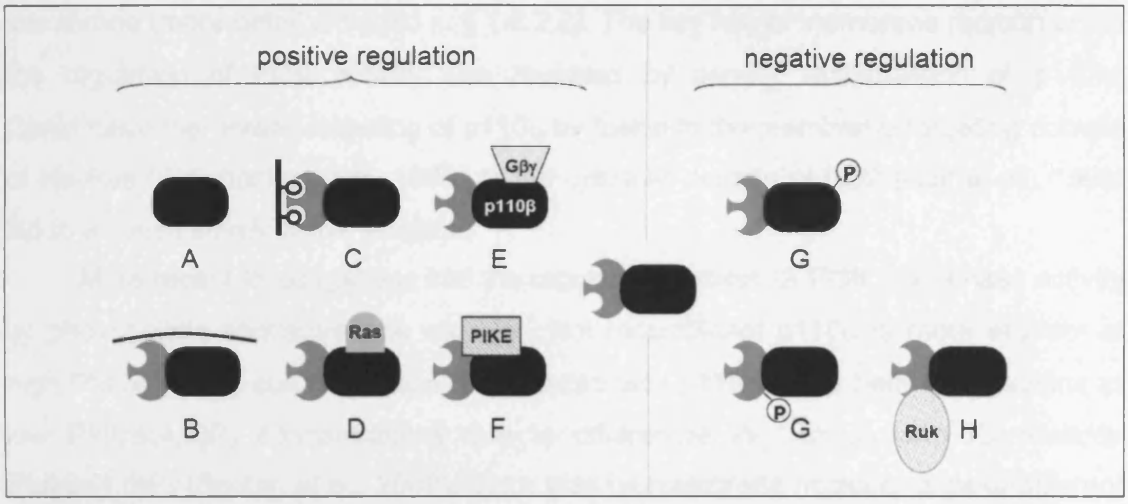

Figure 1.5: The intrinsic PI3K lipid kinase activity is modulated by a variety of mechanisms *in vitro*

Compared to the PI3K activity of non-activated, cytosolic p85-p110 heterodimer, PI3K activity is controlled by the p85 to p110 ratio (A), by subcellular localisation (B), by interaction with protein partners (C, D, E, F, H), and by post-translational modifications (G). More details to each mechanism of regulation are provided below.

In order to simplify this challenging subject, we divided the mechanisms for class IA PI3K regulation into different subjects, such as subcellular localisation, interaction partners, protein kinase activities and post-translational modifications. However, this classification can only be conceptual since each subset of regulating mechanisms is possibly interlinked with other subsets. Thus, the subcellular localisation of a protein might be controlled by an interaction partner, or binding to a protein partner is due to post-translational modifications.

1.3.1 Subcellular localisation of class IA PI3K

Traditionally, proteins have been characterised according to their broad subcellular localisation as being cytosolic, membrane, nuclear etc. However, many proteins are constantly shuttled between different cellular compartments rendering strict definitions redundant. Moreover, within distinct subcellular compartments, microdomains made of unique concentrations of certain molecules are gaining increased importance potentially leading to adjustment of intracellular localisation of many proteins, possibly including class IA PI3Ks.

Class IA PI3Ks are found in the cytoplasm, at the plasma membrane, and in the nucleus. While the pool of class IA PI3Ks is believed to reside in the cytoplasm, a fraction of the p85-p110 complexes translocates to the membrane following cellular stimulation where class IA PI3Ks exert their function as lipid kinases. Membrane recruitment upon stimulation is achieved by interaction of the SH2 domains of the

regulatory subunits with phosphorylated Tyr residues in proteins residing at the plasma membrane (more detail provided in § 1.3.2.2). The key role of membrane recruitment in the regulation of PI3K activity was revealed by genetic manipulation of p110α. Constitutive membrane targeting of p110α by fusion to the membrane-targeting domain of Ha-Ras (Didichenko et al., 1996) or the cytosolic domain of CD2 (Reif et al., 1996) led to a constitutively active enzyme.

More recent investigations into the regulation of class IA PI3K lipid kinase activity by phospholipid concentrations revealed that recombinant p110α is more efficient at high PtdIns(4,5)P_2 concentrations and recombinant p110β is the better lipid kinase at low PtdIns(4,5)P_2 concentrations due to differences in their *in vitro* K_m towards PtdIns(4,5)P_2 (Beeton et al., 2000). Since plasma membrane microdomains of different phospholipid concentrations have been described (Liu et al., 1998), it is tempting to speculate that p110α might be more active than p110β in certain fractions of the plasma membrane (where higher concentrations of phosphoinositides are found).

Emerging evidence is suggesting that class I PI3Ks can also translocate to the nucleus upon cellular stimulation where these enzymes catalyse the phosphorylation of PtdIns(4,5)P_2 to PIP_3 (Bavelloni et al., 1999; Kim, 1998; Marchisio et al., 1998; Neri et al., 1994). The regulation of nuclear PI3K activity seems to be achieved at least to some extent by the nuclear GTPase called PI3K Enhancer (PIKE) (Rong et al., 2003). However, the mechanism and biological relevance of nuclear translocation of class IA PI3K remains to be determined.

1.3.2 Protein-protein interactions

Biological functions involve the formation of protein-protein complexes. Protein-protein interactions have been shown to be critical for the activity, stability, and subcellular localisation of many proteins. They differ based on the composition of the complex, on the affinity of the components to each other and on the longevity of the interaction and can accordingly be divided into homo- and heterocomplexes and into obligate or non-obligate complexes (see Table 1.1). All protein-protein interactions are ultimately driven by the local concentration of the components and the free energy of the complex.

The regulatory and catalytic subunits of class IA PI3Ks contain a multitude of protein-interacting domains. Additionally, class IA PI3Ks were shown to be Ser, Thr and Tyr phosphorylated (more information in § 1.3.4) creating further docking sites for SH2-, phospho-tyrosine binding (PTB)-, C2-, Forkhead-associated (FHA)- and C-terminal region of BRCA-1 (BRCT)- domain containing proteins (Benes et al., 2005; Durocher et al., 1999; Kavanaugh and Williams, 1994; Manke et al., 2003; Sadowski et

al., 1986). It is therefore not surprising, that class IA PI3Ks have been detected in complex with many different protein partners. Here, we first discuss the interaction between p85 and p110 and introduce evidence that suggests this complex being an obligate or non-obligate heterodimer. This is followed by an overview of additional class IA PI3K binding partners.

Table 1.1: Properties of non-obligate and obligate protein complexes
Dimeric protein complexes can be divided into non-obligate or obligate interactions depending on the existence of monomeric (non-obligate) or strictly heterodimeric (obligate) subunits. Different biophysical properties can be attributed to each protein formation. Adapted from (Nooren and Thornton, 2003).

	non-obligate	obligate
Stability	Protomers are independently stable. Monomers are detectable.	Monomeric protomers are not found as stable structures *in vivo*. Only heterodimers are detectable.
Expression (Transcription/ Translation)	Protomers are expressed non simultanously.	Protomers are expressed simultanously.
Interaction	Weak interaction between protomers	Strong interaction between protomers
Interface	Small	Large and hydrophobic

1.3.2.1 p85-p110 protein interaction

The interaction between the regulatory and catalytic subunit of class IA PI3K is important for at least three aspects of PI3K activity regulation which will be discussed in more detail below. First, interaction with p85 enables p110 being shuttled to the plasma membrane following cellular stimulation. This translocation allows interaction with p110 substrates and increases the intrinsic lipid kinase activity. Second, the interaction increases the thermal stability of the unstable, monomeric catalytic subunit and the less stable, monomeric regulatory subunit. Third, binding of p85 to p110 reduces the p110 lipid kinase activity in the basal state which can be increased by interaction of the complex with non-PI3K binding partners following cellular stimulation.

The interaction between the catalytic and regulatory subunit involves the interSH2 (iSH2, also called p110-binding) domain of p85, and the p85-binding domain of p110 (Dhand et al., 1994; Holt et al., 1994; Hu et al., 1993; Klippel et al., 1993; Yu et al., 1998). While the p85 iSH2 domain is sufficient for p110 binding, it does not inhibit p110 activity. The presence of the N-terminal SH2 domain coupled to iSH2 is required for p110 lipid kinase inhibition (Yu et al., 1998). Since inhibition of p110 activity by p85 was shown to be released by interaction of the complex to phosphorylated Tyr residues in pYxxM-motif containing proteins (Rordorf-Nikolic et al., 1995; Yu et al., 1998), the N-terminal SH2-domain of p85 was suggested as a regulator of lipid kinase activity (Yu et

al., 1998). Inhibition of p110 by p85 is likely due to conformational changes imposed onto the catalytic subunit by p85 binding, which is alleviated by interaction of p85 with phosphorylated Tyr residues. Which domain of p85 is involved in these conformational rearrangements is controversial (Chan et al., 2002; Fu et al., 2004; Panayotou et al., 1993). In addition to p110 inhibition by the non-engaged N-terminal SH2 domain of p85, phosphorylation of Ser608 in the iSH2 domain of p85α further reduces p110 lipid kinase activity (Dhand et al., 1994). This reduction might be due to p85-p110 dissociation (Foukas et al., 2004). Further information about phosphorylation of Ser608 is provided in § 1.3.3.

In the traditional model of class IA PI3K regulation described above, it is suggested that p110 and p85 form obligate heterodimers and that regulation of PI3K lipid kinase activity of the obligate heterodimer is mainly steered by interaction with non-PI3K binding partners. This model of obligate heterodimeric class IA PI3K was generated on the basis of observations that revealed high binding affinities between the subunits (Fry et al., 1992) and instability of monomeric p110 (Yu et al., 1998).

Various reports have challenged obligate heterodimericity of class IA PI3K and its implications on PI3K regulation. Thus, when class I PI3Ks are purified from bovine thymus using various chromatographic methods, two catalytically active p110 subunits can be distinguished: p110 in complex with p85, and p110 in what was considered to be a monomeric form (Shibasaki et al., 1991). In contrast to an excess of the catalytic subunit observed in thymic cells, more recent data gained from analysis of p85 KO mice indicate a greater than 30% molar excess of p85 over p110 in WT murine embryonic fibroblasts (MEFs) (Ueki et al., 2002) and WT murine liver cells (Mauvais-Jarvis et al., 2002).

The existence of monomeric class IA PI3K subunits *in vivo* likely has implications on the regulation of the lipid kinase activity. Due to the increased activity of monomeric p110 observed *in vitro* (Shibasaki et al., 1991; Yu et al., 1998), an excess of catalytic subunit over regulatory subunit would probably lead to increased p110 lipid kinase activity. In contrast, monomeric p85 is believed to compete with heterodimeric p85-p110 for binding to pYxxM-motif containing proteins (Ueki et al., 2002). Since monomeric p85 does not possess lipid kinase activity, occupation of pTyr docking sites by monomeric p85 instead of active, heterodimeric PI3K would lead to a decrease in PI3K lipid kinase activity (Luo and Cantley, 2005).

1.3.2.2 Other class IA PI3K binding partners

Class IA PI3Ks have been implicated in a multitude of protein-protein interactions via the diverse protein interaction domains of the catalytic and regulatory subunits. Binding of protein partners can regulate PI3K activity by modulating the intrinsic

enzymatic activity, by localising the enzyme to specific cellular compartments or by disrupting interaction with other binding partners.

In Table 1.2, a summary of class IA PI3K interaction partners and binding properties are given. While this list of proteins is by no means complete, we tried to consider a few examples of interacting proteins for each class IA domain, which are described in more detail below.

Table 1.2: Class IA PI3K interaction partners

Interaction partners of class IA PI3Ks are listed according to the interacting domain in the p85 or p110 subunit starting from the C-terminus. If known, the stimuli and cell type upon which the interaction occurs is stated as well as the biological implications of this interaction. R, receptor, P-tase, phosphatase.

Binding partner	Properties	PI3K	Domain	Stimulation/ cell type	Biological implications	References
Androgen R	Receptor	p85α	C-terminus	Androgen	Lipid kinase activity ↑	(Sun et al., 2003)
Oestrogen R	Receptor	p85α	SH2		Lipid kinase activity ↑	(Simoncini et al., 2000)
c-Kit R	Receptor	p85	SH2		Lipid kinase activity ↑	(Lev et al., 1992; Serve et al., 1994)
EGF R	Receptor	p85	C-SH2		Lipid kinase activity ↑	(Hu et al., 1992)
PDGF R	Receptor	p85	C-SH2		Lipid kinase activity ↑	(Hu et al., 1992)
IGF-1 R	Receptor	p85	SH2		Lipid kinase activity ↑	(Yamamoto et al., 1992)
CD28	Adaptor	p85	SH2	T cells	Lipid kinase activity ↑	(Pages et al., 1994)
CD19	Adaptor	p85	SH2	B cells	Lipid kinase activity ↑	(Tuveson et al., 1993; Buhl and Cambier, 1999)
CD5	Adaptor	p85	C-SH2 N-SH2			(Dennehy et al., 1997)
IRS-1	Adaptor	p85	SH2	Insulin	Lipid kinase activity ↑	(Backer et al., 1992)
BCAP	Adaptor	p85	SH2	B cells		(Okada et al., 2000)
Gab2	Adaptor	p85	SH2			(Gu et al., 2000)
SLP-76	Adaptor	p85	N-SH2	CD3/ T cells		(Shim et al., 2004)
Shc	Adaptor	p85	C-SH2			(Harrison-Findik et al., 1995)
Ezrin	Adaptor	p85	C-SH2			(Gautreau et al., 1999)
Syk	Kinase	p85α, p85β	C-SH2			(Moon et al., 2005)
IkBα	Kinase	p85α	SH2	pV/ T cells		(Beraud et al., 1999)
SHIP	Ⓟ-tase	p85	SH2	B cell		(Gupta et al., 1999)
SHP1	Ⓟ-tase	p85	C-SH2	PDGF/ MCF-7, TRMP		(Cuevas et al., 1999; Yu et al., 1998)
SHP2	Ⓟ-tase	p85α				(Kwon et al., 2005)
Rac	GTPase	p85	BH		Lipid kinase activity ↑	(Zheng et al., 1994; Bokoch et al., 1996; Tolias et al., 1995)
Cdc42	GTPase	p85	BH		Lipid kinase activity ↑	(Zheng et al., 1994)
Grb2	Adaptor	p85	P1	constitutive		(Wang et al., 1995)
α-actinin	Adaptor	p85	P1	NIH-3T3	Binding ↑ by PIP_3	(Shibasaki et al., 1994)
Fyn	Kinase	p85	P1 only	T cells Thrombin/ platelets		(Mak et al., 1996; Pleiman et al., 1994; Prasad et al., 1993)
Lyn	Kinase	p85	P1 only	α-IgM/ B cells		(Yamanashi et al., 1992; Pleiman et al., 1994)
Src, v-Src	Kinase	p85				(Fukui and Hanafusa, 1989; Liu et al., 1993)
Ruk	Adaptor	p85α	SH3		Lipid kinase activity ↓	(Gout et al., 2000)

Binding partner	Properties	PI3K	Domain	Stimulation/ cell type	Biological implications	References
Cbl-b	Adaptor	p85β	SH3	TCR/ T cells EGF/ PC12 cells	Lipid kinase activity ↓	(Hartley et al., 1995; Soltoff and Cantley, 1996)
Dynamin	GTPase	p85	SH3		Dynamin GTPase activity ↑	(Gout et al., 1993)
p85α	Adaptor	p85α	SH3,P1/P2			(Kapeller and Cantley, 1994; Harpur et al., 1999)
α/β/γ -tubulin		p55α/γ	N-terminus	constitutive		(Inukai et al., 2000)
α/β -tubulin		p85	iSH2	constitutive		(Kapeller et al., 1995)
γ -tubulin		p85		Insulin,PDGF		(Kapeller et al., 1995)
Ras	GTPase	p110	RBD		Lipid kinase activity↑	(Rodriguez-Viciana et al., 1994;Rodriguez-Viciana et al., 1996)
Rab5	GTPase	p110β			Lipid kinase activity↑	(Christoforidis et al., 1999; Kurosu and Katada, 2001)
Gβγ subunit		p110β			Lipid kinase activity↑	(Kurosu et al., 1997)

1.3.2.2.1 p85 interaction partners

The N- and C-terminal **SH2 domain** of the regulatory subunits are of fundamental importance for the enzymatic function of class IA PI3K since these domains bind to pTyr residues of activated growth factor receptors and adaptor molecules. In this way, the SH2 domains of p85 dock the p110 enzyme to the plasma membrane and concomitantly increase the intrinsic lipid kinase activity (more information in § 1.3.2.1). Both SH2 domains have high affinity for binding pYxxM, and especially pYMxM. There is, however, a small difference in the specificities of the N- and C-terminal SH2 domains (Panayotou et al., 1993; Songyang et al., 1993).

In addition to the SH2 domain, also the p85 **BH /Rac binding domain** is involved in the positive regulation of PI3K activity. Interaction with small GTPases via the BH domain leads to PI3K activation (Tolias et al., 1995). The BH domain of p85α, which displays sequence homology to GTPase activating proteins (GAPs), was moreover shown to have GAP activity towards Rab proteins, Cdc42, and Rac1 (Chamberlain et al., 2004).

In contrast to SH2 and BH domain, p85 **SH3** binding to the adaptor proteins Ruk and Cbl-b mediates negative PI3K signalling. While Ruk interaction with PI3K leads to the downregulation of the intrinsic lipid kinase activity, Cbl-b was shown to compete with CD28 binding of p85 presumably interfering with positive CD28 lipid kinase signalling (Fang and Liu, 2001); (Fang et al., 2001). Furthermore, the SH3 domain of p85 was shown to bind the proline rich motifs of p85. In line with these findings, p85α and p85β seem to be able to form homodimers, while p55α and p50α, which are devoid of the SH3 domain, exist as monomers if expressed in Sf9 cells (Harpur et al., 1999).

Furthermore, the **proline-rich motifs** of p85 interact with the SH3 domain of Tyr kinases Src, Lyn and Fyn. As described below (see § 1.3.4.2), it is unclear whether interaction with and subsequent phosphorylation by Src family kinases mediates changes in the lipid kinase activity of PI3Ks.

An intriguing interaction partner of the regulatory subunit is tubulin. While the small regulatory subunits p55γ and p55α were shown to constitutively interact with α-, β- and γ-tubulin via their unique N-termini, the large regulatory subunit p85 constitutively interacts with α- and β-tubulin via its iSH2 domain, but binds in an inducible manner to γ-tubulin. Since the small regulatory subunit are evolutionary conserved, while the large regulatory subunits are a relatively new addition to the PI3K subunit pool, one can speculate that the large subunits originally devoid of the tubulin binding sites were under evolutionary pressure to generate tubulin interaction sequences. This anticipation would highlight the importance of the PI3K-tubulin interaction.

1.3.2.2.2 p110 interaction partners

Three main interaction partners of the catalytic subunit have been described. All class IA catalytic subunits contain a Ras-binding domain that shows binding affinity to GTP-bound Ras. Following Ras binding, the C2 domain and catalytic domain undergo molecular rearrangement that affects the conformation of the lipid substrate binding site (Walker et al., 1999). In line with this, interaction of p110 with Ras increases the lipid kinase activity of PI3K (Kodaki et al., 1994). Importantly, Ras binding was also shown to increase lipid kinase activity in previously pTyr-stimulated PI3K, suggesting that Ras- and concomitant pTyr-binding is necessary for full activation of PI3K (Jimenez et al., 2002). Furthermore, Ras was determined as a substrate for p110α protein kinase activity (Foukas and Shepherd, 2004). p110β also interacts with a GTPase called Rab5. The binding of p110β to Rab5 is dependent on sequences only existent in this catalytic subunit isoform. As for Ras-binding, this interaction is dependent on the activity state of the GTPase and increases PI3K activity (Christoforidis et al., 1999; Kurosu and Katada, 2001).

As described above (see § 1.2.1.1.1.2), p110β also uniquely binds Gβγ subunits of trimeric G proteins. This interaction increases its lipid kinase activity synergystically to the binding of pYxxM-motif containing proteins (Kurosu et al., 1997).

1.3.3 Protein kinase activity of PI3K

The protein kinase activity of class IA PI3K plays an important role in the negative regulation of its lipid kinase activity.

p110α and to a lesser extent p110β phosphorylate p85α on Ser608 leading to an 80% decrease in PI3K lipid kinase activity *in vitro* (Carpenter et al., 1993; Dhand et al., 1994; Foukas et al., 2004). Ser608, which is part of the iSH2 domain of p85α, was shown to be an important residue in the interaction with the catalytic subunit, since its mutation causes a decrease in p110 binding (Foukas et al., 2004). Dissociation of p85 from p110 provides a basis for regulation of PI3K lipid kinase activity by Ser608 phosphorylation. In addition to p85α, also p85β is phosphorylated by p110α *in vitro*, its phosphorylation sites remain to be discovered (reviewed in (Vanhaesebroeck and Waterfield, 1999)).

p110β and p110δ both autophosphorylate Ser residues in their C-termini (Ser1070 in p110β and Ser1039 in p110δ, respectively) (Czupalla et al., 2003; Czupalla et al., 2003; Vanhaesebroeck et al., 1999). As for Ser608 phosphorylation of p85α by p110α, Ser autophosphorylation of recombinant p110β and p110δ mediates the downregulation of PI3K lipid kinase activity. Further analysis revealed that p110β autophosphorylation is not enhanced by binding to pYxxM-containing peptides or Gβγ complexes. While p110β autophosphorylation has only been investigated *in vitro*, the role of p110δ autophosphorylation was addressed *in vivo*. CD28 stimulation of T cells increases phosphorylation of Ser1039 in p110δ, which leads to a rapid decrease in p110δ-associated lipid kinase activity (Vanhaesebroeck et al., 1999).

In addition to autophosphorylation and cross-phosphorylation of the regulatory subunit, evidence for the existence of exogenous class IA PI3K substrates is emerging (reviewed in (Foukas and Shepherd, 2004)).

1.3.4 Post-translational modifications of PI3K

Post-translational modifications modulate the activity, localisation and turnover of many eukaryotic enzymes. They are tightly regulated, and selectively control many aspects of cell growth, metabolism, division, motility and differentiation (Hunter, 1995; Posada and Cooper, 1992). Since protein phosphorylation is occurring in as many as a third of proteins in mammalian cells (Hubbard and Cohen, 1993), it is the most intensely studied post-translational modification. Other important protein modifications for cellular signalling are acetylation, methylation, acylation, glycosylation, and ubiquitylation due to their reversibility.

The regulatory and the catalytic subunit of class IA PI3Ks undergo reversible phosphorylation (summarised in Figure 1.6 and Figure 1.7). As discussed below, the biochemical properties and biological significance of these modifications are poorly understood. If possible, implications for the regulation of class IA PI3Ks are given.

1.3.4.1 Post-translational modifications of PI3K catalytic subunits

Phosphorylation of the catalytic subunit on Ser, Thr and Tyr residues has been reported (Figure 1.6). While *in vitro* phosphorylation of Ser and Thr is inhibited by treatment of immunocomplexes with WM and LY294002, Tyr phosphorylation is not (Geltz and Augustine, 1998). It was subsequently shown that p110β and p110δ autophosphorylate on Ser residues (see § 1.3.3). p110α is Ser/Thr phosphorylated by PKCα *in vitro* and this phosphorylation partially inhibits the *in vitro* lipid kinase activity of p110α (Sipeki et al., 2006). Phosphorylation of p110α by PKCα might therefore provide an alternative mechanism for PI3K activity regulation similar to autophosphorylation of p110β and p110δ.

A

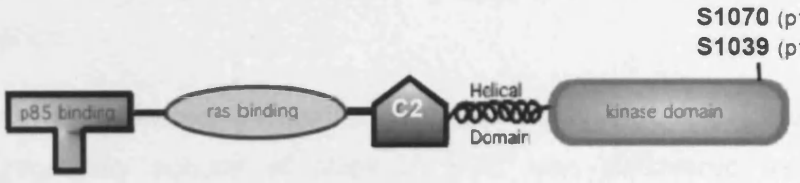

B

Protein	Residue	Kinase	Stimulation		Biological implications	Reference
p110α	Ser	PKCα		*in vitro*	Lipid kinase activity ↓	Sipeki et al., 2006
p110α	Tyr		PDGF R	*in vivo*	Dissociation from R	Roche et al., 1994
p110β	Ser1070	p110β		*in vitro*	Lipid kinase activity ↓	Czupalla et al., 2003
p110β	Tyr		PDGF R	*in vivo*	Dissociation from R	Roche et al., 1994
p110δ	Ser1039	p110δ	CD28 - T cells	*in vivo*	Lipid kinase activity ↓	Vanhaesebroeck et al., 1999
p110	Tyr	Lck	CD4 - T cells	*in vivo*		Mazerolles et al, 1998
p110	Tyr	Syk	BCR	*in vivo*		Craxton et al., 1999
p110	Tyr	Syk, Lyn	H_2O_2 - B cells	*in vivo*	Lipid kinase activity ↔	Qin et al., 2003

Figure 1.6: Summary of class IA PI3K catalytic subunit phosphorylation
(A) Catalytic subunit phosphorylation sites were identified at the C-terminus of p110β and p110δ. (B) Table of reported catalytic subunit phosphorylation events and their biological implications. ↓, decreased; ↔, unchanged.

Tyr phosphorylation of the catalytic subunit is attributed to different Tyr kinases depending on cell type. In T cells, CD4 stimulation enhances Tyr phosphorylation of p110 maximally at 20 min after stimulation due to association of a p110-Lck complex with CD4 (Mazerolles and Fischer, 1998). In B cells, Tyr phosphorylation of p110 was shown to follow cellular stimulation by BCR crosslinking within minutes and is Syk-, but not Btk- or Lyn-dependent (Craxton et al., 1999). In line with this, H_2O_2 treatment of B cells increases Tyr phosphorylation of p110. This phosphorylation is decreased in Lyn-, BCAP- and Syk KO cells, but is unchanged in Btk- and Cbl KO cells. The Tyr

phosphorylation of p110 in B cells does not impact on the intrinsic lipid kinase activity of p110 since *in vitro* PIP_3 generation is the same with p110 from WT, Lyn-, Syk- and Btk KO cells (Qin and Chock, 2003).

Furthermore, p110α was shown to become Tyr phosphorylated following PDGF receptor stimulation *in vivo*, with maximal p110 phosphorylation between 30 and 60 minutes of stimulation. Performing immunodepletion experiments, it was shown that p110 is released from the PDGF receptor in a Tyr phosphorylated form (Roche et al., 1994). Also p110β becomes phosphorylated on Tyr residues following association with activated PDGF receptor (Roche et al., 1998).

Tyr phosphorylation of the catalytic subunit is underexplored. While early studies did not differentiate between the different p110 isoforms, later ones were not able to identify specific Tyr phosphorylation residues or Tyr kinases involved in phosphorylation.

1.3.4.2 Post-translational modifications of PI3K regulatory subunits

The regulatory subunit of class IA PI3K was discovered as an 85 kDa phosphoprotein associated with polyoma middle T antigen and Src (Cohen et al., 1990). p85 phosphorylation of Ser, Thr and Tyr has been detected in several cell types following different stimuli (Figure 1.7).

Ser and Thr phosphorylation of p85 was reported in T cells. While p85α was shown to be Ser phosphorylated independent of TCR engagement, p85β becomes phosphorylated on Thr residue(s) following T cell stimulation (Reif et al., 1993). p85α was subsequently shown to be phosphorylated on Ser608 *in vivo* (Dhand et al., 1994), which leads to the downregulation of the p110 lipid kinase activity (§ 1.3.3). Phosphorylation of Ser608 was also observed in fibroblasts following PDGF stimulation (Foukas et al., 2004).

Also Tyr phosphorylation of the p85 subunit was observed in **T cells**. Following IL-2 stimulation, the Tyr kinase Fyn, but not Lck, was shown to phosphorylate the regulatory subunit and interaction with Fyn induces PI3K activity in unstimulated and even more so in stimulated T cells (Karnitz et al., 1994). Phosphorylation of p85 on Tyr residue(s) is also increased in lymphoblast cells containing a Bcr-Abl fusion protein (Gotoh et al., 1994; Varticovski et al., 1991). In line with this, irradiation of T cells induces Tyr phosphorylation of p85 by Abl which leads to a decrease in PI3K activity (Yuan et al., 1997). Residue Tyr688 in the N-terminal SH2 domain was identified as a p85α phosphorylation site following Bcr-Abl or constitutively active Lck overexpression in T cells. In contrast to previous results, the enzymatic activity of PI3K was unchanged upon Tyr phosphorylation by Abl. However, the interaction of p85α with binding partners was affected (von Willebrand et al., 1998). SHP1, an SH2 domain containing

Tyr phosphatase expressed in cells of hematopoietic origin, was shown to decrease the Lck induced p85α Tyr phosphorylation (Cuevas et al., 1999). The same group subsequently showed that Cos7 cells transfected with a p85-Tyr688Ala construct have decreased Akt phosphorylation compared to WT cells while Cos7 cells transfected with a p85-Tyr688Asp construct show increased phosphorylation of Akt, suggesting that Tyr688 phosphorylation has an impact on the lipid kinase activity of PI3K (Cuevas et al., 2001). It therefore appears that the Tyr kinases Fyn, Lck and Abl do not phosphorylate the same (or at least not the same combination of) p85 Tyr residue(s) in T cells leading to differences in the intrinsic lipid kinase activity of PI3K. It is also possible that rather than the residue involved, the kinetics of Tyr phosphorylation are crucial for the PI3K lipid kinase activity.

Even though signalling cascades in **B cells** have been studied in depth, Tyr phosphorylation of class IA PI3K regulatory subunit has hardly been described. One report indicated that crosslinking of the BCR leads to Tyr phosphorylation of p85, however, this phosphorylation peaked at 20 min of stimulation (Beckwith et al., 1996). It is likely that Tyr phosphorylation of p85 in B cells occurs only at a later stage of stimulation, in contrast to what is observed in T cells.

Tyr phosphorylation of p85 has also been demonstrated in non-leukocyte cells. Following **PDGF receptor** engagement in NIH-3T3 cells, Tyr phosphorylation of the regulatory subunit was revealed (Kaplan et al., 1987). It was subsequently shown that Tyr phosphorylation of p85 inhibited the interaction of the N-terminal SH2 domain to the receptor while binding of the C-terminal SH2 domain was intact (Kavanaugh et al., 1992). When recombinant p85α was subjected to *in vitro* protein kinase assays with recombinant PDGF receptor, Tyr508 was identified as a phosphorylation site. Tryptic phosphopeptide mapping demonstrated that p85α is also phosphorylated on Tyr508 *in vivo* (Kavanaugh et al., 1994). The homologous Tyr residue in p85β (Tyr458) was recently shown to become phosphorylated following pV stimulation of cells (Rush et al., 2005).

Tyr368, Tyr580 and Tyr607 were identified as major p85 Tyr phosphorylation sites following overexpression of p85α and **insulin receptor** (IR) in Cos7 cells (Hayashi et al., 1993). It was previously shown that insulin stimulates the phosphorylation of the regulatory subunit *in vitro* and *in vivo* and that this modification does not change the lipid kinase activity of PI3K (Hayashi et al., 1992; Hayashi et al., 1991; Hayashi et al., 1993). The homologous residue to Tyr607 in p55γ is Tyr341. Tyr341 was shown to be phosphorylated by the insulin receptor in Sf9 and CHO-IR cells and this modification appears not to change the intrinsic lipid kinase activity of PI3K (Pons et al., 1995).

A

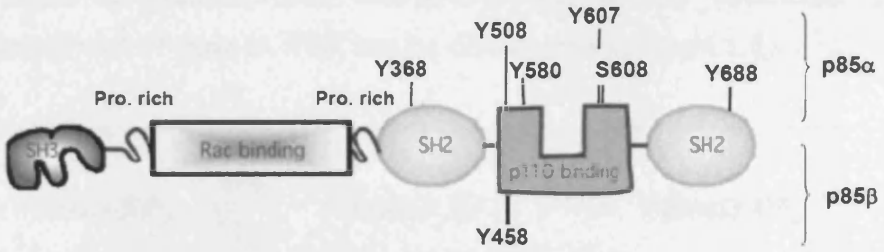

B

Protein	Residue	Kinase/ Phosphatase	Stimulation		Biological implication	References
p85α	Tyr368, 580, 607		IR	*in vivo*	Lipid kinase activity ↔	Hayashi et al., 1993
p85α	Tyr508		PDGF R	*in vivo*	Dissociation from R	Kavanaugh et al., 1994
p85α	Ser608	p110α, p110β	IR, PDGF R	*in vivo*	Lipid kinase activity ↓	Dhand et al., 1994
p85α	Tyr688	Abl Lck/SHP1		*in vivo*	Lipid kinase activity ↔ (dissocation from Zap70/TCR) Lipid kinase activity ↓	Von Willebrand et al. 1998; Cuevas et al., 1999; Cuevas et al., 2001
p85β	Y458		pV	*in vivo*		Rush et al., 2005
p85β	Thr		T cells	*in vivo*		Reif et al., 1993
p85	Tyr	Fyn	IL-2 - T cells	*in vivo*	Lipid kinase activity ↑	Karnitz et al., 1994
p85	Tyr	Abl	Irradiation - T cells	*in vivo*	Lipid kinase activity ↓	Yuan et al., 1997
p85	Tyr		BCR	*in vivo*		Beckwith et al. 1996
p85	Tyr nitration		Peroxynitrite, NONOate	*in vivo*	p85 dissociation from p110	Hellberg et al., 1998; E-Remessy et al., 2005

Figure 1.7: Summary of class IA PI3K regulatory subunit phosphorylation

(A) p85α and p85β phosphorylation sites were identified in different cell types following various stimuli. (B) Table of reported phosphorylation on regulatory subunit and their implications. ↑ increased; ↓, decreased; ↔, unchanged

In addition to protein phosphorylation, **Tyr nitration** of the regulatory subunit was reported. p85 was shown to be Tyr nitrated in macrophages following peroxynitrite and NONOate treatment, two nitric oxide donors. Tyr nitration of p85 appears to abrogate its interaction with p110 (Hellberg et al., 1998). In addition, high glucose and peroxynitrite treatment of endothelial cells also induces Tyr nitration of p85, which correlates with p85 dissociation from p110 and decreased phosphorylation of Akt. Dissociation of p85 from p110 is blocked by a peroxynitrite decomposition catalyst and by a Tyr nitration inhibitor (el-Remessy et al., 2005).

1.4 Downstream effectors of Class IA PI3K

Upon activation of class IA PI3K, the intracellular levels of PIP_3 rapidly increase leading to the recruitment of PH domain containing proteins to the plasma membrane. PH domains are modular segments of about 100 amino acids found in many signalling molecules (Lemmon and Ferguson, 2000; Rameh et al., 1997), and the ability of PH domains to discriminate PIP_3 from other PIs is a central basis for specificity in class IA

PI3K signalling. Recruitment of PH domain containing proteins to the plasma membrane leads to protein-protein interactions and protein activation. Several pathways downstream of class IA PI3K can be distinguished (Figure 1.8).

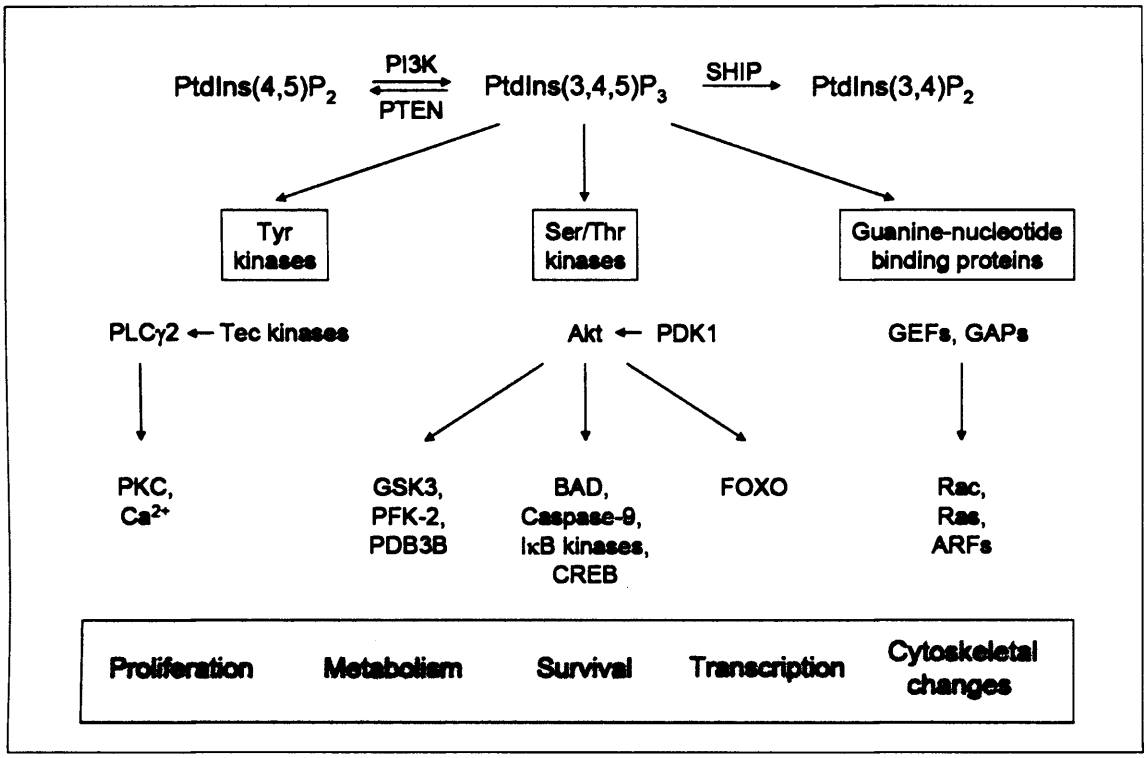

Figure 1.8: Class I PI3K signalling pathways

Generation of PIP_3 at the plasma membrane by PI3Ks leads to the accumulation and activation of Tyr kinases, Ser/Thr kinases and guanine-nucleotide binding proteins amongst others. The signalling pathways originating from these molecules are described in detail below. The phosphatases PTEN and SHIP use PIP_3 as substrates and are therefore involved in the feedback control of PI3K signalling (more detail in § 1.5).

1.4.1 Ser/Thr kinases

A key Ser/Thr kinase containing a PIP_3 binding domain is protein kinase B (PKB, also known as Akt), a protein with fundamental roles in a multitude of cellular processes ranging from cell survival and proliferation to metabolism (Brazil and Hemmings, 2001; Burgering and Coffer, 1995; Datta et al., 1996; Vanhaesebroeck and Alessi, 2000).

Following recruitment to the plasma membrane by means of its PH domain, Akt is phosphorylated at Thr308 and Ser473 (Alessi and Cohen, 1998; Bellacosa et al., 1998). Full enzymatic activation of Akt is only achieved when both residues are phosphorylated. The upstream kinase that targets Thr308 is PDK1, itself a PH domain containing protein (Alessi et al., 1997; Stephens et al., 1998). The protein kinase catalysing the phosphorylation of Ser473 is termed PDK2; its identity is controversial.

In addition to Ser/Thr phosphorylation of Akt, also Tyr phosphorylation has been shown to influence the enzymatic activity of this protein (Conus et al., 2002).

The number of physiological Akt substrates is expanding rapidly (Brazil and Hemmings, 2001; Vanhaesebroeck and Alessi, 2000). The minimal consensus peptide sequence for Akt substrates was identified as Arg-Xaa-Arg-Xaa-Xaa-[Ser/Thr]-Hyd (where Xaa is any amino acid and Hyd is a bulky hydrophobic amino acid) (Andjelkovic et al., 1997; Meier et al., 1997). A study of the Swiss-Prot database in 2001 using Scansite identified this sequence 551 times in 446 protein entries (Nicholson and Anderson, 2002) underlining the potential abundance of Akt substrates. We summarised the more established routes of Akt signalling below.

Akt has been shown to regulate cell survival by phosphorylating a variety of proteins involved in the anti-apoptotic process. One target of Akt is BAD, a protein that binds Bcl-2 and Bcl-X_L thus preventing their anti-apoptotic function (Downward, 1999). Another Akt target involved in the anti-apoptotic process is Caspase-9. Direct interaction, phosphorylation and thus inactivation of Caspase-9 by Akt inhibits the initiation step of apoptosis (Cardone et al., 1998). Furthermore, Akt has been implicated in the regulation of the transcription factor NF-κB by activating I-κB kinases (IKKs). Upon phosphorylation of the inhibitor of NF-κB by IKKs, NF-κB is released and moves to the nucleus where it induces the transcription of anti-apoptotic genes. Similarily, Akt phosphorylates and induces translocation to the nucleus of the transcription factor CREB that promotes transcription of anti-apoptotic/cell survival genes (Du and Montminy, 1998).

Another process in which Akt is involved is the regulation of metabolism. Akt has been shown to phosphorylate and inactivate glycogen synthase kinase 3 (GSK3). This results in the phosphorylation and consequent activation of metabolic and gene-regulatory proteins. Furthermore, 6-phosphofructo-2-kinase (PFK-2), one of the key players in glycolysis, is phosphorylated by Akt *in vitro* (Deprez et al., 1997) and activated as a phosphatase. Consistently, insulin-stimulated activation of PFK-2 is inhibited by WM (Lefebvre et al., 1996). PDB3B, an enzyme catalysing the hydrolysis of cAMP, was further shown to be an Akt target (Wijkander et al., 1998).

The Forkhead (FH) family of transcription factors regulates transcription of genes controlling cell cycle, cell death, and metabolism. FH transcription factors are inactivated by Akt phosphorylation due to prevention of nuclear entry (Burgering and Kops, 2002). This leads to a decrease in transcription of $p27^{Kip}$, a protein involved in the inhibition of cell cycle progression (Dijkers et al., 2000) and of the Fas ligand, which is an inducer of apoptosis (Brunet et al., 1999).

The PH domain containing protein PDK1 is important in the regulation of not only Akt, but also many other AGC superfamily kinases (Williams et al., 2000). This enzyme

catalyses the phosphorylation of the residue equivalent to Thr308 in PKC isoforms (Chou et al., 1998; Dutil et al., 1998), in $p70^{S6K}$ (Alessi and Cohen, 1998; Pullen et al., 1998), in SGK (Kobayashi et al., 1999; Park et al., 1999) and in PKA (Cheng et al., 1998; Toker and Newton, 2000; Vanhaesebroeck and Alessi, 2000). PDK1, itself member of the AGC family of kinases, requires phosphorylation for activation and appears to autophosphorylate (Casamayor et al., 1999). However, PDK1 is not regulated by extracellular signals. It seems more likely that its activation is modulated by interaction with its substrates (Biondi et al., 2001).

1.4.2 Tyrosine kinases

Tec kinases are non-receptor tyrosine kinases that contain N-terminal PH domains. This interaction controls their association with the plasma membrane and thus with Src kinases that catalyse the phosphorylation of Tec family members (Shan et al., 2000). Upon phosphorylation, these proteins are activated (Rawlings et al., 1996; Schaeffer and Schwartzberg, 2000). The importance of the PH domain is shown in one member of the Tec family called Bruton's tyrosine kinase (Btk) which is essential in normal B cell development and function (more details in §1.7.1): mutations in the Btk PH domain cause X-linked agammagloblinaemia in humans and a similar X-linked immunodefiency (Xid) in mice (Li et al., 1995). The important function of Btk for B cell development stems from the essential role of this Tyr kinase in the control of PLCγ (Scharenberg et al., 1998) whose activation is a crucial component for the regulation of intracellular Ca^{2+} levels. PLCγ, itself a PH domain containing protein, hydrolyses PtdIns(4,5)P_2 to produce IP3 and diacylglycerol, which in turn mediate Ca^{2+} release from intracellular stores and activation of PKC (Rhee and Bae, 1997).

1.4.3 Guanine-nucleotide binding proteins

Important targets of the products of PI3Ks are the Rho family of GTPases including Rho, Rac and Cdc42. These proteins coordinate the dynamic organisation of the actin cytoskeleton and the assembly of associated integrin structures. Activation of Rac and Rho is regulated by guanine-nucleotide exchange factors (GEFs) and GTPase-activating proteins (GAPs) both containing PH domains (Cerione and Zheng, 1996). One well-studied Rac-GEF is Vav-1 whose catalytic activity depends on activation by Src kinases. *In vitro* models have suggested that binding of Vav-1 to PIP_3 potentiates Tyr kinase mediated Vav activation (Han et al., 1998). Furthermore, PI3K inhibitors block Rac activation by Vav-1.

There is also evidence of Rac regulation by Arfs (D'Souza-Schorey et al., 1997; Zhang and Xiong, 1999). Arfs are a family of small GTPases involved in the regulation of intracellular membrane trafficking. Arfs are regulated by Arf-GEFs, proteins

containing a PH domain. There is a multitude of data showing that PI3K signalling is involved in Arf function via Arf-GEFs (Venkateswarlu et al., 1999) and Arf-GAPs (Kam et al., 2000; Krugmann et al., 2004).

Furthermore, activated small GTPases can stimulate PI3K activity, thus forming a positive feedback loop (Tolias et al., 1995; Zheng et al., 1994), reviewed in(Welch et al., 2003).

1.5 Feedback control of PI3K signalling

The effects of 3'-phosphorylated PIs generated by PI3Ks are antagonised and/or diversified by PI phosphatases (Maehama et al., 2001; Vanhaesebroeck et al., 2001). Members of this group of enzymes can be divided into 3 families: 3-PI phosphatases, 4-PI phosphatases and 5-PI phosphatases. The two major routes for PIP_3 degradation are mediated by PTEN and SHIPs.

1.5.1.1 PTEN

PTEN (Phosphatase and tensin homologue deleted on chromosome 10) is member of the 3-PI phosphatases family and converts PIP_3 to $PtdIns(4,5)P_2$. PTEN was originally identified as a tumour suppressor and tyrosine phosphatase inactivated by loss of heterozygosity at chromosome 10 (Li et al., 1997; Myers and Tonks, 1997; Steck et al., 1997), but was later found to contain PI phosphatase activity (Maehama and Dixon, 1998). Several mutation and deletions in the PTEN gene are found in various human cancers (Cantley and Neel, 1999) and it was shown to be the lipid phosphatase activity that endows PTEN its tumour suppressor specificity by negative regulation of the PI3K pathway. Consistently, cells lacking PTEN have increased levels of PIP_3 that correlates with activation of Akt (Stambolic et al., 1998).

While PTEN KO mice are embryonic lethal, information gained from PTEN KO heterozygous mice (Di Cristofano et al., 1998; Podsypanina et al., 1999; Suzuki et al., 1998) and mice containing tissue-specific deletions in the PTEN gene (Anzelon et al., 2003; Li et al., 2002; Suzuki et al., 2001), confirmed the potency of PTEN tumour suppressor activity. Cells analysed in the various PTEN KO mice showed hyperproliferation, resistance to apoptosis, lower threshold to activation, and altered migration properties.

Little is known about the regulation of PTEN activity. The crystal structure of PTEN revealed that the protein consists of a phosphatase and C2 domain, which is involved in membrane recruitment of PTEN (Lee et al., 1999). A putative PDZ-binding motif at the C-terminus of the protein appears to mediate interaction with PDZ domain containing proteins. Furthermore, PTEN activity seems to be regulated by protein phosphorylation (reviewed in (Leslie and Downes, 2004)).

1.5.1.2 SHIP

SHIP is an SH2 domain containing member of the 5-PI phosphatase family and dephosphorylates PIP_3 to $PtdIns(3,4)P_2$. Two isoforms of SHIP have been identified in eukaryotes called SHIP1 and SHIP2. These enzymes contain similar substrate specifitiy but differ in their tissue distribution. SHIP1 is mainly found in cells of hematopoietic origin, where it takes part in cytokine signalling (Lioubin et al., 1996). In contrast, SHIP2 is broadly expressed, and participates in growth factor-stimulated signalling. In line with this, SHIP2 KO mice were originally reported to display severe hypoglycaemia and mortality (Clement et al., 2001; Habib et al., 1998; Rohrschneider et al., 2000). More recent data, however, revealed that SHIP2 KO mice are viable, have normal glucose and insulin levels, but display high resistance to weight gain when placed on a high-fat diet (Sleeman et al., 2005). The different KO mice were generated using different gene-targeting strategies likely explaining the different phenotypes.

SHIP proteins are controlled by inhibitory receptors such as FcγRIIb (Liu et al., 1998; Ono et al., 1997) by means of their SH2 domain. The SH2 domain of SHIP binds ITIM-motifs (I/V/L/S-x-Y-x-x-L/V) located in the cytosolic domain of inhibitory receptors. Due to its membrane localisation upon receptor binding, SHIP can dephosphorylate PIP_3 (see also § 1.7.1).

1.6 Experimental inhibition of PI3K function

The analysis of class IA PI3Ks has been challenging for various reasons: stable overexpression of class IA regulatory subunits has a dominant-negative effect on the recruitment of endogenous protein to pYxxM-motif containing proteins. Stable overexpression of the catalytic subunit has not been reported probably due to the instability of monomeric p110. Thus, a variety of class IA PI3K gene-targeting approaches have been employed. However, deletion of either p110 or p85 subunits leads to compensationary expression of non-targeted class IA PI3K subunits hampering analysis (reviewed in (Vanhaesebroeck et al., 2005)).

Therefore, small molecule pharmalogical inhibitors of PI3Ks have been an indispensable tool for the elucidation of the physiological processes in which PI3Ks are involved. IC_{50} values of different drugs against PI3Ks and related protein kinases are summarised in Table 1.3.

1.6.1.1 Broad-spectrum inhibitors

The two inhibitors that have been primarily used to study PI3K function are low molecular weight, cell permeable compounds called Wortmannin and LY294002 (Stein and Waterfield, 2000).

Wortmannin (WM) is a fungal metabolite that irreversibly binds PI3K, resulting in covalent modification of the Lys residue in the catalytic domain of PI3K involved in ATP binding. This inhibitor is a very potent drug with IC_{50} values of 5 nM *in vitro* (Powis et al., 1994). All Class I, II and III PI3K members exert the same sensitivity to WM with the exception of PI3K-C2α, which is at least 10-fold less sensitive (Domin et al., 1997; Virbasius et al., 1996). However, also enzymes of class IV PI3K related kinases such as mTor (Brunn et al., 1996; Withers et al., 1997), DNA-PK (Hartley et al., 1995; Sarkaria et al., 1998), and ATM (Banin et al., 1998) are inhibited by WM although at concentration 10-100-fold higher than the dose required for class I, II and III PI3K. Although potent, WM has a short half-life in aqueous solutions (Woscholski et al., 1994).

LY294002 is a flavonoid-based compound and a competitive inhibitor of ATP binding in the catalytic domain of PI3K (Vlahos et al., 1994). The *in vitro* sensitivity to LY294002 is similar for all class I, II, and III PI3Ks, apart from PI3K-C2α (Domin et al., 1997). However, LY294002 also inhibits mTOR, DNA-PK and protein kinase CK2 with similar potency as PI3K (Brunn et al., 1996; Izzard et al., 1999).

Table 1.3: IC_{50} values of PI3K inhibitors

Class IA PI3Ks can be inhibited by broad-range PI3K inhibitors WM or LY294002 that also target distantly related proteins, or by isoform-specific inhibitors. U: unknown.

	IC_{50} (nM)						
	p110α	p110β	p110δ	p110γ	PI3K-C2	DNA-PK	References
Wortmannin	5	5	5	5	400	250	Powis et al., 1994; Virbasius et al.,1996; Sarkaria et al., 1998
LY294002	1'000	1'000	1'000	1'000	20'000	6'000	Vlahos et al., 1994; Domin et al., 1997; Brunn et al., 1996
PI-103	**1'000**	U	U	U	U	U	
TGX-221	10'000	**5**	100	1'000	>10'000	U	Jackson et al., 2005
IC87114	100'000	75'000	**500**	29'000	>10'000	>100'000	Sadhu et al., 2003
AS604850	450	>2'000	>2'000	**250**	U	U	Camps et al., 2005

1.6.1.2 Isoform-selective PI3K inhibitors

Comparison of the crystal structure of p110γ with bioinformatic data of class IA PI3K revealed that the interior of the ATP binding pocket is highly conserved among class I PI3K, while the residues which line the entrance to the ATP binding pocket are

divergent in their size and charge (Knight et al., 2004). These findings indicate a basis for isoform-specific ihhibitors interacting with the ATP-binding site of PI3K.

PI-103 is a p110α selevtive inhibitor with an IC_{50} for p110α of 1 μM.

TGX-221 is a p110β-specific inhibitor with similar chemical structure to LY294002. This inhibitor is 20-fold more selective for p110β than p110δ and shows more than 1000-fold selectivity for p110β over p110α, p110γ and over a broad range of kinases tested. TGX-221 has minimal inhibitory effect on PI3K-C2α and PI4K. Since the concentration of ATP influenced the IC_{50} value of TGX-221 against p110β, this inhibitor is likely acting as a competitive ATP antagonist (Jackson et al., 2005).

IC87114 is a p110δ-selective inhibitor related to LY294002. IC_{50} values for p110α, p110β and p110γ were more than 200-, 150- and 50-fold higher than for p110δ. No significant inhbition of a variety of protein kinases was detected (Sadhu et al., 2003).

AS604850 is a p110γ-selective inhibitor which is 10-fold more selective for p110γ than for p110β and p110δ. The IC_{50} for p110α is 50 times higher than p110γ. Furthermore, AS604850 is an ATP-competitive drug (Camps et al., 2005).

In summary, isoform-selective inhibitors are very helpful tools to analyse the non-redundant functions of class I PI3K. However, 2 important aspects of PI3K inhibitors need to be considered. First, IC_{50} values are usually generated with recombinant protein performing *in vitro* activity assays. This may or may not reflect the inhibitory effect of a drug *in vivo*. Second, even though a panel of known proteins are normally scanned for their inhibition by a certain drug in order to determine its selectivity, it is likely that the chosen inhibitor decreases the activity of either uninvestigated or unknown proteins.

1.7 B lymphocytes and class IA PI3Ks

Most of the experiments discussed in this thesis were performed using B lymphocytes. We will therefore give an overview of B cell antigen receptor (BCR) signalling and the role of class IA PI3K downstream of the BCR.

1.7.1 B cell antigen receptor signalling

In immature and mature B cells, the BCR is composed of membrane immunoglobulin (Ig) associated with disulfide-linked heterodimers of immunoreceptor tyrosine based activation motif (ITAM)-containing CD79α and CD79β (also called Igα and Igβ, respectively) (Cambier et al., 1994). BCR crosslinking by antigen or anti-receptor Ab mediates clustering of associated Src family kinases which induce phosphorylation of ITAM-motifs (Yamanashi et al., 1991). An important Src kinase in

this process is Lyn. Lyn is constitutively associated with the BCR via acetylation, which anchors the kinase to the membrane and via a unique N-terminal region that interacts with the non-phosphorylated BCR in unstimulated cells. Phosphorylation of ITAM-motifs by Lyn following BCR engagement leads to the recruitment of additional Src family kinases as well as the Tyr kinase Syk, which become Tyr phosphorylated and activated upon recruitment (Clark et al., 1992; Kurosaki et al., 1995).

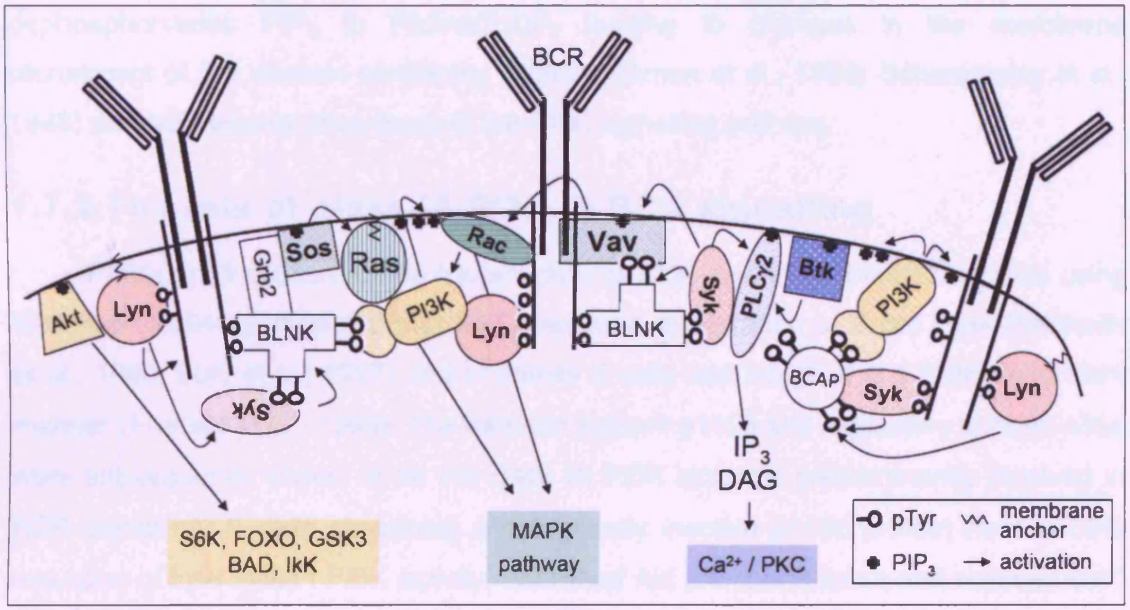

Figure 1.9: BCR signalling cascade

Following BCR crosslinking, tyrosine kinases (in red) enable recruitment of PI3K (in yellow) and adaptor proteins (in white) to the plasma membrane. PI3K activity facilitates translocation of PH domain containing proteins, such as Akt, Btk, PLCγ and Vav. Adaptor molecules function as nucleators of different signalling pathways through binding and activation of mainly SH2 domain containing proteins. Binding of Sos and Vav to adaptors induces Ras and Rac (in green) activity. BCR engagement ultimately leads to activation of PI3K and MAPK pathways and mobilisation of intracellular Ca^{2+} and activation of PKC (in blue).

In parallel, Tyr phosphorylation of B cell specific adaptor proteins such as B cell linker protein (BLNK/SLP-76) and B cell adaptor for PI3K (BCAP) by Lyn and Syk leads to membrane recruitment and subsequent generation of PIP_3 (Li et al., 1999); (Buhl and Cambier, 1999). Btk and PLCγ2 translocate to the plasma membrane by means of their PH domains but also through interaction of their SH2 domains with BLNK (Fu et al., 1998). Following membrane recruitment, Btk is phosphorylated and activated by Src family kinases (Li et al., 1997; Nisitani et al., 1999). Activated Btk and Syk phosphorylate and activate PLCγ2 which mediates the hydrolysis of phosphoinositides, thereby generating inositol-1,4,5-triphosphate (IP_3) and diacylglycerol (DAG) (Fluckiger et al., 1998). This leads to Ca^{2+} mobilisation from intracellular stores and activation of PKC. Furthermore, the guanine-nucleotide exchange factor Vav translocates to the

plama membrane due to its PH and SH2 domains. In conjunction with Sos, which is recruited to the BCR complex via BLNK, activated Vav induces the MAPK pathway.

BCR-mediated signals are inhibited by co-engagement of BCR with the inhibitory receptor FcγRIIB (Ravetch, 1997). The FcγRIIB-mediated inhibition is dependent on the immunotyrosine based inhibitory motifs (ITIM) in the cytosolic domain of FcγRIIB (Amigorena et al., 1992; Muta et al., 1994) and its interaction with SH2 domain containing protein SHIP (Ono et al., 1996). Following membrane recruitment, SHIP dephosphorylates PIP_3 to $PtdIns(3,4)P_2$ leading to changes in the membrane recruitment of PH domain containing proteins (Aman et al., 1998; Scharenberg et al., 1998) and subsequent shut-down of the PI3K signalling pathway.

1.7.2 The role of class IA PI3K in BCR signalling

PI3Ks are important in the transduction of BCR signalling. Inhibitor studies using WM and LY294002 revealed that BRC-mediated proliferation of B cell lines (Beckwith et al., 1996; Buhl et al., 1997) and of primay B cells was inhibited in a PI3K-dependent manner (Fruman et al., 1999). The catalytic subunit p110δ and regulatory subunit p85α were subsequently shown to be the class IA PI3K isoforms predominantly involved in BCR signalling. B cells containing a catalytically inactive p110δ protein have a 60% reduction of total class I PI3K activity, abolished Akt phosphorylation and reduced Ca^{2+} mobilisation leading to completely abrogated *in vitro* proliferation in response to BCR engagement (Bilancio et al., 2006). While the B cell phenotype observed in cells depleted of p85α was similar to the one of p110δ KI mice, no obvious B cell phenotype was detected in mice lacking p85β or p55γ (Fruman et al., 1999; Suzuki et al., 1999). B cells were also not affected by deletion of p110γ (p110γ KO) which instead leads to altered signalling and function of T cells, macrophages, neutrophils and mast cells (Hirsch et al., 2000; Laffargue et al., 2002; Rodriguez-Borlado et al., 2003; Sasaki et al., 2000).

The mechanisms by which BCR crosslinking leads to activation of PI3Ks and its downstream effectors are complex. Class IA PI3Ks are recruited to the plasma membrane following BCR engagement by two mechanisms (Figure 1.10).

If BCR-CD19 crosslinking is induced (left panel of Figure 1.10), the regulatory subunit interacts with phosphorylated Tyr residues in the cytosolic domain of CD19 leading to Akt activation (Buhl and Cambier, 1999; Tuveson et al., 1993). PI3K activation seems to be the primary signalling function of CD19. A CD19 transgene with mutations in the Tyr residues that interact with PI3K is unable to restore CD19 function when introduced into CD19-deficient mice (Wang et al., 2002). Co-ligation of membrane Ig with CD19 was shown to require Vav function for PI3K activation and

subsequent Ca^{2+} mobilisation (Vigorito et al., 2004). It is not clear how Vav proteins, which possess a PH domain and were traditionally considered to act downstream of PI3Ks, influence PI3K activity. One possibility is through activation of Rac proteins which were shown to bind and activate PI3Ks (Bokoch et al., 1996; Tolias et al., 1995).

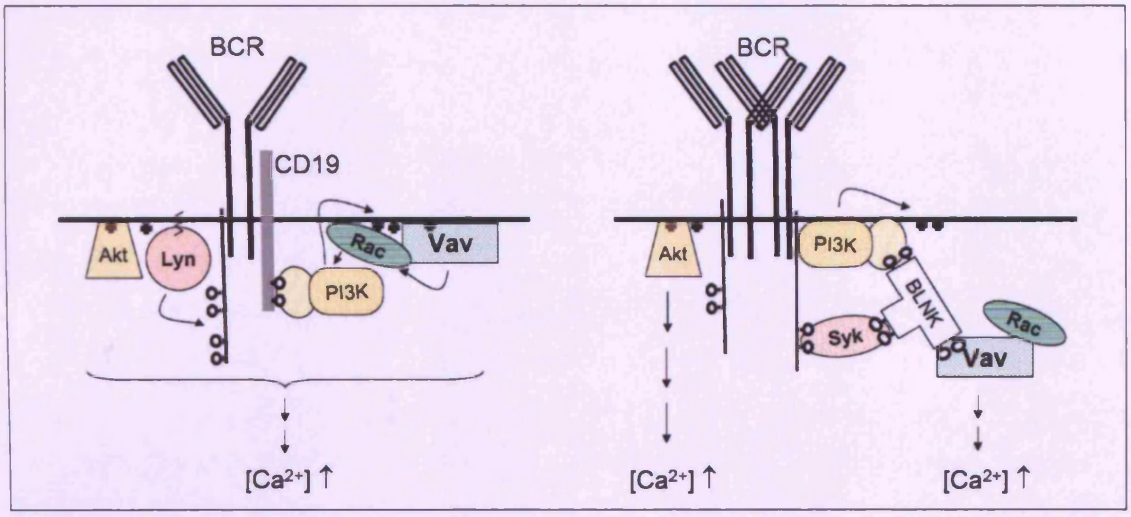

Figure 1.10: PI3K signalling downstream of BCR
Two separate mechanisms for Ca^{2+} mobilisation downstream of the BCR have been suggested: BCR crosslinking to CD19 leads to Vav-dependent PI3K activation, whereas BCR only crosslinking induces Ca^{2+} mobilisation via 2 independent pathways.

In contrast, PI3K activation by BCR only crosslinking (right panel of Figure 1.10) is Vav-independent. However, Ca^{2+} mobilisation after BCR engagement is Vav- and PI3K-dependent, indicating two separate pathways leading to Ca^{2+} flux after BCR only engagement. These findings also explain the incomplete reduction in Ca^{2+} flux by inhibition of p110δ after BCR stimulation (Bilancio et al., 2006). PI3K activation by BCR crosslinking is believed to occur via the recruitment of adaptor/scaffolding molecules such as BLNK, BCAP, Cbl and Gab, which have all been shown to interact with class IA PI3K regulatory subunit through its SH2 domain. The key role of adaptor molecules in BCR signalling was shown in mice lacking BLNK, which exhibit similar defects in B cell function as observed in p85α, p110δ or CD19 KO mice (Jumaa et al., 1999; Pappu et al., 1999).

The Tyr kinase Btk has been implicated as a major down-stream effector of PI3K signalling in B cells. In line with this, membrane recruitment of Btk is blocked by PI3K inhibitors (Varnai et al., 1999). Btk may also stimulate PI3K activity and therefore act as an upstream effector. In Btk-deficient DT40 cells, Akt phosphorylation following BCR engagement is reduced compared to WT cells (Craxton et al., 1999).

Generation of DAG and activation of PKC have been suggested to be the crucial components for B cell proliferation following BCR signalling, since proliferation could be

restored in Btk and p85α deficient cells by low levels of phorbol ester, a DAG analog (Deane and Fruman, 2004; Forssell et al., 1999). However, since mice lacking both p85α and Btk have more severe phenotypes than single KOs, it is likely that PI3K triggers important signals independent of Btk (Suzuki et al., 2003) (see § 1.4).

AIM OF THIS STUDY

While the biological activities of class IA PI3Ks have been investigated in great detail, the biochemical mechanism of their regulation is underexplored (Chapter 1). Mechanisms that have been implied in the modulation of PI3K lipid kinase activity include interaction with binding partners (such as Tyr kinases, Ras and Gβγ subunits of trimeric G proteins), phosphorylation of the PI3K subunits on Ser residues, and the molar ratios of p85 to p110.

The aim of this research project was to explore the biochemical regulation of endogenous (i.e. not overexpressed) class IA PI3K following physiological stimulation. In particular, we strived to

1) identify post-translational modifications in the class IA PI3Ks and investigate their biological role. Our main focus was on the p110δ isoform of PI3K, which is predominantly expressed in cells of hematopoietic origin. Therefore, the WEHI-231 B cell model system (Chapter 2) was used. As described in Chapter 4 and Chapter 5, post-translational modifications in p85 and p110 were assessed in unstimulated *versus* stimulated immature B cells by separation of class IA PI3Ks using 2D-gel electrophoresis and by mass spectrometry (MS). In order to analyse a protein of interest and its modifications by MS, pure and ample protein is a prerequisite. We therefore developed a novel class IA PI3K purification tool based on the interaction of p85 SH2 domains with Tyr phosphorylated residues in YxxM-motifs (Chapter 3). The biological relevance of the observed modifications was explored by comparison of PI3K lipid kinase activities, subcellular localisation and protein-protein binding partners in stimulated *versus* unstimulated conditions

2) analyse the molar equilibrium between regulatory and catalytic subunits (Chapter 6). Over the last couple of years, a vast literature on the existence of free p85 has appeared, mainly in an attempt to explain the increase in PI3K signalling upon insulin stimulation observed in mice in which class IA regulatory subunits have been deleted. In the proposed model, free p85 in WT cells competes with heterodimeric p85-p110 for docking sites on Tyr phosphorylated IRS molecules. Thus, monomeric p85 was put forward as a negative regulator in the PI3K signalling pathway. In order to address the relevance of these findings, we compared the p85 to p110 molar ratio in fibroblasts to those in B cells, in which no p85 excess has been reported. These investigations were employed by affinity and ion exchange chromatography and absolute quantitation (AQUA) MS.

2 MATERIALS & METHODS

2.1 Buffers and Solutions

Company names and catalogue numbers are provided between brackets.

ACK lysis buffer	0.15 M NH_4Cl, 1 mM $KHCO_3$, 0.1 mM Na_2EDTA, pH 7.3
mouse anti-chicken IgM	Mouse anti-chicken IgM, clone M4 (CAMBRIDGE BIOSCIENCES, 8300-01)
goat anti-mouse IgM	AffiniPure F(ab')2 Fragment Goat Anti-Mouse IgM, mu Chain Specific (JACKSON IMMUNORESEARCH LABORATORIES, 115-006-075)
4x SEP buffer	1.5 M Tris-HCl pH 8.8, 0.4% w/v SDS, made up to 1 l with ddH_20
4x SPAC buffer	0.5 M Tris-HCl pH 6.8, 0.4% w/v SDS, made up to 1 l with ddH_20
5x SDS sample buffer	156.25 mM Tris-HCl pH 6.8, 5% w/v SDS, 25% v/v glycerol, 0.0025% w/v bromophenol blue in 10 ml ddH_20. Add 250 mM DTT just before use.
Protein Assay Dye Reagent Concentrate	Dilute according to manufacture's protocol (BIORAD, 500-0006)
Home-made ECL	Solution A: 20 mM Tris-HCl pH 8.5, 0.0192% H_2O_2 Solution B: 20 mM Tris-HCl pH 8.6, 13.2 mg cumaric acid (SIGMA, C9008), 0.868 mg luminol (3-Aminophtalhydrazide, SIGMA, A8511)
Hypotonic buffer	10 mM Tris-HCl pH 7.4, 42 mM KCl, 5 mM $MgCl_2$
Inhibitors (final conc) 50 mM NaF 1 mM $NaVO_4$ 0.05 TIU/mg aprotinin 10 μM leupeptin 0.7 mM pepstatin A 27 μM TLCK 1 mM PMSF 5 μM fenvalerate 5 μM bpVphen 1 μM okadaic acid	 Phosphatase inhibitor (BDH, 102464T) Tyrosine phosphatase inhibitor (SIGMA, S6508) Serine protease inhibitor (SIGMA, A6279) Serine and cysteine protease inhibitor (SIGMA, L2884) Acid protease inhibitor (SIGMA, P4265) Serine protease inhibitor (SIGMA, T7254) Serine protease inhibitor, dissolved in isopropanol, (SIGMA, P7626) PP2B inhibitor (SIGMA, F1428) Potassium Bisperoxo(1,10-phenanthroline)oxovanadate, PTP inhibitor (CALBIOCHEM, 203695) PP1 and PP2A inhibitor, 0.5 mM in ethanol (100 μg in 248 μl) (CALBIOCHEM, 495604)
Lysis buffer	50 mM Tris-HCl pH 7.4, 150 mM NaCl, 1 mM EDTA, 1% Triton X-100
PBS	137 mM NaCl, 2.7 mM KCl, 9.5 mM Na_2PO_4H, 1.4 mM $K_2PO_4H_2$ (SEVERN BIOTECH LTD.)
Raft lysis buffer	25 mM Tris-HCl pH 7.4, 150 mM NaCl, 5 mM EDTA
SDS-PAGE running buffer	0.025 M Tris, 0.192 M glycine, 0.1% w/v SDS, pH 8.3
Stripping buffer	62 mM Tris pH 6.8, 2% SDS, 1M β-mercaptoethanol
TAE buffer	50 mM Tris-Acetate, 1 mM EDTA, pH 8
TBE buffer	89 mM Tris-Borate, 2 mM EDTA
TBST	50 mM Tris-HCl pH 7.5, 150 mM NaCl, 0.1% v/v Tween 20
Transfer buffer	48 mM Tris-HCl pH 8.5, 0.39 M glycine, 0.1% SDS, 20% methanol

PI3K inhibitors IC87114 TGX-221 AS604950 LY294002	p110δ-specific inhibitor (SERONO) p110β-specific inhibitor (SERONO) p110γ-specific inhibitor (SERONO) PI3K inhibitor (TOCRIS, 1130) — provided by Serono scientists (Geneva) to Dr. Vanhaesebroeck
Chromatography buffer A	20 mM Tris, pH 7.6, 1 mM EGTA, 1 mM $MgCl_2$, 10% glycerol, 0.1% octylglucoside
Pervanadate	1.84 g $NaVO_4$ was dissolved in 50 ml ddH_2O, pH adjusted to 10, the solution boiled in the microwave until colourless, made up to 100 ml with ddH_2O (= sodium orthovanadate). 11 µl H_2O_2 (30%) was added to 1 ml sodium orthovanadate and incubated at RT for > 15 min. 2 µl catalase (2 mg/ml) was added and incubated at RT for > 30 min.

2.2 Media

2.2.1 *E. coli* medium

LB medium	12.5 g LB Broth, Miller (Luria-Bertani) (BECTON DICKINSON) in 500 ml ddH_20
LA plates	12.5 g LB Broth, Miller (Luria-Bertani) (BECTON DICKINSON) and 7.5 g Bacto™ Agar (BECTON DICKINSON) in 500 ml ddH_20
Antibiotics	100 µl Ampicillin (Amp)/ml for LB medium and LA plates
	12.5 µl Tetracycline (Tet)/ml LB medium and LA plates
S.O.C. medium	(INVITROGEN, 15544-034)

2.2.2 Mammalian cell culture medium

RPMI 1640 medium, complemented	Roswell Park Memorial Institute (RPMI) medium was purchased from (GIBCO, 52400-025) supplemented with 10% FBS, 5 ml Pen/Strep
RPMI 1640 for WEHI-231 cell culture	supplemented with 10% FBS, 5 ml Pen/Strep, and 0.5 ml 5 x 10^{-2} β-mercaptoethanol
DMEM	Dulbecco's Modified Eagle Medium (GIBCO, 41966-029) was supplemeted with 10% FBS, 5 ml Pen/Strep
Phosphate-free DMEM	(GIBCO, 11971-025)

2.2.3 Chicken cell culture medium

RPMI 1640	RPMI (GIBCO, 52400-025) was supplemented with 10% FBS, 1% chicken serum, 5 ml Pen/Strep
Chicken serum	(GIBCO, 16116-082)

2.3 Antibodies

The source of antibodies (Abs) generated by members of Dr. Vanhaesebroeck's team is called BV laboratory.

Name	Target protein	Source and Cat #	Specification	Concen-tration	WB/IP concen-tration
Akt	Akt	Cell Signalling, 9272	Rabbit pAb		1:1000 (WB)
pS473	Akt	Cell Signalling, 9271	Rabbit pAb		1:1000 (WB)
pT308-77	Akt	Cell Signalling, 9275	Rabbit mAb		1:1000 (WB)
pT308-76	Akt	Cell Signalling, 4056	Rabbit pAb		1:1000 (WB)
Akt-901	Akt	Upstate, 05-901	Mouse mAb		1:1000 (WB)
β-actin	β-actin	Sigma, ac-15	Mouse mAb		1:10000 (WB)
BCAP	BCAP	Provided by Dr. Kurosaki, Riken	Rabbit pAb		1:1000 (WB) 1:1000 (IP)
Btk	Btk	Santa Cruz, sc-1696	Rabbit pAb		1:200 (WB)
Dal1/53	CD45	Babraham Institute, Cambridge	Mouse mAb against cytoplasmic tail		1:1000 (WB)
Dal1/4	CD45	Babraham Institute, Cambridge	Mouse mAb against cytoplasmic tail		1:1000 (WB)
IRS-1-526	IRS-1	Upstate, 06-526	Rabbit pAb		1:1000 (WB)
IRS-2-S919	IRS-2	Provided by Dr. Foukas, LICR, S919	Goat pAb	0.55 mg/ml	1:1000 (IP)
IRS-2	IRS-2	Upstate, 06-506	Rabbit pAb		1:10000 (WB)
Itk	Itk	Pharmingen	Rabbit mAb	0.5 mg/ml	1:1000 (WB)
Lck	Lck	Transduction Laboratories	Mouse mAb	0.25 mg/ml	1:5000 (WB)
Lyn	Lyn	Santa Cruz, sc-15	Rabbit pAb	0.2 mg/ml	1:2000 (WB)
9E10	Myc	Abcam	Mouse mAb		1:1000 (WB)
9B11	Myc	Cell Signalling	Mouse mAb		1:1000 (WB) 1:1000 (IP)
p110α-15	p110α	BV laboratory	Rabbit pAb against C-terminus		1:500 (WB)
p110α-16	p110α	BV laboratory	Rabbit pAb		1:500 (WB)
sc-602	p110β	Santa Cruz	Rabbit pAb against C-terminus	0.2 mg/ml	1:1000 (WB)
SK214/215	p110α	BV laboratory	Rabbit pAb	0.01 mg/ml	1:100 (IP)
p110α-11	p110α	Transduction Laboratories	Mouse mAb	0.25 mg/ml	1:1000 (WB)
p110β-2.1	p110β	BV laboratory	Rabbit pAb against C-terminus		1:100 (IP)
p110β-CT	p110β	BV laboratory	Rabbit pAb		1:300 (IP)
p110γ	p110γ	BV laboratory	Mouse mAb		1:100 (WB)
p110δ-CT	p110δ	BV laboratory	Rabbit pAb against C-terminus	1 mg/ml	1:5000 (WB) 1:1000 (IP)
pS1039	p110δ	BV laboratory	Rabbit pAb against pSer1039		1:1000 + competing peptide (WB)
p55γ	p55γ	Provided by Dr. Asano, Tokyo	Rabbit pAb	0.33 mg/ml	1:1000 (WB)

T15	p85β	BV Laboratory/ Serotec	Mouse mAb	0.35 mg/ml	1:1000 (WB) 1:200 (IP)
T12	p85β	BV laboratory/ Serotec	Mouse mAb		1:1000 (WB) 1:200 (IP)
U10	p85α	BV laboratory/ Serotec	Mouse mAb against BH domain	0.5 mg/ml	1:1000 (WB) 1:200 (IP)
pS608	p85α	Provided by Dr. Foukas, LICR	Rabbit pAb against pS608		1:1000 (WB)
LazAB	p85α, p85β	Provided by Dr. Foukas, LICR	Rabbit pAb against N-SH2	0.5 mg/ml	1:1000 (IP)
p85pan	p85α/ p85β	Upstate, 06-195	Rabbit pAb against N-SH2 and full-length protein		1:5000 (WB) 1:1000 (IP)
U2	p85α/ p85β	BV laboratory	Mouse mAb against N- SH2	0.3 mg/ml	1:1000 (WB) 1:100 (IP)
pThr	phospho-Thr	Cell Signaling	Rabbit pAb	0.1 mg/ml	1:1000 (WB)
4G10	phospho-Tyr	Upstate	Mouse mAb against phospho-tyramine	1 mg/ml	1:5000 (WB)
Src	Src	Provided by Dr. Gout, UCL	Mouse mAb		1:1000 (WB)
Syk-1077	Syk	Santa Cruz, sc1077	Mouse mAb	0.2 mg/ml	1:1000 (WB)
Syk-573	Syk	Santa Cruz, sc-573	Mouse mAb	0.2 mg/ml	1:1000 (WB)
Tubulin	Tubulin	Sigma, T5168	Mouse mAb		1:1000 (WB)

2.4 Cell lines

Cell line	**Species**	**Additional information** (including ATCC catalogue number if available)
A20	*Mus musculus*	Mature B cell line
B16BL6	*Mus musculus*	Melanoma cell line
CT26	*Mus musculus*	Colon carcinoma cell line (CRL-2638)
DT40	*Gallus gallus*	B lymphoma cell line (CRL-2111)
EL-4	*Mus musculus*	T lymphoma cell line (TIB-39)
GIST-430	*Homo sapiens*	Gastrointestinal stromal tumour cell line
HEK-293T	*Homo sapiens*	Kidney cell line
HMC-1	*Homo sapiens*	Immature mast cell line
MDA-MB361	*Homo sapiens*	Breast cancer cell line (HTB-27)
NALM-6	*Homo sapiens*	acute lymphoblastic pre-B cell line
NIH-3T3	*Mus musculus*	Fibroblast cell line (CRL-165)
THP-1	*Homo sapiens*	acute monocytic leukemia cell line
U937	*Homo sapiens*	histiocytic lymphoma cell line (CRL-1593.2)
WEHI-231	*Mus musculus*	Immature B cell line

2.5 DNA primers

Primers were ordered from QIAGEN OPERON.

2.6 Plasmids & bacterial strains

Plasmid	Genotype/ Description	Antibiotic Resistance	Source & catalogue number
pGEX-4T-2	pGEX-4T-2 has a tac promoter followed by a multiple cloning site, thrombin recognition site and glutathione S-transferase gene and β-lactamase gene.	Amp	Amersham Biosciences (27-4581-01)
pBG1	pBG1 is a pGEX-4T-2 plasmid from Amersham with the single-small (ss) peptide inserted. pGEX-4T-2 is restriction digested with *EcoRI* and *SalI* ss: 5' a att tat gtg ccg atg ctg ggc ggc gcc 3'	Amp	N/A
pBG2	pBG2 is a pGEX-4T-2 plasmid from Amersham with the double-small (ds) peptide inserted. pGEX-4T-2 is restriction digested with *EcoRI* and *SalI* ds: 5' a att ggt ggc tac atg gac atg agc aag gac gag tct gtg gac tat gtg ccg atg ctg ggc gcc 3'	Amp	N/A
pBG3	pBG3 is a pGEX-4T-2 plasmid from Amersham with the double-long (dl) peptide inserted. pGEX-4T-2 is restriction digested with *EcoRI* and *SalI* dl: 5' aatt ggc gag agc gac ggt ggc tac atg gac atg agc aag gac gag tct gtg gac tat gtg ccg atg ctg gac atg ggc gcc 3'	Amp	N/A
Strain	**Genotype/ Description**	**Antibiotic resistance**	**Source & catalogue number**
XL1-blue	*recA1 endA1 gyrA96 thi-1 hsdR17 supE44 relA1 lac* [F'*proAB lacI*^{q}*ZΔM15 Tn10* (Tet^r)]	Tet	Stratagene (200249)
TKB1	*E. coli* B F– *dcm ompT hsdS*(r_B–m_B–) *gal λ*(DE3) [pTK Tet^r] Lysogenic for lambda DE3, which carries the T7 polymerase gene under *lacUV5* control.	Tet	Stratagene (200134)
BG1	XL1-blue containing pBG1	Tet, Amp	N/A
BG2	XL1-blue containing pBG2	Tet, Amp	N/A
BG3	XL1-blue containing pBG3	Tet, Amp	N/A
BG4	XL1-blue containing pGEX-4T-2	Tet, Amp	N/A
BG6	TKB1 containing pBG1	Tet, Amp	N/A
BG7	TKB1 containing pBG2	Tet, Amp	N/A
BG8	TKB1 containing pBG3	Tet, Amp	N/A

2.7 Cell culture techniques

All procedures were carried out in a flow hood using antiseptical techniques.

2.7.1 Cryopreservation of cells

Stocks of the various cell lines were kept in liquid nitrogen. To start cultures of frozen cells, aliquots were removed from storage and thawed quickly at 37°C in a water bath before transfer to a tissue culture flask containing the appropriate medium.

To prepare for freezing, cells were harvested by centrifugation at 700 x g for 7 min and resuspended in 100% fetal bovine serum to give a final cell density of 1 x 10^8 cells/ml. 0.5 ml of this cell solution was mixed with 0.5 ml of 20% DMSO, 80% FBS and immediately transferred to sterile cryovials, which were frozen slowly in a polystyrene box containing isopropanol at –80°C overnight. They were subsequently transferred to liquid nitrogen.

2.7.2 Mammalian cell culture

2.7.2.1 Maintenance of mammalian cells

In general, suspension cells were cultured in Roswell Park Memorial Institute (RPMI) 1640 medium and adhesion cells in Dulbecco's Modified Eagle's Medium (DMEM) each supplemented with 10% Fetal Calf Serum and 1% antibiotic solution (Penicillin and Streptomycin). Cells were grown at 37°C in a humidified incubator with 5% CO_2. For further propagation, when cells became confluent, they were either diluted in fresh, prewarmed medium in the case of suspension cells or washed with PBS and trypsin-treated in the case of adhesion cells.

2.7.2.2 Treatment of cells with PI3K inhibitors

WEHI-231 cells were incubated with 5 μM IC87114, 5 μM LY294002, 0.1 μM TGX-221, 1 μM AS604950 or an equivalent volume of DMSO only for 30 min at 37°C. Following treatment with PI3K inhibitors, the cells were either left untreated or stimulated with α-IgM.

2.7.2.3 Antigen stimulation of B cells

B cells were either stimulated with α-IgM (WEHI-231 cells) or α-IgG (A20 cells) in order to crosslink the B cell antigen receptor and to induce a signalling cascade leading to Akt phosphorylation. Cells were therefore split to 1-2 x 10^6 cells/ml and incubated with 10 μg/ml α-IgM or α-IgG for 1-10 min at 37°C. They were subsequently diluted with ice-cold PBS and harvested at 700 x g for 7 min in a cold centrifuge.

2.7.2.4 Treatment of cells with okadaic acid (OA)

OA treatment of cells leads to the accumulation of Ser and Thr phosphorylated proteins since this agent is a potent PP1 and PP2A phosphatase inhibitor. Mammalian cells were seeded at 1-2 x 10^6 cells/ml and incubated with 1 nM okadaic acid for 45 min at 37°C. They were subsequently diluted with ice-cold PBS and harvested at 700 x g for 7 min in a cold centrifuge.

2.7.2.5 Transfection of mammalian cells

HEK-293T cells were transfected with plasmid DNA by calcium phosphate precipitation according to the manufacturer's protocol (INVITROGEN, K2780-01).

2.7.3 Avian cell culture

2.7.3.1 Maintenance of DT40 cells

DT40 cells were cultured in RPMI containing 10% FBS, 1% chicken serum and 1% antibiotic solution. The cells were grown at 39.5°C in a humidified incubator with 5% CO_2. The cells were kept between 5 x 10^5 and 1 x 10^7 cells/ml. Stimulation of DT40 cells with mouse anti-chicken IgM (clone M4, CAMBRIDGE BIOSCIENCES) or pervanadate was performed with 1 x 10^6 cells/ml.

2.8 Nucleic acid manipulation

Centrifugation steps were carried out in an Eppendorf microfuge at 14000 rpm unless otherwise stated. All DNA solutions were stored at –20°C.

2.8.1 DNA preparation methods

2.8.1.1 Small-scale preparations of plasmid DNA

Small-scale plasmid preparations were performed with the GenElute™ Plasmid Miniprep Kit (SIGMA) according to the manufacturer's protocol.

2.8.1.2 Determination of DNA concentration

DNA concentration was determined spectrophotometrically by measuring the optical density (OD) at 260 nm by a Nanodrop ND-1000 spectrophotometer (NANODROP TECHNOLOGIES). Concentrations were then calculated from the equation: OD_{260} =1= 50 µg/ml double stranded DNA.

2.8.1.3 Agarose gel electrophoresis of DNA

Molecular biology grade agarose (HELENA BIOSCIENCES) was dissolved in 1 × TAE buffer to a final concentration of 0.6-1.8%. The solution was boiled in a microwave oven until the agarose was completely melted. The solution was allowed to cool down to approximately 60°C, ethidium bromide was added to a final concentration of 10 µg/ml, and the agarose was poured into a horizontal gel apparatus. After solidification, the chamber was filled with 1 × TAE buffer to run the gel. The DNA samples were mixed with Mass Loading Dye Solution (MBI FERMENTAS), loaded into the slots and run at a constant voltage of 120 mV for 20-30 min. For the determination of the fragment size, either GeneRuler™ 100 bp DNA Ladder Plus or MassRuler™ DNA Ladder, High

Range (both MBI FERMENTAS) were electrophoresed simultaneously. The bands were visualised under UV-light and photographed with Polaroid films.

In order to resolve DNA fragments of 200-300 bp, NuSieve® 3:1 agarose (CAMBREX) was dissolved in 1 x TBE to a final concentration of 3%. The manufacturer's protocol was followed. Briefly, the agarose was slowly added to 1 x TBE and soaked for 15 min, subsequently heated in the microwave oven and held at the boiling point until the agarose was completely melted. After cooling down and adding ethidium bromide, the same procedure was followed as describe for lower percentage agarose gels.

2.8.2 DNA cloning procedures

2.8.2.1 Restriction enzyme digestion of DNA

An appropriate amount of DNA was diluted in 1 × restriction enzyme buffer (MBI FERMENTAS or NEB) to a final volume of 20-100 µl. If required, 1 µl of BSA (MBI FERMENTAS) was added. 5-10 units of the desired restriction enzyme(s) were added and the reaction mixture was incubated between 2 and 4 h at the temperature recommended by the manufacturers (usually 37°C). The reaction product was analysed by agarose gel electrophoresis.

2.8.2.2 Ligation of DNA fragments

In order to anneal synthesised oligonucleotides (provided by QIAGEN), 100 pmol/µl each of an oligonucleotide and its complementary sequence were incubated with 1 x T4 ligase buffer at 100°C for 3 min. The samples were then switched to room temperature (RT) and left to cool down and the annealing reaction to proceed.

An appropriate amount of purified vector and insert DNA – usually in a 3:10 vector-to-insert molar ratio – were diluted in 1 × T4 ligase buffer (MBI FERMENTAS) and 400-800 units of T4 DNA ligase (MBI FERMENTAS) were added. Subsequently, the mixture was incubated at 4°C overnight.

2.8.3 Transformation of competent *E. coli* cells (XL1-blue)

In order to transform competent cells, an aliquot of 100 µl of cells was thawed on ice and mixed with 50 ng DNA of the ligation mix. Cells were kept on ice for 30 min and then heat-shocked (42°C) for 90 s. Upon storage on ice for 2 min, 0.9 ml of S.O.C. medium was added and the cells were recovered for 45 min at 37°C on a shaker. The cells were concentrated thereafter and plated on selective LA plates. Dilution series were made to obtain an optimal colony number when a high number of transformants was expected.

2.8.4 Polymerase chain reaction (PCR)

PCR experiments were routinely performed in a volume of 50 µl in 500 µl PCR tubes. The thermocycler (PELTIER THERMAL CYCLER, PTC-200) was equipped with heatable lids.

The reactions contained 1 x PCR reaction buffer without $MgCl_2$ (SIGMA), 200 µM of each dNTP (MBI FERMENTAS), 2.5 mM $MgCl_2$ (SIGMA), 10 ng template DNA, 2.5 pmol primers and 0.5 units of Taq (SIGMA).

The cycling programs for PCR were optimised for each template-primer combination. The program was started with a denaturation step (94°C, 1 min), followed by 30 cycles consisting of a denaturation step at 94°C for 30 s, an annealing step at 60°C (in some cases slightly higher or lower) for 30 s and an elongation step at 72°C for 2-3 min depending on the length of the fragment amplified. The reaction was terminated by an additional extension at 72°C for 10 min to synthesise incomplete products.

For crude verification of transformation results, 100 µl LB containing the appropriate antibiotic were inoculated and grown for 3 h. 5 µl of the *E. coli* culture was added to 1 x PCR reaction buffer, 200 µM of each dNTP, 2.5 mM $MgCl_2$, 0.5 units of Taq, and 2.5 pmol primers. The PCR reaction was performed as described above.

2.8.5 Sequencing reactions

DNA sequencing reactions were performed by MWG (MWG-BIOTECH AG, Ebersberg, Germany). 1-2 µg of plasmid DNA or PCR DNA sequences were supplied air-dried, in addition to primers at a concentration of 10 pmol/µl.

2.9 Protein analysis and detection

2.9.1 SDS polyacrylamide gel electrophoresis

Sodium Dodecyl Sulfate PolyAcryamid Gel-Electrophoresis (SDS-PAGE) was used for the separation of proteins according to their relative molecular weight (M_r).

The resolving gel (8%) was prepared in the following manner in a Hoefner gel apparatus: 10 ml 30% acrylamide solution , 10 ml 4 x SEP buffer, 18.8 ml water, 250 µl APS (10%) and 25 µl TEMED. After polymerization, the stacking gel was prepared as follows: 2.7 ml acrylamide solution, 5 ml 4 x SPAC buffer, 12.2 ml water, 90 µl APS and 25 µl TEMED. The protein samples, dissolved in SDS sample buffer and boiled for 5 min, and the marker were loaded. The gel was run at constant voltage of 150 V for 5 hours or overnight at 50 V in 1 × SDS-PAGE running buffer.

2.9.2 Two-dimensional gel electrophoresis

Two-dimensional (2D) gel electrophoresis sorts proteins according to two independent properties in two discrete steps: the first-dimension step, isoelectric focusing, separates proteins according to their isoelectric points (pI); the second-dimension, SDS-PAGE, separates proteins according to their molecular weights (M_r, relative molecular weight). Thus, complex mixtures or post-translationally modified proteins can be analysed in more detail than using 1D SDS-PAGE.

2D gel electrophoresis was first introduced by O'Farrell (O'Farrell, 1975) and Klose (Klose, 1975) in 1975. In the original technique, the first dimension separation was performed with ampholyte-containing polyacrylamide gels cast in narrow glas tubes. 2D gel electrophoresis has been more widespread used in the last few years due to a number of improvements, especially the introduction of immobilised pH gradients (IPG) in 2D gel electrophoresis which led to increased reproducibility and sample loading capacity (Gorg et al., 1985{Gorg, 1988 #214); (Gorg et al., 2000).

The work flow of 2D gel electrophoresis can be summarised as follows: after sample preparation, the IPG strips are rehydrated overnight by adding the protein sample. The next day, the first dimension isoelectric focusing is performed followed by IPG equilibration and second dimension SDS-PAGE. Furthermore, the gel is either stained with Coomassie or Silver or the protein transferred to PVDF membranes for immunoblotting analysis.

2.9.2.1 Sample preparation

The method of sample preparation is key to the success of the experiment. The protein fraction loaded on a 2D-PAGE gel must be in a low ionic strength denaturing buffer that maintains the native charges of proteins and keeps them soluble during all steps of 2D electrophoresis. We therefore used a 2D lysis buffer made of 2 M thiourea and 8 M urea (chaotropic agents, (Rabilloud, 1998)), 4% CHAPS (zwitterionic detergent, (Rabilloud, 1999)), 65 mM DTT (reducing agent) and 2% ampholytes (carrier ampholytes to reduce protein precipitation).

Cells were split the day before the experiment, then harvested by centrifuging at 700 x g for 7 min at 4°C, and washed twice with ice-cold PBS. Lysis of 1 x 10^7 cells was performed in 0.8 ml 2D lysis buffer (8 M urea, 2 M thiourea, 4% CHAPS, 65 mM DTT, 2% ampholytes). The cells were incubated for 15 min at RT and passed three times through a 27-gauge needle. To separate the unbroken cells from the lysate, a centrifugation step at 10000 x g for 10 min at 16°C was performed. The protein concentration of the lysate was determined.

If immunoprecipitated protein was analysed by 2D gel electrophoresis, immunoprecipitation was performed as described in § 2.10, however, a low-salt/

detergent free wash step (50 mM Tris-HCl pH 7.4, 10 mM NaCl, 5 mM EDTA) of the beads was incorporated after washing with lysis buffer. The beads were subsequently incubated with 2D lysis buffer for 15 min at RT and the supernatant loaded onto the first dimension of the gel.

2.9.2.2 First dimension isoelectric focusing (IEF)

The isoelectric point of a protein is the specific pH at which its net charge is zero. Proteins are positively charged at pH values below their pI and negatively charged at pH values above their pI. In IEF, proteins move under the influence of an electric field along a pH gradient until their net charge is zero.

For the first dimension isoelectric focusing, we used immobilised pH gradient (IPG) strips (AMERSHAM PHARMACIA BIOTECH). An IPG is created by covalently incorporating a gradient of acidic and basic buffering groups into a polyacrylamide gel at the time it is cast.

200 μg total protein or immunoprecipitated protein in 350 μl 2D lysis buffer containing 0.001% bromophenol blue and 2% ampholytes was spread along the whole length of the IPG reswelling tray. A defrosted, 18 cm IPG strip (Immobiline DryStrip, pH 3-10, AMERSHAM PHARMACIA BIOTECH) was labelled, the plastic backing removed and the strip layed gel-faced down. After 1 h of reswelling, 1 ml of PlusOne DryStrip cover fluid (AMERSHAM PHARMACIA BIOTECH) was added and the lid of the reswelling tray closed. The strip was rehydrated overnight at RT. Thereafter, the strip was transferred to a plastic strip aligner with the gel facing up and a 2 cm electrode strip, which was soaked in 100 μl ddH_20, placed on each side of the strip. The strip was connected to the Multiphor™ II Electrophoresis Unit (AMERSHAM PHARMACIA BIOTECH) and DryStrip cover fluid added. The focussing program was as follows: 300 V gradient for 30 min, 3500 V gradient for 6 h and 3500 V gradient for 20 h. The current and power was maintained at 5 mA and 10 W, respectively for each step.

2.9.2.3 Equilibration of IPG strips

The equilibration step saturates the IPG strip with the SDS buffer system required for the second dimension separation. In addition, proteins are further reduced and alkylated in order to prevent protein streaking in the second dimension. To this end, the strips were emerged for 10 min in IPG equilibration buffer (50 mM Tris-HCl pH 8.8, 6 M urea, 30% glycerol, 2% SDS) containing 1% DTT, followed by 10 min incubation with IPG equilibration buffer containing 245 mM iodoacetamide.

2.9.2.4 Second dimension SDS-PAGE

For the analysis of PI3K proteins, 7-8% single percentage gels were cast in 20 x 22 cm plates. The gel was made of 15 ml 1.5 M Tris-HCl pH 8.8, 12 ml 40%

acrylamide, 33 ml HPLC ddH_2O, 0.6 ml 10% APS and 60 μl TEMED and poured until the gel solution reached 2-3 cm below the top of the lower glass plate.

After equilibration of the strip, melted second dimension overlay agarose solution (0.5% molecular biology grade agarose in SDS-PAGE running buffer containing 0.001% bromophenol blue) was poured on top of the second dimension and the strip transferred. Once the agarose was set, the second dimension was run at 50 mA per gel with cooling in SDS-PAGE running buffer for 4-5 h until the dye front ran out (BioRad, Protean II xi Cell). Subsequently, the samples were analysed either by colloidal Coomassie blue (§ 2.9.3), Silver staining (§ 2.9.4) or by immunoblotting method (§ 2.9.5).

2.9.3 Colloidal Coomassie staining of acrylamide gel

Colloidal Coomassie staining of polyacrylamide gels was performed with the GelCode® Blue Stain Reagent according to the manufacturer's protocol (Pierce, 24592).

Briefly, polyacrylamide gels were fixed in 40% ethanol/10% acetic acid for 1 h to overnight. The gels were subsequently washed 3-5 times with excess ddH_20 and 20 ml of GelCode® Blue were added for 1 h. After staining, the gels were incubated with ddH_20 for another hour to decrease the background staining.

2.9.4 Silver staining of acrylamide gels

After SDS-PAGE, the gel was incubated in a 40% ethanol/10% acetic acid fixating solution for 1 h to overnight. Subsequently, the gel was washed in 50% ethanol and distilled water for 10 min each. The gel was further incubated with 0.02% sodium thiosulphate sensitising solution for 1 min, washed in water for 1 min and then stained in chilled 0.1% silver nitrate for 30 min at 4°C. Thereafter, the gel was washed generously in water for 1 minute and developed in 0.04% formalin, 2% sodium carbonate. The reaction was stopped with 1% acetic acid.

2.9.5 Electroblotting

After SDS-PAGE, proteins were transferred onto a PVDF membrane (Immobilion™-P, Millipore) by electroblotting.

The membrane cut to the same size as the gel was briefly soaked in methanol and rinsed in water. Both the gel and the membrane were pre-equilibrated in 1 x transfer buffer (48 mM Tris-HCl, 386 mM glycine, 1% SDS, 20% methanol), sandwiched between 2 sheets of Whatman 3MM paper and two sponges (both equilibrated in 1 x transfer buffer). The case was then placed in a blotting tank

containing 1 x transfer buffer such that the gel was facing the cathode. Proteins were transferred for 100 Vh.

After the transfer, the membrane was blocked for 1 h to overnight in 5% milk, 1 x TBST. Subsequently, the membrane was incubated with the primary antibody (Ab) overnight at 4°C, washed thoroughly 3 times for 5 min in 1 x TBST and then incubated with the secondary Ab for 1 h at RT. The membrane was washed with 1 × TBST and incubated with ECL™ Western Blotting Detection Reagents (AMERSHAM BIOSCIENCES) or home-made ECL for 2-3 min. The membrane was wrapped in saran foil and exposed to super RX Fuji medical X-ray films (FUJI) for different amounts of time.

Blots were stripped by immersing in stripping buffer (62 mM Tris-HCl pH 7.4, 20% SDS) supplemented with 700 µl β-mercaptoethanol per 100 ml stripping buffer for 30 min at 55°C and then rinsed thoroughly in 1 x TBST.

2.9.6 Determination of protein concentration

The protein concentration of lysates was measured by comparing the spectrometrical absorbance of lysis buffer at 595 nm with the absorbance of the cell lysate. Therefore, 5 µl of the lysis buffer was added to 1 ml of BioRad solution (BIORAD), mixed well and the absorbance measured with a spectrophotometer (Cary 50, VARIAN INC.). This control absorbance was subtracted from the absorbance measured if 5 µl of cell lysate was added to 1 ml BioRad solution. The obtained value for the cell lysate was thereafter multiplied with a constant (24.75) and the dilution factor (200) to give the protein concentration in mg/ml.

2.10 Immunoprecipitation

Cells were harvested by centrifugation at 700 x g for 7 min and subsequently washed twice with ice-cold PBS. The pellet was resuspended in ice-cold lysis buffer (1 ml lysis buffer/10^7 cells, 50 mM Tris-HCl pH 7.4, 150 mM NaCl, 1 mM EDTA, 1% Triton X-100) containing protease and phosphatase inhibitors and incubated for 20-30 min on ice. The lysate was centrifuged at 10000 x g for 10 min and the protein concentration of the supernatant determined. If mass spectrometry (MS) experiments were performed, the lysate was pre-cleared for 2 h with 10-100 µl packed, prewashed protein A/G sepharose beads (AMERSHAM BIOSCIENCES) followed by Ab addition. In all other experiments, this step was omitted and Ab was directly added to the lysate and incubated for two hours to overnight at 4°C. Subsequently, 10-100 µl packed, prewashed protein A/G sepharose beads were added and the lysate incubated at 4°C for two more hours. The beads were washed three times with lysis buffer, two times with lysis buffer containing 0.5 M NaCl and once with 10 mM Tris-HCl, pH 7.4. The

beads were then incubated with 150 µl 5 x SDS sample buffer and boiled for 5 min at 100°C.

More detailed information to each Ab is provided in § 2.3.

2.11 Subcellular fractionation

2.11.1 Separation of cytosolic and membrane fraction

Analysis of the cytosolic and membrane fraction was performed using a protocol described by Susan Pierce (Stoddart et al., 2002).

Approximately 10^8 WEHI-231 or A20 cells were harvested by centrifugation at 700 x g for 7 min and washed twice with ice-cold PBS. 3.5 ml of ice-cold Hypotonic buffer (10 mM Tris-HCl pH 7.4, 42 mM KCl, 5 mM $MgCl_2$) was added to the cell pellet and incubated for 30 min on ice. Three rounds of freeze-thawing were performed. After this, protease and phosphatase inhibitors were added and the lysate subsequently centrifuged at 1000 x g for 10 min. The protein concentration of the supernatant was measured, a sample kept for immunoblotting analysis and the supernatant subsequently centrifuged at 150000 x g for 30 min. The high spin supernatant containing the cytosolic fraction and high spin pellet containing the membrane fraction were analysed by immunoblotting.

2.11.2 Raft fraction analysis

Lipid rafts were isolated by treatment of cell membranes with Triton X-100 and flotation on sucrose gradients.

3 x 10^7 WEHI-231 or A20 cells in 30 ml supplemented RPMI medium were harvested by centrifugation at 700 x g for 7 min, washed twice in ice-cold PBS and lysed in 3.5 ml Hypotonic buffer. The cells were incubated on ice for 30 min, followed by three rounds of freeze-thawing. The lysate was centrifuged at 1000 x g for 10 min. The post-nuclear supernatant was centrifuged for 30 min at 150000 x g. The high spin pellet containing the membrane fraction was resuspended in 1 ml 0.2% Triton X-100 in Raft lysis buffer (25 mM Tris-HCl pH 7.4, 150 mM NaCl, 5 mM EDTA) and incubated for 20 min on ice. 1.7 ml 65% sucrose in Raft lysis buffer was added to the membranes and overlayed with 5 ml 30% and 2 ml 5% sucrose solution in an ultracentrifuge tube. The discontinuous sucrose gradient was centrifuged at 200000 x g for 18 h, and eleven 1 ml fractions were collected from the top of the gradient and analysed by immunoblotting.

2.12 In vivo *labelling with radioactive ATP*

In order to perform a *in vivo* labelling experiment with WEHI-231 cells, 5 x 10^8 cells were washed twice in pre-warmed, phosphate-free DMEM and subsequently incubated with 50 ml phosphate-free DMEM containing 4% dialysed FCS and 10 mM HEPES, pH 7.4 (= Labelling medium) for 30 min at 37°C. After this incubation step, the cells were harvested and resuspended in 27 ml Labelling medium. 2 mCi [γ-^{32}P]ATP was added to 3 ml Labelling medium and added to the cells. The cells were incubated for 6 h at 37°C. Subsequently, the cells were harvested, washed twice with Labelling medium and resuspended in 40 ml fresh Labelling medium. The cells were split into 5 flasks and either left unstimulated or stimulated with 10 μg/ml α-IgM or 500 nM OA. The cells were then washed with ice-cold PBS and handled as described in § 2.10.

2.13 In vitro *PI3K lipid protein kinase assay*

In vitro PI3K lipid protein kinase assays were performed with immunopurified protein after extensively washing the immunocomplex with lysis buffer and 2 x kinase buffer (40 mM Tris-HCl, pH 7.4, 200 mM NaCl, 1 mM EGTA). The reaction took place in a final volume of 80 μl reaction. 40 μl 2 x Kinase buffer and 10 μl lipids (phosphatidylinositol or phosphatidylinositol 4,5-bisphosphate) were added to the beads. A mastermix of Mg/ATP/[γ-^{32}P]ATP (10 mM Mg, 100 μM ATP, 0.25 μl [γ-^{32}P]ATP) was prepared and added as well. The mix was incubated at 30°C for 15 min and the reaction stopped by addition of 100 μl 1 M HCl. The lipids were extracted by addition of 200 μl $CHCl_3$:MeOH (1:1) followed by 80 μl 1 M HCl:MeOH (1:1).

The lipids were separated by thin layer chromatography (TLC). To this end, the lipids were spotted onto a TLC plate pre-treated with Chelating solution (5 g oxalic acid, 1 ml 0.5 M EDTA, 200 ml MeOH). The chromatography was performed using a solution made of propan-1-ol, 2 M acetic acid, 5 M phosphoric acid (65:35:1). The TLC plate was exposed to a phosphoimager plate for detection of radioactivity.

2.14 *Liquid chromatography*

Molecules can be separated by chromatography using differences in their biophysical properties, such as size, charge and hydrophobicity. Liquid chromatography was used in this work for sample fractionation and as front-end separation before MS analysis.

2.14.1 Ion exchange chromatography

Ion exchange chromatography (IEX) separates biomolecules based on differences in their charge. This separation technique depends upon the reversible

adsorption of charged solute molecules to an immobilised ion exchange group of opposite charge. For the separation of class IA PI3K, we used anion exchange chromatography after a protocol by Shibasaki (Shibasaki et al., 1991). The chosen high performance anion exchange chromatography column (Tricorn Mono Q™ 4.6/100 PE column (AMERSHAM BIOSCIENCES)) contained a strong anion exchanger (O-CH_2-CHOH-CH_2-O-CH_2-CHOH-CH_2-$N^+(CH_3)_3$) covalently coupled to a polystyrene/divinyl benzene matrix. The Tricorn Mono Q™ 4.6/100 PE column was chosen because of its high loading capacity, high resolution purification, reproducibility and durability. An Integral 100Q system (APPLIED BIOSYSTEMS, 5-1818-00, 203) was used for high pressure liquid chromatography.

After cell lysis as described in § 2.10, the lysate containing 30 mg total protein in 10 ml lysis buffer was de-salted by applying the protein to 2 pre-cooled gel filtration columns (BIORAD, Econo-Pac 10DG, 732-2010). Elution was performed with 2 x 4 ml cold Chromatography buffer A (20 mM Tris-HCl pH 7.6, 1 mM EGTA, 1 mM $MgCl_2$, 10% glycerol, 0.1% octylglucoside).

The anion exchange chromatography column was equilibrated with 10 column volumes of Chromatography buffer A before adding the lysate. After addition of protein solution, the column was washed with Chromatography buffer A until the baseline was reached, and the protein subsequently eluted using gradient elution (usually from 0 M NaCl to 0.5 M NaCl in 20 column volumes). The protein fractions were harvested and analysed by immunoblotting.

After usage, the column was routinely washed with 3 M NaCl, followed by ddH_2O. For more rigorous cleaning, 1 M NaCl, 1 M NaOH, 1 M HCl, 1 M NaCl were applied.

2.14.2 Reverse phase high pressure liquid chromatography

In reverse phase (RP) liquid chromatography, molecules are separated according to their hydrophobicity (Snyder, 1997). Sample mixtures in a hydrophilic mobile phase are introduced to a column containing a hydrophobic stationary phase. Elution occurs with applications of a hydrophobic phase applied in a fixed (isocratic) or variable (gradient) concentration. RP high pressure liquid chromatography (RP-HPLC) was used in conjunction with MS.

Depending on the hydrophobicity of the analyte, different stationary phases can be used. Small peptides are best separated with columns packed with beads derivatised with octadecyl groups (C18) containing relatively small pore sizes.

LC was performed using an Ultimate™ HPLC system (LC PACKINGS, Amsterdam, Netherlands). The Ultimate system consisted of an auto-sampler (Famos™) that loaded 5 µl sample at 20 µl/min flow rate onto a peptide trap column (0.3 x 1 mm, PepMap, LC PACKINGS) placed at a switching valve (Switchos™). Peptides in the peptide trap column

were washed for 2 min at 20 µl/min with 0.1% formic acid. Peptides were subsequently eluted onto a main analytical column (C18 PepMap, 75 µm x 15 cm) using an elution gradient of 300 nl/min. Solvent A was 0.1% formic acid and solvent B was 80% acetonitrile/0.1% formic acid. Elution was carried out from 5% B to 40% B in 20, 30, 40 min depending on the application.

The eluents of the HPLC runs were analysed on-line by the MS described below.

2.15 Immobilised metal affinity chromatography

Immobilised metal affinity chromatography (IMAC) is a technique that can be used to selectively enrich phosphopeptides in protein digests, and can therefore increase the sensitivity of phosphopeptide detection by MS (Gronborg et al., 2002); (Barnouin et al., 2005).

In IMAC, a stationary phase made of nitrilotriacetic acid (NTA) is chelated to six-coordinate Fe(III) or Ga(III). The interaction between NTA and the metal ion occupies 4 metal coordination bindig sites of Fe(III) or Ga(III), leaving 2 coordination sites free for interaction with phosphorylated amino acids. Although IMAC significantly decreases complex mixtures, some unphosphorylated peptides are retained by the chelating complex, particularly peptides rich in acidic residues (Ficarro et al., 2002; Schlosser et al., 2002).

We performed IMAC experiments following enrichment of PI3K by immunopurification and tryptic digestion of the protein. In a first step, the IMAC beads were prepared from Nickel-NTA-sepharose beads (QIAGEN) by stripping off Ni^{2+} ions and replacing them by Fe^{3+} ions. To this end, 500 µl Ni(II)-NTA-sepharose suspension was washed with 500 µl ddH_2O, treated 2 x with 500 µl 100 mM EDTA, washed 3 x with 500 µl 100 mM acetic acid and subsequently re-charged with 500 µl 100 mM $Fe(III)Cl_3$. The beads were washed 6 x with 100 mM acetic acid and stored at 4°C until use.

In a second step, the digested protein (approximately 1 pmol/µl) was added to 1 µl IMAC beads and incubated for 15 min at RT. The supernatant was removed with an Eppendorf gel loader tip and the beads washed 3 times with 10 µl 10 mM acetic acid and 3 times with 10 µl ddH_2O. The bound peptides were eluted with 2 µl 100 mM ammonium phosphate and analysed by MS.

2.16 Mass spectrometry

2.16.1 Introduction to mass spectrometry

Mass spectrometry (MS) has become the technique of choice for protein identification and increasingly for the investigation of post-translational modifications.

This is due to a number of instrumental advantages of MS over other techniques, such as sensitivity, low sample consumption, accuracy, and possibility to automate (Baldwin, 2004).

Mass spectrometers generally consist of three functional elements: an ionisation source, a mass analyser and a detector.

2.16.1.1 Ionisation

In order to analyse molecules, they must first be ionised and converted into the gaseous phase. The most commonly used ion sources in biological MS are Matrix-Assisted Laser Desorption/Ionisation (MALDI) and Electrospray Ionisation (ESI).

2.16.1.1.1 Matrix-assisted laser desorption/ionisation

This method of soft ionisation was introduced in 1988 by Karas and Hillenkamp (Karas and Hillenkamp, 1988) and Tanaka (Tanaka et al., 1988). In MALDI, the peptide sample is dissolved in a matrix (containing a chromophor), and irradiated with a pulsed nitrogen laser usually at 337 nm. The rapid energy absorption initiates a phase change of the absorbing material from solid to gas, while also inducing ionisation. However, the actual ionisation mechanism by MALDI is not well understood.

2.16.1.1.2 Electospray Ionisation

ESI was developed by Fenn in 1989 (Fenn et al., 1989). ESI allows for the formation of ions from liquid phase samples. The analyte is introduced into a source and passes through an electrospray needle that has a high potential difference in comparison to the inlet of the mass spectrometer. The electric field generates charged droplets which decrease in size by solvent evaporation and Coulomb explosion until desolvated, single ions are formed.

2.16.1.2 Mass analysers

After production of ions in the source, the ions are separated according to their mass-to-charge (m/z) ratio by a mass analyser. The most commonly used mass analysers in biological MS can be divided into four general groups: (1) time-of-flight (TOF), (2) quadrupole, (3) ion trap, and (4) ion cyclotron resonance. In the experiments performed in this thesis, only TOF, quadrupole and ion trap analyser were used and therefore discussed.

2.16.1.2.1 TOF mass analyser

The time-of-flight (TOF) analyser is one of the simplest and most widely used mass analysers. TOF analysers are instruments noted for their nearly unlimited mass range and sensitivity (Cotter, 1989; Roepstorff, 2000). Separation of ions is based on different flight times of ions in a field-free drift region after acceleration in an electric

field. The ions travel the length of the flight tube at a velocity that can be calculated according to the classical equation of kinetic energy. The ions with greater mass will travel slower than the lighter ones and therefore reach the detector later.

2.16.1.2.2 Quadrupole mass analysers

Mass separation in a quadrupole analyser is achieved by establishing an electric field in which ions of a certain m/z value have a stable trajectory through the field (Paul and Steinwedel, 1953). Quadrupole analysers consist of four parallel inert metal rods that are connected electrically. Ions travelling along the z-axis are subjected to the influence of a total electric field made up of a quadrupolar alternating field superposed on a constant field resulting from the application of the potential upon the rods.

Multiple quadrupoles can be applied successively in a mass spectrometer or quadrupoles can be combined with other mass analysers.

2.16.1.2.3 Ion trap mass analyser

Ion trap mass analysers are scanning devices which trap ions in a three-dimensional electric field. Three hyperbolic electrodes consisting of a ring and two endcaps form the core of this instrument. Injected ions are trapped in a radio frequency quadrupole field and then sequentially ejected from the ion trap into an electron multiplier detector.

2.16.1.3 Detector

The ion beam passes through the mass analyser and is then detected and transformed into a usable signal by a detector. In the detector, ions are recorded when hitting a electron multiplier detector plate (multi channel plate, MCP). The signal is amplified by a cascade of electrons which are released if ions come in contact of the plate.

2.16.2 Sample preparation

In order to analyse proteins by MS, peptide fragments are needed. We therefore enzymatically digested protein using trypsin. Trypsin specifically hydrolyses peptide bonds at the carboxylic sides of Lys and Arg residues, unless Pro lies C-terminally of Lys or Arg.

In order to avoid protein contamination (mainly keratin), sample preparation was performed in either a ventilated hood (PCR workstation) or in a clean room (Proteomics Unit, LICR).

In-gel digestion was performed using in-house protocols (Benvenuti et al., 2002). In short, in-gel digestion consists of washing, reducing, alkylating, digesting and extracting the peptides from gel bands. Gel bands were cut into small pieces

(approximately 1 mm^3) and placed into 0.65 ml siliconised tubes. Gel plugs were washed and dehydrated several times by addition of 50% acetonitrile (ACN). The pieces were dried under vacuum and 10 mM DTT in 25 mM ammonium bicarbonate (AmBic) was added. The reaction was left at 50°C for 1 hour. After removing the supernatant, an equal volume of 55 mM iodoacetamide in 25 mM AmBic was added and the reaction was incubated in the dark for 60 min at RT. The supernatant was removed, the gel pieces washed 3 times with 50% ACN and fully dried under vacuum. 50-100 ng trypsin (PROMEGA, 608-274-4330) was added in enough volume to cover the gel pieces. The gel pieces were left rehydrating and more 25 mM AmBic was added to cover the gel pieces. The reaction was incubated at 37°C overnight. Peptides were extracted by removing excess liquid the following morning and adding 50 μl 50% ACN, 5% trifluoroacetic acid 3 times with vigorous vortexing between the extraction steps. Samples were dried under vacuum and stored at -20°C until mass spectrometric analysis.

Samples for LC-ESI-MS were resuspended in 5-10 μl 0.1% formic acid and sonicated for 15 min. The liquid was transferred to 0.2 ml thin wall PCR tubes, which were placed in conical polypropylene vial and closed by addition of a polypropylene snap cap.

Samples for MALDI-TOF MS analysis were prepared using the dried droplet protocol. In short, the sample analyte was mixed with an excess of matrix. Frequently used matrices for MALDI experiments are 2,5-dihydroxybenzoic acid (DHB) and α-cyano-4-hydrocycinnamic acid (HCCA). Typically, 1 μl of sample was mixed with 1 μl of freshly prepared, saturated solution of DHB (SIGMA) or HCCA (AGILENT TECHNOLOGIES). Since DHB is more tolerant to high salt concentrations compared to HCCA and is considered a "cool" matrix as the energy transfer is relatively low, it is more suitable for the analysis of labile modifications on peptides. HCCA on the contrary is a "hot" matrix. Because of the higher transfer of energy this matrix is more suitable to gain structural information of peptides. Samples mixed with matrix were dried under a stream of cold air.

2.16.3 Instrumentation and its operation

Mass spectrometry-based experiments were carried out using instruments located and maintained at the Proteomics Unit of the Ludwig Institute for Cancer Research (Proteomics Unit, Cruciform Building, Gower Street, London WC1E 6BT) unless otherwise stated.

2.16.3.1 MALDI-TOF

Experiments were performed on an Ultraflex TOF/TOF™ (BRUKER DALTONICS). This is a low pressure MALDI-TOF instrument equipped with a nitrogen laser and with LIFT technology.

Samples were spotted onto a stainless steel MALDI plate as described in § 2.16.2 and placed into the Ultraflex TOF/TOF™. Analysis was performed using FlexControl (BRUKER DALTONICS) by averaging the spectra produced from 50 to 300 laser shots depending on the signal-to-noise ratio. Laser intensity was varied depending on the observed signal intensity such that peaks were not saturated. The instrument was externally calibrated using a standard mixture of peptides for the analysis of low molecular weight peptides such as those produced from protein digestion (Calmix, APPLIED BIOSYSTEMS).

Spectra were analysed using FlexAnalysis (Compass software, BRUKER DALTONICS). Background subtraction, smooting and centering were performed using FlexAnalysis. The peaklist was searched against the NCBInr databases using MSFit by Protein Prospector v3.4.1 or v4.0.4 (UCSF) run on a local server. The same search parameters as described in § 2.16.5.2 were used. Protein hits were accepted if the MOWSE score was above 250 and at least 30% of the protein sequence was covered.

2.16.3.2 LC-ESI-Q-TOF

Full-scan acquisitions and most of the multiple reaction monitoring experiments were performed on a Q-TOF™ instrument (MICROMASS, Manchester) coupled to a Nanoflow LC (Ultimate™ HPLC system). The operations of the HPLC are described above (§ 2.14.2).

In the Q-TOF hybrid instrument (Morris et al., 1996); (Morris et al., 1997), two quadrupoles (Q1 and q2) are combined with a time-of-flight mass analyser. When scanning large mass ranges, Q1 operates in the so-called radio frequency (RF) mode allowing for transmission of ions with a wide m/z range to a push-pull region. From there, ions are accelerated orthogonally towards the field-free region of the TOF. In MS/MS experiments, Q1 is used in a static mode allowing for the isolation of desired ions and their transmission to the collision cell (q2) where their fragmentation due to collision induced dissociation (CID) occurs. Fragmented ions are subsequently separated by the TOF analyser.

The ESI mass spectrometers were equipped with nanoflow ion sources and fused silica ESI emitters with 50 µm I.D. tapered to 15 µm at the tip (PicoTip™, NEW OBJECTIVE). Samples were introduced from the eluent of HPLC runs at flow rates of 300 µl/min. Operation parameters were determined empirically by infusing standard peptides. Typical spray tip potentials were 2000-3000 V depending on the tip of the

emitter and the flow rate. Voltages at the orifice of the interface ranged from 40-150 V. The instrument was calibrated using the m/z values of the fragment ions generated from a MS/MS fragmentation of (Glu1)-Fibrinopeptide B.

The instrument was controlled using the Masslynx software (Micromass, WATERS). More detailed running parameters are provided in § 2.16.4.1.

2.16.3.3 LC-ESI-Q-STAR

Multiple reaction monitoring experiments were partially performed with a QSTAR instrument (PE Siex, APPLIED BIOSYSTEMS) coupled to a Nanoflow LC (Ultimate™ HPLC system). This is another hybrid Q-TOF mass spectrometer with ion optics similar to those described above for the Q-TOF™ instrument.

2.16.3.4 LC-ESI-Q-TRAP

Precursor-ion scanning experiments were performed with the hybrid triple quadrupole linear ion trap 4000 Q-TRAP® system (APPLIEDBIOSYSTEMS) coupled to nanoflow chromatography. The Q-TRAP was equipped with a Flow NanoSpray® source controlled using Analyst 1.4 software (MDS-SCIEX). The protein digests were separated using an LC Packings Integrated System (DIONEX) consisting of a FAMOS™ micro autosampler, Switchos™ micro column switching module and UltiMate™ micro pump, a PepMap C18 column (75 µm x 15 cm, LC PACKINGS), and a mobile phase of acetonitrile/0.1% formic acid, with a 45 minute gradient elution and a flow of 0.3 µl/min. Samples were loaded (20 µl injection of a digest reconstituted in 1% formic acid) onto a capillary trap (MICHROM BIORESOURCES) and washed with 0.2% formic acid at a flow rate of 20 µl/min. After approximately 5 min, the capillary cartridge was switched in-line with the analytical column. Post column addition of 80% propan-2-ol was used at a flow rate of approximately 100 nl/min from a syringe pump (connected to a microtee (UPCHURCH) prior to the microionspray head), to improve stability of the spray in negative ion mode.

2.16.4 Peptide sequencing

The main objective of tandem mass spectrometry (MS/MS) is to gain structural information. Sequence information of a certain peptide is gained by its fragmentation into smaller peptides, which are subsequently analysed for their m/z. The fragmentation is achieved by exposing ionised peptides to an inert gas. Upon collision with the gas particles, the peptides undergo fragmentation, a process called collision induced fragmentation (CID). Figure 2.1 shows a schematic representation of the possible fragmentation of the peptide backbone. The nomenclature was proposed by Roepstorff (Roepstorff and Fohlman, 1984) and modified by (Biemann, 1990). Upon fragmentation of a peptide, the charge is retained either by the N- or the C-terminal

side of the molecule. Fragments are named a, b, c in the first case and x, y, z in the latter case. In addition, amino acids such as Pro and carbamidomethylated Cys are prone to generate internal fragment ions. Internal fragments are the result of a double cleavage of the peptide backbone while the central part retains the charge.

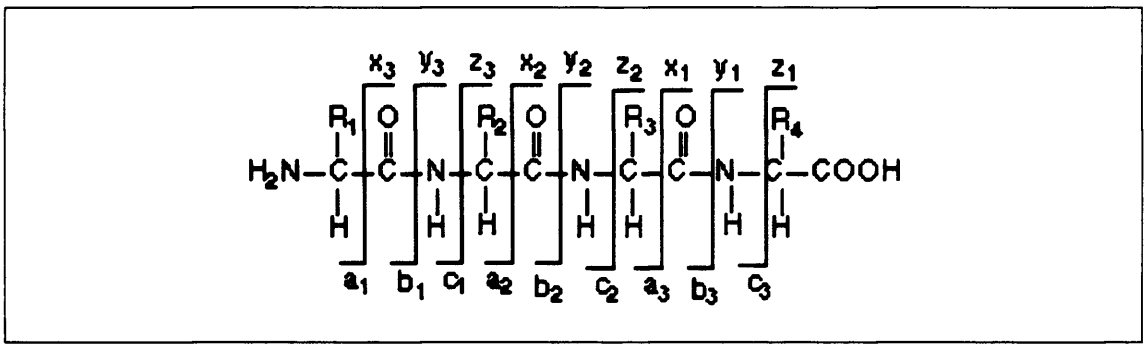

Figure 2.1: Labelling of fragment ions
Ion fragments formed through bond cleavages along the backbone of protonated linear peptides. The labelling of fragment ions in this study will be based upon the generally accepted nomenclature developed by (Biemann, 1990).

When phosphorylated peptides are fragmented under CID conditions, loss of phosphate is frequently the primary mode of fragmentation (Mann et al., 2002). This neutral loss of 80 (HPO_3) or 98 (H_3PO_4) is due to a cleavage at either side of the phospho-ester bond. pSer and pThr readily loose phosphoric acid, H_3PO_4, generating dehydroalanine and dehydroamino-2-butyric acid, respectively. pTyr cannot loose the phosphoric acid as that means disintegrating the aromatic ring, but it looses HPO_3. Due to the energy distribution of the aromatic ring, pTyr is more stable than pSer or pThr. Therefore, pTyr-peptide fragment ions are less abundant and more difficult to detect.

ESI precursor ions are multiply-charged with the distribution of charge states dependent upon both peptide structural properties and instrumentation parameters. Because MALDI ions are singly-charged for the most part, their fragmentation spectra are often dominated by signals arising from cleavage at the acidic residues and sometimes not enough information is present to establish the peptide sequence conclusively. For this reason, we mainly used ESI to perform MS/MS.

2.16.4.1 Data dependent acquisition

If unknown proteins were identified or primary analyses of post-translational modifications performed, data dependent acquisition using the Q-TOF was chosen. Data dependent acquisition allows for the automatic switching from MS to MS/MS experiments whenever an ion of pre-determined nature is detected. We usually set the ion count threshold for switching from MS to MS/MS to 20-40 counts depending on the sample.

2.16.4.2 Multiple reaction monitoring

By performing multiple reaction monitoring (MRM), the mass spectrometer is set to scan over a very small mass range, typically one mass unit. Only one or a few selected m/z (depending on the experimental set-up) are set for detection per run and subsequently chosen by the mass analyser for further fragmentation.

MRM was performed with the Q-TOF, Q-STAR or Q-TRAP. MRM was performed on potential phospho-peptide ions by calculating the precursor mass and daughter mass for the loss of HPO_4 (80 Da) from Tyr phosphorylated peptides. For the Q-TRAP instrument, the MRM builder script (MDS-SCIEX) was used to calculate the precursor and daughter masses, along with the required collision energies. The 4000 Q-TRAP was run in positive ion mode with unit resolution in both Q1 and Q3 and the dwell time for each transition was set to 25 ms up to a total of 80 predicted Tyr phosphorylated peptide ions for a 2 s duty cycle.

MRM experiments were also performed for AQUA peptides and endogenous peptides. The required collision energy was determined empirically for the Q-TOF and Q-STAR, starting from 20 V for m/z = 300 up to 35 V for m/z = 1000. The scan time was set to 0.2 s and the interscan delay to 0.05 s.

2.16.4.3 Precursor-ion scanning on a 4000 Q-TRAP

In precursor-ion scanning, a parent ion that gives rise to the diagnostic fragment ions created by collisions in q2, is selectively detected in the third quadrupole (Q3) of a triple quadrupole instrument. For phosphopeptide analysis, scanning is performed in the negative ion mode. The first quadrupole is scanned over the full mass range and CID is induced in the second quadrupole filled with inert gas. The third quadrupole is set to detect the fragment ions of 79.

Precursor-ion scanning experiments are also possible with Q-TRAP instruments, in which Q3 is replaced by a linear ion trap. Precursor-ion scanning experiments in this thesis were performed on a 4000 Q-TRAP collaboration with Dr Nick Morrice, MRC Protein Phosphorylation unit, University of Dundee, Dundee. The following protocol was used:

Precursor-ion scanning was performed over a mass range of m/z 400-2000 at 500 amu/s, with a ionspray voltage of -2200 V applied to a Picotip FS360-50-15-N (NEW OBJECTIVE) along with ionspray gas (nitrogen). Precursors were collided in q2 with a collision energy ramp of -65-110 V across the mass range. Once precursors of 79 were detected (with a minimum threshold of 2000 cps), the polarity was automatically switched to +2300V (after a 700 ms dwell at 0 V) with the same gas settings and a positive ion enhanced resolution scan was performed at 250 amu/s to determine the charge state of the ion. Enhanced product ion scans (MS/MS) were performed at 4000

amu/s and collision voltages were calculated automatically. Once this duty cycle was completed, the polarity was switched back to negative (after a 700 ms dwell at 0 V) and the cycle repeated.

2.16.4.4 Absolute quantification

Absolute quantitation (AQUA) of endogenous protein by LC-MS can be achieved by comparing peak areas of endogenous peptide with those of known amounts of standard peptide possessing the same amino acid sequence (Barnidge et al., 2003; Barr et al., 1996; Gerber et al., 2003). In contrast to the endogenous peptide, the standard (=AQUA) peptide is synthesised using stable isotopes. While most biophysical properties of the endogenous and AQUA peptide are identical (e.g. the elution from RP-columns and ionisation potential), they differ in molecular weight and therefore in m/z. This difference is subsequently detected by MS and used to distinguish between the endogenous and the AQUA peptide. The work flow of a typical AQUA experiment is depicted in Figure 2.2.

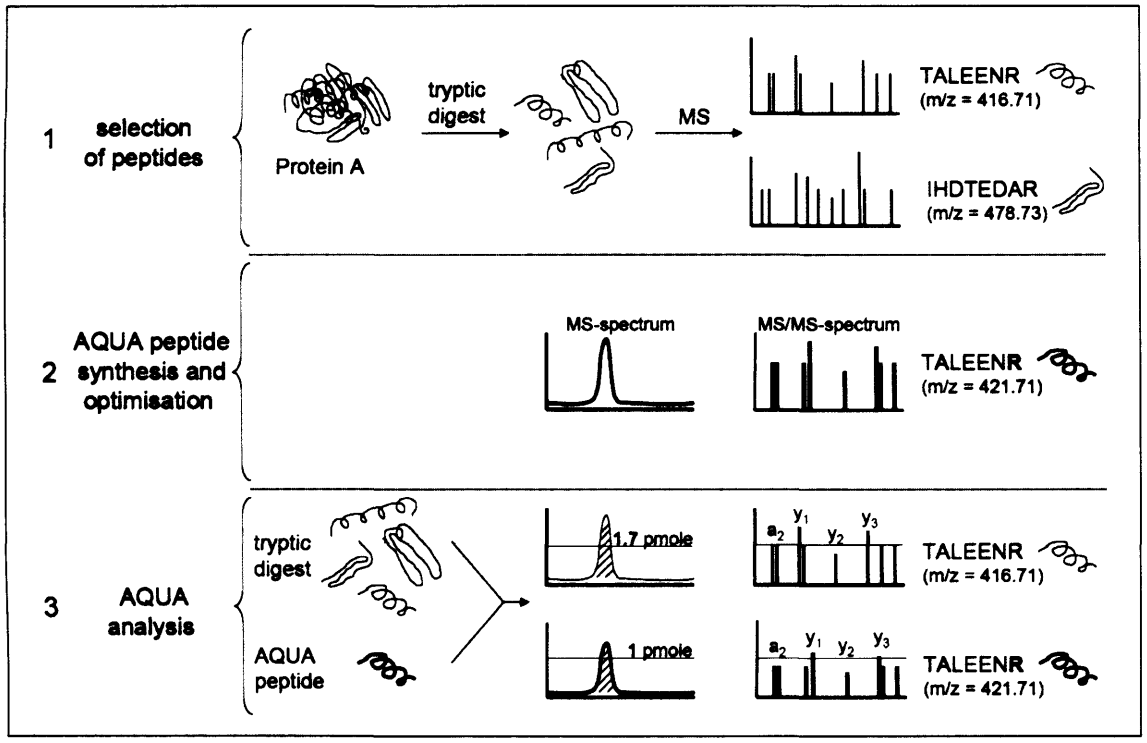

Figure 2.2: Work flow of absolute quantitation (AQUA) MS

In a first step, endogenous peptides of the protein of interest detected by MS are selected for AQUA synthesis based on their detection frequency, amino acid sequence and non-redundancy. In a second step, the isotopically labelled AQUA peptides are analysed for their elution profile from RP-columns, MS/MS-spectrum, detection limit and purity. In a third step, known amounts of AQUA peptides are spiked to protein samples. Endogenous and AQUA peptide are analysed by LC-MS or LC-MS/MS. Comparison of AQUA peptide peak areas with endogenous peptide peak areas permits absolute quantitation of endogenous peptide and protein, respectively.

In a first step, suitable peptides of the protein of interest are selected. The selection is based on the frequency with which the peptide is detected in LC-MS/MS runs in different samples, on the quality of the MS/MS data, on the amino acid composition of the peptide (no Met, Cys and Try due to their chemical reactivity; no Asp-Gly, N-term Gln, N-term Asn due to their chemical instability), on its non-redundancy and on the occurrence of the peptide in different species.

In a second step, the AQUA peptides are diluted in 0.1% formic acid to 10 pmole/µl and subsequently analysed by MALDI and ESI for their molecular weight, purity, elution profile, and MS/MS spectrum.

In a third step, the AQUA peptides are spiked to the protein samples before trypsination (2.16.2) and analysed by LC-MS or LC-MRM. Integrated peak areas of endogenous and AQUA peptide were extracted by MassLynx (WATERS) Quantify software.

2.16.5 Data mining

2.16.5.1 Peak list extraction of MS/MS data

The peak list was created by automatic extraction of all MS/MS data using ProteinLynx of Masslynx V4.0 software (MICROMASS, WATERS). The m/z peaks were centred using background subtraction (35% below the curve), smoothing (Savitzky Golay, 2 smoothings), and 80% percent of peak height for centroids. The output file was generated as a Micromass peaklist in a Mascot compatible file.

2.16.5.2 Database searches

All MS/MS spectra acquired in data-dependent acquisition, precursor-ion scanning or MRM mode were searched against public databases (NCBInr) using the Mascot search engine (MATRIXSCIENCE) run on a local server. Sites of phosphorylation were assigned from manual interpretation of the MS/MS spectra viewed using Masslynx V4.0 software.

The following parameters were generally applied:

The chosen database was NCBInr, with the restriction of *mus musculus* as species. Up to 2 miss-cleavages were allowed after digestion with trypsin, adding carbamidomethylation of Cys as a fixed modification and N-acetylation of protein; oxidation of Met; phosphorylation of Ser, Thr, Tyr, and N-terminal pyro-glutamation as variable modifications. The precursor-ion mass and fragment ion mass accuracy were set to a tolerance of 100 ppm and 100 mmu, respectively.

If other modifications than phosphorylation were analysed, variable modifications were uploaded from the Mascot webserver.

2.16.5.3 Interpretation of MS/MS data output

Protein hits generated by MS/MS data were considered if the MOWSE score (Pappin et al., 1993) of a protein hit was above 40 and at least 2 peptides were identified.

Sites of phosphorylation were assigned from manual interpretation of the MS/MS spectra viewed using MassLynx V4.0 (MICROMASS).

.

3 A NEW TOOL TO PURIFY CLASS IA PI3K

The aim of this study was to 1) investigate post-translational modifications of class IA PI3K and to 2) analyse the molar equilibrium between class IA PI3K regulatory and catalytic subunits using MS amongst other techniques. Protein identification by LC-MS/MS requires approximately 100 ng of protein following SDS-PAGE. Since the stoichiometry of protein phosphorylation is usually low, identification of post-translational modifications presupposes even more protein quantities. Therefore, efficient protein purification methods are required.

One possibility to enrich for proteins is the application of immunoprecipitation (IP) with protein-specific Abs. A variety of PI3K isoform-specific Abs was available at the host laboratory. However, protein purification by IP has disadvantages: first, large-scale IP can be limited by the restricted availability of Abs. And second, high purity of immunoprecipitates might not be ensured by using Abs due to Ab cross-reaction with unspecific proteins.

Another method to purify class IA PI3K is based on the interaction of the two SH2 domains of the regulatory subunit of class IA PI3K with phosphorylated Tyr (pTyr) residues in the cytosolic domain of receptors. PI3Ks were first purified using immobilised full-length PDGF-receptor (Escobedo et al., 1991), which method was subsequently replaced by enrichment of the proteins with short, synthesised PDGF-receptor peptides containing pTyr residues known to be autophosphorylated in activated receptors and coupled to Actigel resin (Fry et al., 1992). Using restricted sequences of the PDGF-receptor instead of whole polypeptides allowed for a greater degree of specificity and higher density of affinity groups per unit volume of the column. The same study also showed that only peptides containing pTyr residues in YxxM-motifs were able to bind class IA PI3Ks. The potential binding sites of PI3K to the human PDGF-β-receptor were further restricted to Y740 and Y751 (Klinghoffer et al., 1996).

Because preliminary results obtained by incubation of cell lysate with synthesised PDGF-R-peptides of the sequence pYVPMLG coupled to Actigel did not reveal purification of pure and/or large quantities of class IA PI3Ks, we designed an alternative purification tool based on the interaction of the regulatory subunit with pYxxM-motifs. Three PDGF-receptor peptides of different lengths all containing at least Y751 of the human PDGF-β-receptor were generated (Figure 3.3; for general workflow see Figure 3.1). The constructs were cloned to the 3' end of the glutathione S-transferase (GST) gene that was under the control of the tac promoter in the plasmid pGEX-4T-2 (AMERSHAM PHARMACIA BIOTECH). Plasmids containing the GST-tagged

PDGF-β-receptor peptide were subsequently transformed into the *E. coli* strain TKB1 (STRATAGENE), which carries a plasmid-encoded, inducible Tyr kinase gene. Following induction of PDGF-receptor-peptide and Tyr kinase gene expression by IPTG, Tyr residues in the PDGF-receptor peptide were phosphorylated by the Tyr kinase. The phosphorylated GST-PDGF-receptor peptides were then affinity purified using glutathione sepharose beads. Murine cell extract was added to the GST-PDGF-receptor peptide-beads (further referred to as 'pTyr-matrix'), and class IA PI3K was purified by interaction of the regulatory subunit with the pTyr residues of the GST-PDGF-receptor peptides in the pTyr-matrix. Below, we describe the cloning and biochemical assessment of the 3 GST-PDGF-receptor-peptides.

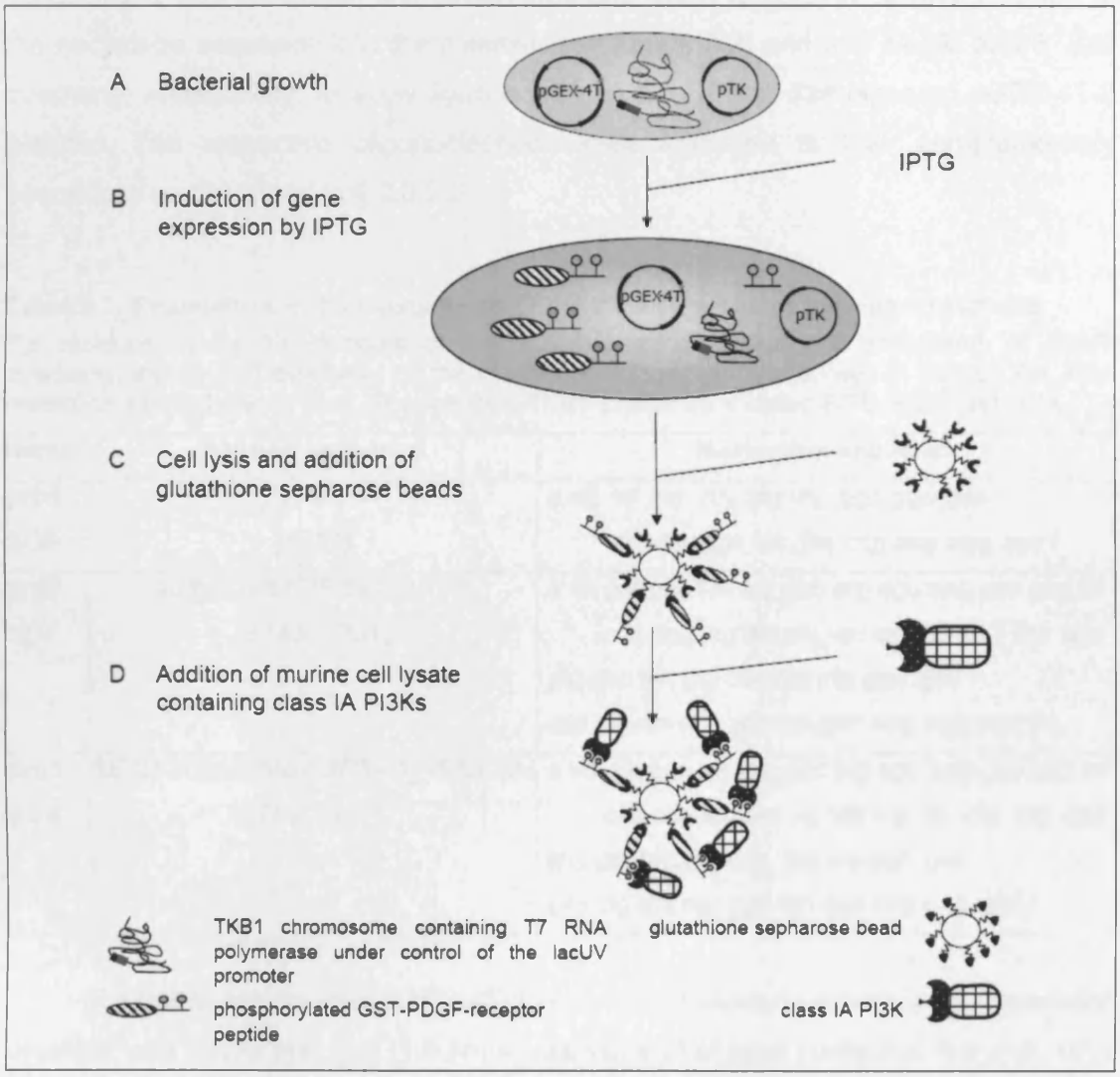

Figure 3.1: Workflow of class IA PI3K purification

(A) Bacterial strains BG6, BG7, BG8 containing different PDGF-receptor peptide lengths were grown and (B) expression of GST-PDGF-peptide and Tyr kinase induced by addition of IPTG. (C) Glutathione sepharose beads were incubated with the bacterial cell lysate allowing for binding of the PDGF-receptor peptide to the beads via its GST-tag. (D) The pTyr-matrix was combined with cell lysate. Class IA PI3Ks were purified by binding of the regulatory subunit to the pTyr residues of the GST-PDGF-receptor peptides.

3.1 Cloning the GST-PDGF-receptor peptides

Previous experiments with biotinylated, phosphorylated PDGF-receptor peptides have indicated that PDGF-receptor peptides of short length (6 amino acids) might not allow access of the regulatory subunit SH2 domains to the pTyr residue lying in proximity of the biotin-tag, and long PDGF-receptor peptides (24 amino acids) might cause peptide aggregation (G. Panayotou, unpublished work).

Therefore, we chose to generate constructs containing PDGF-receptor peptides with three different lengths, called prp1 (PDGF-receptor peptide 1), prp2, and prp3 (peptide and nucleotide sequence provided in Table 3.1).

Nucleotide sequences corresponding to the peptide sequences were designed containing a *NarI* restriction site (which was later used to confirm correct insertion of the nucleotide sequence into the plasmid, see Figure 3.3) and a 5' *EcoRI* and 3' *SalI* overhang, respectively, to allow ligation with an *EcoRI* and *SalI* digested pGEX-4T-2 plasmid. The respective oligonucleotides were annealed to their complementary sequences as described in § 2.8.2.2.

Table 3.1: Peptide/nucleotide sequences of the 3 PDGF-receptor peptide constructs
Tyr residues in the YxxM-motifs of the PDGF-receptor peptide are underlined. 5' *EcoRI* overhang and 3' *SalI* overhang of the nucleotide sequences are shown in italics. The *NarI* restriction site is drawn in bold. The resulting TKB1 strains were called BG6, BG7, and BG8.

Name	Peptide sequence	Nucleotide sequence
prp1 BG6	YVPMLG (Y751)	*a att* tat gtg ccg atg ctg ggc **ggc gcc** ata cac ggc tac gac ccg **ccg cgg** *agc t*
prp2 BG7	GGYMDMSKDESVDYVPML (Y740, Y751)	*a att* ggt ggc tac atg gac atg agc aag gac gag tct cca ccg atg tac ctg tac tcg ttc ctg ctc aga gtg gac tat gtg ccg atg ctg **ggc gcc** cac ctg ata cac ggc tac gac **ccg cgg** *agc t*
prp3 BG8	GESDGGYMDMSKDESVDYVPMLDM (740, Y751)	*a att* ggt ggc tac atg gac atg agc aag gac gag tct cca ccg atg tac ctg tac tcg ttc ctg ctc aga gtg gac tat gtg ccg atg ctg **ggc gcc** cac ctg ata cac ggc tac gac **ccg cgg** *agc t*

In parallel, the plasmid pGEX-4T-2 (AMERSHAM PHARMACIA BIOTECH) was restriction digested with *EcoRI* and *SalI* (1.8 pmol plasmid, 4 µl of each restriction enzyme, 10 µl restriction buffer, made up in 100 µl ddH_2O) for 3 h at 37°C as described in § 2.8.2.1. pGEX-4T-2 contains the GST gene under the control of a tac promoter (a strong hybrid promoter composed of the -35 region of the trp promoter and the -10 region of the lacUV5 promoter/operator), a multiple cloning site at the 3' end of the GST gene, the Amp resistance gene β-lactamase and the lacI repressor gene (see Figure 3.3). GST

belongs to a family of multifunctional enzymes present in all living organisms whose main function is the detoxification of electrophilic compounds, but is used in molecular biology as a protein tag because of its ability to interact in a high-affinity binding with the glutathione tripeptide (ECG) coupled to sepharose (Smith and Johnson, 1988).

The digested plasmid DNA was resolved by electrophoresis in a 0.9% agarose gel and the desired plasmid fragments purified from the gel using the SIGMA QIAquick Gel Extraction Kit. The annealed oligonucleotides prp1, prp2, and prp3 were subsequently ligated into the restricted vector pGEX-4T-2 using 3 different insert-to-vector ratios (350/1, 35/1, 3.5/1). One sample containing no insert was used as a negative control. Ligation was performed as described in § 2.8.2.2.

In order to confirm insertion of the oligonucleotides into pGEX-4T-2 (the resulting constructs were called gprp1, gprp2, and gprp3 on plasmid pBG1, pBG2, and pBG3), the ligation mix was transformed into 100 µl competent XL1-blue *E. coli* cells (STRATAGENE) using 10 µl of ligation mix (samples and negative control) and 1 µl of pGEX-4T-2 as a positive control as described in § 2.8.3 and plated onto Amp-containing LA-plates. 5 colonies of each construct were picked, dipped into 100 µl Amp-containing LB in eppendorf tubes and streaked out on Amp-containing LA-plates. The eppendorf tubes were incubated for 2 h at 37°C with shaking and then boiled at 100°C for 5 min. 5 µl of the culture were added to a PCR mix containing the 5'- and 3'-pGEX sequencing primers (AMERSHAM PHARMACIA BIOTECH) and the PCR reaction was performed as described in § 2.8.4. 10 µl of the samples was analysed by gel electrophoresis at 100 V for 5 h in a 4% NuSieve gel (§ 2.8.1.3). As shown in Figure 3.2, the expected PCR products of 202 bp for pBG1, 238 bp for pBG2, and 256 bp for pBG3 could be detected in the majority of samples analysed.

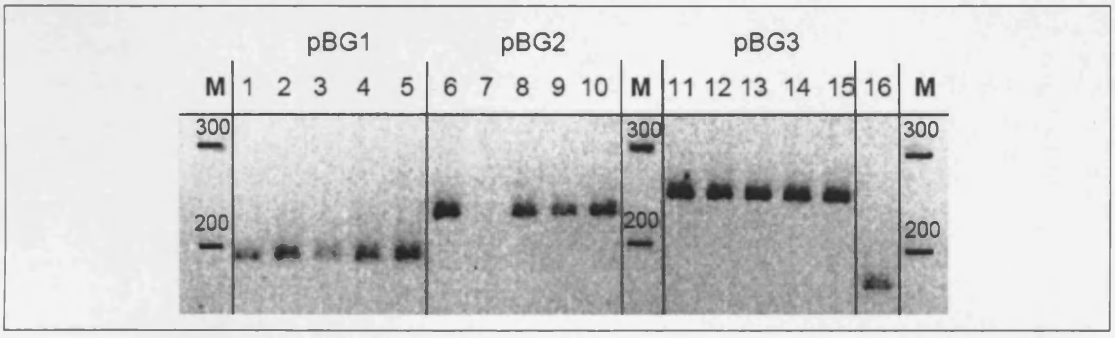

Figure 3.2: Confirmation of correct insertion of prp1, prp2, prp3 into pGEX-4T-2 by NuSieve gel electrophoresis

After transformation of pBG1, pBG2, pBG3 (the three pGEX-4T-2 plasmids containing prp1, prp2, prp3) into competent *E. coli* cells (XL1-blue), 5 colonies resulting from each transformation and 1 colony of the vector only positive control (sample #16) were subjected to PCR with 5'- and 3'-pGEX sequencing primers. The PCR products were analysed after electrophoresis for 5 h at 100 V on a 4% NuSieve agarose gel and corresponded to the expected sizes of 202 bp for sample #1-5 (pBG1), 238 bp for sample #6-10 (pBG2), and 256 bp for sample for #11-15 (pBG3). A low range marker (M) was used to determine the relative size of the PCR products.

Plasmids were extracted from two colonies of each construct containing the insert (colony #1 and #3 of the pBG1 construct, #6 and #8 of pBG2, and #13 and #15 of pBG3) by using the small-scale preparations of plasmid DNA method (§ 2.8.1.1). A restriction digest was performed with *NarI* to confirm correct insertion. The two *NarI* restriction sites of pBG1, pBG2, and pBG3 are shown in Figure 3.3. Two resulting nucleotide fragments of the expected sizes 3130 bp and 1870 bp were detected in all restricted plasmids after agarose gel electrophoresis (data not shown). Each of the two plasmids was subsequently sequenced using 5'- and 3'-pGEX sequencing primers. Plasmids of colony #1, colony #6 and colony #15 contained perfect sequences (data not shown) and were further used. The three XL1-blue strains containing these plasmids were called BG1, BG2, and BG3.

pBG1, pBG2 and pBG3 were transformed into the competent *E. coli* TKB1 strain (STRATAGENE) according to the manufacturer's protocol. TKB1 is a BL21 *E. coli* strain that harbours the gene for T7 RNA polymerase in the chromosome under the control of the lacUV5 promoter and also carries a plasmid-encoded, inducible Tyr kinase gene.

In order to verify correct transformation, the plasmids of the transformed colonies were analysed by PCR, *NarI* restriction digestion and DNA sequencing as described above (data not shown). The TKB1 strains containing perfect sequences of pBG1, pBG2 and pBG3 were called BG6, BG7, and BG8, respectively.

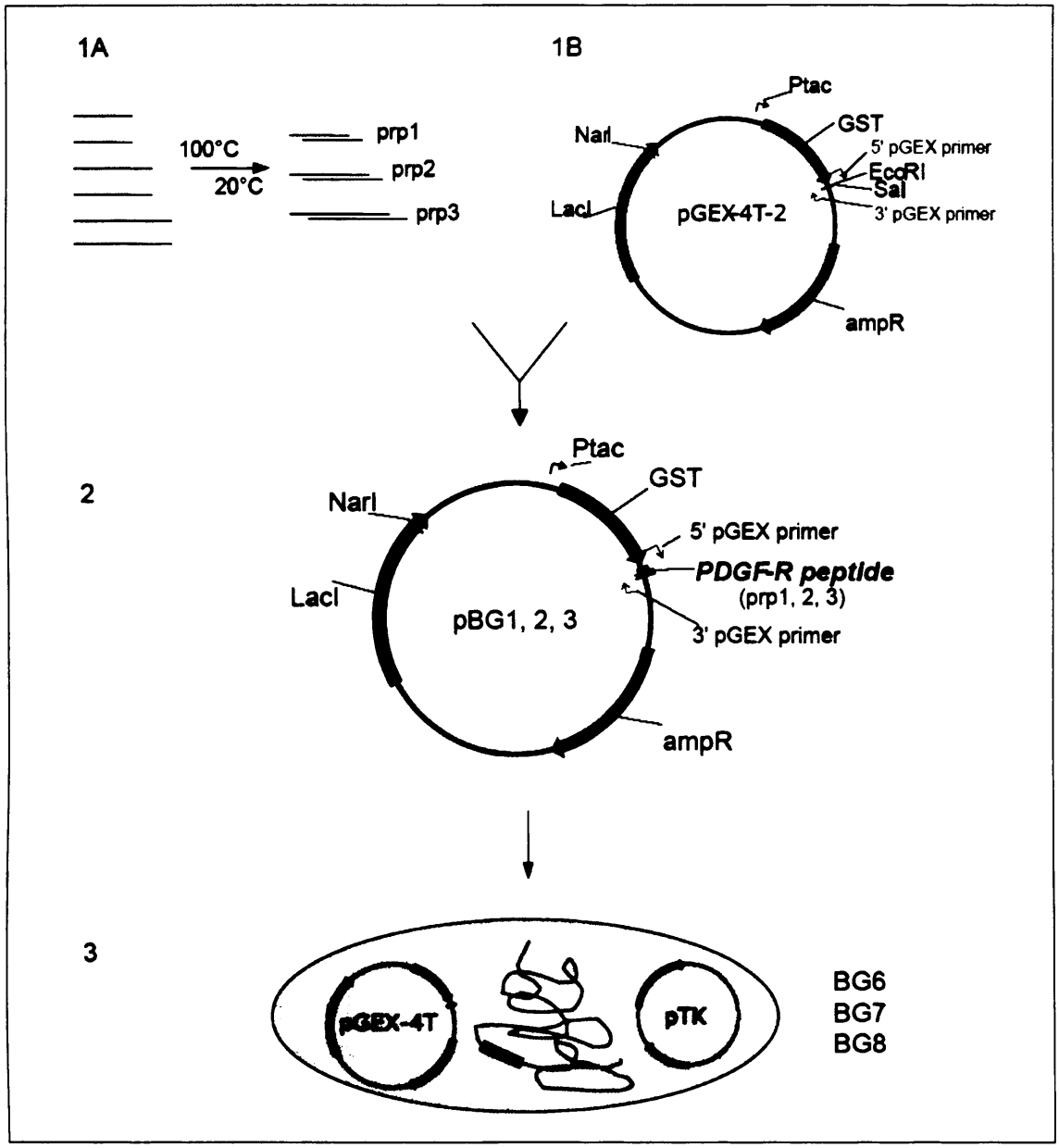

Figure 3.3: Schematic drawing of the cloning procedure leading to TKB1 strains BG6, BG7, and BG8

(1A) The nucleotide sequences of three different PDGF-receptor peptides all containing at least one YxxM-motif were annealed and (1B) the plasmid pGEX-4T-2 restriction digested with *EcoRI* and *SalI*. (2) The 3 constructs prp1, prp2 and prp3 were ligated to the 3' end of the GST gene in pGEX-4T-2 leading to plasmids pBG1, pBG2 and pBG3. (3) The constructs were subsequently transformed into TKB1, an *E. coli* strain carrying an inducible Tyr kinase gene, leading to bacterial strains BG6, BG7, and BG8.

3.2 Assessment of optimal conditions to prepare pTyr-matrix

Before analysing the ability of the affinity system to purify class IA PI3K, we investigated the optimal conditions to prepare pTyr-matrix. First, induction of expression and phosphorylation of the GST-PDGF-receptor peptides (Figure 3.4) and

in a second experiment binding of GST-PDGF-receptor peptides to glutathione sepharose beads (Figure 3.5) were assessed.

The expression of the GST-PDGF-receptor peptides as well as of the Tyr kinase was induced in BG6, BG7 and BG8 by addition of IPTG to the culture medium. Expression of T7 RNA polymerase in TKB1 strains containing GST-tagged PDGF-β-receptor peptides was repressed under normal culture conditions by the LacI protein that binds to the lac promoter. Upon addition of the β-galactosidase isopropyl-beta-D-thiogalactopyranoside (IPTG) to the medium, IPTG binds to the LacI repressor and inhibits its interaction with the lac promoter. T7 RNA polymerase expression occurs and controls protein expression of genes placed downstream of the T7 RNA polymerase binding sites, which was in TKB1 the plasmid-encoded Tyr kinase gene. Additionally, LacI inactivation by IPTG led in our system to the expression of the transformed GST-PDGF-receptor peptide. Its Tyr residues were subsequently phosphorylated by the Tyr kinase.

The manufacturer's protocol (STRATAGENE) was used as a guideline. Briefly, 3 ml Tet- and Amp-containing LB medium was inoculated with BG6, BG7, or BG8 and the cells were grown overnight at 37°C. The bacterial suspension was diluted 1:15 the following day. After 1 h of growth, a sample was removed as uninduced control and the expression and phosphorylation of the GST-PDGF-receptor peptides was induced by addition of IPTG (end concentration 0.4 mM). The culture was further incubated at 37°C for 3-4 h.

Protein expression of all three GST-PDGF-receptor peptides was highly induced after 3 h of IPTG addition (Figure 3.4.A) as determined after resolving protein of BG6, BG7, and BG8 whole cell lysates minus or plus 0.4 mM IPTG on a 15% SDS polyacrylamide gel and staining the protein with Coomassie blue. The shift in protein motility of the different constructs in the 15% SDS polyacrylamide gel corresponds to the moderate difference in size between the 3 constructs with theoretical molecular weights of 27.7 kDa, 28.9 kDa and 29.7 kDa.

In order to analyse the induction of Tyr phosphorylation of the GST-PDGF-receptor peptides, proteins of whole cell lysates of BG6, BG7, and BG8 minus IPTG and 1, 2 and 3 h after IPTG stimulation were separated on a 15% SDS-polyacrylamide gel. The proteins were transferred to a PVDF membrane and analysed for Tyr phosphorylation by immunoblottig using pTyr Ab 4G10 (§ 2.3). As shown in Figure 3.4.B, induction of GST-PDGF-receptor peptide phosphorylation was very efficient. After 1 h, peptide phosphorylation, which was not completely abolished in uninduced cells, had doubled, and after 3 h at least five times as many Tyr residues in the construct were phosphorylated.

We could not detect any major difference in the capacity to be expressed or phosphorylated between the three different GST-PDGF-receptor peptides.

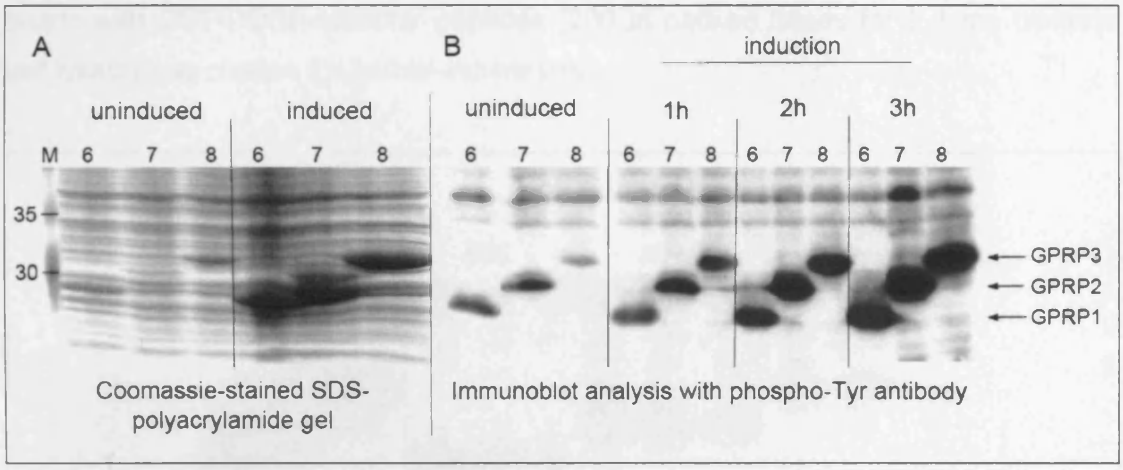

Figure 3.4: GST-PDGF-receptor peptide expression (A) and phosphorylation (B) are greatly induced after IPTG addition to bacterial cell culture medium

(A) Proteins of whole cell lysates of approximately 6 x 10^8 BG6, BG7, BG8 cells were analysed on a 15% SDS polyacrylamide gel before and after IPTG induction. Proteins were detected by Coomassie staining. (B) Proteins of BG6, BG7, and BG8 cell lysates treated without or with IPTG for the indicated times were resolved on a 15% SDS polyacrylamide gel, transferred to a PVDF membrane and subjected to immunoblotting with the pTyr Ab 4G10. Each sample contained approximately 6 x 10^7 cells.

In order to determine the binding capacity of the GST-PDGF-receptor peptides to glutathione sepharose beads, we performed a titration experiment. The three strains BG6, BG7, BG8 were grown and GST-PDGF-receptor peptide expression and phosphorylation induced as described above. After 4 h of IPTG induction, the cells were harvested, resuspended in PBS containing 1 mg/ml lysozyme and inhibitors (ROCHE, complete tablet) and sonicated in order to break open the cell walls. The cell lysate was centrifuged to clear it from debris, the protein concentration determined, and a sample of total cell lysate (TCL) removed for analysis. 0.4 mg of total bacterial protein of each strain was incubated with increasing volumes of glutathione sepharose beads (50, 100, 200 μl) for 2 h at 4°C. After incubation, the glutathione sepharose beads were harvested by centrifugation and the same volume of unbound fraction (supernatant, SN) was compared to TLC by immunoblotting with pTyr Ab after the proteins in samples TCL and SN were resolved by SDS-PAGE and transferred to PVDF membrane. As shown in Figure 3.5, the phosphorylated GST-PDGF-receptor peptide amount contained in the unbound fractions decreased with increasing glutathione sepharose bead volumes for each strain. 50 μl of glutathione sepharose beads bound approximately $^2/_3$ of phosphorylated GST-PDGF-receptor peptides in 0.4 mg total bacterial protein, whereas 200 μl of glutathione sepharose beads was capable of interacting with at least $^3/_4$ of phosphorylated GST-PDGF-receptor peptides. However,

even 200 µl sepharose beads did not bind all GST-PDGF-receptor peptides in 0.4 mg total bacterial protein. Since the aim of developing the pTyr-matrix was to enrich for as much class IA PI3K as possible, the ratio ensuring complete saturation of sepharose beads with GST-PDGF-receptor peptides (200 µl packed beads for 0.4 mg bacterial cell lysate) was chosen for further experiments.

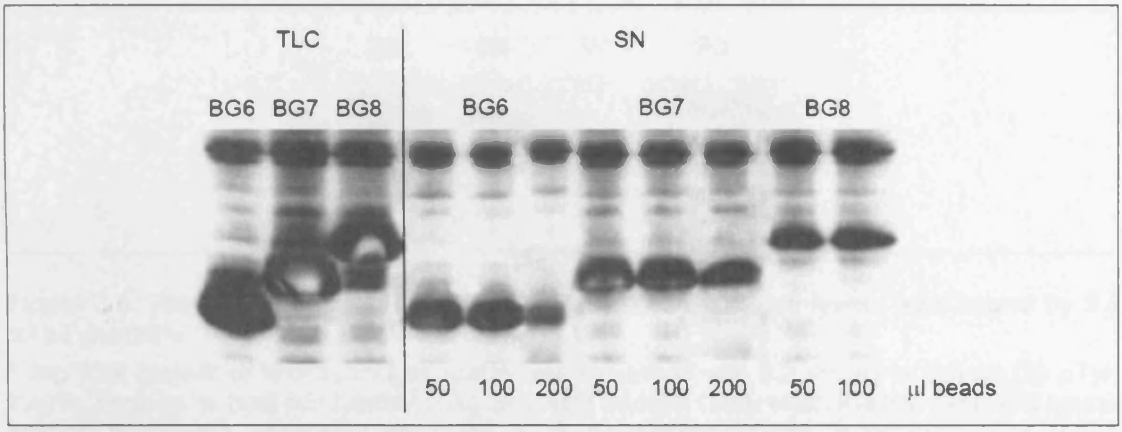

Figure 3.5: Titration experiment assessing the binding capacity of sepharose beads to GST-PDGF-receptor peptides

BG6, BG7, BG8 treated with IPTG were lysed and the protein lysate corresponding to 0.4 mg total protein incubated with 50, 100, and 200 µl glutathione sepharose beads. The total cell lysate (TCL) and unbound fraction (SN) samples containing the same volume were resolved on a 15% SDS polyacrylamide gel, transferred to a PVDF membrane and analysed with the pTyr Ab 4G10. For BG8, only unbound fractions of 50 and 100 µl were analysed.

3.3 Optimal ratio of pTyr-matrix to p110δ protein

As demonstrated in the previous two experiments, the induction of expression, phosphorylation and the binding to glutathione sepharose beads were similar for the three different GST-PDGF-receptor peptide constructs. In order to reduce the complexity of the experiments, we decided to perform the assessments of how much pTyr-matrix was needed to deplete PI3K from murine lysate with BG7 alone. BG7 is the TKB1 strain possessing the medium sized PDGF-receptor peptide. Since we were mainly interested in p110δ, we analysed the pull-down capacity of the pTyr-matrix towards this class IA PI3K isoform.

For this purpose, 5 mg total protein of WEHI-231 B cell lysate (§ 2.10) was incubated with 0.2 ml and 0.5 ml pTyr-matrix, respectively, for 3 h at 4°C. After incubation, the sepharose beads were harvested and washed four times with lysis buffer plus inhibitors. The proteins of total cell lysate (TCL), unbound fraction (SN), wash fraction (W) and bound fraction (PD) were separated by SDS-PAGE, transferred to a PVDF membrane and analysed with a C-terminal p110δ Ab by immunoblotting.

A small amount of free p110δ could be observed in SN if 0.2 ml glutathione pTyr-matrix was added to 5 mg B cell lysate (Figure 3.6.A), whereas most p110δ bound to the glutathione sepharose beads if 0.5 ml pTyr-matrix was used (Figure 3.6.B). Equal amounts of cell lysate were loaded onto the SDS polyacrylamide gel in the TCL and SN sample, whereas three times more volume was loaded in the wash sample (W).

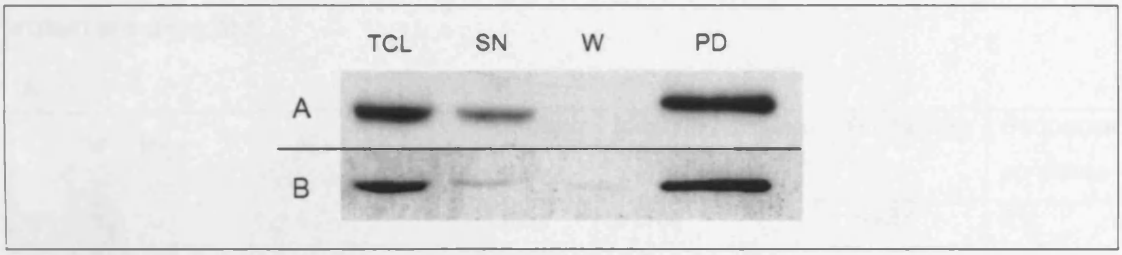

Figure 3.6: The majority of p110δ protein in 5 mg WEHI-231 cell lysate was bound by 0.5 ml pTyr-matrix

5 mg total protein of WEHI-231 cell lysate was incubated with 0.2 ml (A) or 0.5 ml (B) pTyr-matrix. Proteins in total cell lysate (TCL), unbound fraction (SN), wash fraction (W), and bound fraction (PD) were separated on a 8% SDS polyacrylamide gel, transferred to a PVDF membrane and analysed by immunoblotting using CT-p110δ Ab. Same volumes of TLC and SN were loaded. Three times more W and 5 times more PD were loaded per lane.

3.4 Identification of proteins affinity purified by pTyr-matrix

After adaptation and improvement of the most important steps in the purification procedure, we separated the proteins bound to the pTyr-matrix by gel electrophoresis and analysed the protein content by colloidal Coomassie blue staining. 1 ml of pTyr-matrix was incubated with 4 mg induced bacterial protein and 12 mg WEHI-231 lysate was added. Two distinct bands at M_r 110 kDa and 85 kDa were detected. However, many additional protein bands were also observed (data not shown).

It has previously been shown that the interaction between endogenous p85 and phosphorylated PDGF-receptor is of high affinity (Escobedo et al., 1991) and that the interaction is resistant to treatment with solutions containing 2 M NaCl plus 0.5% Triton X-100, 5 M NaCl, 6 M urea, 50 mM pTyr or up to 1 mg of free Y751 phosphopeptide (Fry et al., 1992). We therefore incubated the pTyr-matrix binding p85/p110 with 1 x lysis buffer containing 5 M salt. This additional wash step reduced unspecific binding of proteins to the pTyr-matrix.

As shown in Figure 3.7.A, four major protein bands were detected on a SDS polyacrylamide gel after staining with colloidal Coomassie blue when class IA PI3Ks were purified using the pTyr-matrix generated in BG7. The proteins were cut from the gel, reduced, alkylated, subjected to tryptic in-gel digestion and analysed by LC-MS/MS (§ 2.14, § 2.16). Blasting the sequencing information gained from a full-scan acquisition

against the NCBI database NCBInr using the Mascot program (MATRIXSCIENCE) led to the identification of the following proteins: The protein detected at M_r of 110 kDa was identified as p110β and p110δ, the protein band labelled #2 contained p85α and p85β, protein band #3 was identified as member of the Hsp70 family (see also Table 5.1) and protein band #4 was elongation factor-1γ (see also Table 5.1). In Figure 3.7.B, the significance of the MS results and the coverage of the identified peptides for each protein are depicted.

A

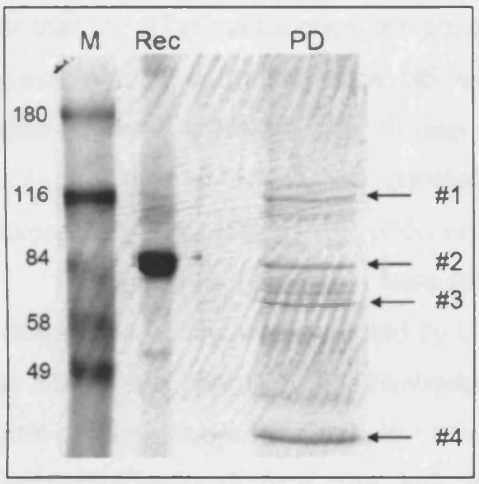

B

Protein band	Identified protein	Probability	Sequence coverage
#1	p110δ	2e-37	8%
	p110β	3e-5	1%
#2	p85α	1e-56	22%
	p85β	1e-25	8%
#3	Hsp70	8e-64	21%
#4	Elongation factor-1γ	8e-67	30%

Figure 3.7: Identification of class IA PI3Ks by LC-MS/MS after pTyr-matrix pulldown
(A) Proteins pulled down by the pTyr-matrix from WEHI-231 cell lysates were separated by SDS-PAGE and stained with colloidal Coomassie blue. The 4 major bands were cut from the gel and the proteins reduced, alkylated, tryptic in-gel digested and subjected to LC-MS/MS. Recombinant class IA PI3K was loaded onto the gel as a control. (B) The table lists the proteins identified by MS, the significance of the obtained MS results and the percentage of sequence coverage for each protein.

3.5 Discussion

Here we present a new class IA PI3K purification tool. It is based on the interaction of phosphorylated YxxM-motifs located in the cytosolic domain of the PDGF-receptor with the two SH2 domains of the regulatory subunit of PI3K. Instead of using synthesised, phosphorylated PDGF-receptor peptides, which were not successful for large-scale purification in our hands, we developed a bacterial system that is expressing and phosphorylating these PDGF-receptor peptides linked to GST protein. The construct can subsequently be purified with glutathione sepharose from bacterial lysate and be incubated with eukaryotic cell lysate to enrich for class IA PI3K.

Because it had previously been reported that short YxxM-containing peptides might be less able to recruit p85 and long YxxM-containing peptides seem to possess a low solubility, we generated three PDGF-receptor peptides of different lengths. These constructs were analysed in parallel for their protein expression level, their ability to

become Tyr phosphorylated and their binding capacity to glutathione sepharose. The constructs performed equally in these experiments.

MS analysis of the four major protein bands pulled down by the pTyr-matrix led to the identification of class IA PI3K. However, p110α was not identified in the 110 kDa protein band and it was also not possible to detect a protein band at 50-55 kDa corresponding to p55α, p50α and p55γ following Coomassie staining of protein gels. These results indicate that p110α and the small regulatory subunits do not occur in similar concentrations as p110β/p110δ, and p85α/p85β, respectively in WEHI-231 cells or that the pTyr-matrix does not possess similar binding affinities towards the different class IA PI3K subunits. Since MS identification of p110α, p55γ, p55α, and p50α was also less well achieved after IP experiments with different Abs raised against class IA subunits (see § 4.7.1), we conclude that these subunits might not be as highly expressed as p110β, p110δ, p85α and p85β in WEHI-231 cells.

Two non-PI3K proteins were also identified by MS. Hsp70, member of the Hsp70 chaperone family, was detected by LC-MS/MS as a protein band running at M_r 70 kDa in SDS polyacrylamide gels. However, this protein was also detected in anti-p110δ and anti-p85 immunoprecipitates, in immunopurifications performed with mixed anti-mouse immunoglobulin G from the IgG fraction of rabbit antiserum, and in pull-downs performed with the synthesised PDGF-receptor peptides coupled to actigel (data not shown). These findings suggest that rather than interacting with class IA PI3K, Hsp70 most probably binds the agarose contained in the matrix used for IP and pull-downs. The second cross-contaminating band was identified as elongation factor-1γ. This protein was also identified by LC-MS/MS in an anti-p110δ IP experiment and in pull-downs with sepharose beads only (Table 5.1). This suggests that elongation factor-1γ cross-reacts with the agarose, excluding specific binding to class IA PI3K.

The advantages of the new purification tool are manifold: it is cheaper than using synthesised, phosphorylated peptides, independent of outside resources for production and an infinite source compared to Abs. This purification tool can in theory enrich for all class IA PI3K. This attribute can be an advantage if an overall analysis is performed (as in absolute quantitation experiments, see chapter 6) or a disadvantage if single subunits are preferred for analysis (chapter 5). Further minor disadvantages of the new purification system over established class IA PI3K subunit enrichment methods are the increased volume of sepharose beads needed leading to increased working volume and cross-contaminating proteins and the increased expenditure of time compared to immunopurification (but not compared to enrichment by synthesised peptide which is also a two-day protocol).

In summary, the pTyr-matrix provided an enrichment method independent of IP and we successfully applied it for the enrichment of class IA PI3K in several different projects of this thesis.

4 INVESTIGATION OF POST-TRANSLATIONAL MODIFICATIONS IN THE REGULATORY SUBUNITS OF CLASS IA PI3KS

Very few, if any, known proteins are merely the simple polymer of the basic 20 primary amino acids but instead contain post-translational modifications. Such modifications have been shown to impact on the biophysical properties of proteins, such as enzymatic activity, protein-protein interaction, protein stability and subcellular localisation, leading amongst others to changes in their functions. In signalling pathways, reversible changes in protein modifications, and thus reversible changes in protein functions, allow for transmission and amplification of signals and subsequent return to basal state after a signal has passed through the cascade. Protein phosphorylation is one of a few post-translational modifications which are reversible due to the concerted action of protein kinases and phosphatases and therefore play an important role in the regulation of signalling molecules.

Phosphorylation of class IA PI3K regulatory subunits on Ser, Thr and Tyr residues upon different stimuli and in different cell types has been described (more information is provided in § 1.3.4.2). In order to gain insight into the regulation of class IA PI3K activity, we investigated post-translational modifications, in particular protein phosphorylation of the regulatory and catalytic subunit. In this chapter, we report on results obtained from analysis of p85 modifications and in chapter 5, post-translational modifications and their possible impact on PI3K function of the catalytic subunit p110δ will be described.

Only six of many reported p85 phosphorylations have been assigned to specific residues in the regulatory subunit p85α (Tyr368, Tyr508, Tyr580, Tyr607, Ser608, Tyr688), and one each in the regulatory subunits p85β (Tyr458) and p55γ (Tyr341). The biological relevance of these phosphorylation sites is often controversial or has not been investigated. Most of the work performed to gain insight into these phosphorylation events has been undertaken with recombinant p85α and not on endogenous protein. In addition, modifications other than phosphorylation have barely been investigated.

We set out to analyse post-translational modifications of endogenous regulatory subunit in the murine immature B cell line WEHI-231. Different electrophoretic and mass spectrometric methods were applied to investigate post-translational modifications in p85 in unstimulated and stimulated cells, the nature of these modifications and the amino acid residues involved. We observed that a variety of modifications existed in p85α of proliferating, but unstimulated WEHI-231 following separation of PI3K on 2D-gels, whereas p85β appeared not to be modified. Further

analysis by immunoblotting and MS revealed that a fraction of these modifications was due to protein phosphorylation in general, and phosphorylation of Y688 in particular. Performing MS, we also detected p85α amino acid residues that underwent protein hydroxylation and amino acid substitutions. We could further demonstrate that the observed modifications in p85α were not restricted to B cells since a similar p85 modification pattern could be observed in different cell types. Some of these modifications in p85α seemed to minor impact binding of p85 to the catalytic subunits. Interestingly, physiological stimulation of B cells leading to BCR crosslinking did not change the variety of modifications observed following 2D-analysis. Only treatment of cells with okadaic acid or pervanadate, two potent inhibitors of protein phosphatases increased protein phosphorylation. These findings indicate that p85α is extensively modified in proliferating cells, but these modifications do not seem to be crucial for changes in the lipid kinase activity observed following cellular stimulation of B cells.

4.1 2D-PAGE analysis reveals post-translational modifications of the regulatory subunit in proliferating B cells

2-dimensional polyacrylamide gel electrophoresis (2D-PAGE) is a powerful technique to (1) separate post-translationally modified proteins from their non-modified or differentially-modified counterparts allowing for the analysis of their stoichiometry, (2) compare their existence in different experimental set-ups, and (3) enrich for certain post-translationally modified protein forms (herein called 'protein species').

2D-PAGE of proliferating NIH-3T3 fibroblasts has revealed multiple p85 protein spots, indicative of post-translational modifications in the regulatory subunit (Cohen et al., 1990). We therefore investigated whether post-translational modifications could be detected by 2D-PAGE in proliferating WEHI-231 cells. For this purpose, total cell lysate of WEHI-231 cells was subjected to isoelectric focusing (IEF) using immobilised pH gradient (IPG) strips. After SDS-PAGE of IEF-separated proteins, electroblotting was performed and the proteins analysed by immunoblotting using different Abs against the regulatory subunits (Figure 4.1).

Multiple p85α spots were detected using a p85α mAb (U10), as well as 1 p85β spot using a combination of two p85β mAbs (T12 and T15) in two independent experiments. We also utilised 2 Abs that recognise both p85α and p85β (U2 mAb and p85pan polyclonal Ab (pAb)), which allowed for detection of 4 main protein spots and depending on the Ab for additional minor protein spots on 2D-immunoblots. A similar variety of p85 protein spots could be detected by p85pan Ab if the regulatory subunits were immunopurified using either p85 (data not shown) or p110δ Abs (Figure 4.2).

These results suggested that differentially modified p85α and to a lesser extent p85β occur in WEHI-231 cells under basal proliferative culture condition.

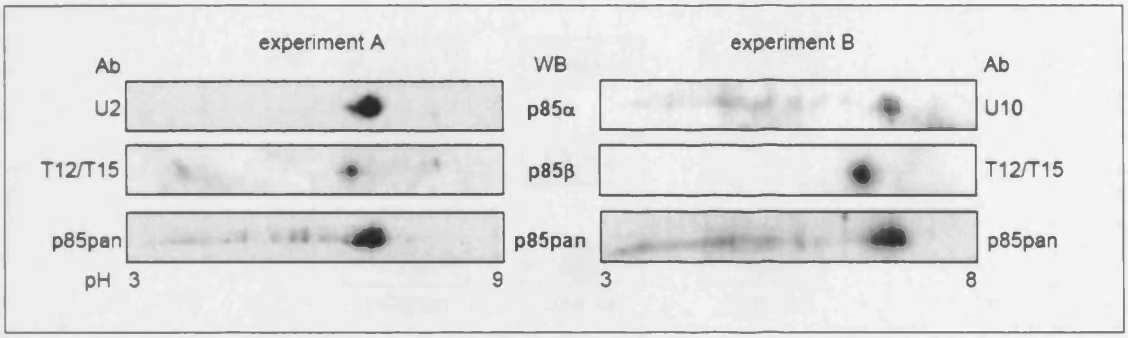

Figure 4.1: p85α protein is extensively modified in unstimulated WEHI-231 B cells
WEHI-231 total cell lysate was resolved by 2D-PAGE and p85 subsequently analysed by immunoblotting using p85-specific Abs. U10: mAb against p85α; T12 and T15: mAbs against p85β; U2: mAb recognising p85α/p85β. p85pan: pAb against p85α/p85β. Sections of two independent 2D experiments are shown.

4.2 Treatment with okadaic acid alters the phosphorylation state of class IA PI3K regulatory subunits, in contrast to stimulation with α-IgM

In order to investigate the nature of the p85 modifications observed following 2D-PAGE from proliferating WEHI-231 cells, we compared the phosphorylation status of the regulatory subunit from unstimulated and stimulated B cells. Thus, WEHI-231 cells were treated with α-IgM or okadaic acid (OA).

Treatment of B cells with α-IgM leads to crosslinking of the B cell antigen receptor (BCR). This induces a complex signalling cascade in B cells, resulting in the phosphorylation of predominantly Tyr residues in proteins and activation/deactivation of many downstream targets, amongst others class IA PI3K (see § 1.7.1). OA is a potent inhibitor of protein phosphatase 1 (PP1) and PP2A, which account for the majority of phosphatase activity in the cytosol (Cohen, 1989). Treatment of cells with OA leads to the accumulation of pSer and pThr residues.

Analysis of the incorporation of phosphate groups into the class IA PI3K regulatory subunit was performed by immunoblotting using phospho-specific Abs following IP and separation of the proteins by 2D-PAGE. In order to monitor successful cellular stimulation, the increase in pSer473 and/or pThr308 of Akt, a key downstream effector of class IA PI3K, was analysed in each experiment (data not shown)

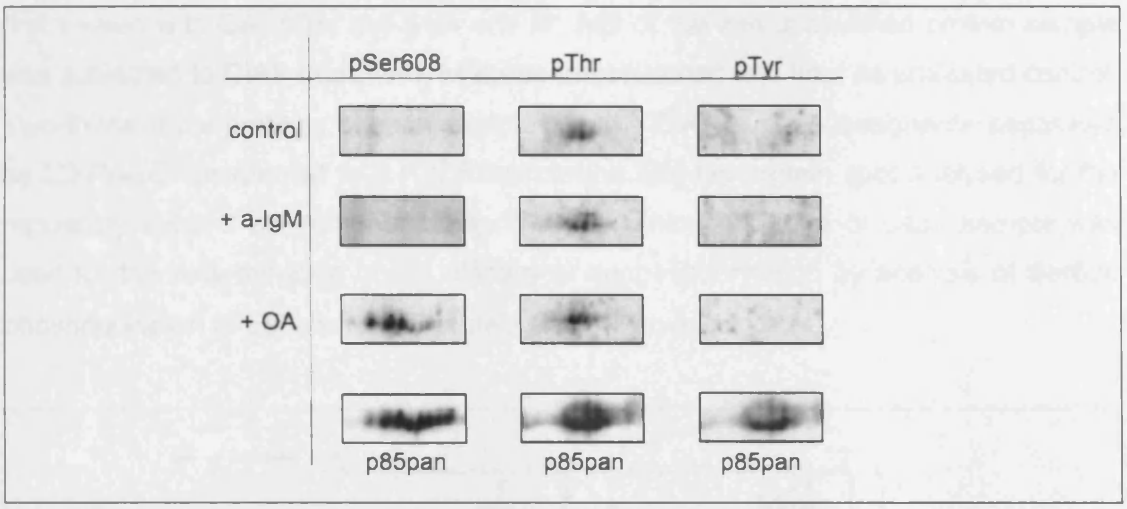

Figure 4.2: The regulatory subunit becomes phosphorylated following OA treatment, but not upon α-IgM stimulation of B cells.

Class IA regulatory subunits were immunoprecipitated from control, α-IgM-stimulated or OA-treated WEHI-231 cells using p110δ Ab followed by analysis for pSer608, pThr and pTyr by immunoblotting.

As shown in Figure 4.2, p85 seemed to be phosphorylated on Thr residues in unstimulated cells. BCR crosslinking did not induce changes in the Thr phosphorylation of p85. These findings are in line with results from 1D-experiments (data not shown). Following OA treatment of cells, an increase in Ser608 and a minor shift in Thr phosphorylation was detected by immunoblotting with phospho-specific Abs. The pattern of Ser608 phosphorylation following OA treatment indicates not only an increase in Ser608 phosphorylation, but possibly also in other modifications not detected with the phospho-specific Abs.

These findings indicate that BCR stimulation does not induce phosphorylation of the regulatory subunit in contrast to OA. Furthermore, residual Thr phosphorylation of p85 detected in unstimulated cells might possibly constitute some of the modifications detected by 2D-immunoblotting with p85 Abs.

4.3 Only a fraction of the post-translational modifications observed in class IA PI3K regulatory subunits are due to protein phosphorylation

Since the analysis of protein phosphorylation by immuoblotting crucially depends on the quality and specificity of the phospho-specific Abs used for detection, we compared the regulatory subunit protein spot pattern detected by Abs to the regulatory subunit before and after *in vitro* dephosphorylation of immunoprecipitated proteins.

This was carried out by *in vitro* treatment of immunoprecipitated regulatory subunit with calf intestine alkaline phosphatase (CIAP). Ser608 phosphorylation of p85α was used as a positive control for the efficacy of CIAP, and cells were therefore

first treated with OA. After cell lysis and IP, half of the immunopurified protein sample was subjected to CIAP treatment, whereas the other half was kept as untreated control. Two-thirds of the proteins of each sample (- and + CIAP) were subsequently separated by 2D-PAGE, transferred to a PVDF membrane and the protein spot analysed for the regulatory subunit by immunoblotting. The remaining one-third of each sample was used for the determination of the efficacy of dephosphorylation by analysis of Ser608 phosphorylation of p85α after 1D-protein separation and blotting.

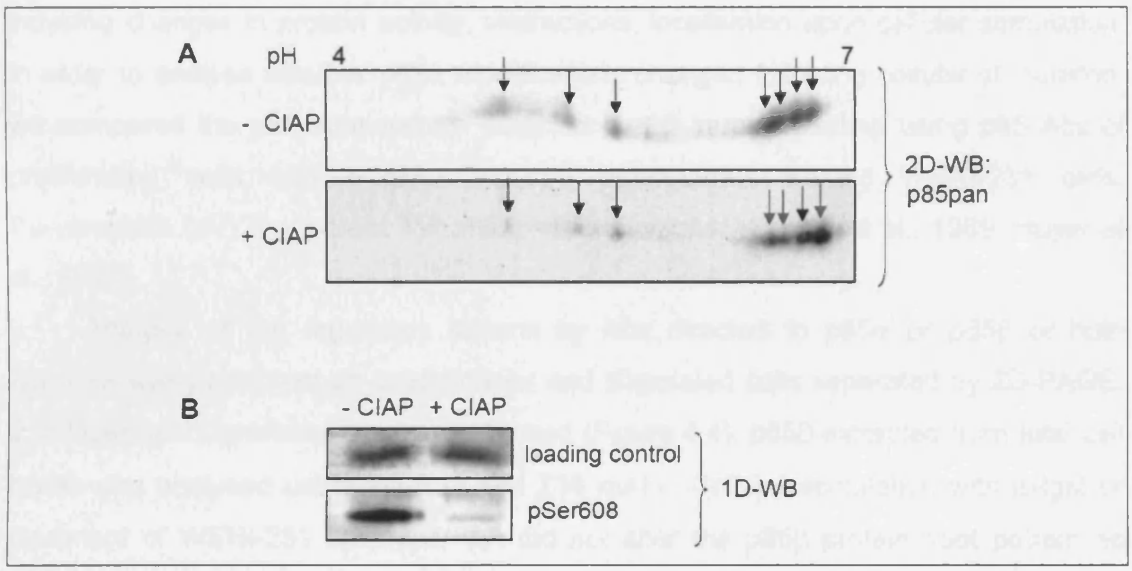

Figure 4.3: p85 protein spots detected on 2D-immunoblots are only partially due to protein phosphorylation

The regulatory subunit was enriched from WEHI-231 cells by immunopurification using a mixture of 4 mAb to p85α and p85β, followed by *in vitro* dephosphorylation using calf intestine alkaline phosphatase (CIAP). (A) 2/3 of the immunocomplex was separated by 2D-PAGE, transferred to a PVDF membrane and analysed for the regulatory subunit by immunoblotting. Arrows are used to indicate p85 protein spots. Green arrows show a decrease, red arrows an increase and black arrow indicate similar p85 protein amounts in the + CIAP compared to the – CIAP sample. (B) 1/3 of the immunocomplex was separated by 1D-SDS-PAGE, transferred to PVDF membrane and analysed for pSer608 of p85α by immunoblotting.

As shown in Figure 4.3.A, dephosphorylation of some p85 spots occurred upon CIAP treatment. When the 4 main p85 protein spots are compared in both samples, a shift in protein spot distribution from acidic to basic pI can be detected in the dephosphorylated *versus* non-treated protein sample, leading to the most prominent spot being the most basic one. However, approximately half of the protein spots (indicated by black arrows in Figure 4.3.A) seemed to be only partially affected or unaffected by phosphatase treatment, suggesting that protein modifications other than phosphorylation exist in the regulatory subunit. As shown in Figure 4.3.B, dephosphorylation of Ser608 occurred under the chosen conditions, indicating successful *in vitro* protein dephosphorylation.

We therefore conclude that the modifications observed in proliferating B cells are potentially due to protein phosphorylation, but also to other protein modifications.

4.4 Post-translational modifications in class IA PI3K regulatory subunits detected by 2D-PAGE are not subject to regulation by physiological stimulation

Reversible protein modifications other than phosphorylation (such as hydroxylation, acetylation, carboxylation, sulfation, nitration) have been implicated in inducing changes in protein activity, interactions, localisation upon cellular stimulation. In order to analyse whether p85α modifications changed following cellular stimulation, we compared the p85 spot pattern detected by 2D-immunoblotting using p85 Abs of proliferating cells with α-IgM, OA and pervanadate treated WEHI-231 cells. Pervanadate (pV) is a potent Tyr phosphatase inhibitor (Fantus et al., 1989; Huyer et al., 1997).

Analysis of the regulatory subunit by Abs directed to p85α or p85β or both isoforms was performed on unstimulated and stimulated cells separated by 2D-PAGE. 2 independent experiments were performed (Figure 4.4). p85β extracted from total cell lysate was analysed using the T12 and T15 mAbs. Cellular stimulation with α-IgM or treatment of WEHI-231 cells with OA did not alter the p85β protein spot pattern as compared to unstimulated samples. Only upon pV treatment, a second p85β protein spot became visible, suggesting modification of this regulatory subunit (Figure 4.4.A). However, since the protein shift was towards a more basic pH, modifications causing more acidic proteins such as phosphorylation, acetylation, carboxylation, hydroxylation, sulfation or nitration could be excluded as the cause for the occurrence of this protein spot.

Analysis of p85α from total cell lysate by 2D-PAGE using the U10 mAb indicated a minor increase of protein spots towards a more acidic pH in all stimulated samples *versus* the control sample, but mainly in OA treated cells. These results were confirmed when total cell lysate was analysed with a p85pan Ab.

Taken together, physiological stimulation of WEHI-231 cells with α-IgM did not induce major changes in the p85 protein spot pattern, suggesting that the modifications detected on 2D-immunoblots are insensitive to BCR crosslinking. When the cells were incubated with less physiological stimuli, such as OA and pV, a shift in the p85 protein pattern could be detected, which was most likely due to protein phosphorylation (Figure 4.2).

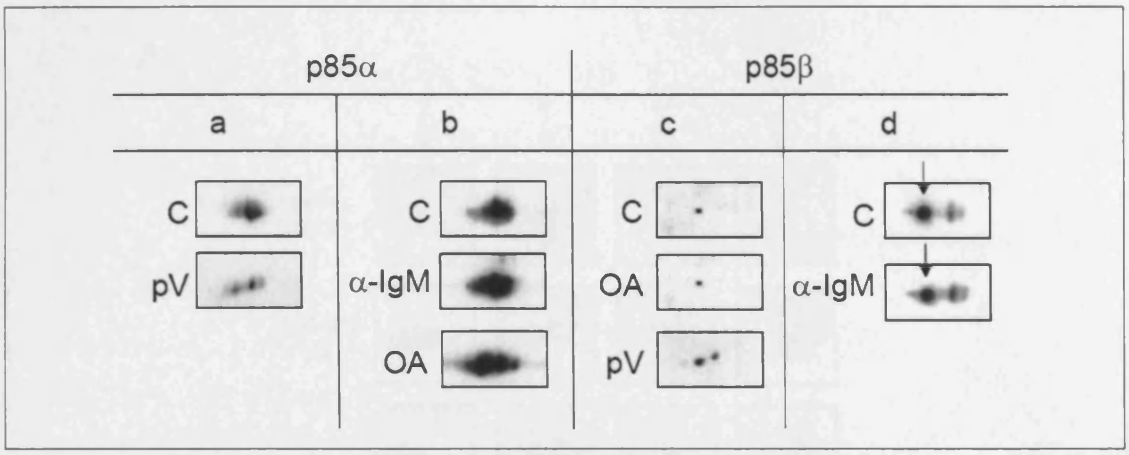

Figure 4.4. Treatment of WEHI-231 cells with OA or pV, in contrast to stimulation with α-IgM, alters the protein spot pattern of the regulatory subunit on 2D-gels

WEHI-231 cells were stimulated with different chemicals (C, control; pV, pervanadate; α-IgM; and OA, okadaic acid) followed by separation of the protein spot pattern of the regulatory subunit by 2D-PAGE and analysis by immunoblotting. Total cell lysate of WEHI-231 cells was analysed using p85α or p85β Abs. a, b, c, d: 4 different experiments.

4.5 p85 modifications revealed in unstimulated cells are common in different cell types

In order to detect whether the modifications observed in p85α were unique to B cells, we analysed in parallel the p85 protein spot pattern from total cell lysates of four different cell types by 2D-PAGE, focusing on cells of murine origin.

We compared the B cell line WEHI-231 with the T lymphoma cell line EL-4, the colon carcinoma cell line CT-26 and the fibroblast cell line NIH-3T3. 2D-immunoblots were analysed using different Abs directed against the regulatory subunits (Figure 4.5.A). This led to the detection of different p85 spot patterns depending on the Ab used. If the 2D-immunoblots were analysed for p85α using the U10 mAb, easily detectable differences were observed between cell types. However, analysis of the same membrane after protein stripping with the mAb U2 resulted in similar p85 protein spot pattern between the different cell lines with decreasing signal intensity toward the more acidic pH. If a pAb against all regulatory subunits was used for analysis ('p85pan'), small differences between the different cell types were detected, which were not as pronounced as the ones detected with U10.

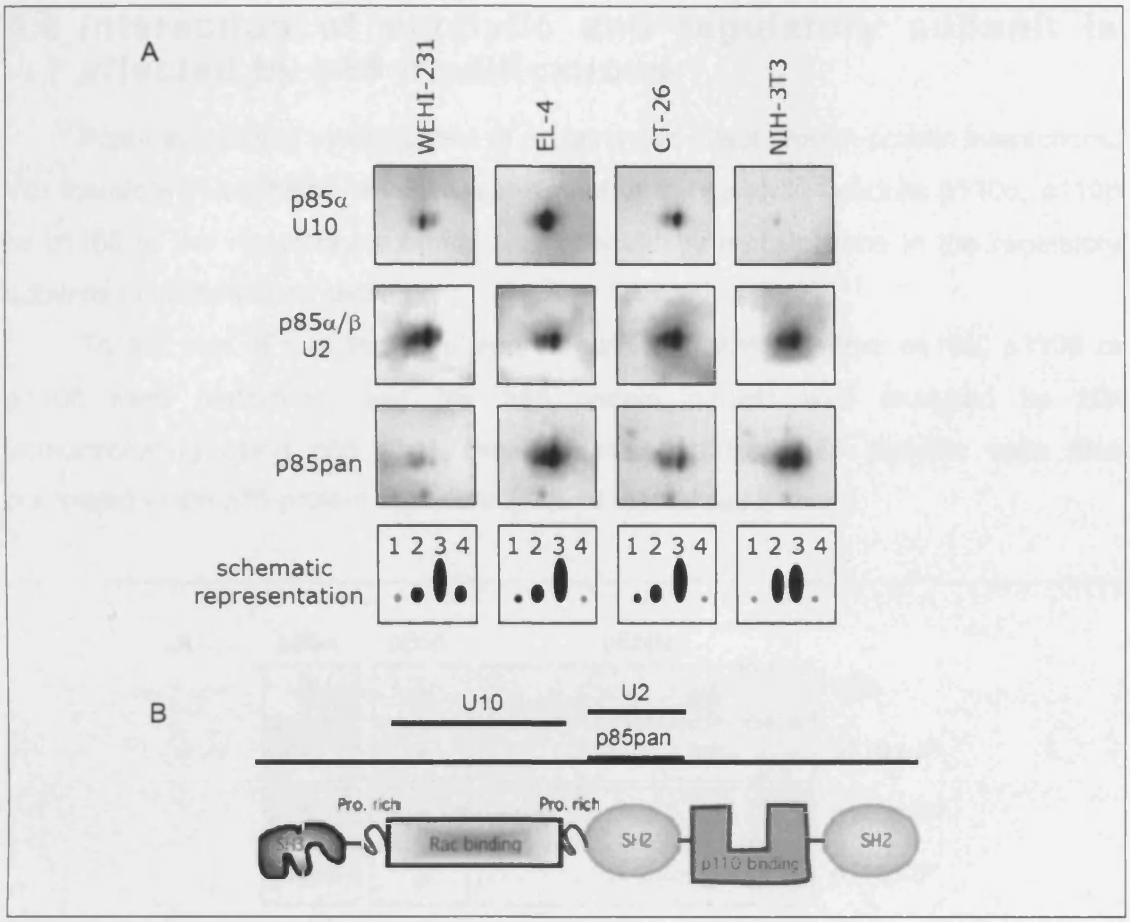

Figure 4.5: p85 post-translational modifications in different murine cell types

(A) Total cell lysate of four different cell lines (WEHI-231, EL-4, CT-26 and NIH-3T3) were separated by 2D-PAGE and analysed for p85α (U10) and p85α/p85β (U2, p85pan). A schematic representation of the spot pattern is given. Sections of the 2D-immunoblots are shown. (B) Schematic drawing of class IA PI3K regulatory subunit (adapted from (Deane and Fruman, 2004)), indicating which domains the different Abs were raised against.

The observed differences may relate to the different epitopes recognised by the different Abs. The epitope recognised by U10 Ab lies within the Rac binding domain (also termed BH domain) and the epitope recognised by U2 lies within the N-terminal SH2 domain, respectively (End et al., 1993). It is thus possible that post-translational modifications in the amino acid sequences to which the Ab binds hampers recognition of these p85 species by the Abs used.

In summary, our data suggest that p85 protein modification in unstimulated cells is common in a variety of cell types. Small differences in the protein pattern seem to occur, suggesting modifications on different amino acid residues in different cell types.

4.6 Interaction of catalytic and regulatory subunit is affected by p85 modifications

Post-translational modifications of proteins can affect protein-protein interactions. We therefore investigated whether recruitment of the catalytic subunits p110α, p110β or p110δ to the regulatory subunits was affected by modifications in the regulatory subunits in unstimulated cells.

To this end, IPs of the regulatory subunit with Abs to either p110α, p110β or p110δ were performed, and the p85 protein pattern was analysed by 2D-immunoblotting using p85 Abs. The immunoprecipitated p85 proteins were also compared to the p85 protein spot variety found in total cell lysate.

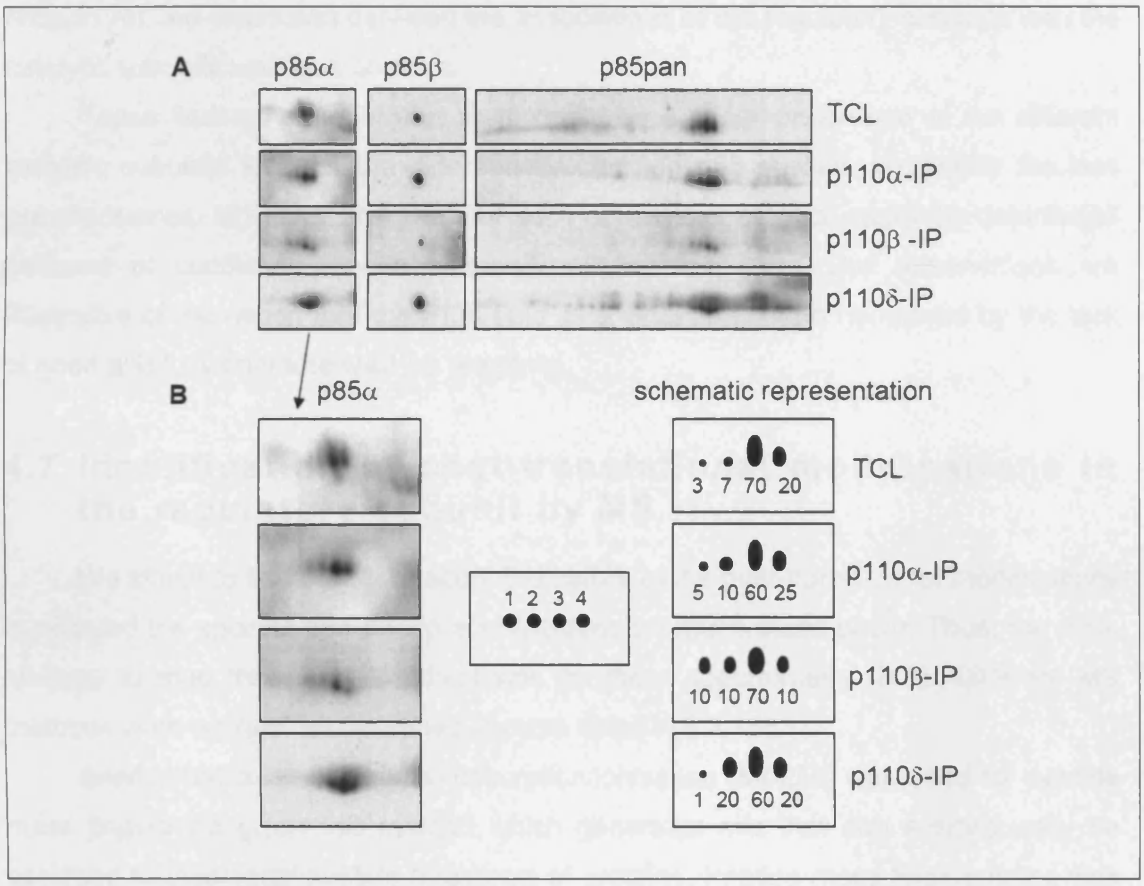

Figure 4.6: Indications that differentially modified p85α subunits are not equally distributed over the 3 distinct p110 class IA catalytic subunits

(A) Total cell lysate (TCL) of WEHI-231 cells analysed by 2D-PAGE was compared to immunoprecipitations (IP) with Abs to p110α, p110β or p110δ. Each sample (TCL and IP) was analysed for p85α, p85β and p85pan with specific Abs. (B) A schematic representation of the p85α protein spot pattern is shown, indicating the percentage of each of the four major protein spots in each of the four samples. Sections of the 2D-immunoblots are shown, representing 1 of 2 independently performed experiments.

As shown in Figure 4.6.A, p85β interacted with all catalytic subunits in a similar way. Since we did not investigate how successful the IP of each catalytic isoform was by analysing the depletion of each catalytic subunit after IP, no statement can be made on the strength of the interaction between p85β and the different catalytic subunits.

The p85α subunit also interacted with all catalytic subunits, but not identically. In Figure 4.6.B, a schematic representation and estimated percentage of each of the four main p85α protein spots of total cell lysate and after IP with different catalytic subunits is shown. This indicates that the p85α protein spot termed number 3 is the most prevalent, whereas protein spot number 4 is mainly found in p110α and p110δ immunoprecipitates. Protein spot number 2 can be primarily observed in IPs of p110δ. However, when the differentially modified p85 protein species are analysed using a p85pan Ab, the distinction between the associations of the regulatory subunits with the catalytic subunits was less obvious.

These findings suggest that there might be a minor preference of the different catalytic subunits towards the differentially modified p85 species, especially the less prevalent ones. However, the scale of such differences can not easily be determined because of conflicting results obtained with different Abs. Our observations are illustrative of the notion that the PI3K field as a whole has been hampered by the lack of good and fully characterised Ab reagents.

4.7 Identification of post-translational modifications in the regulatory subunit by MS

We aimed to find out more about the nature of the post-translational modifications in p85 and the specific p85 amino acid residues on which these occur. Thus, the main strategy to map these modifications was by mass spectrometry (MS). Different MS methods were applied, as described in more detail in § 2.16.

Briefly, matrix-assisted laser desorption/ionisation (MALDI) was used for peptide mass fingerprinting, an MS method which generates m/z that can subsequently be assigned to theoretical peptide fragments of proteins. Peptide mass fingerprinting was used as initial analysis of post-translational modifications of immunoprecipitated proteins. The advantages of this method are the speed of acquisition, the low consumption of sample, the large mass range of analysis and a simple identification of spectra due to predominantly singly-charged peptides. We also used electrospray ionisation (ESI) which, in contrast to MALDI, allows for easier generation of sequencing information. This is because high quality spectra and sequence specificity are generated due to low energy fragmentation. Furthermore, doubly- or triply-charged peptides occurring in ESI generate readily interpretable tandem mass spectra

compared to singly charged peptides produced in MALDI. Another advantage of ESI is the ease with which it can be interfaced with chromatographic and electrophoretic liquid phase separation techniques. Full-scan acquisition by ESI was performed to determine the peptide sequences by assigning m/z of peptides (MS) and their fragments (MS/MS). Full-scan acquisition data were also used to perform error-tolerant searches, in which unexpected modifications, primary sequence variations and enzyme non-specificities are increasing the probability of peptide identification. Once further information on a protein was available that suggested modifications of a specific residue, multiple reaction monitoring (MRM) was applied. In this approach, the mass spectrometer is set to scan over a very small mass range, typically one mass unit. Only one or a few selected m/z (depending on the experimental set-up) are set for detection per run and subsequently chosen by the mass analyser for further fragmentation. The advantage of this method over full-scan monitoring is increased sensitivity. Instead of scanning the most prominent m/z in a complex peptide mixture, in MRM only a small fraction of all m/z will be analysed allowing for detection of less abundant peptides.

4.7.1 Testing the tools: identification of class IA PI3K isoforms by MS

Analysis of post-translational modifications of proteins by MS requires enrichment tools that are specific for the protein of interest only and allow for the purification of large amounts of protein.

As described in § 3.4, the regulatory subunit p85α and p85β and the catalytic subunit p110β and p110δ could be identified by tandem mass spectrometry (MS/MS) from protein samples enriched for class IA PI3K by a pull-down using the pTyr-matrix. However, the described pulldown method does not discriminate between different class IA PI3K isoforms. We therefore tested whether a mAb which recognises p85α and p85β (U2) and a pAb to the p110δ catalytic subunit could be used to purify these specific subunits from WEHI-231 cell lysates.

After incubation of cell lysate with the indicated Abs and protein A or protein G sepharose beads, the protein complexes were vigorously washed, separated by SDS-PAGE and the proteins visualised by colloidal Coomassie staining. As shown in Figure 4.7, two dominant protein bands could be detected at relative molecular weight (M_r) of 110 kDa and 85 kDa using either enrichment method. No such proteins were found in immunoprecipitates of a control Ab (anti-mouse immunoglobulin G from the IgG fraction of rabbit antiserum). Following tryptic in-gel digestion, the peptides were subjected to full-scan acquisition using an ESI-Q-TOF coupled to an HPLC instrument. The sequencing data were extracted with Masslynx (MICROMASS) and searched against

the NCBInr (non redundant) database using Mascot (MATRIXSCIENCE). Details and parameter values for data interpretation can be found in § 2.16.5.

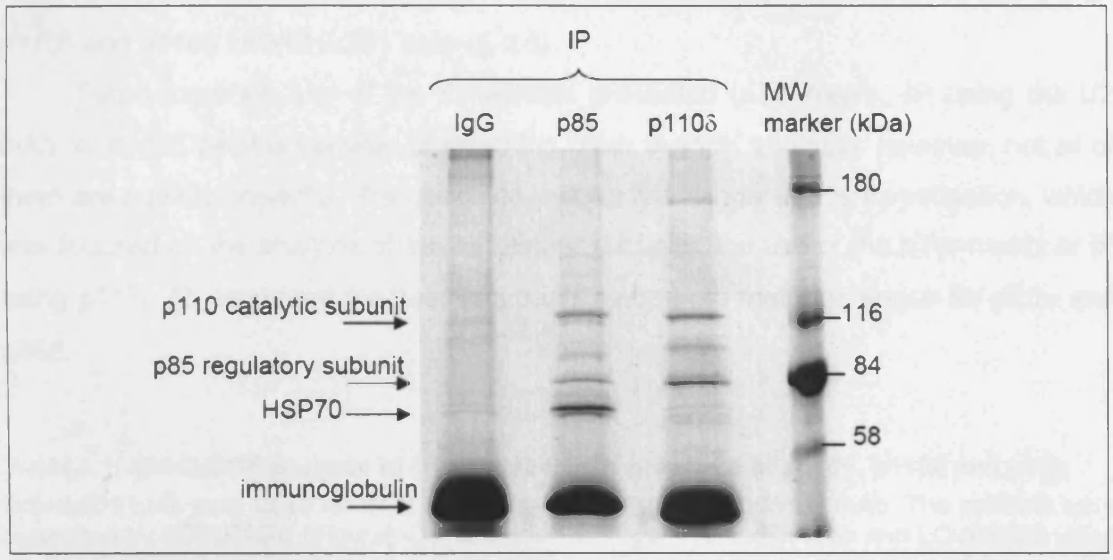

Figure 4.7: Enrichment of class IA PI3K by IP

The regulatory and catalytic subunits were immunoprecipitated from WEHI-231 cell lysate with Abs to either p85α/p85β (p85) or p110δ. The enriched proteins were separated by SDS-PAGE and subsequently visualised by colloidal Coomassie. A mix of anti-mouse IgG immunoglobulins was used as a negative control. The protein bands were extracted and subjected to LC-MS/MS (see Table 4.1).

IP with U2 (p85α/p85β) led to the identification of p110β, p110δ and p85α (Table 4.1). Protein identification with a probability-based MOWSE score (Pappin et al., 1993) above 40 was considered significant. p85β and p110α could not be identified by MS/MS following IP, but could be detected by immunoblotting (data not shown), suggesting that the U2 mAb does not equally enrich for p85α and p85β and/or that p85β and p110α are present at lower levels in WEHI-231 cells compared to the other class IA subunits.

IP with the p110δ Ab resulted in the identification of p110δ, p85α and p85β (Table 4.2). MS analysis also revealed the presence of thymopoietin, a protein with the same M_r as p85α/p85β. Since thymopoietin is not detected in p85 IPs, it is most likely a p110δ Ab crossreacting protein and not part of the p110-p85 protein complex.

Since p85β could be identified when immunoprecipitated with the p110δ Ab and also when pulled down with the pTyr-matrix (§ 3.4), it is likely that the mAb U2 preferentially binds p85α, rather than p85β being available in much minor protein amounts *in vivo*. The abundance of p110α on the other hand seems to be lower than that of p110β and p110δ in WEHI-231 cells, since this subunit could neither be identified by MS after IP using U2 nor after a pulldown with the pTyr-matrix. In fact,

p110α could only be identified by MS analysis if the protein was immunopurified using a p110α Ab (data not shown). Preliminary data obtained by subjecting class IA PI3K to AQUA analysis revealed that p110α is indeed expressed at lower protein levels than p110δ and p110β in WEHI-231 cells (§ 6.6).

Taken together, any of the 3 methods presented (pTyr-matrix, IP using the U2 mAb, or p110δ pAb) is capable of enriching class IA PI3K subunits; however, not all of them are equally powerful. We conclude that for the scope of this investigation, which was focused on the analysis of the regulatory subunits, the use of the pTyr-matrix or IP using p110δ Ab represent the best approach, since both methods enrich for p85α and p85β.

Table 4.1: ESI-Q-TOF analysis of U2 IP reveals the presence of p110β, p110δ and p85α

WEHI-231 cells were used for IP of regulatory subunit with the p85 U2 mAb. The proteins were separated by SDS-PAGE (Figure 4.7), subjected to in-gel tryptic digestion and LC-MS/MS using an ESI-Q-TOF mass spectrometer. Data mining was performed by extraction of the peaklist using MassLynx (MICROMASS) and automated database searches using Mascot demon (MATRIXSCIENCE), with MS/MS ion search parameters as detailed in § 2.16.5. Each identified peptide is given a score according to the MOWSE scoring algorithm, resulting in a total score for each identified protein. m_{Ox} indicates oxidation of methionine residues.

p110β peptide sequences	**experimental m/z**	**exp/ calc delta**	**score**
DSLALGK	352.19	-0.03	20
LNTEETVK	467.22	-0.05	31
DALLNWLK	486.75	-0.06	41
TVVSSEISGK	503.75	-0.05	55
EYNSGDDLDR	592.22	-0.05	40
AAELASGDSANVSSR	717.80	-0.09	43
p110δ peptide sequences	**experimental m/z**	**exp/ calc delta**	**score**
DSLALGK	352.19	-0.03	20
AYTILR	368.70	-0.04	28
FNEALR	375.18	-0.04	39
ALLVNVK	378.73	-0.04	33
SEMHVPSVALR + m_{Ox}	414.53	-0.06	58
QVLWHR	419.72	-0.03	26
NANLSTIK	430.72	-0.04	39
NPGEALDR	436.20	-0.03	32
DALLNWLK	486.75	-0.06	41
HSDNIMIR + m_{Ox}	501.23	-0.03	17
SKNPGEALDR	543.75	-0.05	38
GELLNPAGTVR	563.79	-0.06	38
SNMAATAAFNK + m_{Ox}	571.24	-0.06	74
ITEEEQLQLR	629.80	-0.07	89
FGLIMEAYCR + m_{Ox}	638.27	-0.06	41
LINSQISLLIGK	649.87	-0.08	78
MTPYGCLPTGDR	692.27	-0.08	26
YESYLDCELTK	710.78	-0.08	45
LCDIQPFLPVLR	735.87	-0.09	59
p85α peptide sequences	**experimental m/z**	**exp/ calc delta**	**score**
NLLNAR	350.69	-0.03	25
AENLLR	358.19	-0.03	42
ALYDYK	386.68	-0.04	22
DGTFLVR	404.23	-0.05	24
LLEAIEK	408.23	-0.04	5
LEEDLKK	437.73	-0.04	32

ALYDYKK	450.75	-0.03	17
RLEEDLK	451.75	-0.02	16
ISEIIDSR	466.73	-0.04	59
LLEAIEKK	472.26	-0.07	24
NKAENLLR	479.25	-0.06	14
LYEEYTR	487.2	-0.06	8
EDNIEAVGK	487.73	-0.03	30
YQQDQVVK	504.23	-0.05	29
DTADGTFLVR	547.75	-0.05	55
GLECSTLYR	549.74	-0.06	33
NESLAQYNPK	582.25	-0.07	11
TQSSSNPAELR	595.26	-0.08	16
TAIEAFNETIK	618.80	-0.06	44
YQQDQVVKEDNIEAVGK	654.96	-0.10	15
LRDTADGTFLVR	682.34	-0.06	20
VLSEIFSPVLRF	703.85	-0.12	16
MNSIKPDLIQLR + m_{Ox}	722.37	-0.07	8
IFEEQCQTCER	734.27	-0.11	54

Table 4.2: ESI-Q-TOF analysis of p110δ IPs reveals the presence of p110δ, p85α and p85β
See Table 4.1 for methodical details.

p110δ peptide sequences	**experimental m/z**	**exp/ calc delta**	**score**
ALNDFVK	403.70	-0.05	7
QFCEEAAAHR	406.81	-0.08	24
SEMHVPSVALR + m_{Ox}	414.51	-0.07	11
QVLWHR	419.71	-0.06	14
SEMHVPSVALR	428.20	-0.08	22
NANLSTIK	430.72	-0.06	11
NPGEALDR	436.18	-0.06	12
AYTILRR	446.76	-0.02	9
AKPPPIPAK	459.75	-0.06	24
KLINSQISLLIGK	476.28	-0.07	13
VKFNEALR	488.75	-0.07	15
GRITEEEQLQLR	491.24	-0.09	31
FRGYCER	494.20	-0.06	8
HSDNIMIR + m_{Ox}	501.21	-0.08	5
HEVQEHFPEALAR	521.56	-0.09	1
LKALNDFVK	524.28	-0.07	7
DEQSNPAPQVQKPR	531.89	-0.10	25
SKNPGEALDR	543.74	-0.08	17
TNNSEKFER	562.73	-0.07	7
AAGLPELSCSK	566.74	-0.04	24
SNMAATAAFNK + m_{Ox}	571.23	-0.08	3
QRLEFDISVDCLPR	583.23	-0.09	46
VNWLAHNVSK	584.28	-0.07	18
ITEEEQLQLR	629.79	-0.07	26
FGLIMEAYCR	630.26	-0.07	35
LINSQISLLIGK	649.88	-0.06	54
LCFALYAVVEK	656.82	-0.07	29
VPFILTYDFVHVIQQGK	668.66	-0.12	13
GLHEFDSLRDPEVNDFR	682.62	-0.11	4
MTPYGCLPTGDR	684.27	-0.08	10
MTPYGCLPTGDR + m_{Ox}	692.28	-0.05	26
KLINSQISLLIGK	713.92	-0.06	32
DIQYLKDSLALGK	732.36	-0.1	13
LCDIQPFLPVLR	735.86	-0.08	28
GRITEEEQLQLR	736.35	-0.09	11
DSLALGKTEEEALK	752.36	-0.07	20
ERVPFILTYDFVHVIQQGK	763.72	-0.11	5
DEQSNPAPQVQKPR	797.34	-0.12	10
KPSSVSLWSLEQPFSIELIEGR	834.73	-0.16	23

p85α peptide sequences	experimental m/z	exp/ calc delta	score
DGTFLVR	404.19	-0.05	24
LLEAIEK	408.20	-0.04	5
LRDTADGTFLVR	455.23	-0.07	31
ISEIIDSR	466.72	-0.07	33
LLEAIEKK	472.26	-0.07	24
NKAENLLR	479.23	-0.06	14
LHEYNTQFQEK	479.53	-0.10	10
MNSIKPDLIQLR + m_{Ox}	481.92	-0.07	28
LYEEYTR	487.18	-0.08	8
FPAASSDNTEHLIK	510.56	-0.09	27
TWNVGSSNR	510.72	-0.06	5
YSKEYIEK	530.23	-0.08	17
ISEIIDSRR	544.78	-0.06	17
GLECSTLYR	549.71	-0.06	33
NESLAQYNPK	582.24	-0.07	11
TQSSSNPAELR	595.26	-0.08	16
MHGDYTLTLR + m_{Ox}	611.73	-0.06	19
KGLECSTLYR	613.77	-0.08	9
TAIEAFNETIK	618.77	-0.06	44
YQQDQVVKEDNIEAVGK	654.96	-0.10	15
LRDTADGTFLVR	682.34	-0.06	20
LHEYNTQFQEK	718.80	-0.09	7
MNSIKPDLIQLR + m_{Ox}	722.37	-0.07	8
IFEEQVQTQER	734.27	-0.11	54
FPAASSDNTEHLIK	765.30	-0.09	33
QGCYACSVVVDGEVK	835.82	-0.12	12
TEADTEQQALPLPDLAEQFAPPDVAPPLIK	1109.79	-0.38	1
p85β peptide sequences	**experimental m/z**	**exp/ calc delta**	**score**
HCVIYR	424.19	-0.06	4
TALYDAVK	440.70	-0.03	8
LRDTPDGTFLVR	463.90	-0.08	19
APGPGPPSAAR	489.22	-0.08	2
FLLQHLGR	492.26	-0.06	37
HESLAQYNAK	580.75	-0.07	16
TAIEAFNETIK	618.77	-0.12	35
IFEEQGQTQEK	668.76	-0.13	38
ERPEDLELLPGDLLVVSR	684.00	-0.12	7
LVEAIEQAELDSECYSKPELPATR	916.71	-0.22	16

4.7.2 MS did not allow for identification of post-translational modifications of class IA PI3K regulatory subunits after 2D-PAGE purification

A single 2D-gel protein spot is enriched specifically for a differentially modified residue, due to the isoelectric focusing of proteins in the first dimension. In order to identify post-translational modifications of class IA regulatory subunit by MS, we purified the regulatory subunit from large amounts of starting material (up to 40 mg total cell lysate, compared to 1 mg total cell lysate if the regulatory subunit was analysed by immunoblotting) by using either an p110δ Ab, p85 Ab (data not shown) or the pTyr-matrix (data not shown). The protein complex was separated by 2D-PAGE and the proteins visualised by colloidal Coomassie.

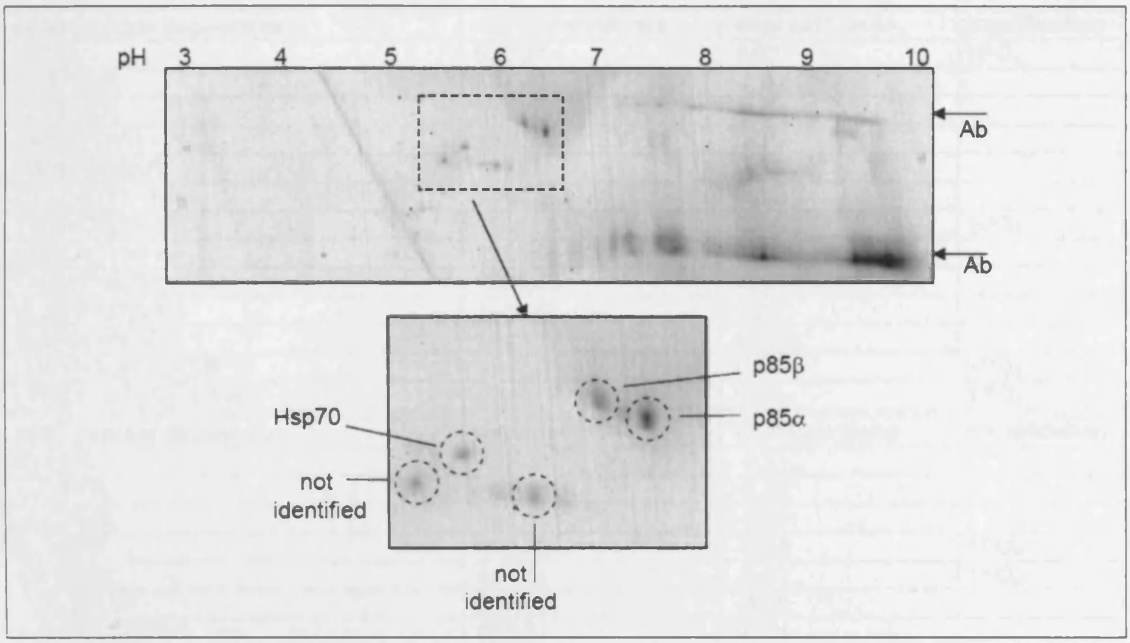

Figure 4.8: 2D-PAGE of regulatory subunit separates p85α from p85β

The regulatory subunit of class IA PI3K was immunoprecipitated using an Ab to p110δ and subjected to 2D-PAGE. Proteins were visualised by colloidal Coomassie staining. The most abundant protein spots with a M_r of 85 kDa were cut from the gel. After tryptic in-gel digestion, the resulting peptides were analysed by MALDI-TOF and identified as p85α, p85β and HSP70 (see Table 4.3).

The protein spot pattern detected with Coomassie (Figure 4.8) did not entirely correspond to the one seen in experiments performed by immunoblotting. Instead of revealing a multitude of protein spots at the M_r of 85 kDa, we could only discover 3 protein spots. This might be due to high specificities of the p85 Abs to low stoichiometry p85 species or to differential binding of the p85 species to the PVDF membrane.

Nevertheless, the different protein spots were cut from the gel and subjected to reduction, alkylation and in-gel tryptic digestion. The peptides were analysed by peptide mass fingerprinting using MALDI-TOF or MS/MS using ESI-Q-TOF (data not shown). p85α and p85β were identified (Table 4.3). However, even though we could detect more than one p85α spot in certain experiments, and potentially phosphorylated peptides were identified using peptide mass fingerprinting (Table 4.3), no regulatory subunit phospho-peptide could be sequenced using LC-MS/MS.

Table 4.3: Identification of p85α and p85β by MALDI-TOF after 2D-PAGE

Peptide mass fingerprinting was used to identify class IA PI3K regulatory subunit. The peptide sequences corresponding to the experimental m/z are indicated on the left, followed by the error between experimental and theoretical m/z. Delta values >0.1 indicate low significance of identification, but were listed if the peptides were identified in other experiments by MALDI-TOF or ESI-Q-TOF. m_{Ox} indicates oxidation of methionine and N_{acetyl} acetylation of asparagines residues.

p85α peptide sequences	experimental m/z	exp/ calc delta	modification
EYDR	662.24	0.03	$1PO_4$
DGTFLVR	807.43	-0.02	
LYEEYTR	973.45	-0.01	
SAEGYQYR + N_{acetyl}	1015.46	0.01	
TWNVGSSNR	1020.5	0.01	
DTADGTFLVR	1094.56	0.01	
TWNVGSSNR	1100.58	0.11	$1PO_4$
NESLAQYNPK	1163.59	0.01	
TAIEAFNETIK	1236.63	-0.01	
VLSEIFSPVLFR	1406.82	0.01	
EIQRIMHNHDK	1420.70	-0.01	
LHEYNTQFQEKSR	1759.96	0.1	$1PO_4$
LYEEYTRTSQEIQMK	2239.12	0.15	$1PO_4$
p85β peptide sequences	**experimental m/z**	**exp/ calc delta**	**modification**
EYLER	709.35	-0.11	
AVYPFR	752.39	-0.02	
DGTFLIR	821.45	-0.02	
AVYPFR	832.34	-0.04	$1PO_4$
DGTFLIR	901.41	-0.01	$1PO_4$
RDGTFLIR	977.46	-0.09	
FLLQHLGR	983.57	-0.01	
YQQDQVVK	1007.49	-0.03	
AGAEGFQYR + N_{acetyl}	1040.45	-0.02	
KINEWLGIK	1100.55	-0.09	
TSQELQMKR + m_{Ox}	1120.57	-0.02	
TWYVGKINR	1136.61	-0.01	
IQGEYTLTLR	1193.64	-0.01	
TAIEAFNETIK	1236.62	-0.01	
SRIAEIHESR	1277.68	0.07	$1PO_4$
TQAEEMLSGKR	1329.68	0.07	$1PO_4$
VALQALGVADGGER	1355.74	0.01	
DQYLVWLTQK	1373.63	-0.02	$1PO_4$
EYDQLYEEYTR	1508.65	-0.01	
GCYACSVVVDGDTK	1638.89	0.15	$1PO_4$
EREPEDLELLPGDLLVVSR	2050.10	-0.01	
EREPEDLELLPGDLLVVSR	2130.16	0.04	$1PO_4$
IPPSGGEGDGSEPVPDFPVLLLER	2477.16	-0.04	
EVAGPVGLEVLEPPTLPLHQALTLR	2520.44	-0.01	
DGHYGFSEPLTFCSVVELISHYR	2807.23	-0.01	$1PO_4$

4.7.3 Similar post-translational modifications are revealed in endogenous and overexpressed p85α protein

In order to increase the probability to detect and identify post-translationally modified p85 proteins by MS, we transiently overexpressed bovine p85α in HEK-293T cells, a cell line known for its ability to be readily transfected by calcium phosphate precipitation transfection (see § 2.7.2.5 and § 6.4.1).

Total lysates from WEHI-231 cells and p85α overexpressing HEK-293T cells were subjected to 2D-PAGE, followed by transfer of proteins to PVDF membranes. Overexpression of p85α in HEK-293T cells was successful as determined by immunoblotting using p85pan Abs (Figure 4.9), leading to a 10-fold increase in p85α level compared to WEHI-231 cells. If a longer exposure time was chosen for the membrane containing WEHI-231 cell sample (endogenous p85α) and shorter exposure

time for the membrane containing p85α overexpressing HEK-293T cell sample, the similarity of the protein spot pattern of the two samples was revealed (right panel of Figure 4.9), confirming similar p85α protein modification patterns even if the protein was highly overexpressed.

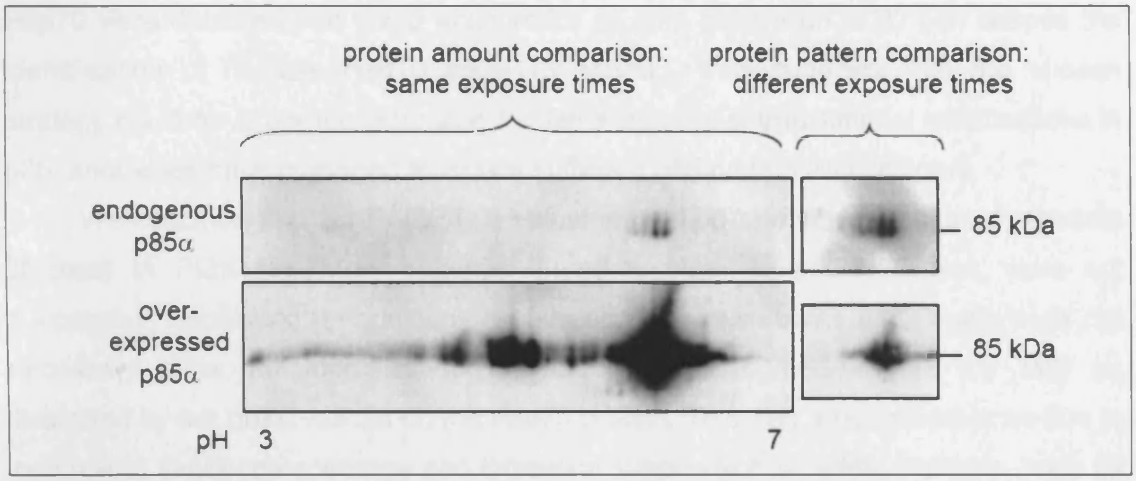

Figure 4.9: Endogenous and overexpressed p85α have a similar 2D-PAGE spot pattern

Total cell lysates of WEHI-231 and p85α overexpressing HEK-293T cells were subjected to 2D-PAGE. Analysis of the regulatory subunit spot pattern was performed by immunoblotting using a p85pan Ab. Two different exposure times are shown in order to demonstrate successful overexpression of p85α in HEK-293T cells (left) and pattern similarity between the 2 samples (right). Sections of the 2D-immunoblots are shown.

4.7.4 MS did not allow for identification of overexpressed p85 protein after 2D-PAGE

p85α overexpressed in HEK-293T cells was purified by Abs (data not shown) or by using the pTyr-matrix and resolved by 2D-PAGE. Following staining by colloidal Coomassie, protein bands were excised and analysed by MS/MS. Unfortunately, we could not identify p85α using this procedure, despite the observation that the Coomassie-stained gel closely resembled the p85 immunoblotting pattern (Figure 4.10). The 9 spots shown in Figure 4.10 could either not be assigned to a specific protein (spot 1; data not shown) or were identified as the Hsp70 chaperone protein (spot 2, 3, 4, 5, 6, 7, 8, 9; data not shown).

We have observed that Hsp70 can bind to the agarose used for IP or pull-down (data not shown). As shown in Figure 4.8, Hsp70 runs at a similar M_r as the class IA regulatory subunit if separated by gel electrophoresis, accounting for the incorrect assessment on 2D gels. Several potential explanations can be given for the presence of Hsp70 in these experiments. Compared to IP, we used higher amounts of sepharose beads in the pTyr-matrix approach, possibly leading to increased Hsp70 'contamination'. In addition, it is possible that Hsp70 is complexed to the

overexpressed p85 subunit. Indeed, heat shock protein expression is often induced by transfection or overexpression of proteins, possibly as a cellular reaction to expression of 'higher than normal' levels of a protein. Induction of Hsp70 has also been found when only one subunit of a multimeric protein is expressed.

It is of interest to note that no changes in post-translational modifications of Hsp70 were detected that could account for its spot pattern on a 2D gel, despite the identification of multiple Hsp70 spots by MS/MS. This suggests that the chosen strategy could have been challenging to map sites of post-translational modifications in p85, should we have managed to isolate sufficient p85 protein from 2D gels.

We conclude that 2D-PAGE is a valuable method to analyse analytical amounts of class IA PI3K regulatory subunits. Large amounts of p85, however, were not successfully separated. In addition, visualisation of protein trains on 2D-gels does not necessary allow for identification of post-translational modifications by MS, as illustrated by our observations on the Hsp70 protein. This may amongst other be due to incomplete sequence coverage and ionisation suppression of acidic peptides, such as the ones containing phosphate-, sulfate-, or carboxy-groups.

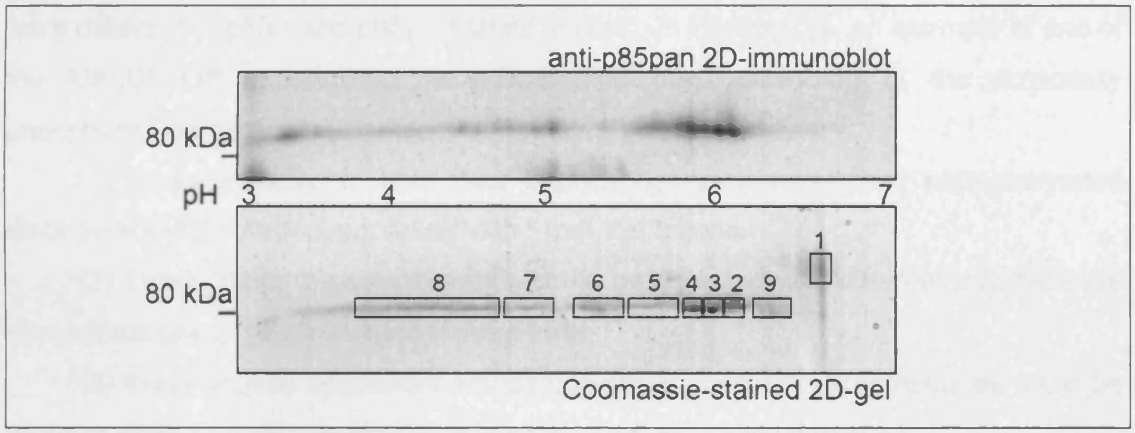

Figure 4.10: Similarities in the spot pattern of overexpressed, immunoprecipitated p85α between immunoblot and Coomassie-stained gel

Bovine p85α was overexpressed in HEK-293T cells and purified using the pTyr-matrix. 1/50 of the sample was used for immunoblotting; the remainder was used for visualisation of proteins by colloidal Coomassie blue on 2D-gels. The numbered boxes indicate gel pieces subjected to tryptic in-gel digestion and LC-MS/MS. Spot number 2-8 were identified as Hsp70, number 1 could not be assigned to a protein. Sections of the 2D-gel/-immunoblot are shown.

4.7.5 MALDI-TOF analysis of the regulatory subunit after 1D-PAGE reveals a variety of potentially phosphorylated p85α and p85β species

Since the 2D-PAGE approach to identify post-translational modifications by MS was not successful, we next performed MS analysis on p85 isolated from 1D-polyacrylamide gels following IP using Abs to p85 or p110δ, or using the pTyr-matrix

(Figure 3.7, Figure 4.7). The protein bands were cut from the gel, reduced, alkylated, subjected to in-gel tryptic digestion followed by identification of the peptides by peptide mass fingerprinting using MALDI-TOF, in order to gain broad insight into the possible modification sites occurring in the regulatory subunit. Once potentially modified residues were determined, the aim was to sequence the relevant peptides by ESI-MS/MS. In order to decrease the complexity of the database searches, peptide mass fingerprinting data were only searched against NCBInr using pSer, pThr, pTyr as variable post-translational modifications, even though previous experiments suggested that other modifications than phosphorylation were likely occurring in p85α (see § 4.3) In contrast, when database searches with MS/MS data were performed, a variety of additional potential modifications were included in the analysis.

Trypsinised peptides were either spotted directly onto MALDI metal plates containing a saturated solution of the matrix chemical 2,5-DHB or first purified over a zip-tip to remove salt and other small molecules interfering with the ionisation process.

As can be seen in Table 4.4, peptide mass fingerprinting of 6 independent experiments identified 51 peptides of p85α (sequence coverage of 63%) and 24 peptides of p85β (35% sequence coverage). 19 potentially phosphorylated peptides were detected in p85α and p85β (marked in bold). In Figure 4.11, an example of one of the MALDI-TOF experiments is shown. The most promising of the potentially phosphorylated peptides (marked • in Table 4.4) were

(1) those detected in both their unphosphorylated (m=x) and phosphorylated state (m =(x+80)). Peptides marked with * met this criterion.

(2) those phospho-peptides which could be detected with different m/z because of modifications or miscleavages (marked with °).

(3) those peptide sequences whose potentially phosphorylated residues could be found in p85α and p85β in their equivalent sequences (marked with ♦).

Amongst the potentially phosphorylated peptides detected by MALDI-TOF was the peptide containing Y368 of p85α (MHGDYTLTLRK), whose phosphorylation was identified in insulin-stimulated cells. Furthermore, Y499 of p85β (EYLERFR) was detected as a potentially phosphorylated peptide, whose equivalent Tyr residue in p85α (Y508) was shown to be phosphorylated in PDGF-stimulated cells. We also identified the peptide containing Y688 of p85α and Y458 of p85β, but only in their unphosphorylated state. Y508, Y607, S608 of p85α, amino acid residues that had also been identified as phospho-group acceptors, were located in amino acid sequences not detected by MALDI-TOF.

Table 4.4: Identification of potentially phosphorylated p85 peptides by MALDI-TOF analysis of immunopurified regulatory subunits.

Potentially phosphorylated peptides are in bold, peptides detected in their unphosphorylated and phosphorylated state are marked with *, phospho-peptides identified with different m/z are marked with °, phospho-peptides found in p85α and p85β are marked with ♦. m_{Ox} indicates oxidation of methionine.

p85α peptide sequences	experimental m/z	exp/ calc delta	modification
NLLNAR	700.43	0.03	
AENLLR	715.36	-0.05	
LSQASSK	720.37	-0.02	
LEEDLK	746.46	0.06	
DGTFLVR	807.42	-0.02	
LLEAIEK	815.48	-0.01	
LLYPVSK *	819.47	-0.02	
ALYDYKK	900.49	0.05	
AENLLRGK	900.52	-0.04	
ISEIIDSR	932.61	0.11	
LLEAIEKK	943.54	-0.04	
KQAAEYR	**945.50**	**0.08**	**1PO4**
NKAENLLR	957.65	0.11	
LYEEYTR	973.44	-0.02	
• **LLYPVSK ***	**979.56**	**0.13**	**1PO4**
DTADGTFLVR	1094.58	0.04	
GLECSTLYR	1098.58	0.06	
NESLAQYNPK	1163.64	0.06	
TQSSSNPAELR	1189.61	0.03	
MHGDYTLTLRK	1206.66	0.07	
TAIEAFNETIK *	1236.67	0.02	
• **TAIEAFNETIK ***	**1316.79**	**0.17**	**1PO4**
LRDTADGTFLVR	1363.84	0.08	
RTAEAFNETIK	1392.79	0.04	
• **KGLECSTLYR °**	**1400.68**	**-0.08**	**2PO4**
VLSEIFSPVLFR	1406.95	0.1	
MNSIKPDLIQLR	1427.85	0.05	
MHGDYTLTLRK + m_{Ox}	**1430.69**	**0.03**	**1PO4**
EIQRIMHNHDK + m_{Ox}	1436.77	0.07	
IFEEQCQTQER	1467.74	0.09	
GDFPGTYVEYIGR *	1473.86	0.11	
• **MNSIKPDLIQLR ♦** + m_{Ox}	**1523.86**	**0.09**	**1PO4**
FPAASSDNTEHLIK	1529.90	0.09	
MNSIKPDLIQLRK	1556.03	0.08	
AIEILISTEWNER	1573.90	0.08	
AIEILISTEWNER	1574.00	0.12	
• **GDFPGTYVEYIGR ***	**1633.63**	**0.01**	**2PO4**
YQQDQVVKEDNIEAVGK	1963.05	0.04	
TATGYGFAEPYNLYSSLK	1982.15	0.1	
EREEDIDLHLGDILTVNK	2109.37	0.14	
ESSKQGCYACSVVVDGEVK *	2130.27	0.13	
ISPPTPKPRPPRPLPVAPGSSK *	2276.47	0.06	
• **ESSKQGCYACSVVVDGEVK * °**	**2290.09**	**0.08**	**2PO4**
• **ISPPTPKPRPPRPLPVAPGSSK ***	**2356.34**	**0.02**	**1PO4**
YGFSDPLTFNSVVELINHYR	2371.24	0.03	
• **GLECSTLYRTQSSSNPAELR °**	**2443.16**	**0.05**	**2PO4**
• **QGCYACSVVVDGEVKHCVINK °**	**2544.19**	**0.02**	**1PO4**
TAIEAFNETIKIFEEQCQTQER	2685.34	0.02	
TEADTEQQALPLPDLAEQFAPPDVAPPLLIK	3327.6	-0.04	
GSLVALGFSDGPEARPEDIGWLNGYNETTGER	**3567.54**	**-0.03**	**2PO4**
YLADLPNPVIPVAVYNEMMSLAQELQSPEDCIQLLK	**4277.82**	**-0.04**	**2PO4**
p85β peptide sequences	**experimental m/z**	**exp/ calc delta**	**modification**
AVYPFR *	752.41	-0.02	
LLYPVSK *	819.47	-0.02	
DGTFLIR *	821.45	-0.02	
• **AVYPFR ***	**832.31**	**-0.08**	**1PO4**

• **DGTFLIR ***	901.41	-0.01	**1PO$_4$**
LYEEYTR	973.44	-0.02	
• **LLYPVSK ***	**979.56**	**0.13**	**2PO$_4$**
FLLQHLGR	983.69	0.11	
EYLERFR	**1092.57**	**0.07**	**1PO$_4$**
TAIEAFNETIK *	1236.62	-0.02	
• **TAIEAFNETIK ***	**1316.79**	**0.17**	**1PO$_4$**
EYDQLYEEYTR	1508.66	0.03	
GCYACSVVVDGDTK	1530.77	0.07	
MNSLKPDLMQLRK	1574.01	0.1	
RMNSLKPDLMQLRK + 2 m_{Ox}	1633.79	-0.04	
• **RMNSLKPDLMQLR *** + m_{Ox}	**1697.87**	**0.03**	**1PO$_4$**
ERPEDLELLPGDLLVVSR *	2050.23	0.08	
GFLLALPAAVVTPEAAAEAYR	2130.32	0.08	
• **ERPEDLELLPGDLLVVSR ***	**2130.38**	**0.08**	**1PO$_4$**
RAPSPDTAVHALASAFGPLLLR *	2260.37	0.05	
• **RAPSPDTAVHALASAFGPLLLR ***	**2290.09**	**-0.02**	**2PO$_4$**
LVQEHVEEQDAAPPALPPKPSK	2380.39	0.06	
IPPSGGEGDGSEPVPDFPVLLLER	2477.34	0.03	
EVAGPVGLVLEPPRLPLGQALTLR	2520.44	-0.08	
TAIEAFNETIKIFEEQGQTQEK	2554.40	0.05	
LVEAIEQAELDSECYSKPELPATR	2748.39	0.02	

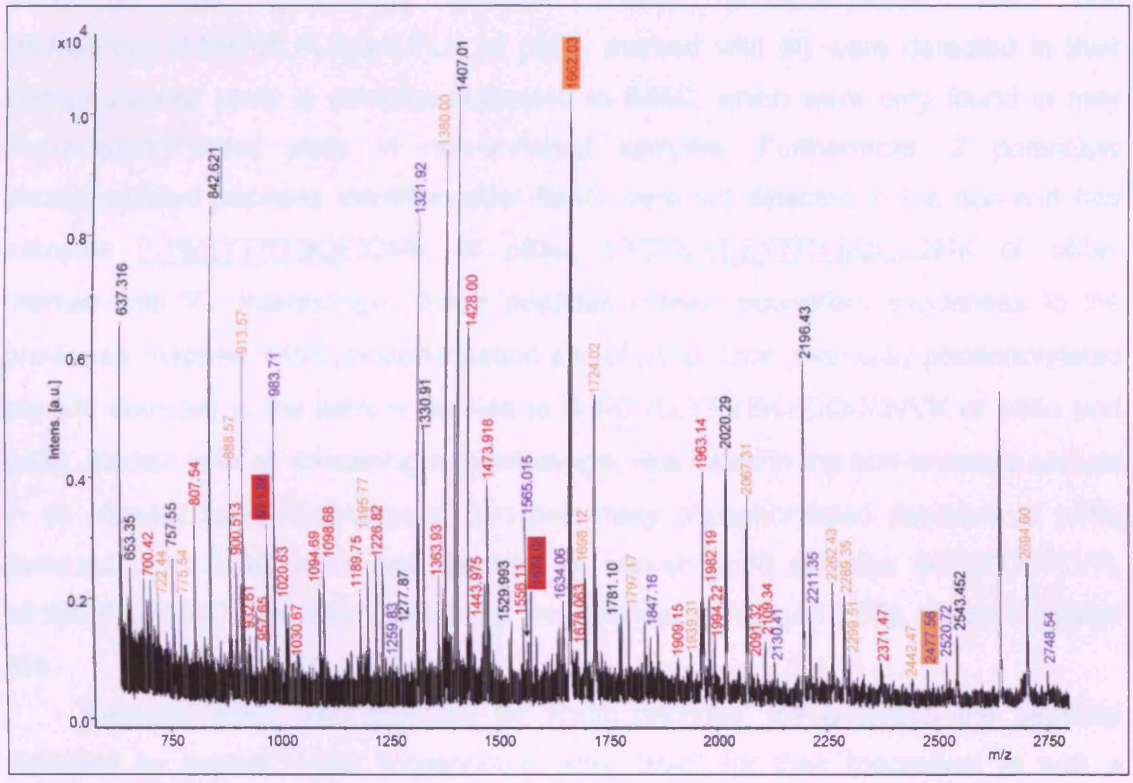

Figure 4.11: MALDI-TOF peptide mass fingerprinting spectrum of immunoprecipitated class IA PI3K regulatory subunit

The regulatory subunit was enriched by IP of p110δ, followed by SDS-PAGE separation and Coomassie brilliant blue staining. Protein bands were cut from the gel, reduced, alkylated and subjected to in-gel tryptic digestion. The peptides and DHB were spotted onto a MALDI metal plate and analysed by MALDI-TOF. m/z peaks corresponding to p85α, p85β and thymopoietin are shown in red, pink and orange, respectively. Underlined m/z correspond to trypsin peptides.

4.7.6 IMAC enrichment increased the detection of phosphorylated p85 residues

Immobilised metal ion affinity chromatography (IMAC) can be used for the enrichment of phosphorylated proteins and peptides ((Andersson and Porath, 1986; Cutillas et al., 2005). The separation principle of IMAC is based on electronic interaction of analyte molecules with metal ions immobilised to a stationary phase. Because of the composition of the metal chelate affinity chromatography column, phosphorylated peptides and acidic peptides preferentially bind to the column and can therefore be separated from non-phosphorylated peptides.

In order to enrich for phosphorylated peptides from tryptic digests of class IA PI3K regulatory subunits, we performed IMAC prior to MALDI-TOF analysis. Table 4.5 lists the peptides detected by peptide mass fingerprinting after IMAC enrichment of 2 independent experiments. Two peptides (TATGYGFAEPYNLYSSLK of p85α containing the previously mapped pY688 phosphorylation site, and EVAGPVGLVLEPPRLPLGQALTLR of p85β, marked with ⊗) were detected in their phosphorylated state in samples subjected to IMAC, which were only found in their non-phosphorylated state in non-enriched samples. Furthermore, 2 potentially phosphorylated peptides identified after IMAC were not detected in the non-enriched samples (LYEEYTRTSQEIQMK of p85α, EYDQLYEEYTRTSQELQMK of p85β, marked with ∇). Interestingly, these peptides contain equivalent sequences to the previously mapped Y458 phosphorylation site of p85β. One potentially phosphorylated peptide detected in the sample applied to IMAC (LLYPVSKYQQDQVVK of p85α and p85β, marked with ♣) containing a miscleavage, was found in the non-enriched sample in its cleaved form. Furthermore, two potentially phosphorylated peptides of p85α detected after IMAC were also detected in non-enriched samples (KGLECSTLYR, MHGDYTLTLRK), the latter containing the previously mapped Y368 phosphorylation site.

Because IMAC also enriches for acidic peptides, we analysed the peptides detected by peptide mass fingerprinting after IMAC for their theoretical pI with a computational tool that calculates the estimated pI of an amino acid sequence using pK values of amino acids described in (Bjellqvist et al., 1982). The majority of all non-phosphorylated peptides shown in Table 4.5 contain a theoretical pI<5 (excluding peptide RMNSLKPDLMQLR for calculations) compared to an average pI ≈ 7 for randomly picked peptides from Table 4.3. However, the majority of potentially phosphorylated peptides enriched by IMAC contain a pI >5, suggesting IMAC binding is due to phosphorylation. Only the potentially phosphorylated peptides LYEEYTRTSQEIQMK of p85α and EYDQLYEEYTRTSQELQMK of p85β have a pI <5,

suggesting IMAC enrichment because of both the acidity of the peptide and protein phosphorylation.

Table 4.5: Potentially phosphorylated p85 peptides identified by MALDI-TOF after IMAC enrichment

Potentially phosphorylated peptides are in bold, peptides found in IMAC sample that were found non-phosphorylated in non-IMAC samples are marked with ⊗, phospho-peptides only found in IMAC samples are marked with ∇, phospho-peptides also found in non-enriched samples are marked with ♣.

p85α sequences	experimental m/z	exp/ calc delta	modification	pI
EDNIEAVGK	974.46	-0.03		4.14
EGNEKEIQR	1102.53	-0.02		4.79
EDNIEAVGKK	1102.53	-0.04		4.68
KGLECSTLYR	**1400.66**	**0.07**	**2P**	**8.2**
MHGDYTLTLRK + m_{Ox}	**1430.69**	**0.03**	**1P**	**8.36**
IFEEQCQTQER	1467.61	-0.03		4.09
YQQDQVVKEDNIEAVGK	1962.97	-0.02		4.32
LLYPVSKYQQDQVVK ♣	**1967.84**	**-0.04**	**2P**	**8.43**
TATGYGFAEPYNLYSSLK ⊗	**2061.80**	**-0.06**	**1P**	**5.66**
EREEDIDLHLGDILTVNK	2109.07	-0.06		4.29
LYEEYTRTSQEIQMK ∇	**2158.93**	**0.05**	**3P**	**4.79**
QGCYACSVVVDGEVKHCVINK	**2544.19**	**0.02**	**1P**	**6.72**
p85β sequences	**experimental m/z**	**exp/ calc delta**	**modification**	**pI**
TQAEEMLSGK + m_{Ox}	1109.50	-0.01		4.53
EGNEKEMQR + m_{Ox}	1136.46	-0.04		4.79
IFEEQGQTQEK	1336.64	-0.01		4.25
EYDQLYEEYTR	1508.64	-0.09		4.00
RMNSLKPDLMQLR+ 1 m_{Ox}	1617.81	-0.03		10.84
RMNSLKPDLMQLR+ 2 m_{Ox}	1633.83	-0.02		10.84
LLYPVSKYQQDQVVK ♣	**1967.84**	**-0.04**	**2P**	**8.43**
YQQDQVVKEDSVEAVGAQLK	2234.18	0.02		4.32
EVAGPVGLVLEPPRLPLGQALTLR ⊗	**2602.01**	**-0.04**	**1P**	**6.24**
EYDQLYEEYTRTSQELQMK ∇	**2694.27**	**0.10**	**3P**	**4.25**
LVEAIEQAELDSECYSKPELPATR	2748.36	0.08		4.14

4.7.7 Confirmation of phosphorylated Tyr688 of p85α in proliferating WEHI-231 cells by multiple reaction monitoring

As shown in Table 4.1 and Table 4.2, LC-MS/MS analysis of the regulatory subunit did not reveal phosphorylated residues although we identified a variety of potentially phosphorylated peptides by MALDI-TOF. We therefore applied LC-MRM.

Before analysing the regulatory subunit for novel phosphorylation sites by MRM using potentially phosphorylated residues detected by MALDI, we were interested in the identification of previously mapped p85 phosphorylation sites. The mass spectrometric data gained by peptide mass fingerprinting and MS/MS experiments revealed that MS analysis allowed for the identification of unphosphorylated Y368, Y508, Y580 and Y588, whereas identification of Y607 and S608 was not possible. Therefore, LC-MRM was only performed with m/z of peptide sequence containing

phosphorylated Y368, Y508, Y580 and Y688. The MS/MS data for each total ion chromatogram (TIC) peak were extracted and compared to *in silico* MS-product data of the chosen peptide (Protein Prospector, UCSF). As shown in Figure 4.12.A, a doubly-charged peptide containing phosphorylated Y688 was identified from WEHI-231 cells if MRM was performed with $[M+2H]^{2+}$=687.9. Most of the m/z peaks of the MS/MS spectrum shown could be assigned to fragment ions of the TATGYGFAEPYNLYSSLK peptide. Fragment ions are generated if a peptide bond undergoes two or more fragmentation events (Aebersold and Goodlett, 2001). Empirical observations showed that internal fragments often occur if either proline or aspartic acid residues are present, which was the case for the investigated peptide.

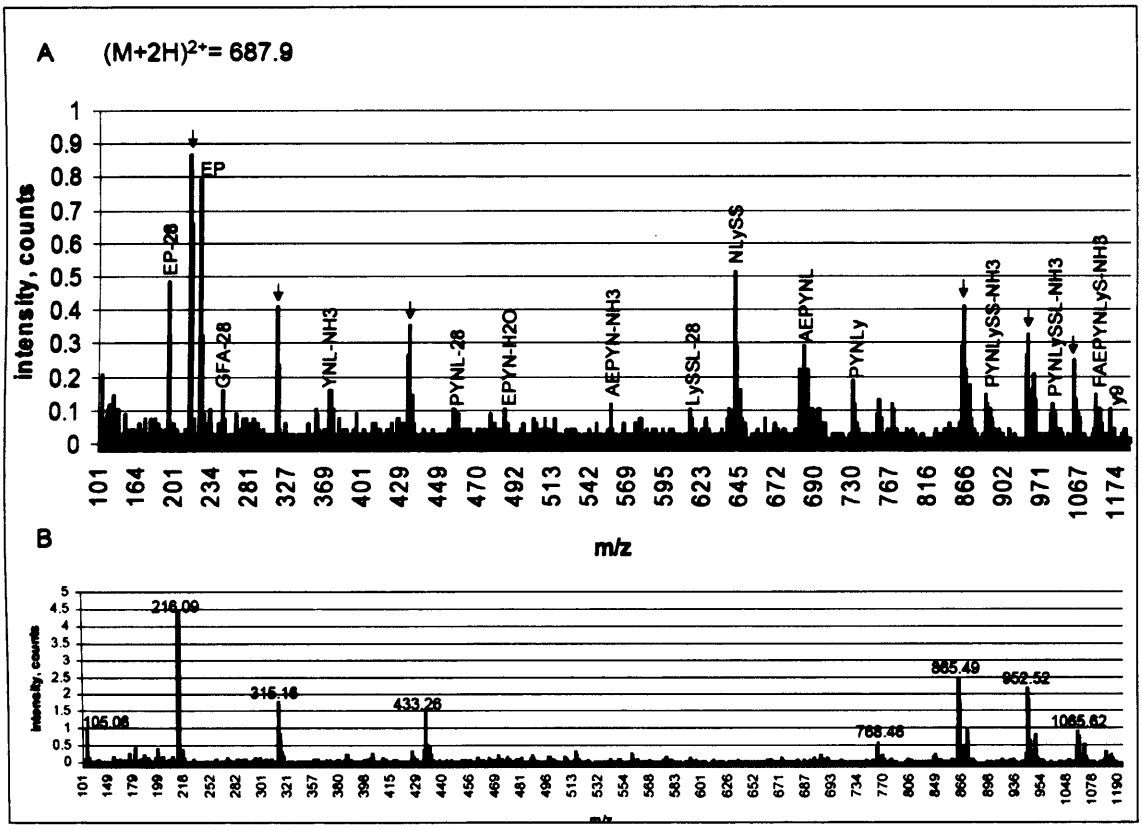

Figure 4.12: Identification of pY688 in WEHI-231 cells by MRM

(A) MRM was performed with tryptic digests of immunopurified regulatory subunit producing the MS/MS spectra of m/z = 687.9. The MS/MS data of each peak in the total ion chromatogram (TIC) were compared to *in silico* collision induced dissociation (CID) and the m/z peaks were labelled accordingly. Unassigned m/z peaks are marked with an arrow. (B) The majority of the unassigned m/z peaks were also found in a second TIC peak of the same MRM run, indicative of contaminating ions (B).

m/z peaks depicted with an arrow in the MS/MS spectrum of $[M+2H]^{2+}$=687.9, which represented most of the unassigned m/z in the spectrum, were also found in a closely eluting peptide TIC peak of this LC-MS/MS run shown in Figure 4.12.B, indicative for contaminating ions. Y688 has been previously identified as a phosphorylation site in overexpressed p85α and its identification here in endogenous,

not overexpressed condition using MS techniques indicates that our MS approach is, in principle, capable of identifying phosphorylation sites.

Performing the same experiment with the m/z of phospho-peptides containing Y368, Y508 and Y580, respectively, did not lead to identification of these phosphorylated residues.

4.7.8 Analysis of protein phosphorylation by MRM MS did not uncover novel phosphorylation sites

After successful identification of phosphorylated Tyr688 in p85α, we performed MRM experiments with p85 samples enriched by immunopurification or pTyr-matrix pull-down and selected for different m/z corresponding to potentially phosphorylated p85α or p85β peptides identified by MALDI-TOF. For every run, the total ion chromatogram (TIC) of each selected ion was extracted using MassLynx V4.0, the sequencing information within each peak accumulated, centred and smoothed and the sequencing data scanned against the NCBI nr using Mascot. Unfortunately, none of the investigated m/z led to the identification of a predicted phospho-peptide.

4.7.9 Error-tolerant searches reveal hydroxylation and amino acid substitutions of p85α

When the results of an MS/MS search are reviewed, there are often a number of spectra that remain unmatched. If that given spectrum contains adequate information (reasonable number of fragment ion peaks at usable signal to noise ratio) causes for failure to find a peptide match are underestimated mass measurement errors, incorrect determination of precursor charges, non-specificity of the enzyme used for digestion, unsuspected chemical and post-translational modifications, and unreported peptide sequences. Error-tolerant searches by Mascot allow for addressing the latter three challenges.

We performed error-tolerant searches on the complete p85 dataset gained from various experiments in order to reveal post-translational modifications other than phosphorylation that could account for the modifications of class IA PI3K regulatory subunit detected on 2D-PAGE in unstimulated cells (see § 4.1). Table 4.6 lists the modifications occurring in class IA PI3K regulatory subunit revealed by error-tolerant searches. The output data of the error-tolerant searches were assigned from manual interpretation of the MS/MS spectra viewed using MassLynx V4.0 (Figure 4.13).

Table 4.6: Identification of post-translational modifications and primary sequence alterations performing error-tolerant searches

LC-MS/MS data were analysed in error-tolerant searches for enzyme non-specificity, chemical and post-translational modifications, and amino acid alterations. Output data of error-tolerant searches were assigned from manual interpretation of the MS/MS spectra using MASSLYNX V4.0.

p85α peptide sequences		experimental m/z	exp/ calc delta	modification
VLSEIFSPVLFR		703.86	0.05	
VLSEIFSpVLfR	A	727.86	0.04	P_{OH}, $F_{(OH)2}$
LLEAIEK		408.22	0.03	
LVEAIEKK	B	465.28	0.02	L136V
FPAASSDNTEHLIK		765.36	0.02	
FPAASSENTEHLIK	C	772.40	-0.01	D281E
ISEIIDSR		466.76	0.01	
ISEIVDSR	D	459.74	0.01	I539V

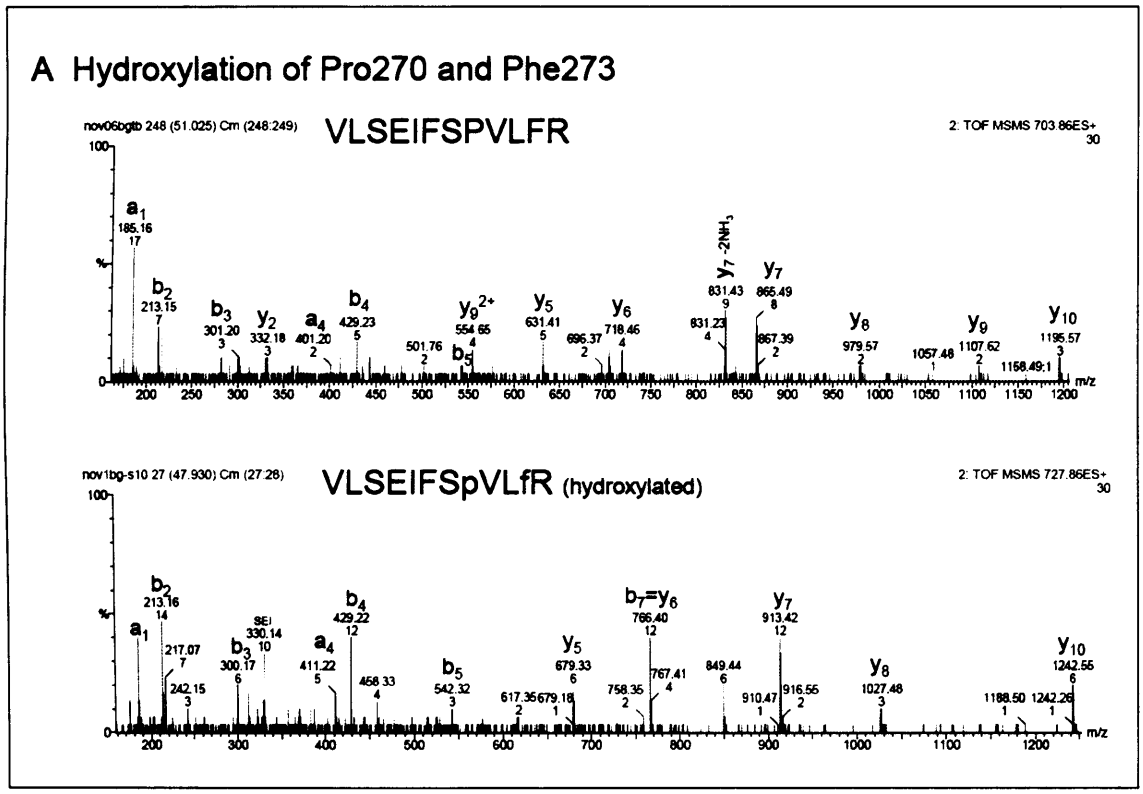

B Amino acid variation of Leu136

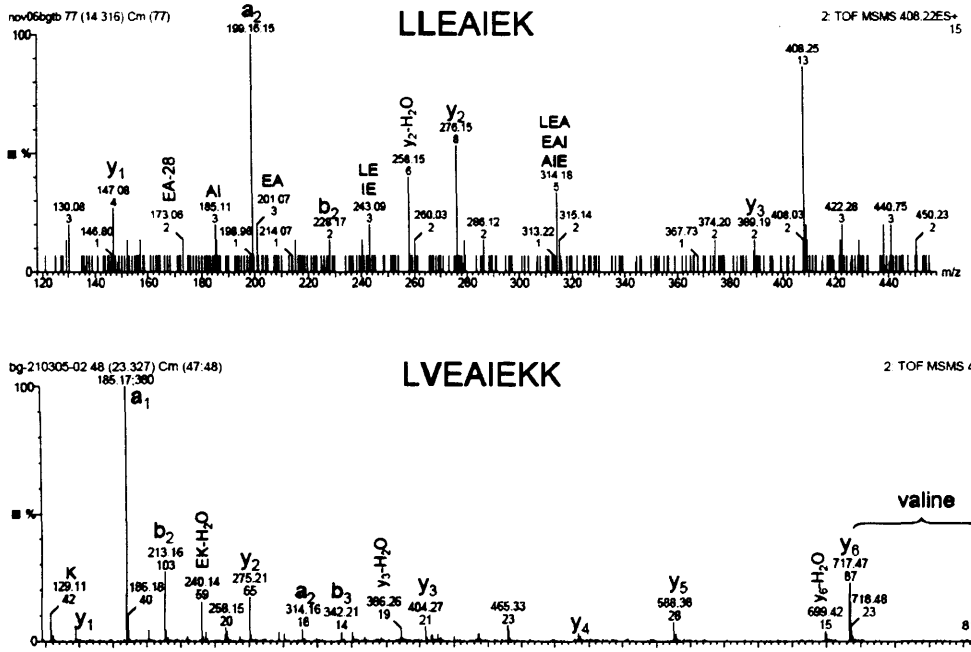

C Amino acid variation of Asp281

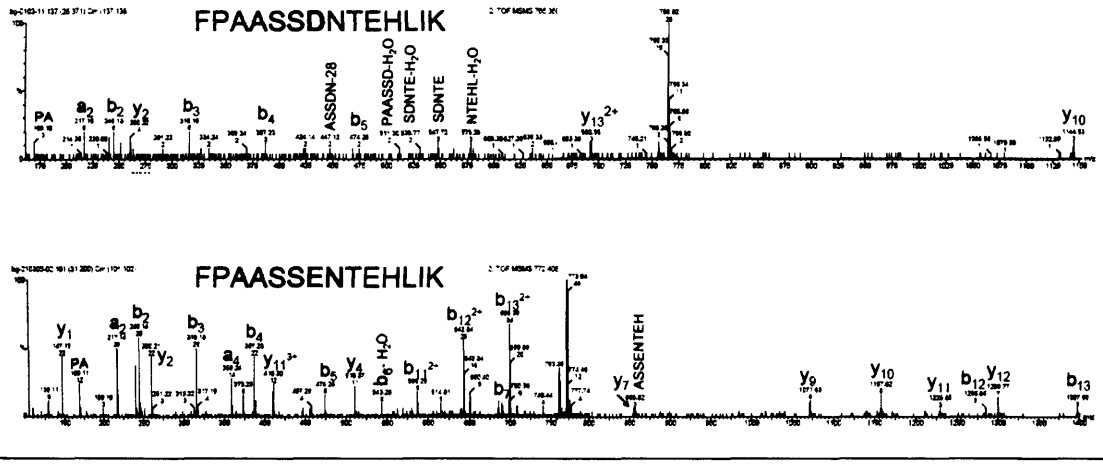

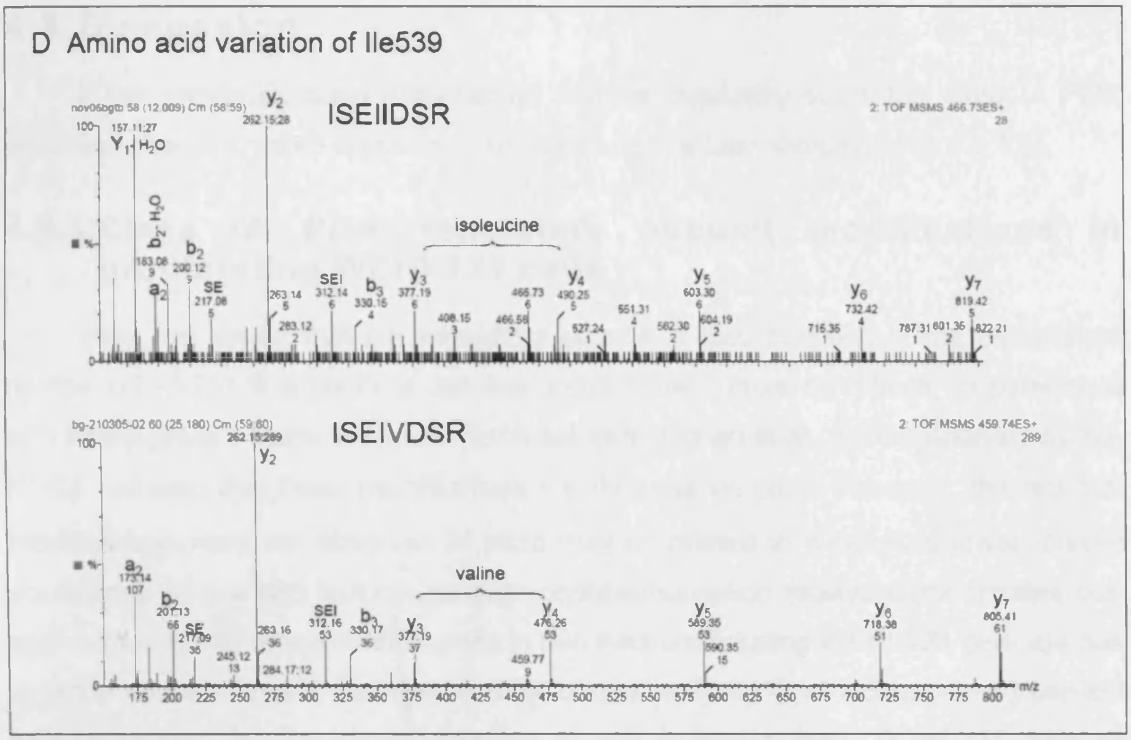

Figure 4.13: Mass spectra of modifications in p85α identified by error-tolerant searches
Output data of error-tolerant searches were assigned from manual interpretation of the MS/MS spectra using MASSLYNX V4.0. (A) MS/MS spectra of unmodified and hydroxylated Pro270 and Pro273; (B, C, D), amino acid variations in the primary sequence of p85α.

The modified residues cluster in the Rac-binding domain of p85α, with one amino acid substitution detected in the inter-SH2 domain, also termed p110 binding domain (Figure 4.14). The Rac-binding domain, a 200-residue region also named breakpoint cluster region-homology (BH) domain, is responsible for the GAP activity of p85. It has been shown to interact with a variety of GTPases, such as Rac1 and Cdc42 (Tolias et al., 1995; Zheng et al., 1994).

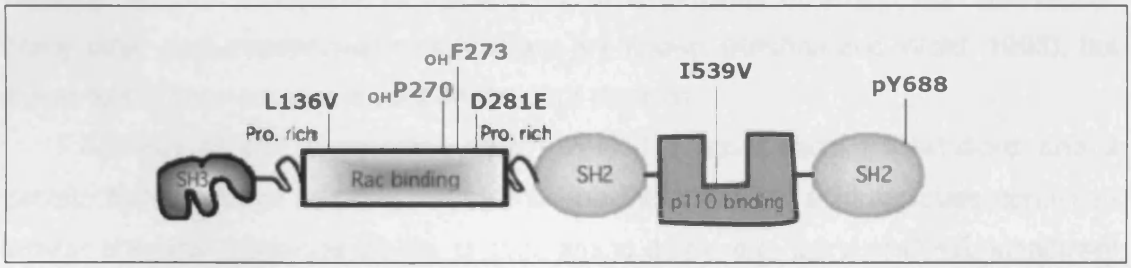

Figure 4.14: Schematic representation of the identified amino acid modifications in p85
Performing error-tolerant searches by MS, 5 amino acid modifications of p85α were identified in addition to the phosphorylated Tyr688 detected by MRM MS.

4.8 Discussion

It has previously been documented that the regulatory subunit of class IA PI3K becomes phosphorylated on several residues upon cellular stimulation (§ 1.3.4.2).

4.8.1 Class IA PI3K regulatory subunit modifications in proliferating WEHI-231 cells

Here, we report that the regulatory subunit is also modified in the established murine WEHI-231 B lymphoma cell line under basal culture conditions, in agreement with investigations made in murine fibroblast cells (Cohen et al., 1990). Analysis by 2D-PAGE revealed that these modifications mainly occur on p85α. However, the fact that modifications were not observed in p85β may be related to a possible lower relative abundance of this p85 isoform. *In vitro* dephosphorylation assays demonstrated that approximately half of the modifications in p85 from proliferating WEHI-231 cells are due to protein phosphorylation as revealed by 2D-gel analysis. This finding is in agreement with indications for Thr phosphorylation of p85 in unstimulated WEHI-231 cells as revealed by immunoblotting using pThr Abs and with our MS identification of Y688 phosphorylation site in p85α from WEHI-231 cells cultured under basal conditions. Unfortunately, detailed MS analysis of peptides derived from the regulatory subunit only provided indications for potentially phosphorylated amino acid residues without the capacity to confirm this by sequencing of the peptides of interest.

The remaining other half of the post-translational modifications in p85 from unstimulated WEHI-231 cells are most likely due to modifications other than phosphorylation. Since the pI values of the p85 species that are resistant to phosphatase treatment are more acidic than the main p85 protein 2D gel spot, we speculate that the changes in pI could be due to hydroxylation, acetylation, sulfation/ nitration, specific proteolysis of the N- and/ or C-terminus or amino acid alterations. Many other post-translational modifications are known (Krishna and Wold, 1993), but these do not have a major impact on the pI of proteins.

Analysis of p85 sequencing data revealed 3 amino acid substitutions and 2 protein hydroxylations in p85α. Since the substituted amino acid residues contained similar chemical properties as the original amino acids, e.g. L→V or D→E, significant changes in the isoelectric point of p85α are not expected. However, unless mutant protein was to be expressed and analysed by 2D-PAGE, these modifications can not be excluded from being part of the observed p85α spot pattern. The substituted residues of L136, D281 and I539, which were found in their non-modified and modified form in WEHI-231 cells, are also found in p85α sequences of other mammalian species, for example V136 is present in *homo sapiens*. The frequency with which these

amino acids are mutated gives reason to believe that their specificity is not crucial for p85 function. Analysis of the p85α nucleotide sequence revealed that the amino acid substitutions are likely due to single nucleotide polymorphisms (SNPs). SNP could either occur in a subpopulation of WEHI-231 cells or exist on one p85α allele only. SNP analysis of class IA PI3K regulatory subunit genes revealed mutation of amino acid M326 to Ile in p85α (Hansen et al., 1997). This SNP is associated with reduced binding affinity of p85α to IRS-1, but not IRS-2 (Algenstaedt et al., 2004). Further SNPs have been detected in the intronic sequence of the p85α gene, and have therefore no impact on p85α amino acid sequence (Barroso et al., 2003); (Suzuki et al., 2004). In contrast to amino acid substitutions detected by MS, protein hydroxylation is likely to reduce the pI of a protein thereby influencing the protein spot pattern detected on 2D gels. However, hydroxylation of proteins during sample preparation for MS analysis due to oxidative conditions can not be excluded as the cause for the identified hydroxylated amino acids in p85α even though reducing agents are added to the sample in each step in order to prevent oxidation.

The modifications detected in unstimulated cells are mainly found in the BH domain of p85α, with one amino acid alteration in the inter-SH2 domain and one in the C-terminal SH2-domain. Since class IA PI3K regulatory subunits are adaptor proteins, it is likely that the modifications identified here are involved in the regulation of protein-protein interactions. This is at least true for pY688 in the C-terminal SH2-domain, which has been implicated in the reduction of p85α interaction with tyrosine phosphorylated proteins (von Willebrand et al., 1998).

4.8.2 Class IA PI3K regulatory subunit modifications in α-IgM stimulated WEHI-231 cells

In order to gain insight into the biological significance of these modifications, p85 post-translational modifications were analysed in WEHI-231 cells activated with physiologically relevant stimuli. No increase in p85 protein phosphorylation was detected by immunoblotting analysis after BCR triggering, even though the downstream effector PKB showed increased phosphorylation, indicative for effective cellular stimulation. In addition, the overall 2D gel spot pattern did only change very marginally upon stimulation. Only when cells were treated with okadaic acid or pervanadate, two powerful inhibitors of phosphatases, S608 and global Thr phosphorylation were increased and the 2D gel spot pattern of p85 significantly changed. We were surprised not to find any changes in protein phosphorylation, especially Tyr phosphorylation, of p85 upon physiological stimulation of B cells. Tyr phosphorylation of p85 on different p85 residues in different cell types upon

physiological stimulation has been reported by various research teams (for more information see § 1.3.4.2). In addition, we documented phosphorylation of Y688 by MS in unstimulated B cells and this phosphorylation was previously shown to be increased upon cellular stimulation of T cells. However, it is possible that BCR crosslinking undergoes different signalling pathways than TCR crosslinking or stimulation of cells with growth factors/hormones. In line with this, stimulation of B cells induces Tyr phosphorylation of the regulatory subunit only after 20 minutes of BCR crosslinking (Beckwith et al., 1996), while other stimuli induce modification of p85 much earlier. We conclude that under the conditions used for cellular stimulation of WEHI-231 cells, the class IA PI3K regulatory subunit does not undergo significant protein phosphorylation or, in fact, any post-translational modifications that would lead to changes in the isoelectric point of the protein.

4.8.3 Biochemical role of class IA PI3K regulatory subunit modifications

In order to gain knowledge of the biochemical roles of these modifications, we analysed the protein spot pattern in different cell types, and following p110 IP in B cells. Minor differences in the 2D gel spot pattern of p85 were found in 4 different murine cell systems using a p85 Ab whose epitope lied within the Rac-binding domain. However, no differences could be detected if p85 Abs were used whose epitopes lied within the N-terminal SH-2 domain. It is therefore possible that the same type of modification (e.g. protein phosphorylation) occurs on different amino acid residues in the regulatory subunit in different cell types. Thus, if one of the amino acids within the Rac-binding domain was modified, one would expect the Rac-Ab to bind this sequence with lower affinity. If the same modification occurred on another residue in a different cell line, differences in the Ab signal using the Rac-Ab, but not using the N-SH2 Ab should be detectable between the cell types. Observations made in stimulated cells, where different p85α amino acid residues have been implicated in phosphorylation in different cell types, e.g. pY508 in PDGF-responsive, pY580 in insulin-responsive and pY688 in immune-responsive cells (see § 1.3.4.2) are in line with this hypothesis.

We also investigated whether the modifications observed in p85 were related to its interaction with the distinct p110 catalytic subunits. Therefore, the 3 class IA catalytic subunits were immunopurified with p110 isoform-specific Abs. Modest differences in the protein spot pattern of the regulatory subunit could be detected after IP with different p110 Abs, suggesting that the interaction of the regulatory and catalytic subunits was partially dependent on the observed modifications. These findings also suggest that some of the modifications of p85α detected in unstimulated cells may occur on amino acid residues located in the p110-binding domain of the regulatory

subunit, such as Ile539 residue which was modified to Val as detected by MS. An alternative explanation for these observations could be that the p110-specific modifications are catalysed by the catalytic subunits.

5 BIOCHEMICAL ANALYSIS OF P110δ IN B CELL ANTIGEN RECEPTOR STIMULATED IMMATURE B CELLS

Signal transduction through the BCR changes dramatically during B cell development resulting in growth arrest and apoptosis in immature B cells and leading to proliferation in mature B cells. Apoptosis in immature B cells serves to remove overreactive or unresponsive lymphocytes. The initial response in immature and mature B cells to BCR engagement seems to be similar, leading to a transient increase in Akt and Erk phosphorylation (Bilancio et al., 2006) followed by a decrease in PI3K-dependent PI levels within 1 h of stimulation (Carey and Scott, 2001). However, the PIP_3 concentration in α-IgD stimulated B cells (which do not undergo growth arrest or apoptosis) returns to basal levels after 4-8 h of BCR engagement, while PIP_3 levels remain low in α-IgM stimulated immature B cells. BCR crosslinking of immature B cells leads to a concomitant long-term decrease in the phosphorylation of the PI3K effector S6K, downregulation of c-myc expression and upregulation of $p27^{Kip1}$ inducing G1 growth arrest (Carey and Scott, 2001).

BCR engagement induces a complex signalling cascade described in § 1.7. Briefly, following B cell stimulation by antigen, the Tyr kinases Lyn and Syk are recruited to the BCR and activated, and increase phosphorylation of adaptor molecules. PI3Ks are subsequently recruited to the plasma membrane by association of their SH2 domains with pTyr residues in adaptor molecules. Membrane recruitment leads to PI3K activation and PIP_3 generation. This induces the accumulation of proteins into a signalosome ultimately increasing MAP kinase and PI3K signalling pathway activation and Ca^{2+} flux. Mouse-gene targeting and inhibitor studies have documented an important role for p85α and p110δ in B cell development and function (Beckwith et al., 1996; Bilancio et al., 2006; Clayton et al., 2002; Fruman et al., 1999; Jou et al., 2002; Okkenhaug et al., 2002; Suzuki et al., 1999). Inactivation of PI3K impairs BCR-mediated proliferation as a consequence of reduced PIP_3 generation and Ca^{2+} mobilisation.

In order to gain insight into the molecular mechanism of p110δ activation and subsequent de-activation following BCR engagement in immature B cells, we analysed post-translational modifications, lipid kinase activity, subcellular localisation and binding partners of p110δ following α-IgM stimulation. Our results confirm the dependence of PI3K signalling on p110δ following BCR crosslinking, and indicate that the increase in PI3K activity is not due to enhanced intrinsic lipid kinase activity, but to alterations in p110δ binding partners, which likely influences p110δ subcellular localisation. These changes might be due to enhanced Tyr phosphorylation of p110δ, which is primarily

found in the p110δ isoform of class IA PI3Ks and mainly detected in B cells. Furthermore, we present a panel of novel, potential PI3K interaction partners – in unstimulated and stimulated immature B cells.

5.1 Time-course of Akt phosphorylation following BCR engagement

In order to investigate the time course of BCR-induced PI3K activation, we analysed the phosphorylation state of the PI3K downstream effector Akt following BCR engagement of the immature B cell line WEHI-231. As shown in Figure 5.1, in unstimulated cells little Akt was phosphorylated compared to α-IgM stimulated cells. The phosphorylation of Akt increased steadily over a period of 10 min of stimulation. Analysis of Akt phosphorylation beyond 10 min of stimulation indicates a slow decrease to basal levels within 1-2 h of stimulation (Bilancio et al., 2006; Gold et al., 1999).

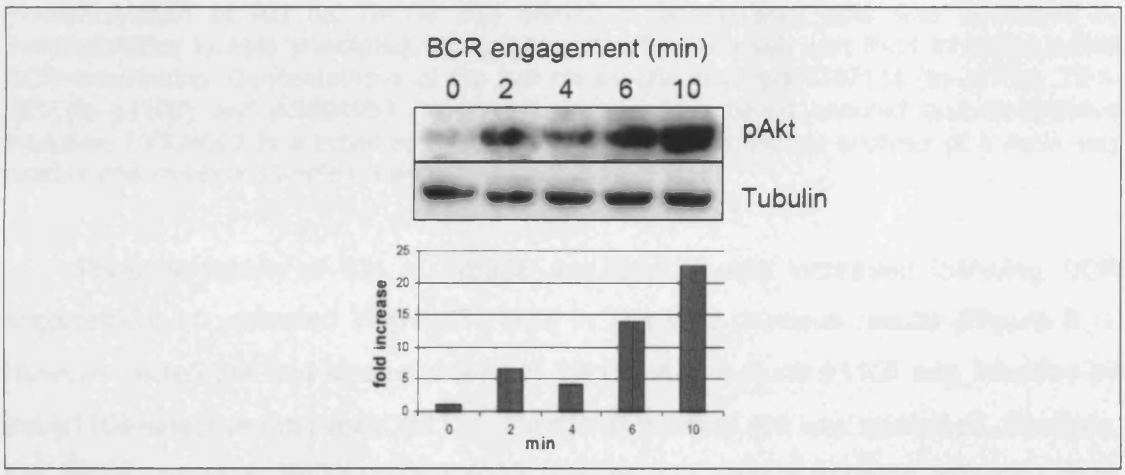

Figure 5.1: BCR engagement of WEHI-231 cells induces phosphorylation of Akt

WEHI-231 cells were treated for the indicated time points with α-IgM leading to crosslinking of BCR. The phosphorylation state of the PI3K downstream effector Akt following stimulation was analysed by immunoblotting. Immunoblotting analysis of tubulin protein amounts was used to confirm equal gel loading. Relative quantitation of immunoblot signals is shown in the lower panel of Figure 5.1.

5.2 p110δ lipid kinase activity is critical for Akt phosphorylation following BCR engagement in WEHI-231

In order to dissect which class IA PI3K catalytic subunit was responsible for the increase in PI3K activity following BCR engagement in WEHI-231 cells, the α-IgM induced phosphorylation of Akt was analysed following pretreatment of cells with PI3K pharmacological inhibitors. To this end, WEHI-231 cells were pre-treated for 30 min with isoform-specific and broad-spectrum inhibitors against PI3K subunits (Figure 5.2).

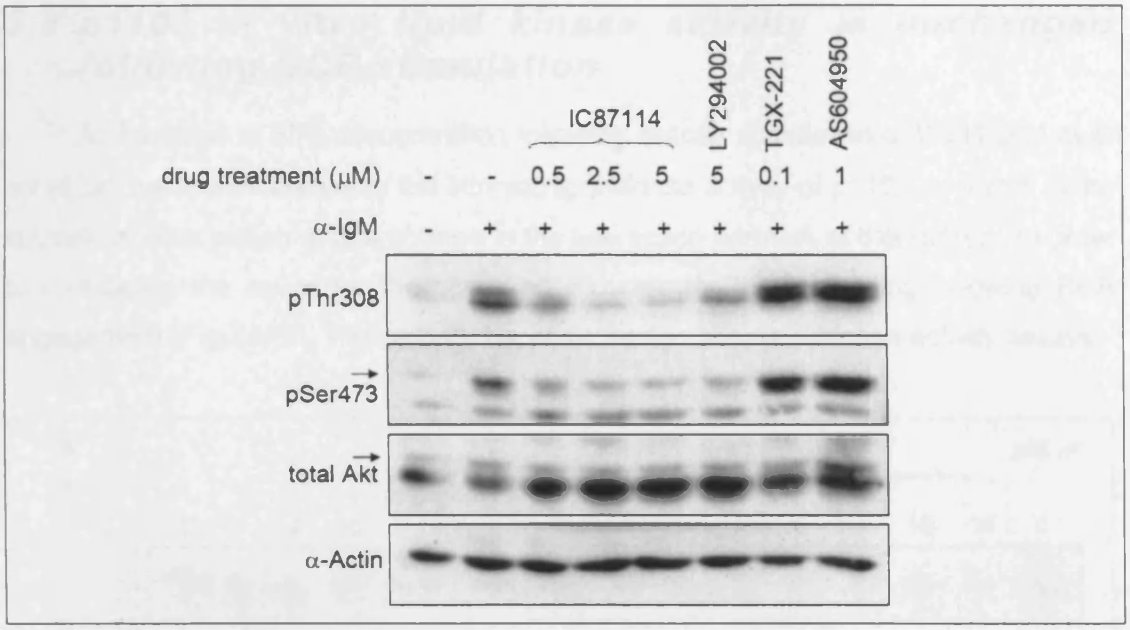

Figure 5.2: p110δ is the critical class IA PI3K subunit following BCR engagement
Phosphorylation of Akt on Thr308 and Ser473 in unstimulated cells was compared by immunoblotting to cells stimulated with α-IgM and cells pretreated with PI3K inhibitors before BCR crosslinking. Concentrations of the isoform-specific inhibitors IC87114 (to p110δ), TGX-221 (to p110β) and AS604950 (to p110γ) were chosen which ensured isoform-selective inhibition. LY294002 is a broad-spectrum PI3K inhibitor. Immunoblot analysis of α-Actin was used to ensure equal sample loading.

Phosphorylation of Akt at Thr308 and Ser473 was increased following BCR engagement of untreated WEHI-231 cells in line with previous results (Figure 5.1). However, when the lipid kinase activity of the catalytic subunit p110δ was inhibited by the p110δ-selective inhibitor IC87114, phosphorylation of Akt was abolished. Similarly, the broad-spectrum inhibitor LY294002 blocked Akt phosphorylation following BCR engagement. In contrast, inhibition of p110β or p110γ activity by TGX-221 and AS604950, isoform-selective inihibitors to p110β and p110γ, did not lead to a reduction in Akt phosphorylation. On the contrary, inhibition of p110β and p110γ activity led to an increase in Akt phosphorylation compared to α-IgM stimulated, untreated cells. Analysis of p110α contribution to Akt phosphorylation was not possible at the time, because no p110α isoform-specific inhibitor was available to us.

These results suggest that p110δ is primarily responsible for the increase in Akt phosphorylation in WEHI-231 cells following BCR crosslinking. Since phosphorylation of Akt is a direct cause of PIP_3 generation, we conclude that p110δ is the main producer of PIP_3 under the chosen conditions. These results confirm previous observations in our laboratory (Bilancio et al., 2006).

5.3 p110δ in vitro *lipid kinase activity is unchanged following BCR stimulation*

An increase in PIP_3 concentration following cellular stimulation of WEHI-231 cells could be due to an increase in the intrinsic lipid kinase activity of p110δ, to a shift in the subcellular localisation or to a change in the interaction partners of this protein. In order to investigate the cause for the observed increase in PI3K signalling following BCR engagement (Figure 5.1, Figure 5.2), we performed *in vitro* lipid kinase activity assays.

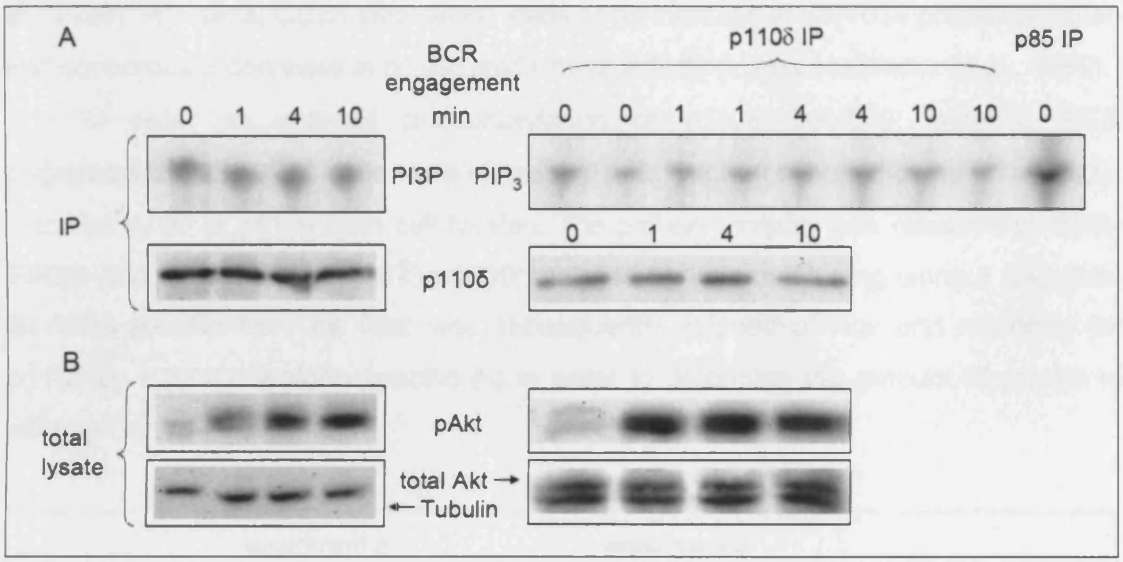

Figure 5.3: The intrinsic lipid kinase activity of p110δ does not increase following BCR engagement

WEHI-231 cells were stimulated with α-IgM for the indicated time points and *in vitro* lipid kinase activity assays were subsequently performed. (A) Immunoprecipitated p110δ was subjected to *in vitro* lipid kinase assays using PI (left panel) or PtdIns(4,5)P_2 (right panel) as substrates. The incorporation of radioactive phosphate into PtdIns was measured by autoradiography. Immunoprecipitated p85 was used as a positive control for the *in vitro* lipid kinase activity assay. A fraction of the p110δ-IP was used to determine equal p110δ enrichment after each time point of stimulation by immunoblotting with p110δ-specific Ab. (B) Total cell lysate of each time point of stimulation was analysed by immunoblotting for phosphorylation of Akt. Immunoblot analysis of total Akt or tubulin was used to ensure equal sample application.

To this end, WEHI-231 cells were left untreated or stimulated with α-IgM for different lengths of time. Following cell lysis, p110δ was immunoprecipitated using a p110δ-specific Ab and subjected to *in vitro* lipid kinase activity assays using phosphoinositides as substrates as described in § 2.13. As shown in Figure 5.3, equal amounts of 3'-phosphorylated phosphoinositides were detected by autoradiography following separation of lipids by thin layer chromatography independent of cellular stimulation, suggesting that p110δ activity was unaltered upon cellular stimulation of WEHI-231 cells. Neither the choice of PI3K substrate (PI or PtdIns(4,5)P_2) nor the time of stimulation seemed to have an effect on p110δ *in vitro* lipid kinase activity. These

results indicated that the increase in Akt phosphorylation observed following BCR engagement was most likely not due to an increase in intrinsic p110δ lipid kinase activity.

5.4 BCR engagement results in a modest decrease in p110δ Ser1039 phosphorylation

Autophosphorylation of Ser1039 located in the C-terminus of p110δ has been implicated in the downregulation of its intrinsic lipid kinase activity (Vanhaesebroeck et al., 1999). In T cells, CD28 stimulation leads to an increase in Ser1039 phosphorylation and concomitant decrease in p110δ lipid kinase activity (Vanhaesebroeck et al., 1999).

In order to address phosphorylation of p110δ Ser1039 following BCR engagement, WEHI-231 cells were stimulated with α-IgM for the indicated time points, followed by IP of p110δ from cell lysates. The protein complex was resolved by SDS-PAGE and phosphorylation of Ser1039 analysed by immunoblotting using a phospho-Ser1039-specific Ab. The filter was subsequently stripped of Abs and reprobed for p110δ by a p110δ isoform-specific Ab in order to determine the amount of protein in each gel lane.

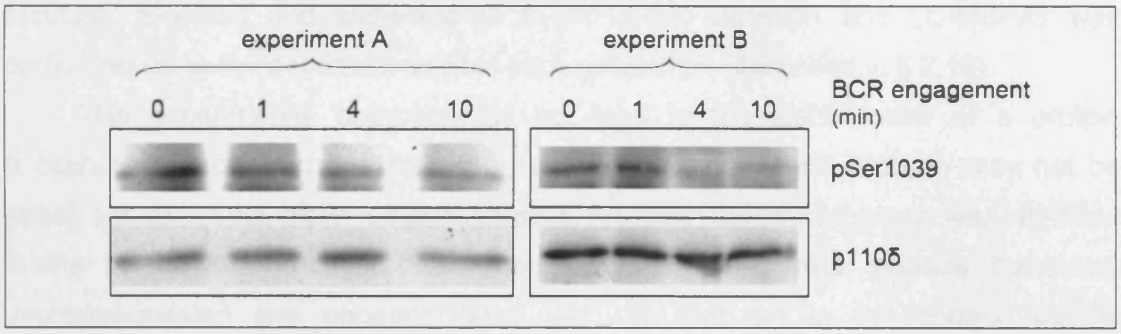

Figure 5.4: BCR engagement induces a small decrease in p110δ Ser1039 phosphorylation
p110δ was immunoprecipitated from total cell lysate of unstimulated or α-IgM stimulated WEHI-231 cells. The immunocomplex was separated by SDS-PAGE, the proteins transferred to a PVDF membrane and p110δ analysed for Ser1039 phosphorylation using a pSer1039-specific Ab. After stripping of proteins from the filter, total p110δ protein was analysed as a loading control.

BCR stimulation of WEHI-231 cells led to a small decrease in Ser1039 phosphorylation compared to the basal state and this decrease in phosphorylation was dependent on the time of stimulation (Figure 5.4). In contrast to the observations made from *in vitro* lipid kinase activity assays, which indicated unaltered intrinsic lipid kinase activity of p110δ following cellular stimulation of WEHI-231 cells (§ 5.3), this result suggests that p110δ lipid kinase activity is increased following B cell stimulation pre-

supposing that the phosphorylation state of Ser1039 can be used as a readout for instrinsic lipid kinase activity.

The changes observed in Ser1039 phosphorylation following B cell stimulation could potentially be due to decreased autophosphorylation or increased protein phosphatase activity. We therefore compared p110δ protein interaction partners from unstimulated and α-IgM stimulated B cells by MS following co-IP experiments using a p110δ-Ab (see § 5.6), but did not detect any protein phosphatase interacting with p110δ. Furthermore, we analysed the protein interaction partners of peptide sequences containing non-phosphorylated *versus* phosphorylated Ser1039. To this end, a peptide made of the p110δ C-terminal amino acid sequence KVNWLAHNV**S**KDNRQ containing Ser1039 (in bold) and a second peptide made of the same amino acid sequence, but containing phosphorylated Ser1039 were coupled to Actigel beads. These constructs were used to pull-down potential p110δ interacting partners from 20 mg WEHI-231 cell lysates. Beads uncoupled to peptides were also incubated with WEHI-231 cell lysate in order to determine which proteins unspecifically interacted with the Actigel beads (Control). The pulled-down proteins were resolved by SDS-PAGE. The protein gel was subsequently fixed and proteins stained with colloidal Coomassie blue (Figure 5.5.A). Gel lanes were cut into sections of equal size and molecular weight. Proteins were reduced, alkylated and subjected to tryptic in-gel digestion and LC-MS/MS was performed using the peptide content of each gel section (described in § 2.16).

This experimental approach did not lead to the identification of a protein phosphatase. However, the interaction between substrate and enzyme may not be strong enough to pull-down the phosphatase. A protein called Acrogranin was identified in the pull-down of Actigel beads coupled to the C-terminal peptide containing unphosphorylated and phosphorylated Ser1039, but not in the control sample containing beads only (Figure 5.5.B/C). Acrogranin, also known as proepithelin and PC-cell-derived growth factor (PCDGF), is the largest member (67 kDa) of a family of growth modulators and has been implicated in the contribution to tumorigenesis in diverse cancers (He et al., 2002; Matsumura et al., 2006; Ong and Bateman, 2003). These findings implicate that Acrogranin might interact with the C-terminal domain of p110δ independent of Ser1039 phosphorylation.

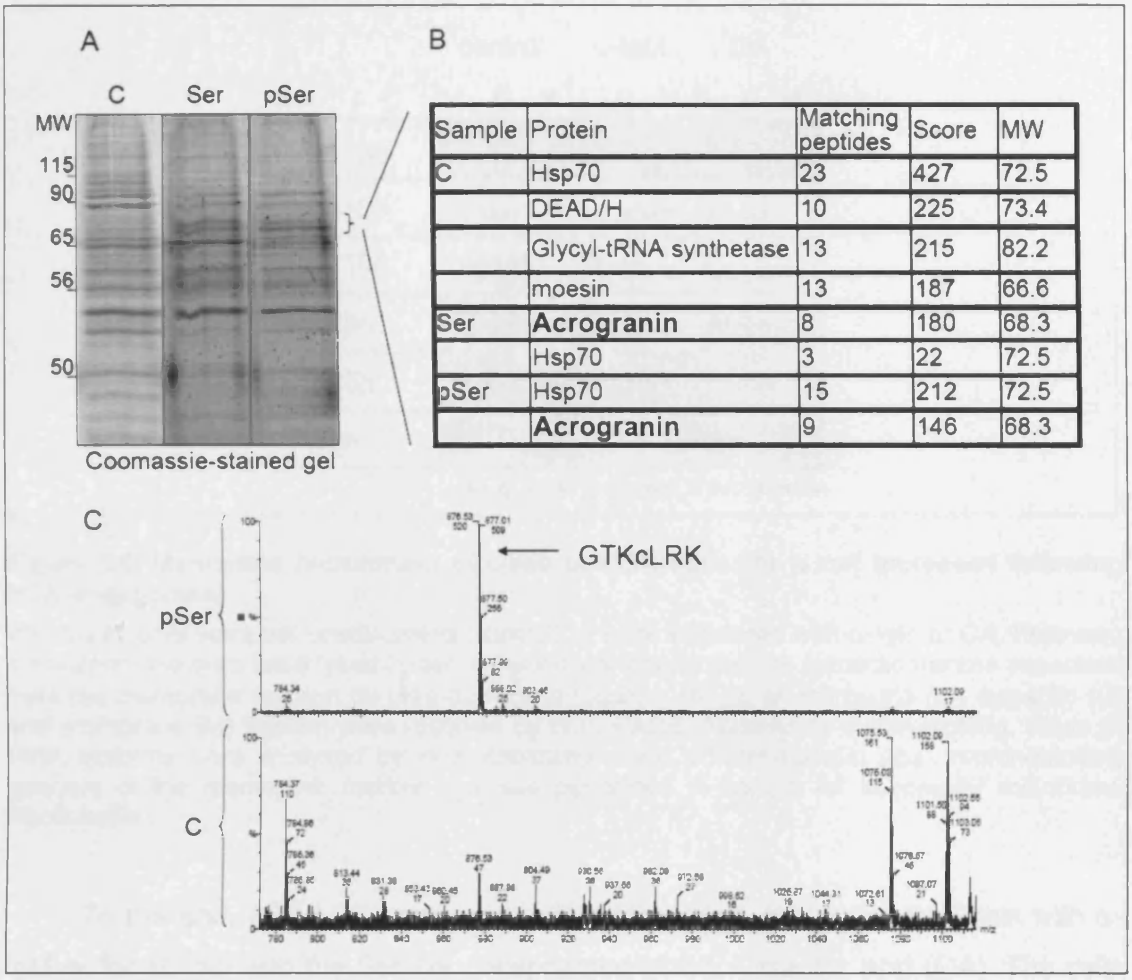

Sample	Protein	Matching peptides	Score	MW
C	Hsp70	23	427	72.5
	DEAD/H	10	225	73.4
	Glycyl-tRNA synthetase	13	215	82.2
	moesin	13	187	66.6
Ser	**Acrogranin**	8	180	68.3
	Hsp70	3	22	72.5
pSer	Hsp70	15	212	72.5
	Acrogranin	9	146	68.3

Figure 5.5: Identification of Acrogranin as potential p110δ interacting partner by LC-MS/MS

(A) Pull-downs of beads only (Control), beads coupled to a peptide made of the p110δ C-terminal amino acid sequence containing Ser1039 (Ser) and beads coupled to a peptide made of the same amino acid sequence, but containing phosphorylated Ser1039 (pSer) were separated by SDS-PAGE and the protein gels stained with colloidal Coomassie blue. (B) Identification of Acrogranin by LC-MS/MS from the gel piece of Ser and pSer sample indicated in (A). (C) Comparison of LC-MS data of one peptide of Acrogranin (m/z = 876.53) in the LC-MS run of the control sample (C) and pSer sample (pSer).

5.5 p110δ is not recruited to the plasma membrane following B cell stimulation

The subcellular localisation of class IA PI3K subunits was analysed from unstimulated and stimulated B cells in order to determine whether membrane recruitment of class IA PI3K isoforms could contribute to increased PI3K signalling following BCR stimulation (Figure 5.1).

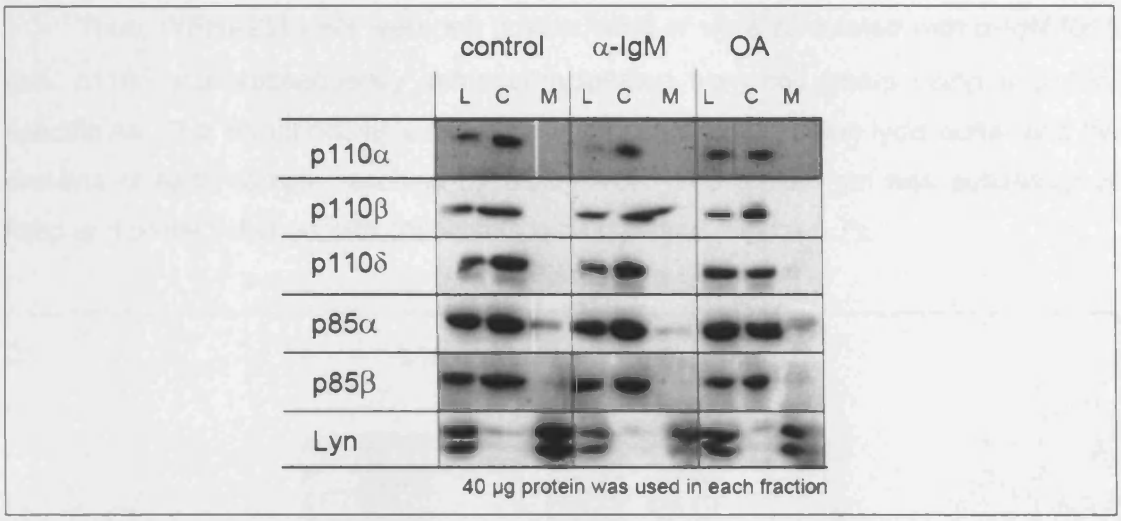

Figure 5.6: Membrane recruitment of class IA PI3K subunits is not increased following BCR engagement

WEHI-231 cells were left unstimulated (control) or were stimulated with α-IgM or OA. Following stimulation, the cells were lysed under hypotonic conditions and the cytosolic fraction separated from the membrane fraction by ultra-high centrifugation. 40 µg of cell lysate (L), cytosolic (C) and membrane (M) fraction were resolved by SDS-PAGE, followed by electroblotting. Class IA PI3K isoforms were analysed by immunoblotting using isoform-specific Abs. Immunoblotting analysis of the membrane marker Lyn was performed to control for successful membrane fractionation.

To this end, WEHI-231 cells were left unstimulated, stimulated for 5 min with α-IgM or for 30 min with the Ser/Thr phosphatase inhibitor okadaic acid (OA). The cells were subsequently lysed under hypotonic conditions and the membrane and cytosolic fraction separated by ultra-high centrifugation (§ 2.11). As shown in Figure 5.6, the majority of class IA PI3K protein from unstimulated, α-IgM stimulated and OA treated WEHI-231 cells was detected in the cytosolic fraction after cellular fractionation. The membrane-coupled protein kinase Lyn was used as a control for successful cellular fractionation.

These results suggest that class IA PI3Ks are not targeted to the plasma membrane following BCR stimulation in WEHI-231 cells. This finding implies that the increase in PI3K signalling observed following α-IgM stimulation of WEHI-231 cells is not due to membrane recruitment of p110δ.

5.6 PI3K interaction partners change following BCR engagement

The binding partners of p110δ in basal state and after α-IgM stimulation of WEHI-231 cells were analysed by MS in order to identify potential protein interaction partners that could be responsible for the increase in PI3K signalling following α-IgM stimulation of B cells.

Thus, WEHI-231 cells were left unstimulated or were stimulated with α-IgM for 5 min. p110δ was subsequently immunoprecipitated from cell lysate using a p110δ-specific Ab. The immunocomplexes were vigorously washed using lysis buffer and the proteins of each sample resolved by SDS-PAGE. The protein gel was subsequently fixed and protein stained with colloidal Coomassie blue (Figure 5.7).

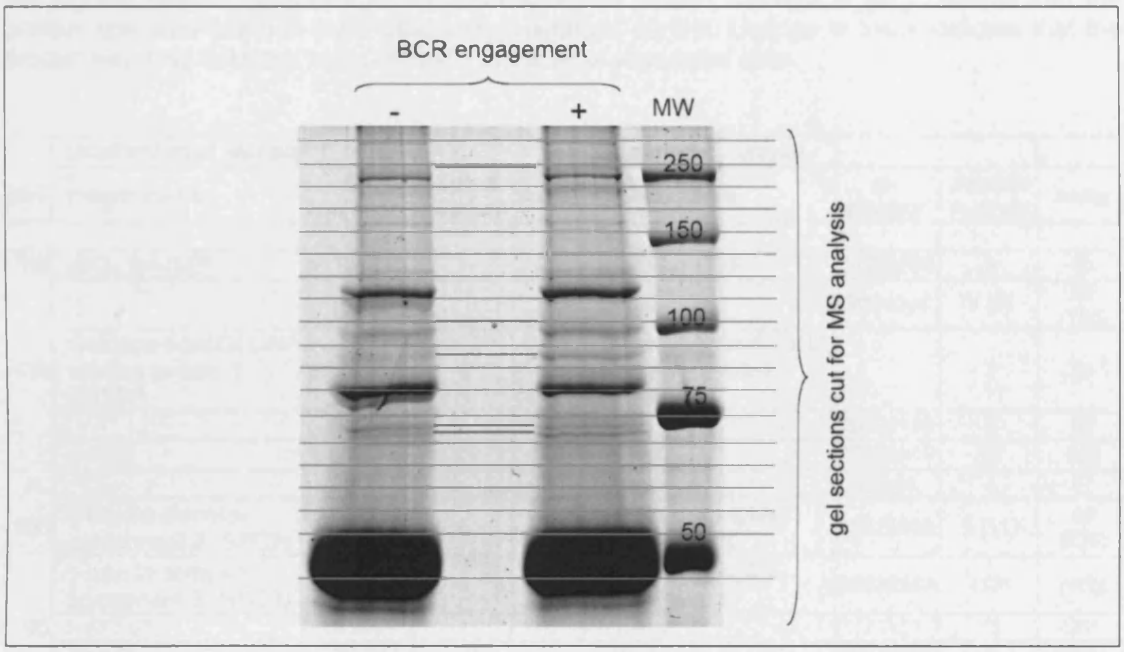

Figure 5.7: Differences in the potential interaction partners of p110δ immunoprecipitated from unstimulated and α-IgM stimulated WEHI-231 cells

WEHI-231 cells were left unstimulated or stimulated with α-IgM for 5 min. p110δ was immunoprecipitated from total cell lysate and resolved by SDS-PAGE. The protein gel was subsequently stained with colloidal Coomassie blue leading to the detection of small differences (marked with red line) in protein content between sample of unstimulated and stimulated cells.

In order to analyse the potential interaction partners of p110δ (and its regulatory subunit) in an unbiased manner, gel lanes were cut into sections of equal size and molecular weight as depicted in Figure 5.7, and gel pieces of unstimulated and stimulated sample were stored in separate tubes. Proteins in each sample were reduced, alkylated and subjected to tryptic in-gel digestion. LC-MS/MS was performed of the peptide content of each gel section.

LC-MS/MS analysis of two independent experiments performed as described above led to the identification of the proteins listed in Table 5.1 and Table 5.2. Proteins marked in grey were also identified by MS in pull-downs of WEHI-231 cells using plain beads only and are therefore likely enriched in p110δ IPs due to their binding capacity to agarose and/or protein A/G.

Table 5.1: Potential interaction partners of p110δ from untreated and α-IgM stimulated WEHI-231 cells

p110δ was immunopurified using a p110δ Ab from unstimulated and α-IgM stimulated WEHI-231 cells and the immunocomplexes were resolved by SDS-PAGE. The Coomassie stained gel was cut into pieces of equal size and molecular weight and the proteins reduced, alkylated and in-gel digested with trypsin. The peptides were analysed by LC-MS/MS. The experiment was performed twice and each sample was analysed two times by MS (4 MS runs in total). Peptide numbers and scores were taken from the first LC-MS/MS run of the first experiment. Proteins indicated in italics were only detected in 1 of the 2 experiments. Numbers in brackets indicate the highest peptide number and score for a certain protein. Listings in grey indicate that the protein was also found in plain bead-only (negative) control. Listings in black indicate that the protein was only detected by LC-MS/MS in the IP of stimulated cells.

	Unstimulated sample				**Stimulated sample**			
MW	protein name	gi-number	peptide number	score	protein name	gi-number	peptide number	score
200	p200 Arf-GEF	51704830	1	21	p200 Arf-GEF	51704830	3	60
					IRS-2	*3024044*	*1 (9)*	*25 (125)*
130	Damage-specific DNA binding protein 1 (DDB1)	5353754	5	60	Damage-specific DNA binding protein 1 (DDB1)		7	85
					PARP-1	20806109	3	83
	p110δ	22758919	11	149	p110δ	22758919	27	802
					nucleolin	70844	4	87
100	γ-tubulin complex component 2 (GPC2)	19526968	4	64	γ-tubulin complex component 2	19526968	2 (11)	50 (234)
	γ-tubulin complex component 3 (GPC3)	39930567	4	42	γ-tubulin complex component 3	*39930567*	*(13)*	*(406)*
90	*HSP90**	*123681*	*3*	*117*	*HSP90**	*123681*	*15*	*388*
	*Gp96**	*6755863*	*1*	*40*	*Gp96**	*6755863*	*2*	*95*
	p85β	3379321	NA	NA	p85β	3379321	14	243
85	p85α	91175	4	457	p85α	91175	14	392
	Thymopoietin	6755817	18	497	Thymopoietin	6755817	17	403
75	HSP70*	1661134	5	52	HSP70*	1661134	5	103
	Immunoglobulin	NA	NA	NA	Immunoglobulin	NA	NA	NA
50	*Gi28175231*	*28175231*	*2*	*84*	*Gi28175231*	*28175231*	*1*	*49*
	γ-tubulin	19527246	2	45	γ-tubulin	19527246	2	15
	*eEF-1a**	*72870*	*1*	*56*	*eEF-1a**		*2*	*32*
35	P0	6671569	3	42	P0	6671569	1	37
	Proliferin 2-precursor	91201	1	36	Proliferin 2-precursor	91201	1	29
25	Hist1h4i, h	51311	3	50	Hist1h4i, h	51311	2	27
	Immunoglobulin	NA	NA	NA	Immunoglobulin	NA	NA	NA

We identified p200 Arf-GEF, damage-specific DNA binding protein 1 (DDB1), γ-tubulin complex component 2/3 (GPC2, GPC3), γ-tubulin, histone 1h4i, thymopoietin and p85α/p85β in p110δ IPs independent of B cell stimulation. Of these proteins, γ-tubulin has previously been implicated in constitutively binding p85α, p55α and p55γ (Inukai et al., 2000; Kapeller et al., 1995). Furthermore, GPC2 and GPC3 have been shown to constitutively interact with γ-tubulin (Murphy et al., 1998). Thymopoietin was identified as a cross-contaminating protein of the p110δ Ab (§ 4.7.1). **Arf-GEF**, **DDB1** and **histone** are to the best of our knowledge novel potential PI3K interaction partners.

BCAP, caprin-1, NEDD1 and Ras-GTPase-activating protein SH3-domain binding protein (G3BP) were also identified by MS in p110δ IPs (Table 5.2). BCAP has been reported to interact with the regulatory subunit of class IA PI3K (Okada et al., 2000) and NEDD1 was recently shown to bind to the γ-tubulin ring complex (Haren et al., 2006). However, **caprin-1** and **G3BP** are novel potential PI3K interaction partners.

Proteins marked in bold in Table 5.1, were only detected by LC-MS/MS in the p110δ IP following BCR engagement of WEHI-231 cells. These are IRS-2, PARP-1 and nucleolin. IRS-2 is known to interact with the regulatory subunit of PI3K (although not downstream of BCR); **PARP-1** and **nucleolin** are novel potential PI3K interaction partners.

Table 5.2: Potential p110δ binding partners

This table includes p110δ binding partners which were detected in the IP after α-IgM stimulation of WEHI-231 cells from the first experiment. However, because the LC-MS/MS run of the control cells was not as efficient as the one of the stimulated cells, it is possible that the indicated proteins also bind p110δ in unstimulated cells.

MW	protein name	gi-number	peptide number	score
90	BCAP	13878195	4	82
80	caprin-1	42558248	2	71
70	NEDD1	82592513	4	76
50	Ras-GTPase-activating protein SH3-domain binding protein (G3BP)	7305075	5	76

Data-dependent acquisition allows for automatic switching from MS to MS/MS experiments whenever an ion of pre-determined nature is detected. If, however, the count of a certain ion is below the set threshold for automatic switching or if more than 3 ions are detected simultaneously, the ion will not be chosen for fragmentation. In order to verify that the absence of proteins in unstimulated samples is not due to the settings of the automatic switching, we manually analysed selected LC-MS and LC-MS/MS spectra of peptides derived from unstimulated and stimulated samples (Figure 5.8, Figure 5.9).

Peak integrated areas of peptides related to proteins listed in Table 5.1 and Table 5.2 were compared with peak integrated areas of unrelated (control) peptides. This analysis revealed similar protein amounts of p110δ, p85α and p200 Arf-GEF in the p110δ IP of unstimulated and stimulated WEHI-231 cells (Figure 5.8). Analysing integrated peak areas of nucleolin and BCAP peptides exposed 2 times higher base peak intensity (BPI) values in samples derived from stimulated WEHI-231 cells compared to samples derived from control cells, suggesting that twice as much nucleolin and BCAP was pulled down in p110δ IPs from cell lysates of stimulated cells (Figure 5.9). 3-, 5- and 100-fold more PARP-1, IRS-2 and caprin-1 peptides were detected by MS in p110δ-IP samples of stimulated WEHI-231 cells compared to control

cells (Figure 5.9). The increase in BPI values following peak integration of peptides derived from stimulated cells is qualitative.

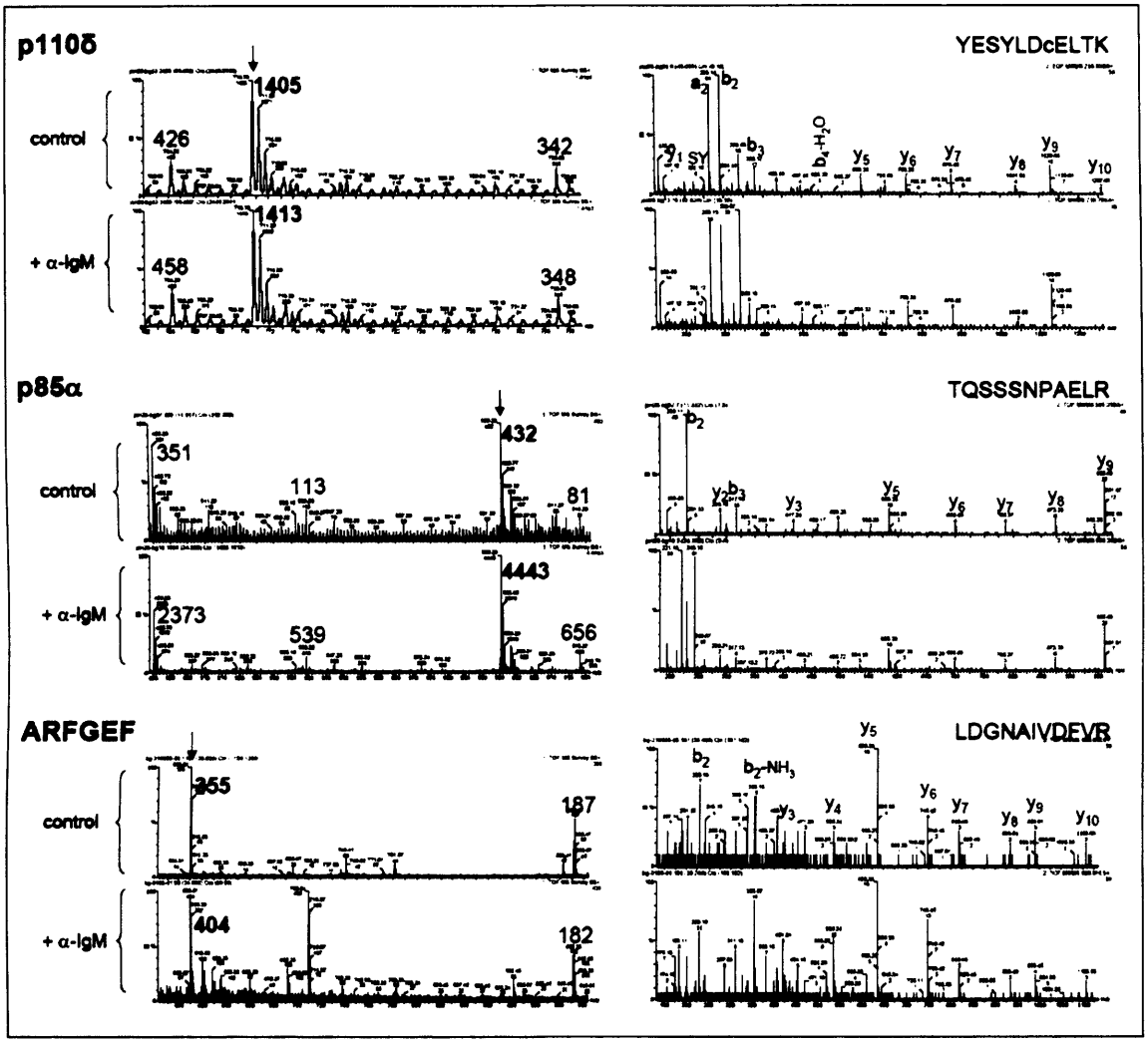

Figure 5.8: Comparison of LC-MS spectra depicting integrated peak areas of peptides derived from control *versus* α-IgM stimulated WEHI-231 cells

LC-MS runs of p110δ IP samples derived from unstimulated and stimulated cells were analysed for protonated peptides of proteins listed in Table 5.1 and Table 5.2. The peptide peak containing the respective m/z is marked with an arrow. The integrated peak area of independent ions are shown for comparison. On the right, the MS/MS spectra are shown belonging to the parent ions marked with an arrow in the MS spectra (left).

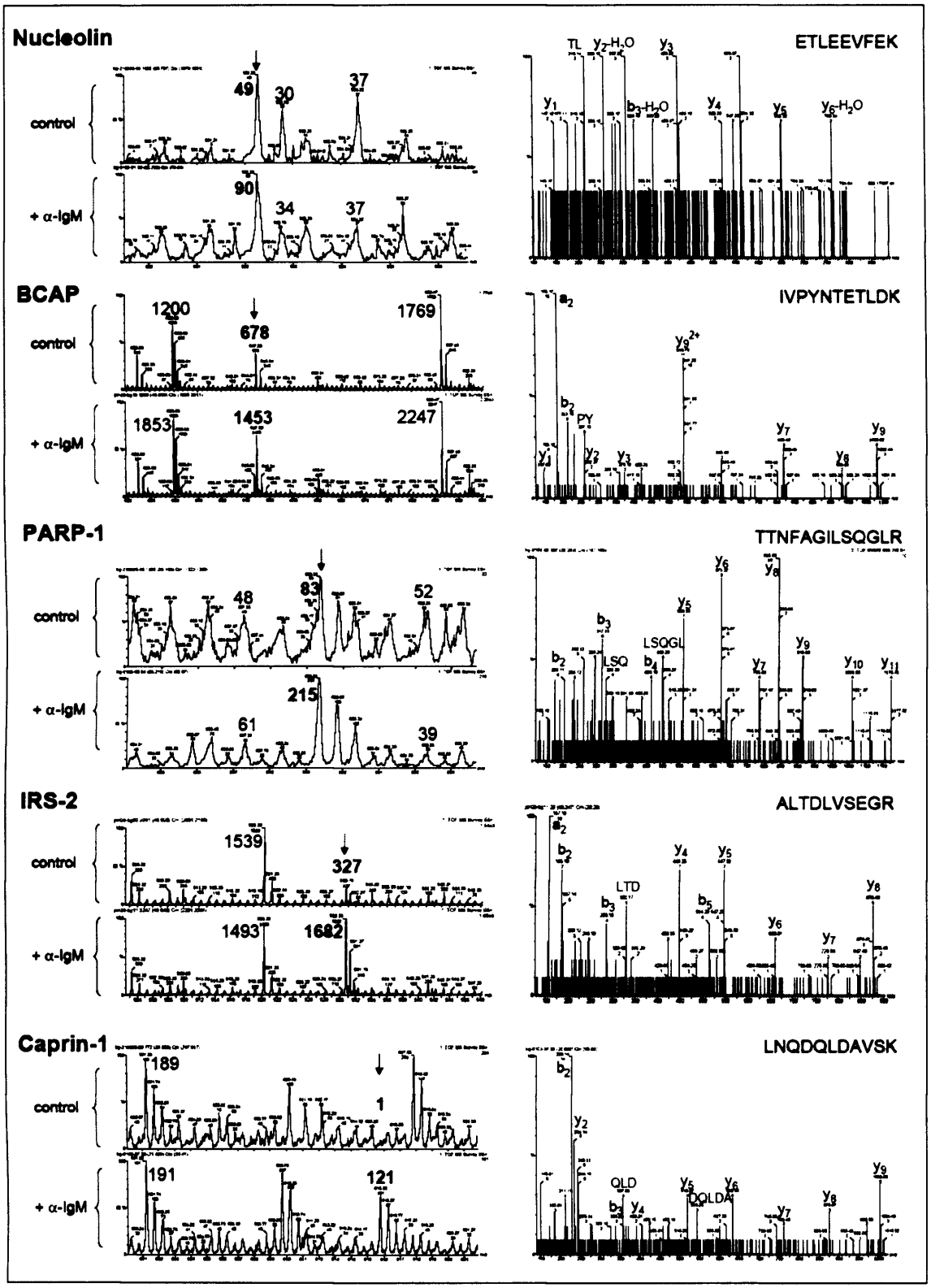

Figure 5.9: Comparison of LC-MS spectra depicting integrated peak areas of peptides derived from control *versus* α-IgM stimulated WEHI-231 cells

LC-MS runs of p110δ IP samples derived from unstimulated and stimulated cells were analysed for protonated peptides of proteins listed in Table 5.1 and Table 5.2. The peptide peak containing the respective m/z is marked with an arrow. The integrated peak area of independent ions are shown for comparison. On the right, the MS/MS spectra are shown belonging to the parent ions marked with an arrow in the MS spectra (left).

Analysis of IRS-2 by LC-MS/MS following p110δ IP of α-IgM stimulated WEHI-231 cells revealed Ser573 as a novel phosphorylation site in IRS-2 (Figure 5.10). This residue has to the best of our knowledge not been identified as a phosphorylation site in murine or human IRS-2, and its equivalent Ser residue in IRS-1 has not been determined as a phosphorylation site.

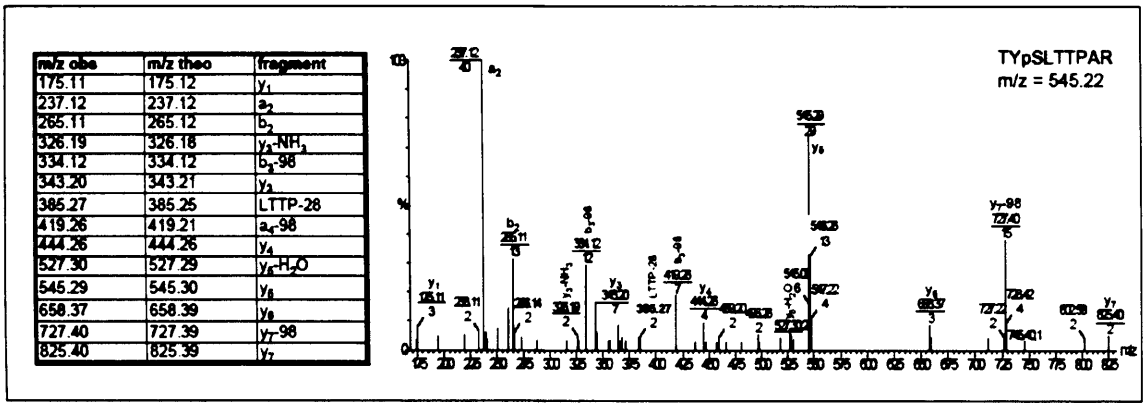

m/z obs	m/z theo	fragment
175.11	175.12	y_1
237.12	237.12	a_2
265.11	265.12	b_2
326.19	326.18	y_3-NH_3
334.12	334.12	b_3-98
343.20	343.21	y_3
385.27	385.25	LTTP-28
419.26	419.21	a_4-98
444.26	444.26	y_4
527.30	527.29	y_5-H_2O
545.29	545.30	y_5
658.37	658.39	y_6
727.40	727.39	y_7-98
825.40	825.39	y_7

Figure 5.10: Ser573 identified as novel phosphorylation site in IRS-2 by LC-MS/MS
LC-MS/MS analysis of IRS-2, which was pulled down in a p110δ-IP from α-IgM stimulated WEHI-231 cells, revealed phosphorylation of Ser573 in murine IRS-2. The MS/MS spectrum of the peptide TYpSLTTPAR is shown on the right, and fragment ion m/z are listed on the left.

In order to corroborate the interaction between p85-p110δ and BCAP or IRS-2, we analysed immunoprecipitates of p110δ, p110α, IRS-2 and BCAP by immunoblotting for class IA PI3K isoforms and IRS-1, IRS-2 and BCAP (Figure 5.11). To this end, WEHI-231 cells were left unstimulated or stimulated with α-IgM. Following cell lysis, proteins were immunoprecipitated with respective Abs and the immunocomplexes resolved by SDS-PAGE. The immunoblots were incubated with the indicated Abs after electroblotting. Between Ab incubations, the filter was stripped of proteins if different primary Abs were used for analysis. Total cell lysate of unstimulated and stimulated WEHI-231 cells was analysed for Akt phosphorylation by immunoblotting (Figure 5.11.A) in order to control for successful stimulation conditions.

Immunoblotting results shown in Figure 5.11.B and Figure 5.11.C confirm the interaction of p85-p110δ with BCAP and IRS-2. While interaction of IRS-2 with all class IA PI3K isoforms increased following BCR engagement, analysis of BCAP interaction with class IA PI3Ks was more variable. Furthermore, IRS-1 was also shown to interact with p110δ in B cells.

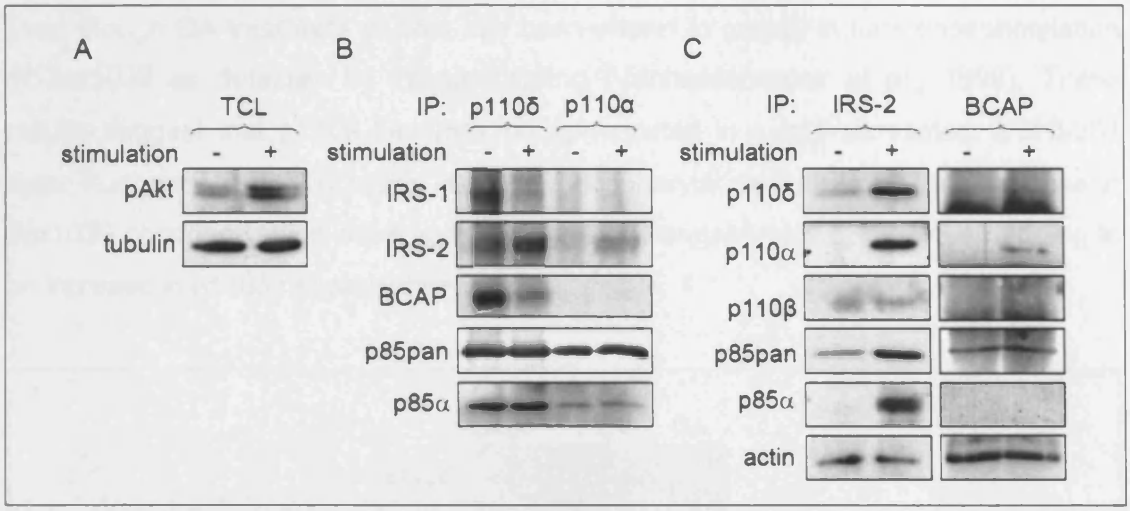

Figure 5.11: Co-IP analysis of class IA PI3K with IRS and BCAP

(A) Total cell lysate (TCL) of control and α-IgM stimulated WEHI-231 cells was analysed by immunoblotting for Akt phosphorylation and tubulin. (B) IPs using Abs to p110δ and to p110α from unstimulated and stimulated WEHI-231 cell lysates were resolved by SDS-PAGE and subjected to electroblotting. Immunoblot sections are shown. (C) IPs using Abs to IRS-2 and BCAP from unstimulated and stimulated WEHI-231 cells were resolved by SDS-PAGE and subjected to elelctroblotting. Immunoblot sections are shown.

5.7 Net phosphorylation of p110δ is increased following BCR engagement

Changes in the protein-protein binding affinities following cellular stimulation are often due to alterations in protein phosphorylation of the interacting proteins. Protein domains interacting specifically with phosphorylated residues have been revealed. SH2-, PTB-, and C2-domains can interact with pTyr (Benes et al., 2005; Kavanaugh and Williams, 1994; Sadowski et al., 1986), while BRCT-, and FHA-domains were shown to bind pSer/Thr (Durocher et al., 1999; Manke et al., 2003). Since IRS-2 contains a PTB domain and an additional, uncategorised amino acid sequence shown to interact with pTyr and PARP-1 contains a BRCT domain, we analysed the phosphorylation state of p110δ following BCR engagement by *in vivo* labelling experiments with radioactive ATP (§ 2.12).

For this purpose, WEHI-231 cells were incubated with 0.4 mCi [γ-^{32}P]ATP for 6 h and were subsequently stimulated with α-IgM or OA (Ser/Thr phosphatase inhibitor, positive control). Following cell lysis, p110δ was immunoprecipitated and the complex resolved by SDS-PAGE. Incorporation of [γ-^{32}P]ATP into proteins was measured by exposure of the dried gel to phospho-imager plates.

As shown in Figure 5.12, incorporation of radioactive phosphate into p110δ was increased following α-IgM and OA stimulation of WEHI-231 cells. Surprisingly, phosphorylation of p110δ upon BCR engagement was higher than in OA treated cells

even though OA treatment of cells has been shown to greatly induce phosphorylation of Ser1039 as detected by immunoblotting (Vanhaesebroeck et al., 1999). These results suggest that p110δ becomes phosphorylated in α-IgM stimulated WEHI-231 cells. Furthermore, the increase in p110δ phosphorylation outweighs the decrease in Ser1039 phosphorylation observed following BRC engagement (Figure 5.4) leading to an increase in p110δ net phosphorylation.

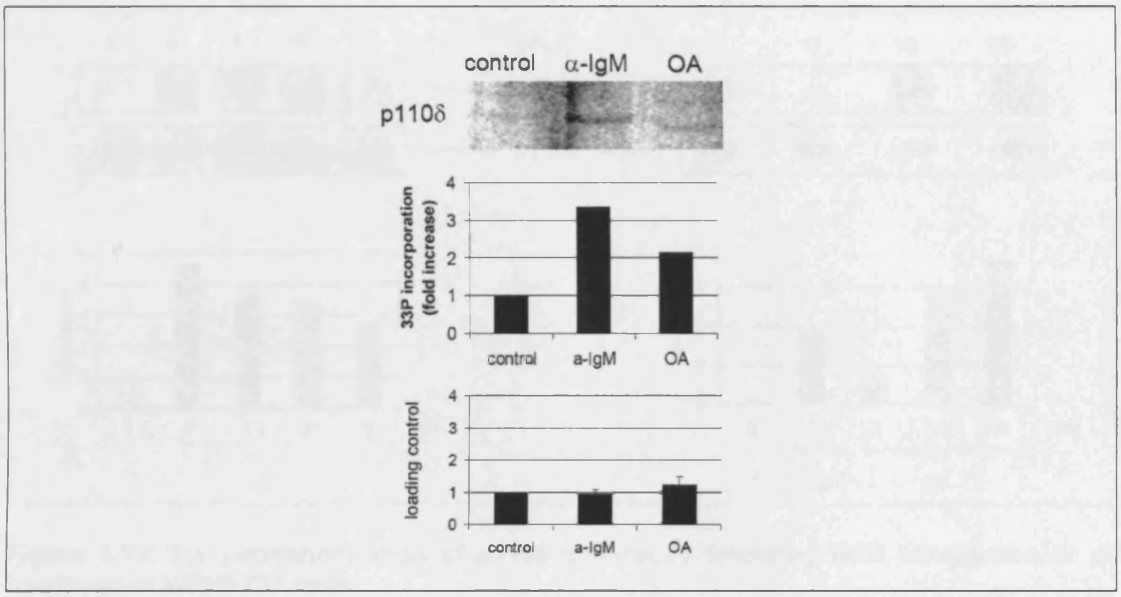

Figure 5.12: BCR engagement of immature B cells induces net phosphorylation of p110δ
In vivo labelling of WEHI-231 cells with [γ-^{32}P]ATP was followed by stimulation of B cells with α-IgM or OA. p110δ was immunoprecipitated with an Ab raised against its C-terminus and the immunocomplex resolved by SDS-PAGE. The gel was stained with colloidal Coomassie blue and dried. [γ-^{32}P]ATP incorporation was measured by exposure of the dried gel to phospho-imager plates.

5.8 B cell stimulation induces Tyr phosphorylation of p110δ

Tyr phosphorylation of class IA PI3K catalytic subunit has been demonstrated in chicken DT40 B cells following BCR engagement (Craxton et al., 1999) or H_2O_2 treatment (Qin and Chock, 2003). We therefore analysed whether the increase in net phosphorylation detected following BCR engagement of WEHI-231 cells could be due to an increase in Tyr phosphorylation of p110δ.

WEHI-231 cells were stimulated for the indicated times with α-IgM or pV (pervanadate, Tyr phosphatase inhibitor). Following cell lysis, p110δ was immunoprecipitated and the immunocomplex resolved by SDS-PAGE. Phosphorylation of immunoprecipitated proteins was analysed by immunoblotting with anti-phospho-Tyr Ab.

As shown in Figure 5.13.A, Tyr phosphorylation of p110δ was induced and peaked shortly after BCR crosslinking in WEHI-231 cells. pV treatment also enhanced Tyr phosphorylation of p110δ (Figure 5.13.B). In contrast, treatment of cells with the Ser/Thr phosphatase inhibitor OA did not alter p110δ Tyr phosphorylation (not shown).

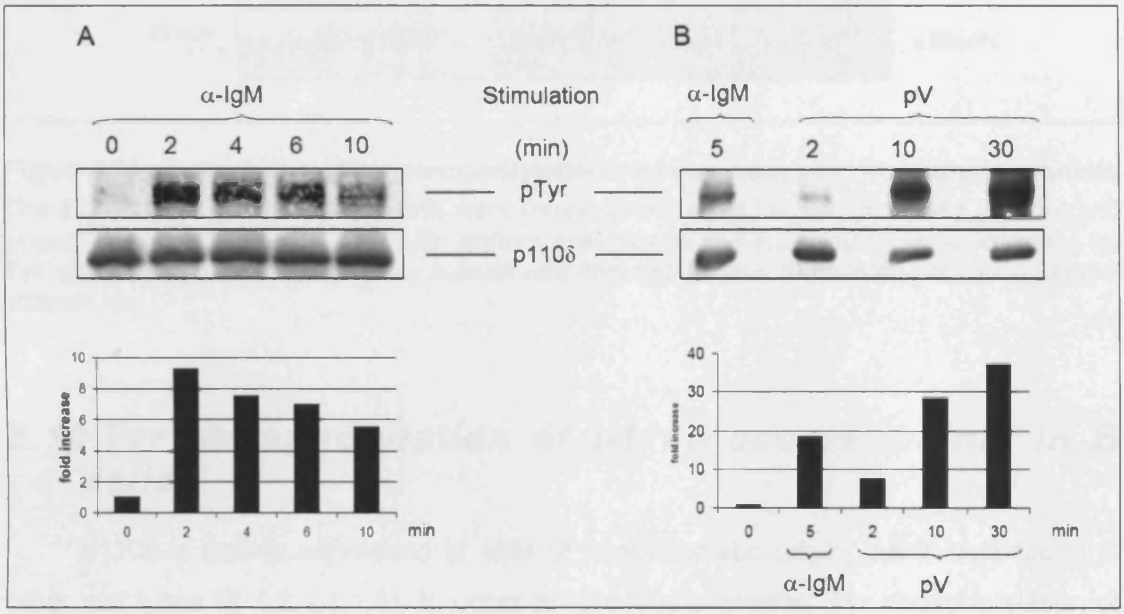

Figure 5.13: Tyr phosphorylation of p110δ is induced following BCR stimulation or pV treatment of WEHI-231 cells

WEHI-231 cells were stimulated for the indicated time points with α-IgM or pV and p110δ immunoprecipitated from cell lysates. Tyr phosphorylation of p110δ was analysed by immunoblotting with anti-pTyr Abs. Following stripping of proteins off the PVDF membrane, p110δ was analysed by immunoblotting with p110δ-specific Abs.

5.9 p110δ, but not p110α or p110β, becomes Tyr phosphorylated following BCR crosslinking

In order to address whether Tyr phosphorylation was common in all 3 class IA PI3K catalytic subunits under the chosen stimulation conditions, p110α, p110β and p110δ were immunoprecipitated from unstimulated and α-IgM stimulated WEHI-231 cells. The immunoprecipitated proteins were resolved by SDS-PAGE and Tyr phosphorylation analysed by immunoblotting. Following stripping of proteins off the filter, the amount of regulatory subunit detected by immunoblotting in each IP was used as a control for equal p85 immunoprecipitation and equal gel loading.

As shown in Figure 5.14, it was mainly p110δ that became Tyr phosphorylated following BCR engagement, with some low level Tyr phosphorylation of p110β.

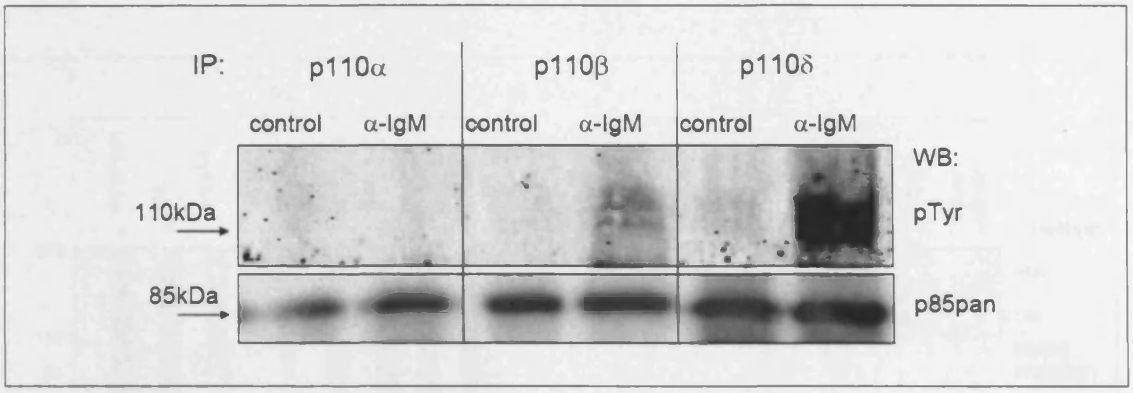

Figure 5.14: Comparison of Tyr phosphorylation between class IA PI3K catalytic subunits
The 3 class IA PI3K catalytic subunits were immunoprecipitated from unstimulated (control) and α-IgM stimulated WEHI-231 cells with isoform-specific Abs and analysed by immunoblotting for Tyr phosphorylation. The regulatory subunit was detected in each IP by immunoblotting using a p85pan Ab.

5.10 Tyr phosphorylation of p110δ occurs mainly in B cells

p110δ is mainly expressed in cells of hematopoietic origin, but is also found in other cell types (§ 1.2.1.1.1.3). In order to investigate whether Tyr phosphorylation of p110δ occurs in cell types other than immature B cells, we tested a panel of p110δ expressing cell lines: murine mature B cells (A20); human immature B cells (NALM-6); murine T cells (EL-4); human gastrointestinal stromal sarcoma cells (GIST); human mastocytoma cells (HMC-1); murine melanoma cells (B16BL6) and breast cancer cells (MDA-MB361). Since results described in § 5.8 indicated that pV treatment of WEHI-231 cells induced Tyr phosphorylation of p110δ, pV was used as a stimulus.

In order to determine whether pV stimulation induced overall protein Tyr phosphorylation, total cell lysates of the indicated cell lines were first analysed by pTyr immunoblotting. As shown in Figure 5.15.A, induction of Tyr phosphorylation following pV treatment was successful in all cell types, even though least effective in EL-4 cells. After stripping of proteins of the filter, p110δ protein expression levels in total cell lysate were compared in each cell type by immunoblotting using an anti-p110δ Ab. This analysis revealed variable p110δ protein amounts in different cell types and undetectable levels of p110δ in the breast cancer cell line MDA-MB361.

Nevertheless, all cell types were subsequently treated with pV for 30 min and p110δ was immunoprecipitated following cell lysis. The proteins were resolved by SDS-PAGE, electroblotted to PVDF filters and the immunoblot was incubated with pTyr-specific Abs. As shown in Figure 5.15.B, Tyr phosphorylation of p110δ following pV treatment of cells mainly occurred in B cells (immature, mature, murine, human).

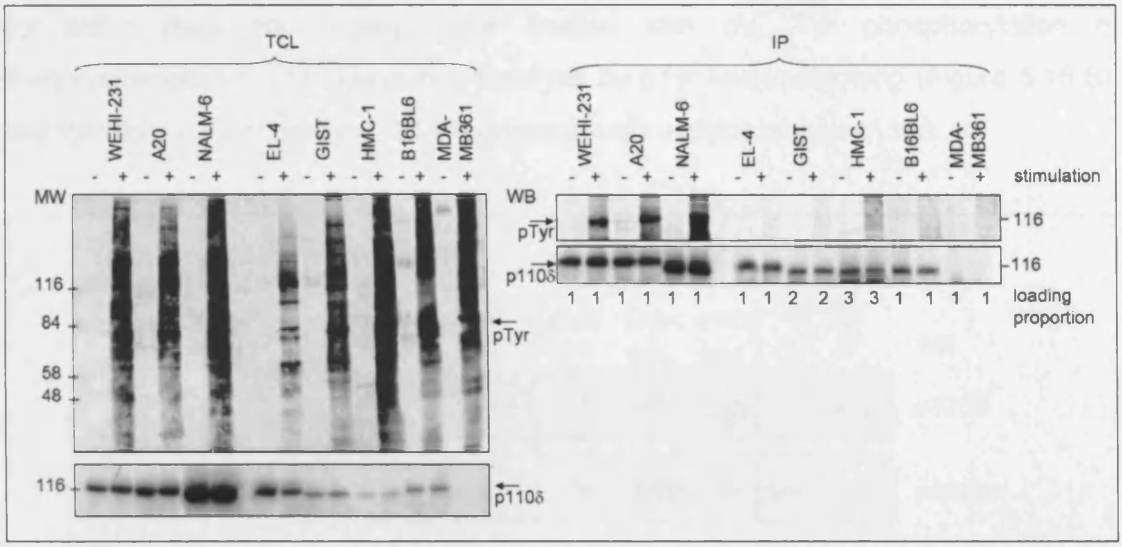

Figure 5.15: p110δ is phosphorylated on Tyr residue(s) mainly in B cells

(A) Total cell lysate of various cell lines separated by SDS-PAGE and electroblotted to PVDF filter was analysed by immunoblotting for Tyr phosphorylation following pV treatment. The filter was reprobed with a p110δ Ab after stripping of proteins (lower panel). (B) Immunoprecipitated p110δ was analysed by immunoblotting with a pTyr-specific Ab for Tyr phosphorylation following pV treatment of various cell lines. The filter was reprobed with a p110δ Ab after stripping of proteins.

5.11 pV stimulation of HEK-293T cells overexpressing p110δ did not induce Tyr phosphorylation of p110δ

Overexpression of p110δ was desirable in order to identify phosphorylated Tyr residues by MS. Since transfection of leukocytes by electroporation or calcium phosphate precipitation was not successful (data not shown), we used HEK-293T cells, a cell line that can easily be transfected.

10^6 HEK-293T cells were transiently transfected with 10 μg plasmid DNA containing murine or human p110δ cDNA in combination with 10 μg plasmid DNA containing bovine p85α or p85β cDNA using the calcium phosphate precipitation protocol (§ 2.7.2.5). Following cell lysis, total cell lysate was resolved by SDS-PAGE and analysed by immunoblotting for PI3K isoforms. Endogenous p110δ and p85 protein amounts expressed in WEHI-231 or HEK-293T transfected with vector only (-) were compared to overexpressed p110δ/p85 from HEK-293T cells. Overexpression of human and murine p110δ was successful following calcium phosphate precipitation transfection compared to HEK-293T cells transfected with vector only. Higher p110δ protein expression was observed upon co-overexpression of class IA PI3K regulatory subunits.

However, when HEK-293T cells transfected with murine p110δ and bovine p85α (or p85β, data not shown) were treated with pV, Tyr phosphorylation of immunoprecipitated p110δ was not observed by pTyr immunoblotting (Figure 5.16.B). We therefore did not perform MS experiments with overexpressed p110δ.

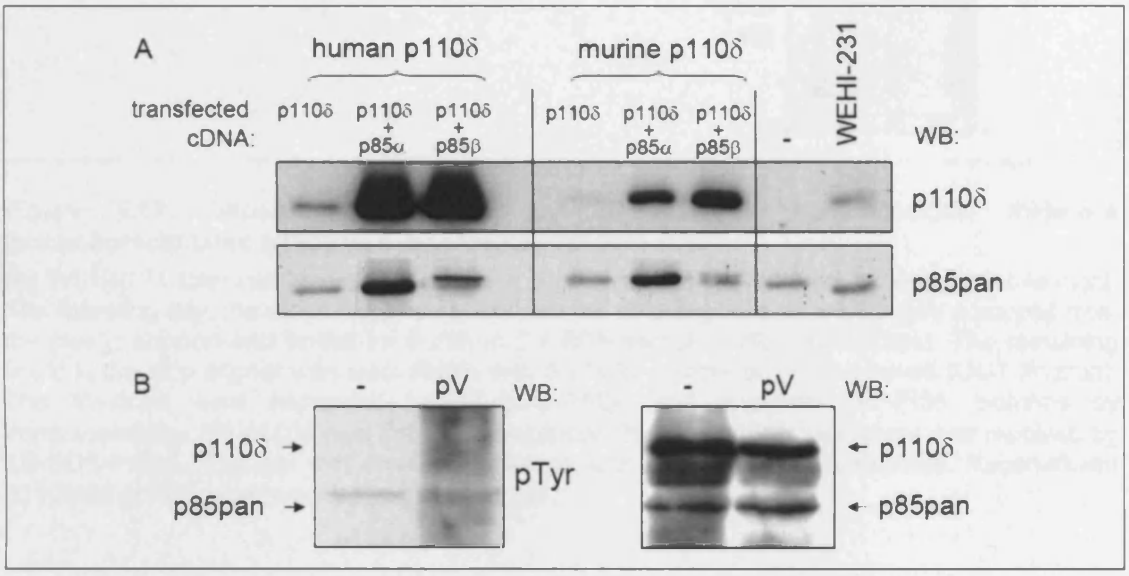

Figure 5.16: pV stimulation of HEK-293T cells does not induce Tyr phosphorylation of overexpressed p110δ

(A) HEK-293T cells were transfected with vector only (-), a DNA plasmid containing human or murine p110δ, and a combination of plasmid containing p110δ and bovine p85α or p85β. PI3K isoform expression in HEK-293T cells was compared to endogenous protein expression in WEHI-231 cells. Cell lysates were analysed by immunoblotting with Abs to p110δ and p85pan. (B) p110δ was immunoprecipitated from pV stimulated HEK-293T cells, which were previously transfected with p110δ and p85α cDNA. Phosphorylation of p110δ was analysed by pTyr immunoblotting (right panel). Following stripping of proteins, the filter was incubated with Abs to p110δ and p85pan.

5.12 MS analysis of p110δ did not reveal phosphorylated Tyr residue(s)

In order to determine the site(s) of Tyr phosphorylation of endogenous p110δ, MS analysis was performed. To this end, the catalytic subunit was immunoprecipitated from WEHI-231 cell lysate and the proteins resolved by 2D-PAGE in order to enrich for phosphorylated species. However, as shown in Figure 5.17.A, 2D-PAGE analysis of p110δ was not feasible due to the incapability of the catalytic subunit to enter the first dimension of 2D-gels (IPG strips (shown below) and tube gels (data not shown)). We therefore resolved immunoprecipitated p110δ from co-immunoprecipitating proteins by 1D-SDS-PAGE (Figure 5.17.B).

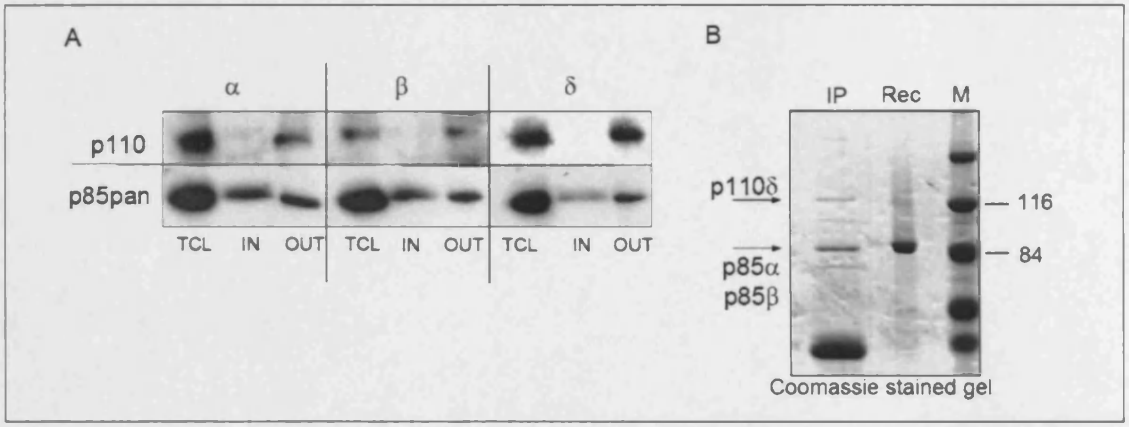

Figure 5.17: Separation of p110 by 2D-PAGE is not feasible, therefore immunoprecipitated p110δ was resolved by 1D-SDS-PAGE

(A) WEHI-231 total cell lysate (TCL) was applied to IPG strips and left to rehydrate overnight. The following day, the strips were removed from the strip aligner and the 1D-gels scrapped from the plastic support and boiled for 5 min in 5 x SDS-sample buffer (IN fraction). The remaining liquid in the strip aligner was also diluted with 5 x SDS-sample buffer and boiled (OUT fraction). The fractions were separated by 1D-SDS-PAGE and analysed for PI3K isoforms by immunoblotting. (B) p110δ was immunoprecipitated from WEHI-231 cell lysate and resolved by 1D-SDS-PAGE. The gel was fixed and stained with colloidal Coomassie blue. Recombinant p110/p85 protein was resolved in the same gel.

p110δ immunoprecipitated from α-IgM stimulated WEHI-231 cells was analysed by MS following SDS-PAGE and in-gel protein digestion.

For preliminary analysis, MALDI mass fingerprinting was applied (detailed information to MALDI mass fingerprinting is provided in § 4.7.5). This led to the identification of 5 p110δ peptides that could potentially be phosphorylated on Tyr residues (Figure 5.18). The amino acid sequence surrounding these Tyr residues were analysed *in silico* for their conservation between class IA catalytic subunits using ClustalW, for their probability to become phosphorylated (NetPhos and Proscan) and to be part of a SH2-binding motif (Motifscan). We also analysed the probablity of these Tyr residues to become phosphorylated by a panel of protein kinases (Motifscan, NetPhosK, GPS). Using Swiss PDB viewer, we investigated the exposure to the surface of the 5 Tyr residues in order to estimate the accessibility of this amino acid to protein kinases. This analysis was performed by overlaying the primary structure of p110δ with the solved crystal structure of p110γ.

Further analysis of the 5 potentially phosphorylated Tyr residues by LC-MS/MS, LC-MRM and error-tolerant searches of MS-data did not allow for identification of phosphorylated residues (more detailed information to each method is provided in § 4.7). Moreover, IMAC enrichment or precursor-ion scanning (in collaboration with Dr. N. Morrice, MRC Phosphorylation Unit, University of Dundee, UK) of p110δ did also not reveal phosphorylated Tyr residues.

	sequence	conserved class IA (clustalW)	predicted (netPhos) (proscan*)	SH2-binding motif (motifscan)	kinase (motifscan) (NetPhosK*) (GPS**)	accessibility (spdbv)
Y239	EQPEEYALQVN	Yes	0.18	Itk (0.6/0)	Abl**, Lyn**, IR**	exposed
Y395	LCFALYAVVEKA	No/Yes	0.25		Itk, Lck (0.5/0)	exposed
Y670	LIMEAYCRGST	Yes	0.44			not exp.
Y812	LRMTPYGCLPT	Yes	0.89	SHIP (0.4/0)		exposed
Y963	YCERAYTILRR	Yes	0.78*	Shc (0.6/0)	EGFR* (0.6/1) Fyn**, Lck**	med. exp.

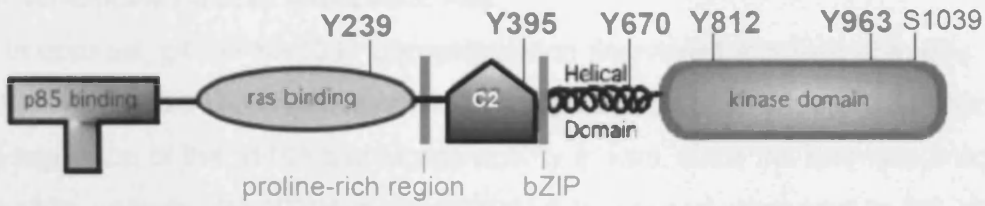

Figure 5.18: Potential p110δ phospho-peptides identified by MALDI mass fingerprinting

MALDI analysis of trypsinised p110δ revealed 5 potentially phosphorylated peptides. These peptides were analysed for their conservation between class IA PI3K (ClustalW) and for their probability to become phosphorylated using prediction programs NetPhos and Proscan. Furthermore, the Tyr residues were analysed for their probability to be part of a SH2 binding motif (Motifscan) and to be phosphorylated by kinases (Motifscan, NetPhosK, GPS). The Swiss PDB viewer was used to investigate the position of the Tyr residue in the catalytic subunit tertiary structure using the p110γ structure as a template.

5.13 Discussion

5.13.1 Critical role for p110δ in BCR sigalling

Stimulation of B cells by BCR crosslinking leads to PI3K activation. The critical component in PI3K signalling following BCR engagement seems to be p110δ. This was confirmed by pharmacological studies using PI3K-isoform specific inhibitors to p110β, p110δ, and p110γ to analyse Akt phosphorylation following BCR engagement, which was decreased by inhibition of p110δ, but not p110β or p110γ. Interestingly, inhibition of p110β and p110γ by isoform-specific inhibitors led to *enhanced* Akt phosphorylation following BCR crosslinking, indicative for a negative feedback loop on PI3K signalling exerted by these isoforms in B cells.

In order to gain insight into the regulation of p110δ activity in B cells following cellular stimulation, we performed diverse biochemical analyses.

5.13.2 *In vitro* lipid kinase activity of p110δ is unchanged following BCR engagement

BCR engagement did not impact on the intrinsic lipid kinase activity of p110δ as determined by *in vitro* lipid kinase activity assays. The generation of 3-phosphorylated

PIs by p110δ was similar if cells were unstimulated or stimulated with α-IgM prior to the assay. This result was independent of the lipid substrate used (PtdIns/PtdIns(4,5)P_2). Our findings are in line with previous reports which have shown that the *in vitro* lipid kinase activity of immunoprecipitated PI3K did not increase in stimulated DT40 cells compared to unstimulated control (Qin and Chock, 2003). However, the p110δ fraction which becomes activated following BCR engagement might be too small in order to measure a difference in the *in vitro* lipid kinase activity of the whole p110δ population immunoprecipitated with p110δ-specific Abs.

In contrast, p110δ Ser1039 phosphorylation decreased modestly following BCR crosslinking. The Ser1039 residue of p110δ has previously been shown to be important in the regulation of the p110δ lipid kinase activity *in vitro*, since the lipid kinase activity of Ser1039 mutants (Ser1039Asp, Ser1039Glu) is reduced compared to WT p110δ. Furthermore, phosphorylation of this site correlates with a decrease in PI3K lipid kinase activity in human T cells upon CD28 stimulation (Vanhaesebroeck et al., 1999). Thus, if CD28 stimulation of T cells was comparable to α-IgM stimulation of B cells, a decrease in pSer1039 following α-IgM stimulation of WEHI-231 cells would indicate an *increase* in p110δ lipid kinase activity. However, the impact of Ser1039 phosphorylation on p110δ lipid kinase activity in T cells might be distinct from B cells due to differences in concomitant p110δ phosphorylation which control the lipid kinase activity. It is further possible that the decrease in Ser1039 phosphorylation was too minor to measure a difference in the *in vitro* lipid kinase activity assay.

5.13.3 BCR stimulation of WEHI-231 cells does not lead to p110δ membrane recruitment

Fractionation experiments to separate cytosolic from membrane fraction of unstimulated and α-IgM stimulated WEHI-231 cells (and mature A20 B cells, data not shown) revealed cytosolic localisation of all class IA PI3Ks, while the membrane marker Lyn was detected in the membrane fraction. This finding indicates that the increase in PI3K signalling following BCR engagement is also not due to recruitment of the catalytic subunit to the membrane. However, it is possible that the lysis conditions used in this experimental set-up were chosen too stringently to reveal membrane localisation of class IA PI3Ks. Furthermore, the number of PI3K molecules recruited to the membrane following cellular stimulation might be very small compared to the cytosolic pool, not allowing for its detection by immunoblotting.

Another possibility is that not membrane recruitment but changes in the *nuclear* localisation of p110δ is the decisive factor in BCR signalling of immature B cells. As will

be described in more detail below, p110δ appears to be found in close contact with a variety of nuclear proteins.

5.13.4 p110δ is Tyr phosphorylated upon BCR crosslinking

In vivo labelling experiments revealed increased phosphorylation of p110δ following BCR engagement of WEHI-231. This increase was at least partially due to enhanced phosphorylation of Tyr residues. Tyr phosphorylation of p110δ rose quickly following cellular stimulation and decreased to its half-maximum within 10 min of stimulation. We further provide evidence that mainly p110δ is Tyr phosphorylated in B cells, since only a modest increase in Tyr phosphorylation of p110β, but no significant Tyr phosphorylation of p110α was detected upon BCR engagement. Comparative analysis of murine p110δ, with p110α and p110β amino acid sequences disclosed 8 Tyr residues in p110δ whose equivalent Tyr residue was only present in p110β. Tyr395, which was identified as a potential phospho-acceptor by MS, was one of these 8 Tyr residues.

We could further demonstrate that Tyr phosphorylation of p110δ preferentially occurred in B cells. For this purpose, Tyr phosphorylation of p110δ was compared by immunoblotting in a panel of p110δ-expressing cell lines that were treated with the Tyr phosphatase inhibitor pV. Only immature and mature B cells of murine and human origin showed a significant increase in p110δ Tyr phosphorylation following pV treatment. Furthermore, pV treatment of HEK-293T cells in which p110δ was transiently overexpressed did also not induce p110δ Tyr phosphorylation. These findings indicate that a B-cell specific Tyr kinase might be involved in p110δ phosphorylation. Studies performed in DT40 cells have shown that the catalytic subunit of class IA PI3K is Tyr phosphorylated following BCR engagement (Craxton et al., 1999). Tyr phosphorylation of p110 following BCR engagement was unchanged in Btk- and PLCγ-deficient cells compared to wild-type cells, decreased in Syk-deficient DT40 cells, and increased in Lyn-deficient cells. Also DT40 cells treated with H_2O_2 had enhanced Tyr phosphorylation of p110, and Syk- and Lyn-deficient cells showed dampened phosphorylation (Qin and Chock, 2003). These findings indicated that Syk, Lyn or an effector of these kinases is likely to be responsible for p110δ phosphorylation. Applying the GPS prediction algorithm to p110δ, Syk is predicted to phosphorylate Tyr55 and Tyr523 in p110δ, which are not part of the potentially phosphorylated Tyr residues revealed by MS. In contrast, Lyn is predicted to phosphorylate Tyr239, Tyr523 and Tyr723. Tyr239 was identified as a potential p110δ Tyr phosphorylation site by MALDI mass fingerprinting.

Even though it was not possible to identify a phosphorylated Tyr residue in p110δ by LC-MS/MS, we could detect 5 p110δ peptides with potentially phosphorylated Tyr residues by MALDI mass fingerprinting (Tyr239, Tyr395, Tyr670, Tyr812, and Tyr963). These residues and their surrounding sequences were analysed by several biocomputational tools. Tyr670 is not exposed to the protein surface and is also not predicted to become phosphorylated by a Tyr kinase or to encompass a SH2 binding motif, and is therefore an unlikely candidate for Tyr phosphorylation. Also Tyr963 is not well exposed to the protein surface and therefore less likely to be phosphorylated. In contrast, Tyr239 is exposed, predicted to be phosphorylated by Lyn and could potentially constitute an Itk binding site. Also Tyr395 is exposed to the protein surface and phosphorylation of Tyr395 seems probable due to the sequence homology of the Tyr395 flanking region of p110δ to p110β, but not p110α. Furthermore, phosphorylated Tyr812 could constitute a binding site for SHIP.

Following α-IgM stimulation of WEHI-231 cells, IRS-2, PARP-1 and caprin-1 interacted with p110δ. Some of these interaction partners might bind to p110δ due to its Tyr phosphorylation. This will be discussed in more detail below.

5.13.5 Interaction partners of p110δ in unstimulated B cells

By performing co-IP experiments from proliferating, but not α-IgM stimulated WEHI-231 cells, known and novel PI3K interaction partners were detected by MS. Figure 5.19 shows a hypothetical model of the PI3K interaction partners and the subcellular localisation of p85-p110δ due to the respective interaction. The potential PI3K interaction partners were compared to information obtained from the yeast 2-hybrid database available at Afcs gateway, from pSTIING and BIND database in conjunction with literature data. Although the associations of the novel potential PI3K interaction partners detected in unstimulated cells were unlikely due to unspecific interaction with matrix because we compared these data with a bead-only control, it is possible that purification of these proteins occurred because of unspecific Ab association. The interaction partners and nature of the complex will be discussed below.

The interaction between **BCAP** and PI3K is likely due to binding of class IA PI3K regulatory subunit to pTyr residues in YxxM-motifs of BCAP. BCAP is a B cell-specific adaptor molecule containing 4 YxxM p85-binding motifs (Okada et al., 2000) and has been shown to become Tyr phosphorylated within minutes of BCR engagement (Inabe and Kurosaki, 2002). p85 association with BCAP was observed in unstimulated B cells, and rapidly increased and subsequently decreased following cellular stimulation (Okada et al., 2000). Comparison of our MS/MS data gained from

unstimulated *versus* stimulated WEHI-231 cells indicated a small increase in BCAP association with PI3K following cellular stimulation. In contrast, immunoblotting data revealed a large decrease in binding of p110δ to BCAP upon α-IgM stimulation of WEHI-231 cells. The discrepancy between these findings might be due to small differences in the length of stimulation. However, it seems that in proliferating WEHI-231 cells a fraction of BCAP is constitutively phosphorylated thereby providing docking sites for p85.

The interaction between **γ-tubulin** and PI3K has previously been reported. γ-tubulin was shown to bind p55α and p55γ constitutively, while binding to p85 following cellular stimulation (Inukai et al., 2000; Kapeller et al., 1995). γ-tubulin is part of the centrosome and other microtubule-organising centres and stabilises the minus-end of microtubules. It has been suggested that PI3Ks could be involved in the regulation of microtubule stability or in the regulation of vesicle budding/fusion located at microtubules.

GPC2, **GPC3** and **NEDD1** interact with γ-tubulin to form a so-called γ-tubulin ring complex (Haren et al., 2006; Murphy et al., 1998). Thus, their identification in p110δ IPs is likely due to their binding to γ-tubulin rather than to direct binding of p85 or p110.

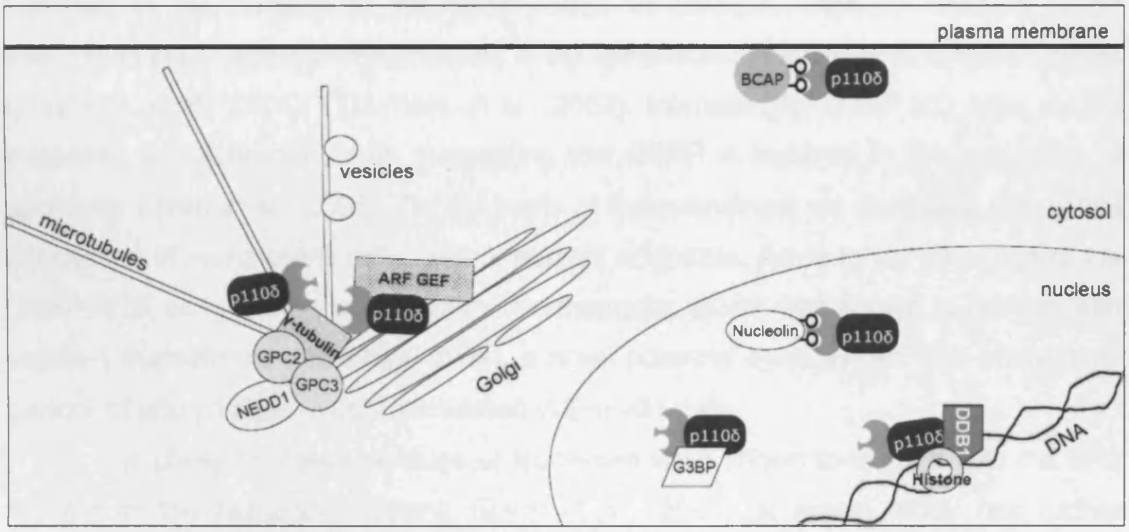

Figure 5.19: Hypothetical model of potential PI3K interaction partners and subcellular localisation in unstimulated WEHI-231 cells

Co-IP experiments using p110δ-specific Abs revealed a variety of potential PI3K interaction partners in unstimulated cells. Data gained from the literature allowed drawing some conclusions about the nature of their interaction with class IA PI3Ks. Details to each interaction partner can be found below.

p200 Arf-GEF is a novel potential PI3K interaction partner. This protein does not contain any known domain or motif which could explain binding to p85 or p110.

p200 Arf-GEF is a Brefeldin A-sensitive guanine nucleotide exchange factor for small GTPases of the ADP ribosylation factor (Arf) family (Mansour et al., 1999) and is localised at the Golgi. Vesicle transport from the Golgi to the plasma membrane is regulated by Arf and occurs along microtubules. Therefore, regulation of vesicle transport could possibly link the interaction of PI3K to p200 Arf-GEF with PI3K to the γ-tubulin ring complex. However, interaction between p200 Arf-GEF and PI3K has to be verified using independent Abs or techniques.

The 4 potential PI3K interaction partners G3BP, nucleolin, DDB1 and histone H4 are proteins detected in the nucleus in proliferating and/or stimulated cells. Since class IA PI3Ks have been shown to translocate to the nucleus following cellular stimulation (Neri et al., 1994), it is possible that a fraction of class IA PI3Ks reside in the nucleus in proliferating WEHI-231 cells.

Ras GTPase activating protein SH3 domain binding protein (**G3BP**) is a novel potential PI3K interaction partner and its interaction with PI3K can not easily be deduced from primary sequence analysis or literature data. G3BP is a RasGAP interacting endonuclease that cleaves AU-rich regions in mRNA, thereby targeting mRNA for rapid degradation. Following growth factor stimulation, G3BP is phosphorylated on Ser residues and translocates to the nucleus (Barnes et al., 2002). Since proliferating WEHI-231 cells can be compared to stimulated cells, G3BP is likely localised in the nucleus in WEHI-231 cells. In contrast, unphosphorylated G3BP assembles in so-called stress granules in the cytoplasm in response to cytotoxic stress (Tourriere et al., 2001); (Tourriere et al., 2003). Interestingly, G3BP KO mice exhibit increased apoptotic cell death suggesting that G3BP is involved in the regulation of apoptosis (Zekri et al., 2005). On the basis of these findings, we speculate that α-IgM stimulation of immature B cells, which induces apoptosis, leads to translocation of the G3BP-PI3K complex to the cytoplasm. Furthermore, G3BP was shown to interact with caprin-1 (Katsafanas and Moss, 2004), a novel potential cytoplasmic PI3K interaction-partner of p85-p110δ in α-IgM stimulated WEHI-231 cells.

Tyr phosphorylated residues of **Nucleolin** were shown to interact with the SH2 domain of the regulatory subunit (Barel et al., 2001). A recent study has further revealed that interaction of nucleolin with the class IA PI3K regulatory subunit was increased in endothelial cells following induction of fluid flow (Huddleson et al., 2006). Qualitative MS analysis revealed a small increase of nucleolin associated with PI3K in α-IgM stimulated WEHI-231 cells compared to control samples. Nucleolin is a multifunctional protein that plays a key role in ribosome biogenesis and in nuclear organisation (Ginisty et al., 1999). Although generally considered a nuclear protein, nucleolin can also be present in the cytoplasm and cell surface (Borer et al., 1989). In fact, translocation from the nucleus to the cytosol was observed in apoptotic B cells (Mi

et al., 2003). This suggests that the nucleolin-PI3K complex, residing in the nucleus in proliferating WEHI-231 cells, might translocate to the cytosol following α-IgM stimulation of WEHI-231 cells. Nucleolin also interacts with the PH domain of IRS-1 and IRS-2 (Burks et al., 1998), and with PARP-1 (Borggrefe et al., 1998). However, since IRS-2 and PARP-1 were only detected in association with PI3K in stimulated cells, whereas nucleolin was found in co-IPs of unstimulated and stimulated WEHI-231 cells, we conclude that the interaction between PI3K and nucleolin is probably not via IRS-2 or PARP-1

No information is available about the interaction between PI3K and damage DNA binding protein 1 (**DDB1**) and no known PI3K interaction domain or motif in DDB1 could be detected. DDB1 forms a heterodimeric complex with DDB2. DDB expression and activity increase following UV irradiation of cells leading to increased nucleotide excision repair. Furthermore, DDB1 was recently shown to interact with Cul4 to form an ubiquitin E3 ligase complex which ubiquinates histones in response to UV irradiation (Groisman et al., 2003). Since we also detected **histone H4** in the p110δ IPs by MS, we speculate that the interaction between PI3K, DDB1 and histone H4 occurs in proximity of DNA.

In addition to co-IP experiments, we also performed pull-down assays of WEHI-231 cell lysates using peptides corresponding to the C-terminal sequence of p110δ. These peptides contained non-phosphorylated or phosphorylated Ser1039. Analysis of pulled-down proteins by MS led to the identification of Acrogranin. Acrogranin is an epithelial tissue growth factor that has been implicated in the progression of many cancers. It has been shown to stimulate MAPK, PI3K and FAK kinase pathways. We speculate that the potential interaction of Acrogranin to p110δ might have a role in the regulation of p110δ activity.

In summary, in unstimulated, but proliferating immature B cells p110δ likely exists in the cytoplasm associated with BCAP, p200 Arf-GEF and the γ-tubulin ring complex. Association with the latter two proteins might suggest involvement of p110δ in vesicular traffic. A fraction of p110δ might also be found in the nucleus, where it seems to bind proteins involved in DNA and RNA metabolism.

5.13.6 Interaction partners of p110δ following BCR engagement

In order to further determine the impact of p110δ Tyr phosphorylation on PI3K signalling and of BCR crosslinking in immature B cells, we analysed by MS proteins immunoprecipitated by p110δ Abs from α-IgM stimulated WEHI-231 cells. IRS-2, PAPR-1 and caprin-1 were identified as novel potential p85-p110δ interaction partners

downstream of the BCR. A hypothetical model of PI3K interactions and subcellular localisation following BCR engagement is shown in Figure 5.20.

The interaction between p85-p110δ and insulin receptor substrate (**IRS**)-2 increased by more than 5-fold following BCR engagement as determined by qualitative MS analysis and immunoblotting of co-IP experiments. This interaction is likely due to binding of the regulatory subunit SH2 domains to phosphorylated Tyr residues in YxxM motifs of IRS-2. IRS contains multiple YxxM motifs to which p85 can bind (Backer et al., 1992). Since also the interaction of p110α with IRS-2 was increased upon cellular stimulation, binding of PI3K to IRS-2 via p85 is emphasised. Two further domains of IRS-2 could be involved in p85-p110δ binding. First, a pTyr binding (PTB) domain which interacts with pTyr residues located in NPxY sequences (He et al., 1996). p110δ contains two Tyr residues with similar flanking sequences: Tyr474 is part of YxPE and Tyr484 lies within HPxYxPA. Second, amino acid sequence 591-733 of IRS-2, but not IRS-1 was shown to interact with IR and IGF-R in a pTyr-dependent, but NPxY-independent manner (He et al., 1996). We therefore hypothesise that IRS-2 might bind p110δ via pTyr residue(s).

Involvement of IRS-2 downstream of the BCR has not been reported and it is therefore not evident how IRS-2 is coupled to the BCR. Unlike the IL-4 receptor, which has been implicated in IRS-2 signalling in B cells (Johnston et al., 1995), the immunoglobulin-associated CD79α/β do not possess Tyr residues in NPxY motifs in their cytosolic domains which could provide docking sites for IRS-2. However, the IRS-2-specific amino acids sequence 591-733 binding to phosphorylated Tyr residues might provide this interaction. Furthermore, IRS-2 contains a PH domain implicated in the binding to PIs (Razzini et al., 2000), which might induce interaction with the BCR. Interestingly, nucleolin, a potential novel p85-p110δ protein partner in proliferating WEHI-231 cells, was shown to bind to the PH domain of IRS-2, thereby inhibiting insulin-stimulated Tyr phosphorylation of IRS-2 (Burks et al., 1998). Interaction between the nucleolin-PI3K complex and IRS-2 might therefore provide a negative feedback loop in BCR signalling. In addition, it is not clear how phosphorylation of IRS-2 downstream of the BCR might be achieved. IRS-2 cannot be phosphorylated on YxxM motifs by the BCR complex, since BCR does not contain kinase activity. Janus kinases have been implicated in IRS-2 phosphorylation downstream of receptors lacking kinase activity (Johnston et al., 1995; Kellerer et al., 1997) and those kinases might possibly phosphorylated IRS-2 downstream of the BCR. However, it has also been suggested that the IRS pathway is independent of the JAK pathway in hematopoietic cells (Uddin et al., 1997).

A novel IRS-2 phosphorylation site on Ser573 was determined by LC-MS/MS. Ser phosphorylation of IRS seems to regulate insulin signal transduction by blocking IRS interaction with IR (Tanti et al., 1994) or by inducing IRS degradation (Pederson et al., 2001). Ser phosphorylation was shown to be catalysed by different Ser kinases, amongst other class IA PI3K (Lam et al., 1994; Tanti et al., 1994) and Akt (Guo et al., 1999; Paz et al., 1999). Indeed, Ser573 lies within an acceptor sequence for Akt phosphorylation. Ser phosphorylation of IRS-2 by Akt might therefore provide a regulatory feedback loop in WEHI-231 cells.

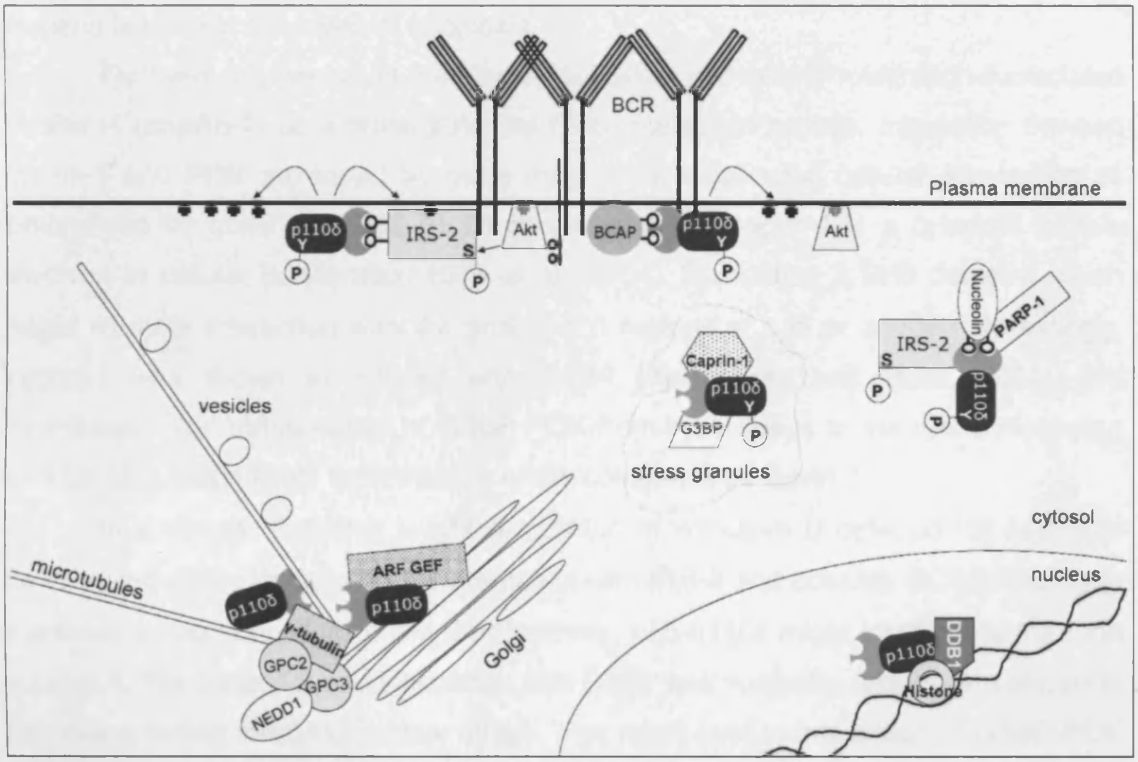

Figure 5.20: Hypothetical model of PI3K interaction partners and subcellular localisation following BCR engagement of WEHI-231 cells

Co-IP experiments using p110δ-specific Abs revealed a variety of potential PI3K interaction partners in unstimulated cells. Data gained from the literature allowed drawing some conclusions about the nature of their interaction with class IA PI3K. Details to each interaction partners can be found below.

A potential novel PI3K interaction partner in α-IgM stimulated WEHI-231 cells is **PARP-1**. The interaction between PARP-1 and p85-p110δ was increased by 4-fold following BCR engagement of WEHI-231 cells. In addition to the identification of PARP-1 in p110δ co-IPs, p110δ and p110β were also identified in PARP-1 IPs (T. Helleday, Institute for Cancer Studies, University of Sheffield, personal communication). Interaction between PARP-1 and PI3K could be mediated by dimerisation of the basic leucine zipper regions (bZIP) of p110δ/p110β and PARP-1. PARP-1 also contains a BRCT domain which can bind phosphorylated Ser/Thr residues; however, since p110δ

Ser1039 phosphorylation is decreased following BCR stimulation, this is unlikely to happen unless unidentified pSer/pThr residues exist in p110δ. PARP-1 is activated by broken DNA and catalyses the reversible modification of proteins with ADP-ribose. Poly(ADP-ribosyl)ation of histones and other nuclear proteins contributes to the survival of proliferating cells following DNA damage (reviewed in (Ame et al., 2004)). During apoptosis, PARP-1 is one of the first proteins cleaved by caspases (Kaufmann et al., 1993). Interestingly, PARP-1 has also been shown to interact with nucleolin. We therefore speculate that translocation of PARP-1 by PI3K-nucleolin complex to the cytosol following BCR engagement of WEHI-231 cells might inhibit DNA repair in the nucleus leading to the onset of apoptosis.

Furthermore, we could identify Cytoplasmic Activation/Proliferation-Associated Protein-1 (**caprin-1**) as a novel potential PI3K interaction protein. Interaction beween caprin-1 and PI3K increased by more than 100-fold following cellular stimulation as determined by qualitative MS. As its name suggests, caprin-1 is a cytosolic protein involved in cellular proliferation (Grill et al., 2004). It contains 2 SH3 domains which might mediate interaction with the proline-rich regions of p85 or p110δ. Interestingly, caprin-1 was shown to interact with G3BP (Katsafanas and Moss, 2004). We hypothesise that translocation of G3BP-PI3K from the nucleus to the cytosol following cellular stimulation leads to interaction of the complex with caprin-1.

In summary, following α-IgM stimulation of immature B cells, p110δ seems to be recruited to the membrane by interaction with IRS-2 and possibly BCAP leading to increased phosphorylation of Akt. Furthermore, p85-p110δ might translocate from the nucleus to the cytosol due to interaction with G3BP and nucleolin, which were shown to become cytosolic following cellular stress. This might lead to interaction of G3BP-PI3K with caprin-1 and of nucleolin-PI3K with IRS-2.

6 INVESTIGATION OF THE P85 TO P110 EXPRESSION RATIO IN MAMMALIAN CELLS

The role of the regulatory subunit of class IA PI3K in resting cells appears to be stabilisation of the catalytic subunit and inhibition of its lipid kinase activity. Following cellular stimulation, p85 was shown to recruit p110 to the plasma membrane and to release inhibition on the lipid kinase activity by interaction of p85 SH2 domains with Tyr phosphorylated proteins (Rordorf-Nikolic et al., 1995; Yu et al., 1998; Yu et al., 1998).

It was therefore surprising that mice with targeted deletion of one or more p85 genes, which leads to p85 *and* p110 protein reduction, exhibit enhanced PI3K signalling in insulin responsive cells (Chen et al., 2004; Fruman et al., 2000; Terauchi et al., 1999; Ueki et al., 2002). Subsequent analysis revealed that forced overexpression of class IA PI3K regulatory subunits in skeletal muscle cells leads to a decrease in Akt phosphorylation (Ueki et al., 2000), indicating that excess p85 might compete with p85-p110 for pTyr-binding sites. Furthermore, a 30% excess of p85 over p110 in WT mouse embryonic fibroblasts (Ueki et al., 2002) and in liver cells (Mauvais-Jarvis et al., 2002) was reported. Based on this information, a model attributing a negative role of p85 to PI3K signalling was proposed: in WT cells, surplus, thus free p85 competes with heterodimeric p85-p110 for pTyr binding sites in receptor tyrosine kinases or adaptor molecules thereby dampening PI3K signalling. In p85 KO cells, expression of monomeric p85 is preferentially reduced leading to enhanced access of heterodimeric p85-p110 to pTyr binding sites and to increased PI3K signalling.

In insulin-responsive tissue of p85 KO mice, however, the PI3K signalling pathway is skewed due to "knock-on" effects of regulatory subunit gene deletion. Analysis of class IA PI3K isoform expression in p85α KO cells revealed decreased levels of p110 protein and increased protein expression of p55α, p50α or p85β. Furthermore, PTEN protein expression is increased in heterozygous p85α KO mouse embryonic fibroblasts (Ueki et al., 2002) and IRS-2 phosphorylation is increased in cells gene-targeted for p55α/p50α and p85β (Chen et al., 2004; Ueki et al., 2002). A further challenge to the model described above arises from the quality of the Abs used in immunodepletion experiments to demonstrate excess of p85 over p110 in insulin-responsive cells (Mauvais-Jarvis et al., 2002; Ueki et al., 2002).

In order to address whether monomeric p85 exists *in vivo* or whether class IA PI3Ks are obligate heterodimers, knowledge of binding affinities of the monomers to each other and *in vivo* molarities of the subunits is crucial. Interaction between the regulatory and catalytic subunit was shown to be very tight, withstanding high concentrations of salt, urea or detergent (Fry et al., 1992; Kazlauskas and Cooper,

1990). These data indicate that dissociation of p85 and p110 is unlikely. Free regulatory subunit could also exist if p85 was expressed in excess of p110 provided that monomeric p85 is stable. Pulse-chase experiments of cells overexpressing p110α and p85α compared to overexpression of p85α on its own, revealed that the half-life of monomeric p85α is more than 3 times shorter than that of p85α associated with p110α (Brachmann et al., 2005). These data indicate that the existence of monomeric p85 *in vivo* is not likely.

We aimed at investigating the p85 to p110 ratio in mammalian cells. Immunoprecipitation, immunodepletion and ion exchange chromatography experiments were performed to analyse the presence of monomeric and dimeric class IA PI3K subunits *in vivo*. Furthermore, we set out to analyse the absolute protein amounts of each subunit by absolute quantitation (AQUA) mass spectrometry. Analysis of these experiments did not reveal any evidence of free p85 indicating that class IA PI3Ks are obligate heterodimers. We provide an alternative model to monomeric p85 for the observed increase in PI3K activity in insulin-responsive cells of p85 KO mice.

6.1 Class IA PI3K isoform expression in fibroblasts and leukocytes

We compared the p85 to p110 ratio in murine fibroblasts and in leukocytes given that different phenotypes of PI3K signalling were observed in these cell types of p85α KO mice. While studies in p85α KO mice revealed that PI3K signalling is upregulated in insulin-responsive cells following insulin stimulation leading to enhanced insulin sensitivity (Fruman et al., 2000; Terauchi et al., 1999), downregulation of PI3K signalling in p85α KO B cells following BCR engagement was believed to dampen B cell proliferation and development (Fruman et al., 1999; Suzuki et al., 1999).

We first analysed the PI3K protein amounts by immunoblotting using various class IA PI3K Abs in cell extracts of NIH-3T3, A20 and WEHI-231 cells (Figure 6.1). This analysis revealed that relative expression levels of p110α were similar in each cell line tested, but p110β and p110δ protein expression followed an inverse correlation: p110β protein levels were high in fibroblasts and low in leukocytes; in contrast, p110δ protein expression was low in fibroblasts and high in leukocytes. Variation in the protein expression of class IA isoforms in different cell types has been reported (Hu et al., 1993; Vanhaesebroeck et al., 1997). Remarkably, depending on the Ab used for immunoblotting, the relative p85 protein expression in fibroblast and leukocytes was variable. Using Abs whose epitopes lie within the BH/Rac binding domain of p85, the p85 expression levels were higher in leukocytes compared to fibroblasts (U10, T12/T15). In contrast, if Abs were used whose epitopes lie within the N-terminal SH2

domain, similar protein expression levels were noted in all cell types (U2, p85pan). It is possible that p85 modifications occurring within the recognition site of the Ab might interfere with Ab binding (see § 4.5).

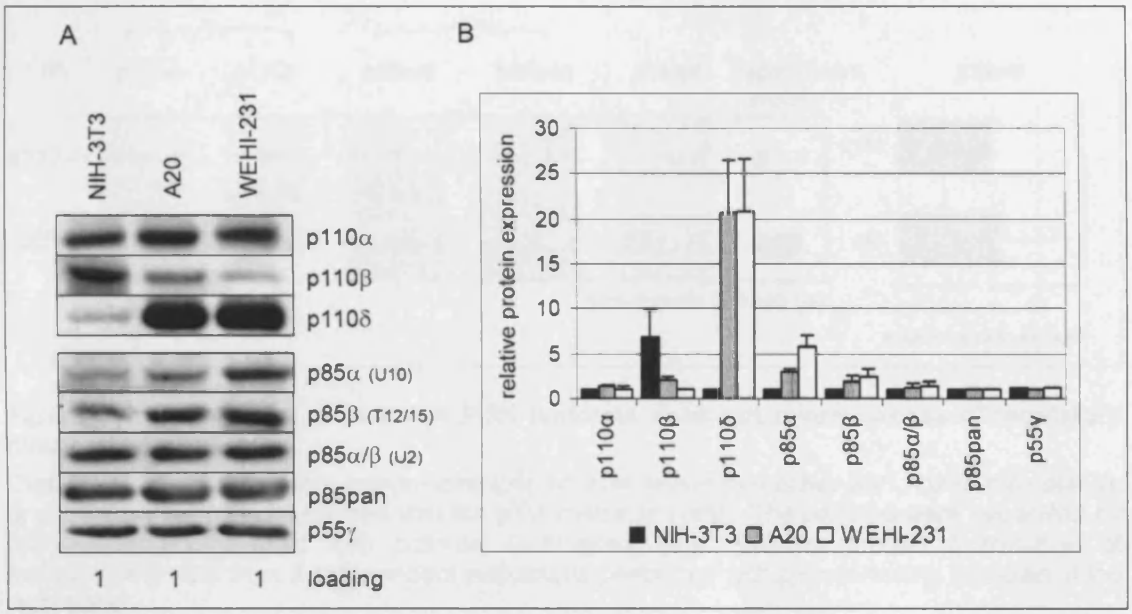

Figure 6.1: Relative protein expression of class IA PI3K isoforms in fibroblasts and leukocytes

The same amount of total cell lysate of the indicated cell lines was analysed for class IA PI3K subunit protein expression. (A) Immunoblot using Abs to the different class IA PI3K isoforms. (B) Relative quantitation of class IA PI3K isoforms based on immunoblot signals in A. The protein expression levels of each subunit are standardised against the lowest protein amount detected in any of the 3 cell types analysed.

6.2 Purification of class IA PI3K by various methods mediates equal amounts of p85 and p110 protein

In order to address whether class IA PI3K regulatory and catalytic subunits exist in equimolar amounts or whether one subunit prevails over the other, we performed class IA PI3K enrichment experiments. By comparing protein amounts visualised by colloidal Coomassie blue of p110-IP with p85-IP, an excess of one subunit over the other should be detectable.

Therefore, class IA PI3Ks were immunoprecipitated from leukocytes with Abs to catalytic subunits (p110α and p110δ) or to regulatory subunits. In addition, class IA PI3Ks were purified using the pTyr-matrix, which interacts with the SH2 domain of p85 (§ 3). The enriched protein were separated by SDS-PAGE and visualised by colloidal Coomassie blue (Figure 6.2). Densitometric analysis of the protein bands at M_r of 110 and 85 kDa revealed equal amounts of catalytic and regulatory subunits in the purified fractions of the various enrichment methods. These data argue against the existence of molar excess of one subunit over the other.

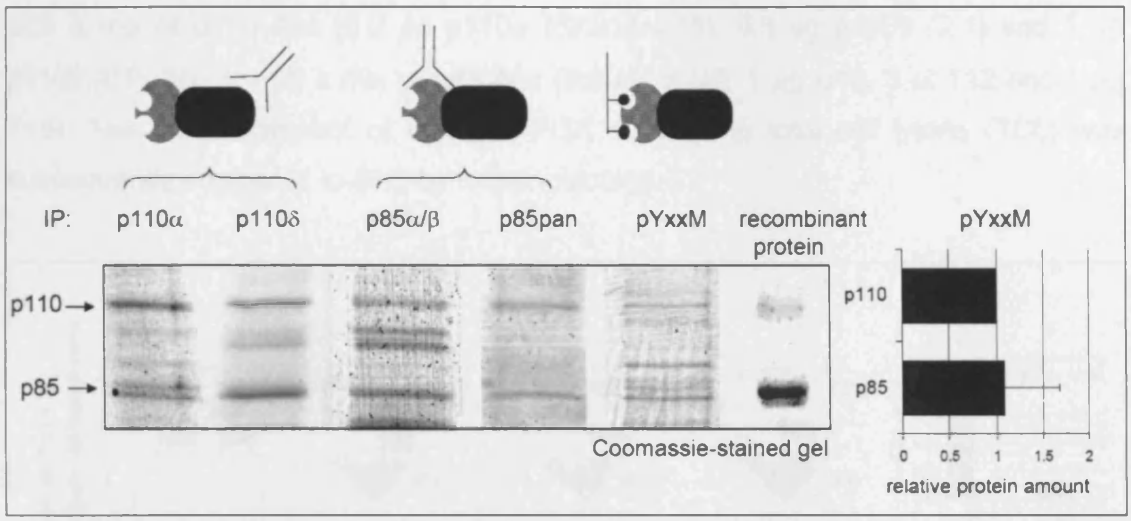

Figure 6.2: Enrichment of class IA PI3K isoforms does not reveal excess of regulatory over catalytic subunit.

Class IA PI3K subunits were immunoprecipitated from leukocytes either with Abs to the catalytic or regulatory subunit or enriched with the pTyr-matrix (pYxxM). The proteins were separated by SDS-PAGE and stained with colloidal Coomassie blue. Relative protein quantitation of densitometric data from 3 independent pull-downs performed with pYxxM-matrix is shown in the right panel.

6.3 Immunodepletion of one subunit does not give rise to free remaining subunits

We next performed sequential IP experiments of class IA PI3K subunits and compared the protein amount of catalytic and regulatory subunits in total cell lysate (TCL) with supernatant (SN) by immunoblotting. A schematic drawing of immunodepletion experiment is shown in Figure 6.3. If class IA PI3Ks were obligate heterodimers, immunodepletion of the catalytic subunit would lead to equal amounts of regulatory and catalytic subunits in the third supernatant (SN3) (Figure 6.3.A). In contrast, immunodepletion of the catalytic subunit from cell lysates containing a 30% molar excess of the regulatory subunit (non-obligate heterodimers) would reveal a 300% excess of the regulatory subunit in SN3 (Figure 6.3.B) if 85% of all class IA PI3K protein was depleted. Since class IA PI3Ks were immunodepleted with an Ab-mix against the regulatory and in a separate experiment against the catalytic subunit, a molar excess of any subunit should be detectable using this method.

Conditions to perform immunodepletion experiments were established using WEHI-321 cell extracts (§ 6.3.1). These experiments were followed by analysis of 3 different methods of regulatory subunit depletion (§ 6.3.2) and by determination of PI3K immunodepletion from NIH-3T3 and A20 cell lysates. In § 6.3.4, we present a summary of immunodepletion experiments performed with WEHI-231, A20 and NIH-3T3 lysates.

Unless otherwise stated, 1 mg of total cell lysate was subjected to sequential IP with a mix of p110 Abs (0.2 μg p110α (SK214+215), 0.3 ug p110β (2.1) and 1 μg p110δ (CT) Ab) or with a mix of p85 Abs (0.8 μg of U2, 1 μg U10, 3 μl T12 and 1 μg T15). The protein amount of class IA PI3K subunits in total cell lysate (TCL) was subsequently compared to SN3 by immunoblotting.

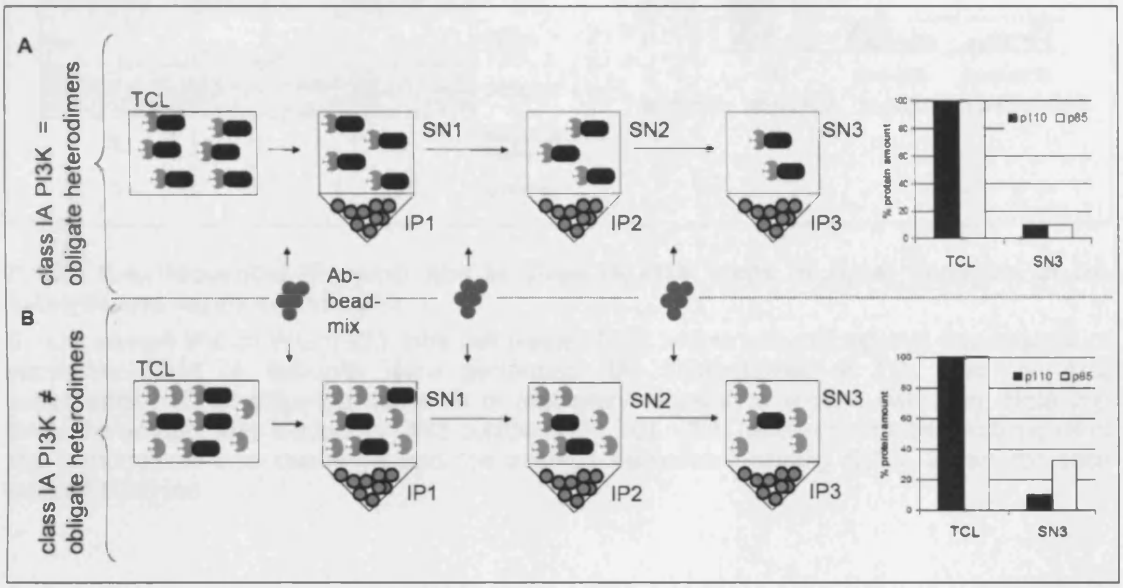

Figure 6.3: Schematic representation of immunodepletion experiments

Immunodepletion experiments are performed by 3 rounds of IP with an Ab-mix to the regulatory or catalytic class IA subunits. In each round, more class IA PI3Ks are being depleted from total cell lysate (TCL). Immunodepletion with Abs raised against the catalytic subunit is shown. If class IA PI3Ks were obligate heterodimers (A), one would expect similar depletion of p85 and p110 in the third supernatant (SN3). If class IA PI3Ks were non-obligate heterodimers (B), one would expect to detect an excess of the regulatory over catalytic subunit in SN3.

6.3.1 Immunodepletion of WEHI-231 cell extracts

Sequential immunodepletion as described in § 6.3 was performed with WEHI-231 cell extracts. In Figure 6.4.A, immunoblots of total cell lysate and SN3 after depletion with p85 or p110 Ab-mix of 3 independent immunodepletion experiments are shown. Relative quantitation of chemiluminescence signals after incubation of the filter with Abs to p110α, p110δ, p85α and p85pan are summarised in Figure 6.4.B. In the latter figure, the signal obtained for total cell lysate of each isoform in each experiment (minus background signal) was set as 100% and the signal values for SN3 were calculated relative to this amount. The average and standard deviation (SD) of the 3 experiments are shown.

More than 80% of the regulatory and catalytic subunit were found to be depleted after 3 sequential IP of class IA PI3K IP. A small excess of p110 following p85 IP and a small excess of p85 following p110 IP was detected.

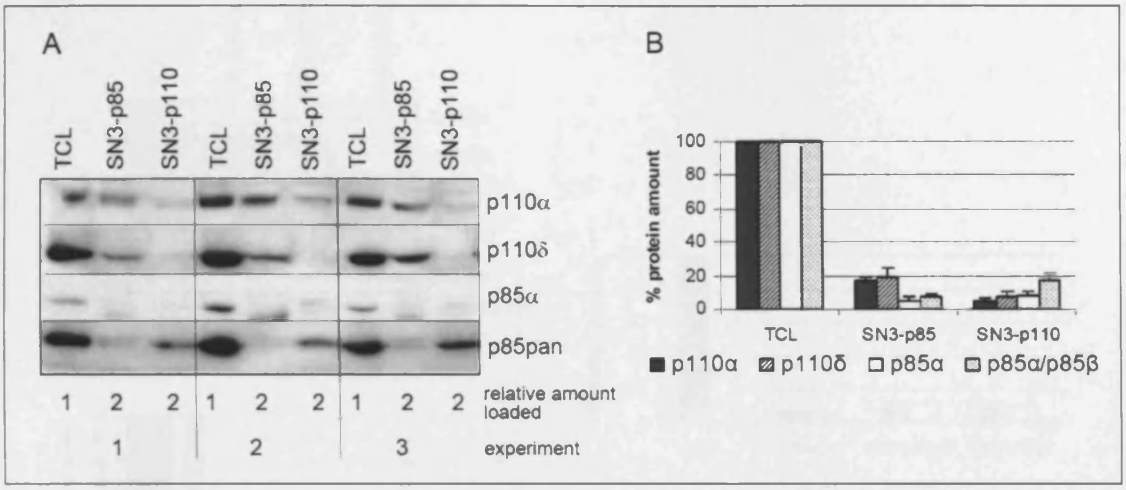

Figure 6.4: Sequential IP using Abs to class IA PI3K leads to equal depletion of the catalytic and regulatory subunit

3 independent IPs on WEHI-231 total cell lysate (TCL) with an Ab-mix against the catalytic or regulatory class IA subunits were performed. (A) Immunoblots of TCL and the third supernantant (SN3) following depletion of regulatory or catalytic subunit depletion. Note that twice the amount was loaded for SN3 compared to TCL. (B) The chemiluminescence signal of the immunoblots was quantified and the average depletion including SD is shown for each subunit analysed.

6.3.2 Comparison of 3 different regulatory subunit enrichment methods

In order to further examine the efficacy of immunodepletion experiments, we compared 3 depletion approaches, which differentially enrich for the regulatory subunit. p85 was depleted from 1 mg WEHI-231 cell extract by 3 rounds of IP with either 0.8 μg p85pan pAb or 0.8 μg U2 mAb, or by 3 rounds of p85 pull-down with 100 μl of pTyr-matrix. Figure 6.5 shows immunoblots of p110α, p110β, p110δ, and p85α/β detected in TCL and SN3 samples (A) and relative quantitation of the chemiluminescence signal after incubation of the filter with PI3K Abs (B) as described in § 6.3.1. The average relative protein amount of p110 and p85 in TCL is compared to SN3 (C).

The data revealed similar depletion efficiencies of class IA PI3K with the different methods used and indicated no molar excess of the catalytic over the regulatory subunit.

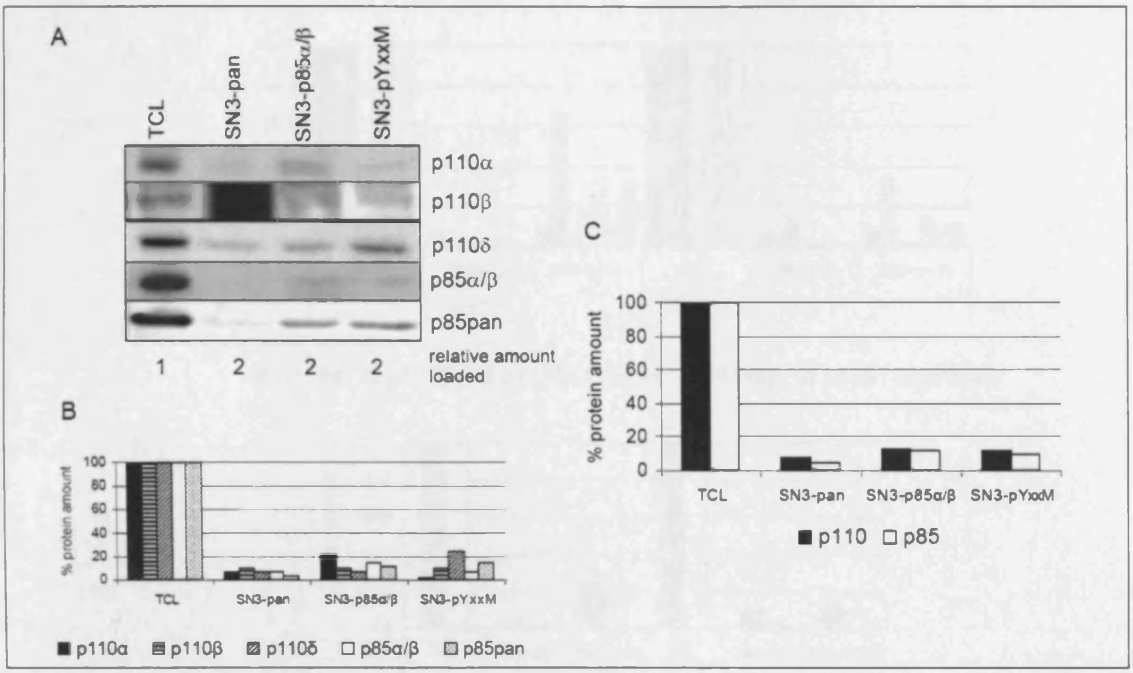

Figure 6.5: Depletion of class IA PI3K from WEHI-231 cells using different p85 enrichment methods

The regulatory subunit was depleted from total cell lysate (TCL) by 3 sequential IPs with p85pan pAb or U2 mAb or by 3 rounds of pull-down with the pTyr-matrix (pYxxM). (A) Immunoblotting of class IA PI3K isoforms in samples of TCL and SN3 derived from the 3 different depletion methods. (B) Relative quantitation of the chemiluminescence signal after immunoblotting with class IA PI3K Abs by comparing the protein amount in TCL and SN3. (C) Relative quantitation of the average p110 and p85 protein amount detected in TCL and SN3.

6.3.3 Immunodepletion in NIH-3T3 and A20 cell extracts

In order to compare the results obtained for WEHI-231 cells with the two cell lines used in § 6.1, we performed immunodepletion experiments with A20 and NIH-3T3 cell extracts. As shown in Figure 6.6.A, relative quantitation of class IA PI3K isoforms after p85 immunodepletion (SN3-p85) revealed more than 80% depletion of regulatory and catalytic class IA PI3K subunits in NIH-3T3 and A20 cells. In contrast, immunodepletion using a p110 Ab-mix mediated only 40-60% depletion of p110β, while depletion of p110α and p110δ was similar to previous experiments. Since significantly more p110β was found in NIH-3T3 and slightly more p110β seems to exist in A20 compared to WEHI-231 (Figure 6.1), we probably did not use enough p110β Ab to deplete the protein. However, average depletion of the regulatory subunit correlated with average depletion of the catalytic subunit in SN3-p110 (Figure 6.6.B). These data indicate that the equimolarity between the regulatory and catalytic subunit is maintained in the depleted fraction.

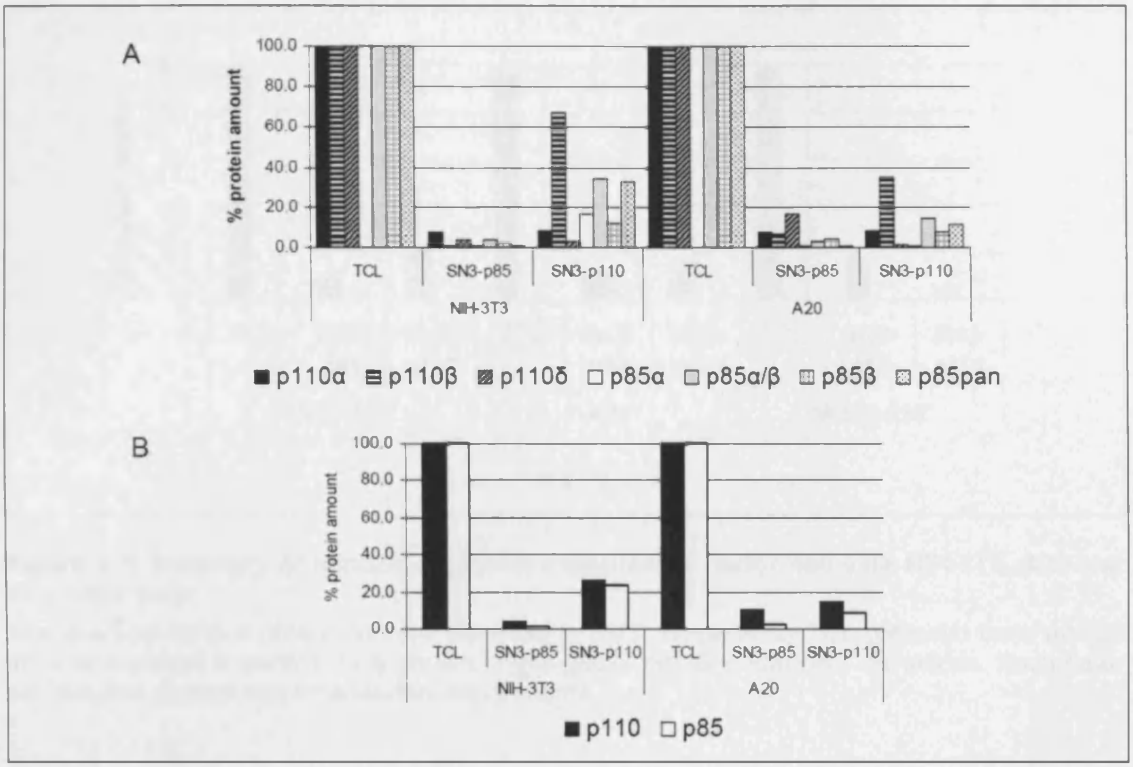

Figure 6.6: Immunodepletion of NIH-3T3 or A20 using PI3K Abs to class IA PI3K does not expose excess of one class IA PI3K subunit over the other

Class IA PI3K subunits were depleted from NIH-3T3 and A20 total cell lysate (TCL) by 3 rounds of IP with a mix of Abs to p85 or p110. The class IA PI3K protein amount detected by PI3K Abs in SN3 was compared to the TCL sample by immunoblotting. (A) Relative quantitation of depleted fraction compared to TCL for each PI3K subunit. (B) Quantitation of p110 and p85 protein levels shown in A.

6.3.4 Summary of immunodepletion experiments

In Figure 6.7, a summary of the average relative quantitation and SD of the immunoblot signals of all immunodepletion experiments performed with the different cell lines is shown.

No significant excess of one class IA PI3K subunit over the other could be detected by immunodepletion experiments in fibroblasts or leukocytes.

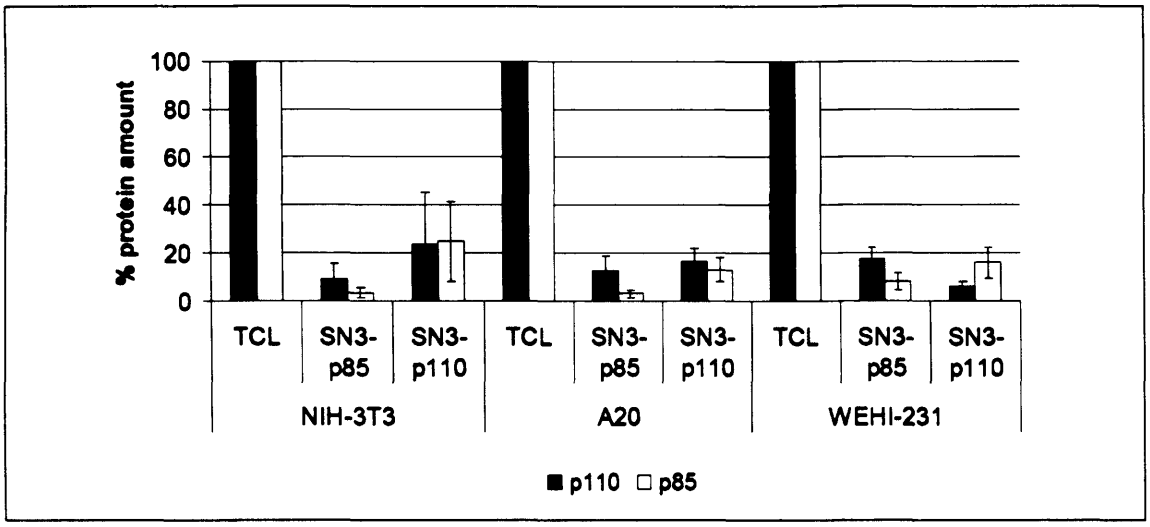

Figure 6.7: Summary of immunodepletion experiments performed with NIH-3T3, A20 and WEHI-231 cells

The average relative protein amount detected in SN3 compared to TCL gathered from various immunodepletion experiments is shown in this graph including standard deviations. Each data-set includes at least two independent experiments.

6.4 Ion exchange chromatography of class IA PI3K subunits indicates that p85/p110 are obligate heterodimers

Ion exchange chromatography separates biomolecules based on differences in their charge characteristics. In anion exchange chromatography, a strong anion exchanger is coupled to an inert resin. Application of negatively charged proteins to anion exchange chromatography columns leads to binding of the protein to the stationary phase, while increasing the ionic strength in the mobile phase subsequently elutes the protein from the column.

Since monomeric class IA PI3Ks likely possess different charge characteristics than heterodimeric PI3K, ion exchange chromatography was expected to separate monomeric and heterodimeric class IA PI3K isoforms. We therefore used anion exchange chromatography to analyse the p85 to p110 ratio of class IA PI3K subunits *in vivo*.

6.4.1 Ion exchange chromatography of overexpressed p85α and p85α/p110α

In order to investigate whether the elution profiles of monomeric regulatory subunit could be discriminated from elution profiles of heterodimeric regulatory subunits by anion exchange chromatography, p85α was overexpressed in HEK-293T cells with or without p110α and subjected to anion exchange chromatography. To this end, 20 µg pSG5 plasmid DNA (STRATAGENE) containing the cDNA sequence of bovine p85α or

bovine p110α under the control of SV40 early promoter were transiently transfected into HEK-293T cells by calcium phosphate precipitation (§ 2.7.2.5). Following cell lysis, the lysate was desalted by gel filtration and proteins subsequently subjected to anion exchange chromatography as described in § 2.14.1. 1 ml eluate fractions were collected and analysed for p85α and p110α by immunoblotting (Figure 6.8).

p85α was found to elute at higher salt concentrations than endogenous p110α in cells overexpressing p85α, suggesting that the p85α protein detected by immunoblotting in Figure 6.8.A is overexpressed, i.e. monomeric p85 protein. A longer exposure of the same filter revealed additional p85α, which presumably includes endogenous p85α, co-eluted with endogenous p110α. When bovine p85α was co-expressed with bovine p110α in HEK-293T cells (Figure 6.8.B), the proteins eluted at the same ionic strength. Furthermore, the elution profile of overexpressed p85α/p110α matched the elution profile of endogenous p110α. These data indicate that monomeric p85 can be separated from heterodimeric p85-p110 by anion exchange chromatography.

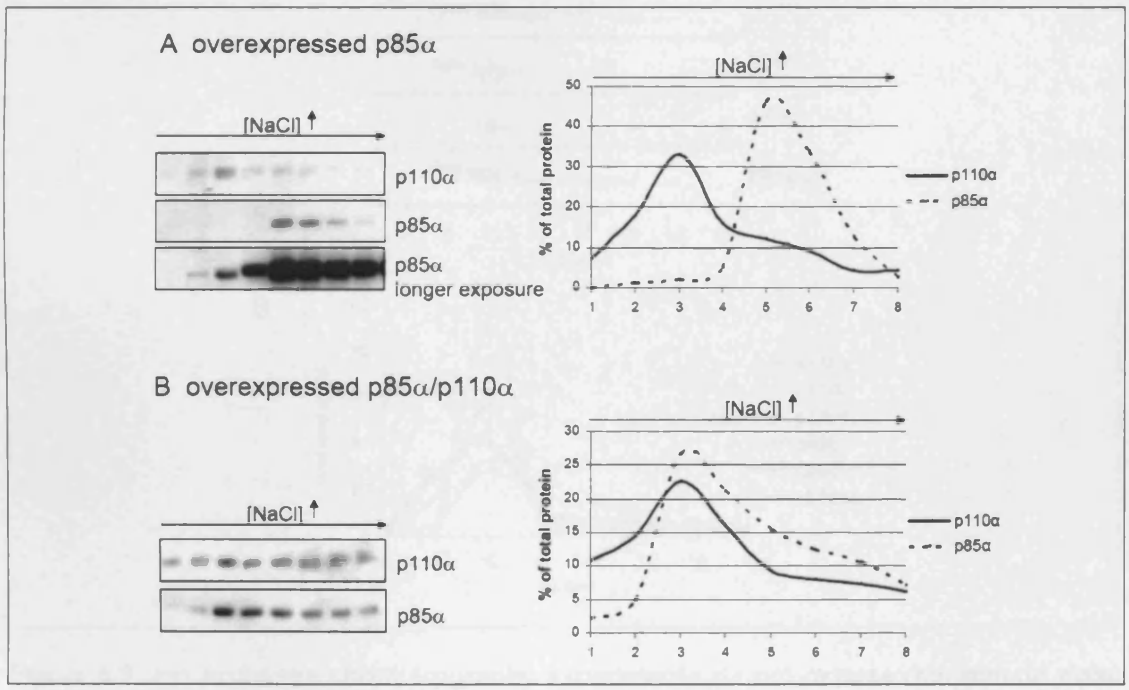

Figure 6.8: Anion exchange chromatography analysis of overexpressed p85α +/- p110α
HEK-293T cells were transiently transfected with bovine p85α without (A) or with (B) bovine p110α using the calcium phosphate transfection method (INVITROGEN). Total cell lysate was subsequently subjected to anion exchange chromatography. The fractions were analysed for class IA PI3K subunits by immunoblotting with Abs to p85α and p110α (left panel). The elution profiles based on immunoblotting signals of each subunit in the two experimental set-ups are shown (right panel).

6.4.2 Endogenous class IA PI3K subunits co-elute from anion exchange chromatography columns

Total cell lysate of WEHI-231 cells was subjected to anion exchange chromatography under the same conditions as used for HEK-293T cells described in § 2.14.1. Eluate fractions were analysed by immunoblotting using Abs to the class IA PI3K isoforms (Figure 6.9.A, only fractions 8-15 of 50 are shown since only modest PI3K signals were detected in other fractions) followed by quantitation (Figure 6.9.B). The results shown in Figure 6.9 are a representative example of 3 independent experiments.

From Figure 6.9 it is clear that all PI3K subunits co-elute within a few chromatography fractions, indicating that p85 and p110 exist as heterodimers *in vivo*.

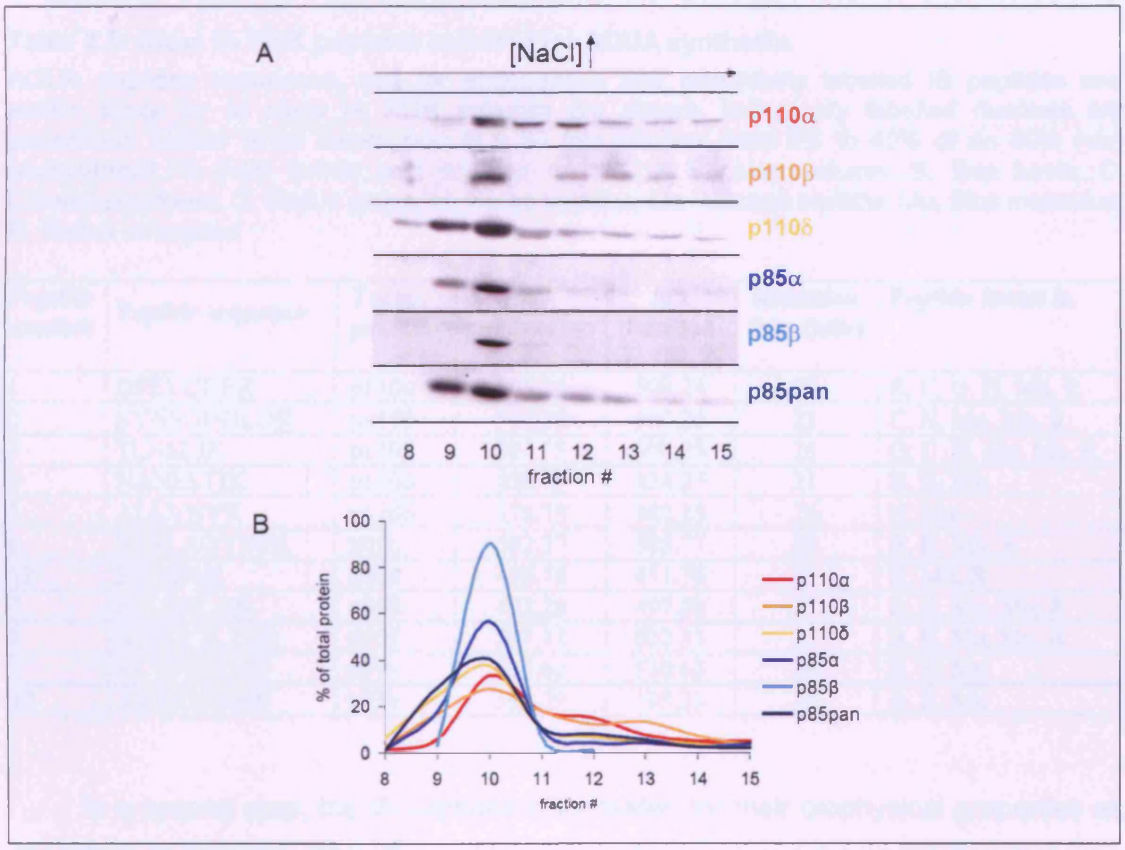

Figure 6.9: Ion exchange chromatography experiments do not expose monomeric class IA PI3K subunits

Total cell lysate of WEHI-231 cells was fractionated by anion exchange chromatography. Each fraction was analysed by immunoblotting for class IA PI3K. (A) Immunoblotting of different class IA PI3K. (B) Relative quantitation of PI3K protein amounts obtained from immunoblotting analysis.

6.5 AQUA analysis allows for quantitative class IA PI3K protein determination

In order to quantify the protein concentration of each class IA PI3K isoform in different cell types, we applied absolute quantification MS. This method is described in more details in 2.16.4.4. Briefly, an internal standard (IS) peptide containing the same sequence as an endogenous peptide following proteolysis is spiked to the cell sample at known concentrations. MS is subsequently used to quantify the endogenous peptide by comparison of peak integrated areas of endogenous and IS peptides.

In a first step, class IA PI3K isoforms were analysed by LC-MS/MS and suitable peptides for AQUA selected as described in 2.16.4.4. Some of their biophysical properties are listed in Table 6.1.

Table 6.1: Class IA PI3K peptides selected for AQUA synthesis.

AQUA peptides sequences, m/z for endogenous and isotopically labelled IS peptides and elution times for all class IA PI3K subunits are shown. Isotopically labelled residues are underlined. Elution times correspond to a 30 min gradient from 5% to 40% of an 80% (v/v) acetonitrile/0.1% (v/v) formic acid solution on a C18 PepMap column. B, Bos bovis; C, Cricetulus griseus; G, Gallus gallus; H, Homo sapiens; Ma, Macaca mulatta; Mu, Mus musculus; R, Rattus novegicus

Peptide number	Peptide sequence	Target protein	m/z endogenous	m/z labelled	Retention time (min)	Peptide found in
1	DPEVQDF<u>R</u>	p110α	503.24	508.24	28	B, C, G, H, Mu, R
2	EYNSGDDLD<u>R</u>	p110β	592.25	597.25	23	C, H, Ma, Mu, R
3	TLNSL<u>I</u>K	p110β	394.75	398.25	26	G, C, H, Ma, Mu, R
4	NANLST<u>I</u>K	p110δ	430.75	434.25	21	B, H, Mu
5	ALL<u>V</u>NVK	p110δ	378.75	382.25	26	H, Mu
6	NES<u>L</u>AQYNPK	p85α	582.27	585.77	20	B, H, Mu, R
12	ISEI<u>I</u>DS<u>R</u>	p85α	466.76	471.76	31	H, Mu, R
7	FLLQHLG<u>R</u>	p85β	492.28	497.28	27	B, H, Ma, Mu, R
8	IQGEYTLTL<u>R</u>	p85β	597.33	602.33	32	B, H, Ma, Mu, R
9	HCVIYSTA<u>R</u>	p55γ	525.62	530.62	24	B, H, Mu
10	TWFVEDIN<u>R</u>	p55γ	590.29	595.29	32	B, H, Mu

In a second step, the IS peptides were tested for their biophysical properties as described in 2.16.4.4. The IS peptides were also analysed for correlation between peptide abundance and integrated peak areas and for their detection limit (Figure 6.10). These experiments revealed that the integrated peak areas obtained by LC-ESI-MS of IS peptides are linear with respect to the amount of peptide analysed and that the detection limit of the IS peptides analysed by LC-ESI-Qtof is below 50 fmole.

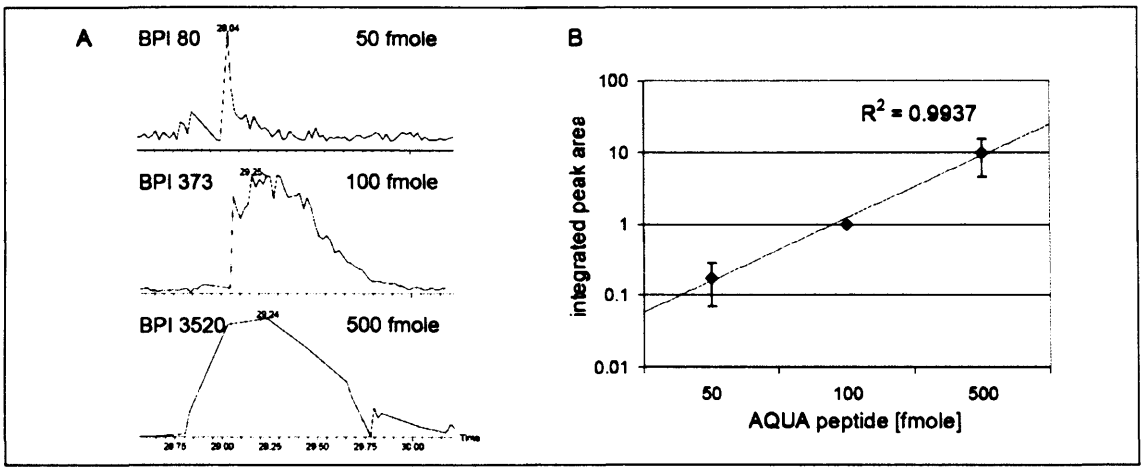

Figure 6.10: Integrated peak areas obtained by LC-ESI-MS of IS peptides are linear with respect to the amount of peptide analysed

(A) Detection of increasing ion counts by analysis of increasing amounts IS peptide amounts for IS peptide nr. 1 (p110α). (B) Average standard curve constructed by plotting the amount of IS peptide against the respective integrated peak areas.

Absolute quantitation of endogenous class IA PI3K subunits (step 3) is described in more detail below. In summary, the IS peptides were spiked to the protein samples (e.g. peptide number 1-4 in p110 samples) before trypsination and analysed by LC-MS or LC-MRM.

6.5.1 Class IA PI3K cannot be detected by MS when isolated from total cell lysate separated by SDS-PAGE

Absolute quantitation of proteins is most exact if least purification steps are involved during which the protein can be lost. We therefore aimed to perform AQUA MS with total cell lysate. To this end, total cell lysate of WEHI-231 cells was separated by SDS-PAGE, the protein stained by colloidal Coomassie blue, protein of M_r 110, 85, 55, and 50 kDa cut from the gel, reduced, spiked with IS peptides and trypsinised.

Since the sample capacity of the nanoLC column was less than 1 ng, saturation of the column was reached if digested protein from 2 mg total protein was applied to RP-LC. 2 mg total protein, however, did not allow for the detection of endogenous class IA PI3K peptide either by LC-MS or LC-MRM (data not shown).

6.5.2 IP of class IA PI3Ks prior to AQUA analysis allows for the sensitivity required for absolute protein quantitation by AQUA

Because PI3K quantitation by MS following SDS-PAGE separation of total cell lysate was not feasible with our instrumentation, we performed two different IP approaches to enrich for class IA PI3K isoforms by IP using either an Ab-mix to p85, or an Ab-mix to p85 and p110. Each IP was divided into 2 fractions containing 2/3 or 1/3

of the sample in order to assess for MS ionisation suppression effects (see below). The immunocomplexes were resolved by SDS-PAGE and the protein gel stained by colloidal Coomassie (Figure 6.11.A). In parallel, samples of TCL and SN were analysed for class IA PI3K isoforms by immunoblotting. This revealed that the majority of class IA PI3K was depleted from total cell lysate after each IP (Figure 6.11.B).

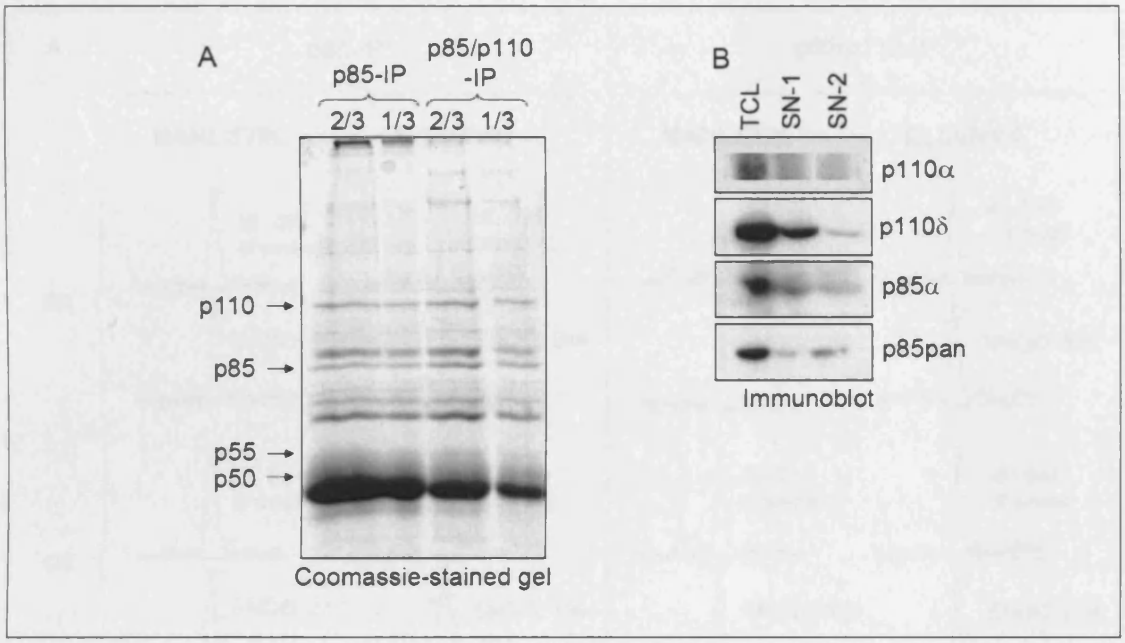

Figure 6.11: Enrichment of class IA PI3K subunits using 2 different approaches
Class IA PI3Ks were immunoprecipitated with an Ab-mix either to p85 (U2, U10, T12, T15) or to p85/p110 (U2, anti-p110α and -p110δ Ab). (A) Coomassie-stained gel of the IPs and M_r of class IA PI3K subunits. (B) TCL and IP-SN samples were analysed for class IA PI3K subunits by immunoblotting using isoform-specific Abs.

Peptide quantitation of endogenous p110δ after LC-MS is shown in Figure 6.12. The integrated peak areas of IS peptides nr. 4 and nr. 5 were compared to integrated peak areas of endogenous peptide for sample 2/3 and 1/3 of both IPs (Figure 6.12.A). In order to obtain mean values, the endogenous p110δ amounts in sample 2/3 and 1/3 calculated from known amounts of IS peptide were extrapolated to 1 (by multiplying with 1.5 and 3, respectively), and the average and SD of each experiment calculated (Figure 6.12.B). The endogenous, average p110δ amount was 2.9 +/- 0.37 pmole if Abs to p85 were used *versus* 3.6 +/- 0.44 pmole if Abs to p85/p110 were used. The lower p110δ amount detected in the p85-IP correlates with inferior depletion efficiency of p110δ as observed by immunoblotting (Figure 6.11.B).

Signals generated by ESI could possibly be suppressed by co-elution of several species from the LC column, thereby competing for ionisation. However, the integrated peak areas of 2 pmole IS peptide compared with endogenous peptide were similar in sample 2/3 and sample 1/3 (containing 66% and 33% of the IP, respectively). This

revealed that ionic intensities were not significantly affected by differences in protein amounts suggesting that signal suppression effects are negligible. Furthermore, calculated protein amounts of endogenous p110δ were similar if integrated peak areas of IS peptides nr. 4 and nr. 5 were compared. This suggests that the choice of p110δ peptide is not crucial for the determination of endogenous protein amounts.

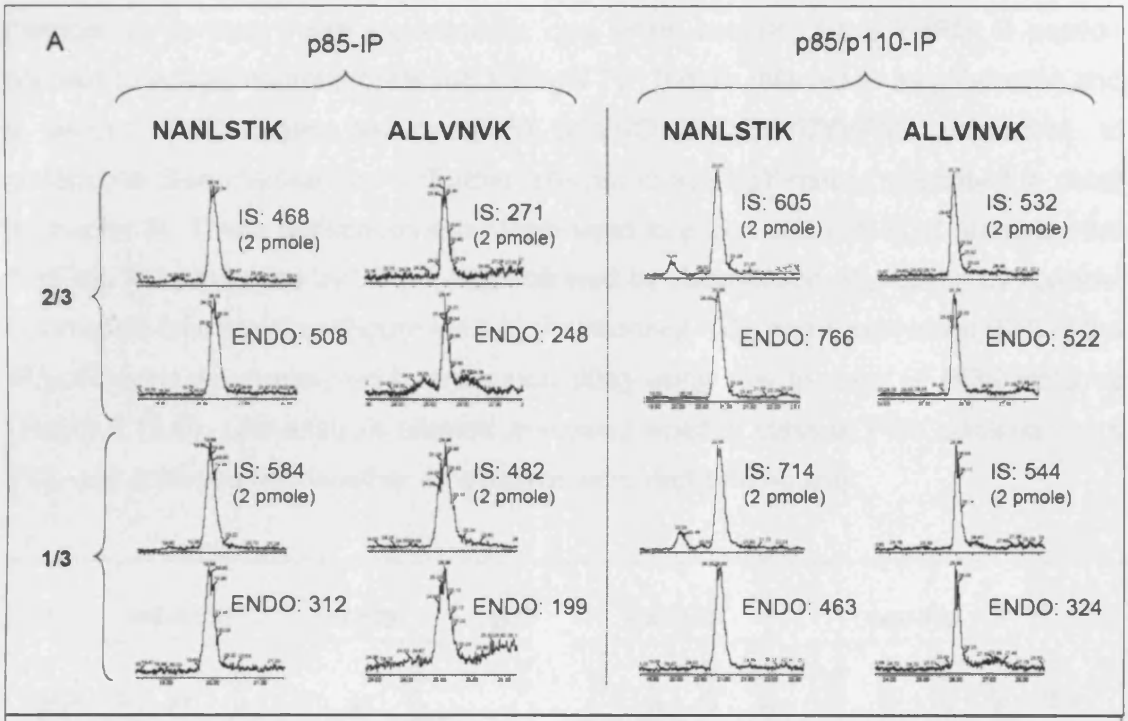

B

			NANLSTIK			ALLVNVK				
			counts	pmole	pmole/1	counts	pmole	pmole/1	average	stde
p85-IP	2/3	IS	468	2.00		271	2.00			
		ENDO	508	2.17	3.26	248	1.83	2.75		
	1/3	IS	584	2.00		482	2.00			
		ENDO	312	1.07	3.21	199	0.83	2.48	**2.92**	**0.37**
p85/ p110-IP	2/3	IS	605	2.00		532	2.00			
		ENDO	766	2.53	3.80	522	1.96	2.94		
	1/3	IS	714	2.00		544	2.00			
		ENDO	463	1.30	3.89	342	1.26	3.77	3.60	**0.44**

C

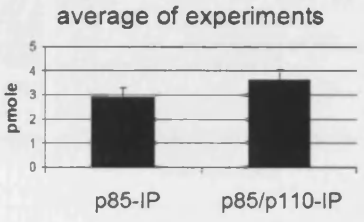

Figure 6.12: Absolute quantitation of p110δ from WEHI-231 cells

p110 protein samples of p85- or p85/p110-IP (Figure 6.11) were spiked with 2 pmole of all p110 IS peptides and analysed by LC-MS. (A) The LC-MS spectra and corresponding base peak intensities (BPI) of endogenous ($m/z_{NANLSTIK}$=430.75, $m/z_{ALLVNVK}$=378.75) and IS peptides nr. 4 and nr. 5 ($m/z_{NANLSTIK}$=434.25, $m/z_{ALLVNVK}$=382.25) were extracted by MassLynx Quantify software. (B) BPI values of endogenous p110δ peptide were compared to BPI values of IS peptides. This allowed for calculations of respective endogenous p110δ protein amounts in each sample. Extrapolation to 1 revealed the amount of endogenous p110δ protein in the IP before sample separation into 2/3 and 1/3. (C) The average amount of endogenous p110δ (plus SD) immunoprecipitated from WEHI-231 cells using p85-Abs or p85/p110-Abs is shown.

6.5.3 Absolute quantitation of class IA PI3K isoforms enriched from WEHI-231 and NIH-3T3 cells

We used two different affinity matrices for the isolation of class IA PI3K isoforms in order to eliminate artefacts in protein quantification due to protein enrichment. PI3Ks were either immunoprecipitated with a mix of isoform-specific Abs to the regulatory and catalytic subunits or pulled-down with the pTyr-matrix. We used two independent pTyr-matrices to perform these experiments: one which consist of the YVPMLG peptide coupled to Actigel matrix (containing a single Tyr; further referred to as pY-matrix) and a second GST-tagged peptide (GST-GG**Y**MDMSKDESVD**Y**VPML) absorbed to glutathione-*S*-sepharose matrix (further referred to as pYpY-matrix; described in detail in chapter 3). These purification tools were used to enrich class IA PI3K proteins from 7-15 mg TCL, resolved by SDS-PAGE followed by visualisation of proteins by colloidal Coomassie blue staining (Figure 6.13.A). Additionally, TCL and supernatant (SN) of the IP/pull-downs were analysed by immunoblotting using Abs to class IA PI3K isoforms (Figure 6.13.B). This analysis allowed assessing whether class IA PI3K depletion from TCL was achieved and whether all isoforms were depleted equally.

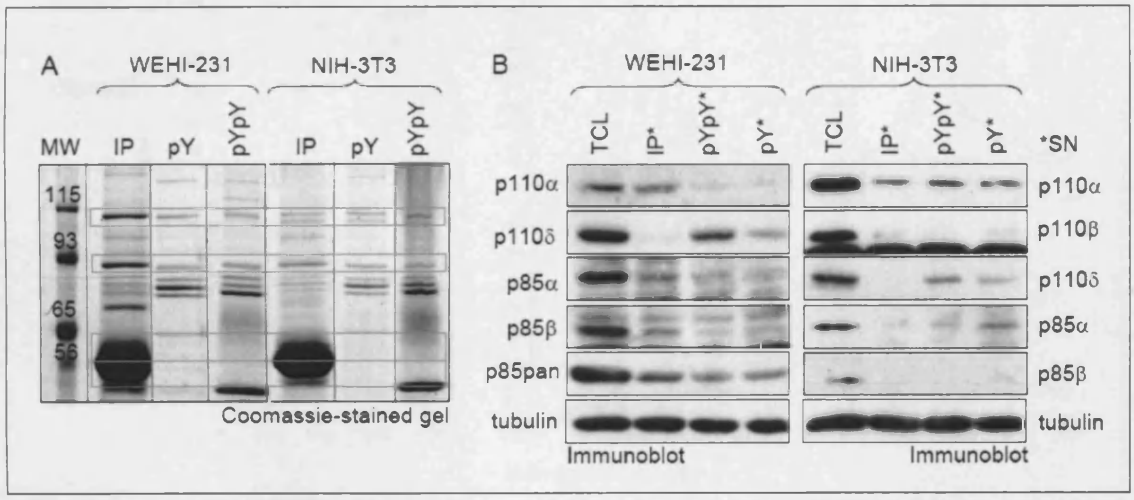

Figure 6.13: Enrichment of class IA PI3K isoforms by 3 different approaches from WEHI-231 and NIH-3T3 cells

(A) Class IA PI3Ks were purified from WEHI-231 or NIH-3T3 cells by affinity chromatography (IP using a mix of isoform-specific Abs or pull-down using pTyr-matrix containing 1 (pY) or 2 (pYpY) phosphorylated Tyr residues in a YxxM-motif). The complex was separated by SDS-PAGE and proteins visualized by colloidal Coomassie blue. Gel sections excised for further analysis are indicated by grey boxes. (B) Protein depletion was assessed by immunoblotting for class IA PI3K isoforms of total cell lysate (TCL) compared to supernatant (SN) following IP or pull-down.

Figure 6.14 shows integrated peak areas of 2 pmole IS peptides (dotted line) and endogenous peptides (solid line) immunoprecipitated from WEHI-231 or NIH-3T3 cells. While the protein amount of p110α was low in both leukocytes and fibroblasts, p110β protein levels were high in fibroblast and low in leukocytes. As expected, p110δ protein

expression was low in fibroblasts compared to leukocytes. The overall level of class IA PI3K regulatory subunit protein expression was similar in leukocytes and fibroblasts, with protein expression of p55α and p50α being undetectable (data not shown). Remarkably, p85β protein expression was higher than that of p85α, previously suggested to be the most abundant p85 isoform in most cell types (Ueki et al., 2002).

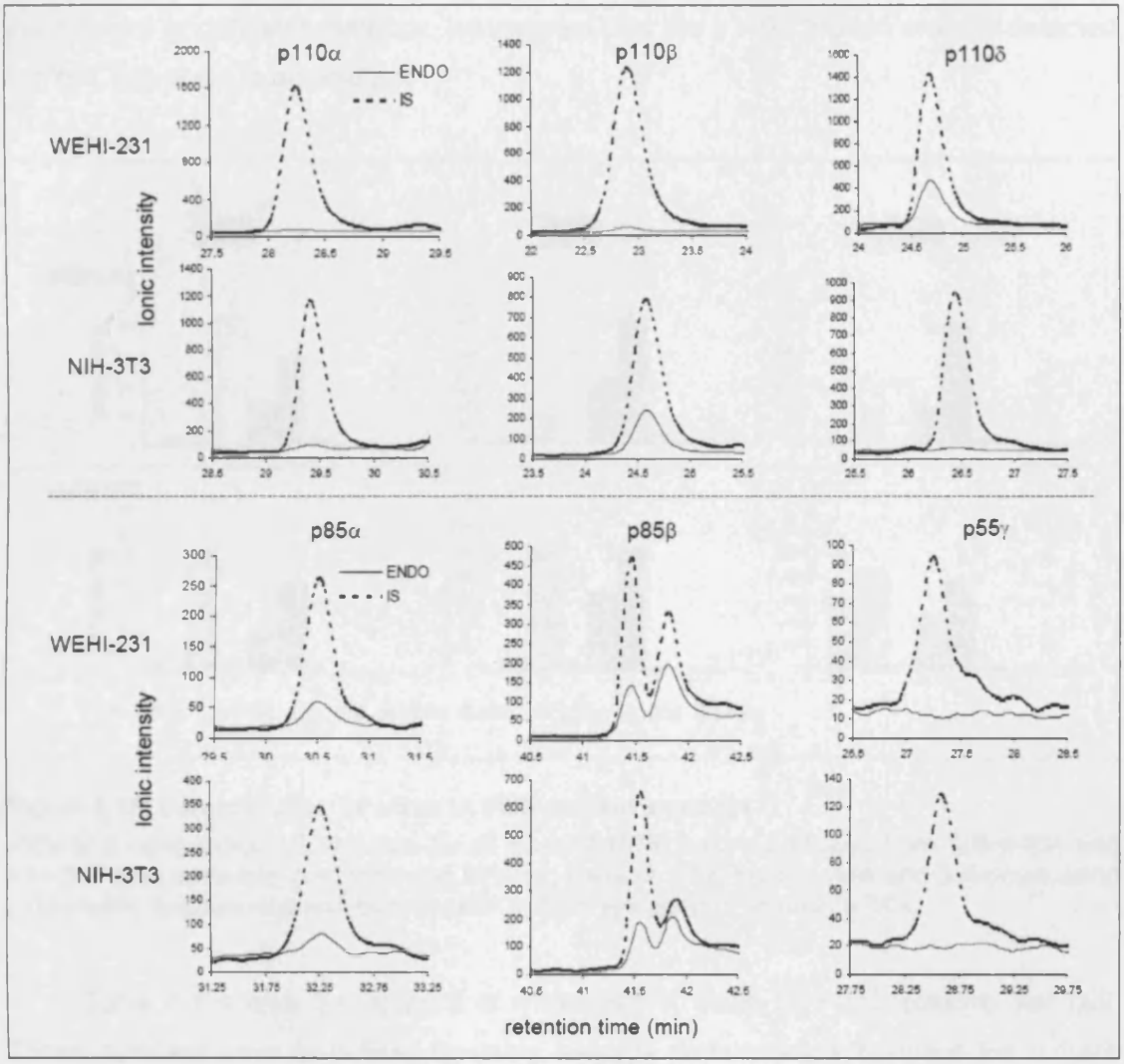

Figure 6.14: Extracted ion chromatograms (XIC) of class IA PI3K isoforms
Graphs depict XICs of endogenous (ENDO) and IS (IS, 2 pmole) peptides for all class IA PI3K isoforms immunoprecipitated from WEHI-231 and NIH-3T3 cells.

The integrated peak areas obtained from the 3 affinity chromatography experiments (IP, pY, pYpY) were processes and the concentration of each endogenous protein calculated in pmole/mg TCL (Figure 6.15). These analyses revealed that similar protein amounts were detected following IP and pull-down of WEHI-231 cells for p110α, p110β, p85α and p85β each, but the amounts differed for p110δ between IP and pull-down. This finding is in line with immunoblotting data shown in Figure 6.13.B

indicating that p110δ is not entirely depleted from WEHI-231 cells following pull-down using pTyr-matrices. In NIH-3T3 cells, similar protein amounts for each class IA PI3K isoform were detected following IP or pull-down, apart from p110α, which was 3 times more abundant following pYpY pull-down than following IP or pY pull-down (marked with an arrow in Figure 6.15). Since immunoblotting data shown in Figure 6.13.B do not reveal differences in p110α protein amounts in the SN following enrichment between the different enrichment methods, we suspect that the p110α protein amount detected in pYpY pull-down is an artefact.

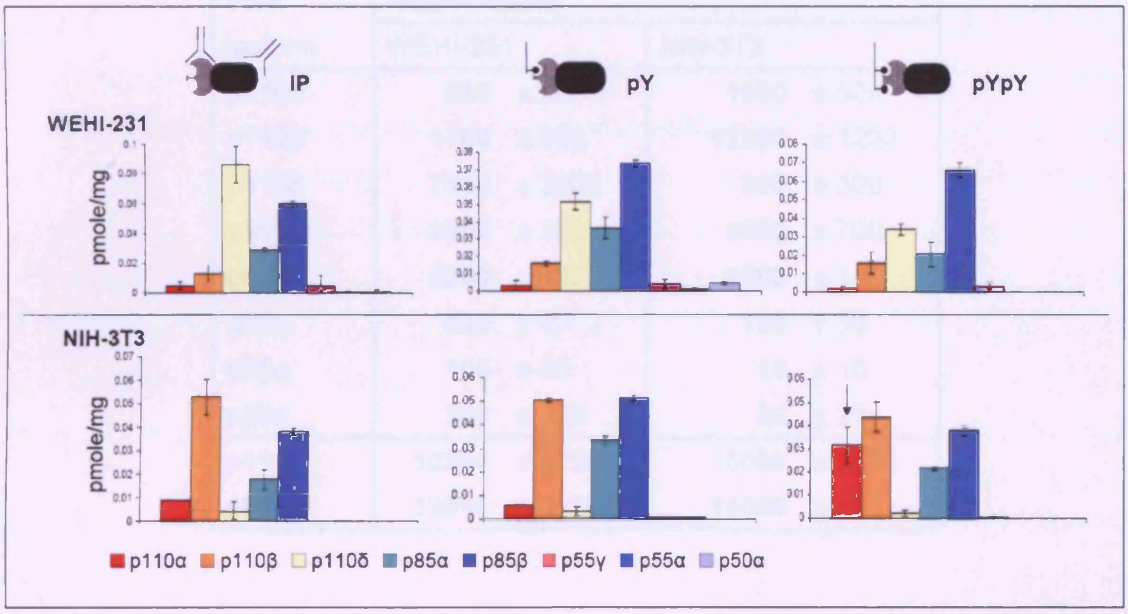

Figure 6.15: Determination of class IA PI3K protein amounts
XICs of 2 independent LC-MS runs for all class IA PI3K isoforms isolated from WEHI-231 and NIH-3T3 cells were analysed following IP using class IA PI3K specific Abs and pull-down using pTyr-matrix. Endogenous amounts of each isoform are given in pmole/mg TCL.

Table 6.2 shows the amount of molecules of class IA PI3K isoforms per cell. These numbers were calculated by using average protein amounts minus the outliers for p110α and p110δ obtained following the 3 enrichment methods. A standard curve of WEHI-231/NIH-3T3 cells per volume lysis buffer was used to determine how much TCL (in mg) was obtained from a certain number of cells (data not shown). This analysis revealed that WEHI-231 and NIH-3T3 cells overall express very similar numbers of class IA PI3K isoform, namely approximately 25,000 molecules of p110 and p85/cell. In addition, the total of all catalytic subunits matches the total of all regulatory subunits, indicating that there is no excess of p85 in the cell lines used here. p110α protein expression was low in both cell lines (below 2,000 molecules/cell), compared to p110β (12,300 and 1,700 molecules/cell in NIH-3T3 and WEHI-231, respectively) and p110δ (800 and 7,900 molecules/cell in NIH-3T3 and WEHI-231, respectively). The amount of

p85β (approximately 9,000 molecules/cell) was more than double that of p85α (4,000 molecules/cell), while p55γ, p55α, p50α protein expression is below 500 molecules/cell in these cell lines.

Table 6.2: Average class IA PI3K protein amounts in WEHI-231 and NIH-3T3 cells
An average amount of class IA PI3K molecules/cell was calculated by using the values of each enrichment method shown in Figure 6.16. The sum of all catalytic and regulatory subunit protein amounts are shown at the bottom.

PI3K isoform	Molecules/cell	
	WEHI-231	NIH-3T3
p110α	**620** ± 20	**1900** ± 500
p110β	**1700** ± 300	**12300** ± 1200
p110δ	**7900** ± 2900	**800** ± 300
p85α	**3900** ± 600	**5000** ± 700
p85β	**8000** ± 1200	**9500** ± 100
p55γ	**530** ± 60	**100** ± 50
p55α	**100** ± 50	**10** ± 10
p50α	**300** ± 300	**30** ± 20
p110	**10300** ± 3220	**15000** ± 2000
p85	**12900** ± 2210	**14000** ± 880

6.6 Discussion

Over the last couple of years, a vast literature on the existence of free p85 has appeared, mainly in an attempt to explain the increase in PI3K signalling upon insulin stimulation observed in mice in which class IA regulatory subunits have been deleted. In the proposed model, free p85 in WT cells competes with heterodimeric p85-p110 for docking sites on Tyr phosphorylated IRS molecules. Thus, monomeric p85 was put forward as a negative regulator in the PI3K signalling pathway.

Various data have cast doubts on this model:

1) Monomeric p85 seems to be unstable. A recent study addressing the phenotype of p110$\alpha^{+/-}$/p110$\beta^{+/-}$ mice revealed that heterozygous loss of p110α and p110β leads to a decrease in the protein expression of the regulatory subunit (Brachmann et al., 2005). These findings were confirmed by RNAi experiments, in which a loss of p110 protein caused instability of the p85 protein. In addition, pulse-chase experiments of cells transfected with p85 or p85-p110 revealed a 3-fold higher

degradation rate of free p85 compared to its heterodimeric counterpart (Brachmann et al., 2005).

2) Monomeric p85 does not necessarily compete with p85-p110 for pTyr docking sites. p85α overexpression in muscle cells correlates with a decrease in *in vitro* lipid kinase activity compared to non-transfected cells (Ueki et al., 2000). This experiment helped to establish the hypothesis that free p85 might oust p85-p110 heterodimer from pTyr binding sites. However, further investigations have shown that an excess of p85 over p110 does not always impact on PI3K lipid kinase activity. Thus, in p85α-deficient brown adipose cells reconstituted with p85α, a 4-fold excess of p85 over p110 does not reduce the *in vitro* lipid kinase activity in pTyr-IPs, compared to p85α KO cells reconstituted with similar p85α to p110 protein levels (Ueki et al., 2003). Furthermore, the *in vitro* lipid kinase activity of pTyr immunoprecipitated PI3K was similar in WT and $p85\alpha^{+/-}$ MEF cells, despite an allegedly 40% excess of p85 over p110 in WT cells (Ueki et al., 2002). Also no difference in the *in vitro* lipid kinase activity of pTyr immunoprecipitated PI3K was observed when WT brown adipose cells were compared to $p85\beta^{-/-}$ cells, which were shown to contain a 30% decrease in monomeric p85 compared to WT cells (Ueki et al., 2002). Unfortunately, the experiment which would resolve matters has not been presented yet: Comparison of the p110 and p85 protein amount in pTyr immunoprecipitates of WT versus $p85^{+/-}$ cells. This should result in reduced levels of p110 protein in pull-downs of WT compared to $p85\alpha^{+/-}$ cells if monomeric p85α exists and competes for pTyr docking sites.

3) The PI3K signalling pathway is skewed in p85 gene-targeted mice. Analysis of PI3K protein expression levels revealed that homozygous or heterozygous loss of the regulatory subunit leads to concomitant distortion of the p110 and untargeted p85 protein expression (Fruman et al., 2000; Fruman et al., 1999; Suzuki et al., 1999; Terauchi et al., 1999). Furthermore, PTEN expression is increased in murine cells of $p85\alpha^{+/-}$ origin (Ueki et al., 2002), and IRS-2 phosphorylation is enhanced in cells deficient of p55α/p50α and p85β (Chen et al., 2004; Ueki et al., 2003). These finding indicate that in insulin-responsive cells, deletion of p85 leads to many "knock-on" effects which likely impact on PI3K signalling.

Despite the challenges described above to the hypothetical model of free p85 in insulin-responsive cells, it is emerging that p85α protein expression can be increased by several chemical agents in these cells, correlating with a reduction in PI3K activity. Thus, the corticosteroid dexamethasone induces p85α protein expression due to an increase in p85α mRNA in cultured muscle cells (Giorgino et al., 1997). Treatment of these cells with dexamethasone concomitantly reduces IRS-1 protein expression and PI3K lipid kinase activity. Similar observations were made when WT skeletal muscle

cells were compared to skeletal muscle cells of p85α KO mice following growth hormone (GH) treatment (Barbour et al., 2005). GH treatment induces p85α protein expression levels in WT cells compared to untreated control, while p85α protein levels remain low in $p85\alpha^{+/-}$ cells. In this system ($[p85\alpha]_{WT+GH}$> $[p85\alpha]_{WT}$ > $[p85\alpha]_{HET}$), the *in vitro* lipid kinase activity of PI3K associated with IRS-1 decreases in WT cells stimulated with growth hormones compared to unstimulated WT cells, but increases in $p85\alpha^{+/-}$ cells. Furthermore, overexpression of the cellular retinol-binding protein-1 (CRBP-1) appears to decrease PI3K activity by inducing dissociation of p85 and p110 (Farias et al., 2005). However, in order to draw conclusions about the existence of free p85, the expression levels of all catalytic subunits and IRS/adaptor molecules have to be analysed.

Because of the controversial data published on the p85 to p110 ratio, we performed different biochemical analyses in order to investigate whether monomeric p85 exists in murine WT fibroblasts and leukocytes.

Since the concept of monomeric p85 in WT cells of insulin-responsive tissue is primarily based on immunodepletion experiments (Ueki et al., 2002), we analysed by immunoblotting PI3K protein amounts of fibroblasts and leukocytes before and after sequential IP. This analysis did not reveal an excess of one subunit over the other. We frequently observed minor differences between depletion of catalytic subunit and regulatory subunit, however, these laid within the coefficient of variation of the method.

Under native conditions, monomeric p85 is expected to have different biophysical characteristics than p110-bound p85. In ion exchange chromatography, separation of molecules is based on differences in their charge characteristics. Thus, monomeric p85 is expected to elute at different ionic strength than p110-bound p85 from ion exchange chromatography. To formerly address this assumption, the protein lysates of HEK-293T cells overexpressing p85α or p85α-p110α were analysed by ion exchange chromatography. Indeed, p85α overexpressed in HEK-293T cells eluted from the column at higher salt concentrations than p85α co-expressed with p110α. Subsequent analysis of endogenous class IA PI3K isoforms from WEHI-231 cells revealed that all PI3K isoforms elute in the same fractions suggesting that they do not possess monomeric p85. We have not addressed by ion exchange chromatography whether monomeric p110 exists for two reasons. First, monomeric catalytic subunit is believed to be thermally labile (Yu et al., 1998) and therefore non-existent. Second, transient overexpression of p110 in HEK-293T cells was not successful (§ 5.11), probably due to instability of monomeric p110 (Yu et al., 1998) or its toxic effect on cells (Yip et al., 2004).

A variety of MS strategies for the quantitation of protein expression levels in cells have been developed. However, the majority of these methods only allow for relative quantitation of expressed protein. The stable isotope labelling by amino acids in cell culture (SILAC) approach allows for *in vivo* incorporation of isotopically labelled amino acids into proteins. This method enables large-scale relative protein and post-translational modifications quantitation of cell culture cells, but not primary tissues (Ong et al., 2002). Another variation of the stable isotope quantitation methods, which can also be employed for primary tissue samples, is the isotope coded affinity tag (ICAT) method (Gygi et al., 1999). In this post-harvesting approach, proteins are isotopically labelled with chemicals that covalently bind to cysteine residues. Peak area measurements with an internal standard (PAIS) allows for protein quantitation between different samples without metabolic labelling by comparison of endogenous peptides with an internal standard added to the samples before protein digestion (Cutillas et al., 2005). However, all these methods only allow for relative quantitation of expressed proteins. In order to quantify the absolute protein amounts of class IA PI3K isoforms, we used the absolute quantification (AQUA) MS strategy (Gerber et al., 2003; Kirkpatrick et al., 2005). The AQUA method is based on the use of an isotope labelled IS that is spiked at known concentrations to cell samples. This IS peptide mimics an endogenous peptide of the target protein, except that it is enriched in stable isotopes. Analysis of the proteolysed sample by MS results in the detection and quantitation of both the endogenous peptide and isotope-labelled IS peptide.

11 IS peptides with equivalent sequences to class IA PI3K isoform peptides were validated using different MS approaches. We determined the detection limit of the peptides in our instrumentation, their elution times from RP chromatography columns, and ruled out ionisation suppression by endogenous peptides. Furthermore, equal endogenous protein amounts were compared with different IS peptides to the respective protein (if applicable). This confirmed the independence of the IS peptide sequence for absolute quantitation of endogenous protein.

AQUA analysis of class IA PI3Ks was not feasible with protein of whole cell lysate due to the low abundance of these proteins. We therefore investigated the absolute PI3K protein amounts following IP and pull-down using pTyr-matrices. Although not ideal because of protein loss during enrichment, the depletion of each isoform was monitored by immunoblotting and optimal conditions for protein enrichment established in order to ensure that all class IA PI3K are equally enriched.

The analysis of endogenous class IA PI3K isoforms by AQUA revealed similar amounts of class IA PI3K in NIH-3T3 and WEHI-231 cells, amounting to approximately 25,000 molecules/cell. In addition, the total of all catalytic subunits matches the total of all regulatory subunits, indicating that there is no excess of p85 in the cell lines used

here. p110α protein expression was surprisingly low in both cell lines (below 2,000 molecules/cell), compared to p110β (12,300 and 1,700 molecules/cell in NIH-3T3 and WEHI-231, respectively) and p110δ (800 and 7,900 molecules/cell in NIH-3T3 and WEHI-231, respectively). Remarkably, the amount of p85β (approximately 9,000 molecules/cell) was more than double that of p85α (4,000 molecules/cell), indicate that p85β is the most prevailing regulatory subunit in the two cell lines tested, contrary to previous reports in MEFs (Ueki et al., 2002). p55γ, p55α, p50α protein expression is below 500 molecules/cell in these cell lines.

Since our data presented in this chapter do not support the existence of an excess of p85 over p110, we would like to present an alternative model to the existence of monomeric p85 that could explain an increase in PI3K activity of insulin-responsive cells in p85-KO mice. First, we discuss how PI3K activity might be modified *in vivo*. An increase in endogenous PIP_3 concentration as observed in p85 KO cells could be mediated by an increase in class IA PI3K activity or a decrease in the activity of PTEN/SHIP. Changes in the net activity of these molecules could be due to

1) alterations in the protein concentration of class IA PI3K or PTEN/SHIP. Indeed, the protein expression levels of the different class IA PI3K (Chen et al., 2004; Fruman et al., 2000; Terauchi et al., 1999; Ueki et al., 2002) and PTEN (Ueki et al., 2002) are modulated in p85 KO cells. In p85α-KO mice, p110 protein levels are decreased suggesting a *decrease* in PI3K activity. In addition, non-targeted p85 protein expression levels are increased. However, this rise in p85 protein does not seem to compensate for the loss of p85 protein due to gene manipulation as determined by immunoblotting using p85pan Abs (Ueki et al., 2002). Furthermore, PTEN protein expression was shown to be increased in $p85\alpha^{+/-}$ cells, while SHIP expression was unchanged (Ueki et al., 2002). These findings would also indicate a *decrease* in PI3K signalling. Furthermore, in p85-KO mice PI3K activity in cells of insulin-sensitive tissue increases following insulin stimulation, whereas PI3K activity decreases in B and T cells following stimulation of B- and T cell receptor, respectively (Fruman et al., 1999; Suzuki et al., 1999). These findings suggest that it is not the concentration of total p85 which is crucial for the observed changes in PI3K activity.

2) modulations in the intrinsic activity of class IA PI3K or PTEN/SHIP, e.g. PI3K activity could be enhanced by a decrease in Ser phosphorylation or an increase in Ras binding or SHIP activity could be decreased by Tyr phosphorylation (Habib et al., 1998). The intrinsic PI3K lipid kinase activity measured following IP using either Abs to pTyr or p110 are *decreased* in $p85\alpha^{-/-}$ and $p55\alpha/p50\alpha^{-/-}$ cells (Chen et al., 2004; Terauchi et al., 1999; Ueki et al., 2002). PTEN or SHIP activity has not been studied.

3) changes in the subcellular localisation of the lipid kinase or phosphatase, e.g. by an increase in IRS phosphorylation or membrane recruitment of monomeric p110 or of PTEN/SHIP. Indeed, Tyr phosphorylation of IRS-2 seems to be enhanced by deletion of p85 (Chen et al., 2004; Ueki et al., 2002), possibly allowing for increased amounts of PI3K to be recruited to the plasma membrane and to be activated. Although *in vitro* lipid kinase assays following IRS-2 IP revealed enhanced PI3K activity, the increase is not enough to impact on total lipid kinase activity following pTyr IP.

In summary, these findings indicate that the phenotypes observed in p85-deficient cells of insulin-sensitive tissue are probably not mediated by changes in protein concentrations of PI3K or PTEN/SHIP or by changes in the intrinsic PI3K activity. Thus, the increase in PIP_3 production in p85 KO cells could be due to an increase in PTEN/SHIP activity or to membrane recruitment of monomeric p110 or PTEN/SHIP. Since monomeric p110 seems to be unstable (Yu et al., 1998), we present a hypothetical model explaining an increase in PIP_3 concentration in p85 KO cells independent of class IA PI3K.

In p85-KO mice, IRS phosphorylation in cells of insulin-sensitive tissues is unchanged or mildly increased (Chen et al., 2004; Ueki et al., 2002). It is likely that less regulatory and catalytic subunit binds to phosphorylated IRS following cellular stimulation in p85 KO cells, because less p85 exists. Thus, other molecules, which usually do not associate with IRS due to lower binding affinities compared to p85, might engage with IRS. The janus kinase JAK and lipid phosphatase SHIP are such candidates, since they both possess SH2 domains (Al/lazikani, 2001). JAKs have been shown to interact with and phosphorylate IRS-1 (Wang et al., 1997) and SHIP (Giallourakis et al., 2000). Interaction of JAK with IRS might therefore lead to the observed increase in IRS phosphorylation in p85-KO mice. Interaction of JAK with SHIP could further lead to phosphorylation and inactivation of SHIP (Habib et al., 1998) mediating an increase in PIP_3 concentration.

In hematopoietic cells, JAK activation seems to be independent of IRS (Uddin et al., 1997), possibly explaining why p85 deletion in insulin-responsive cells leads to an increase in PI3K activation while p85-deficient B and T cells have decreased PI3K signalling.

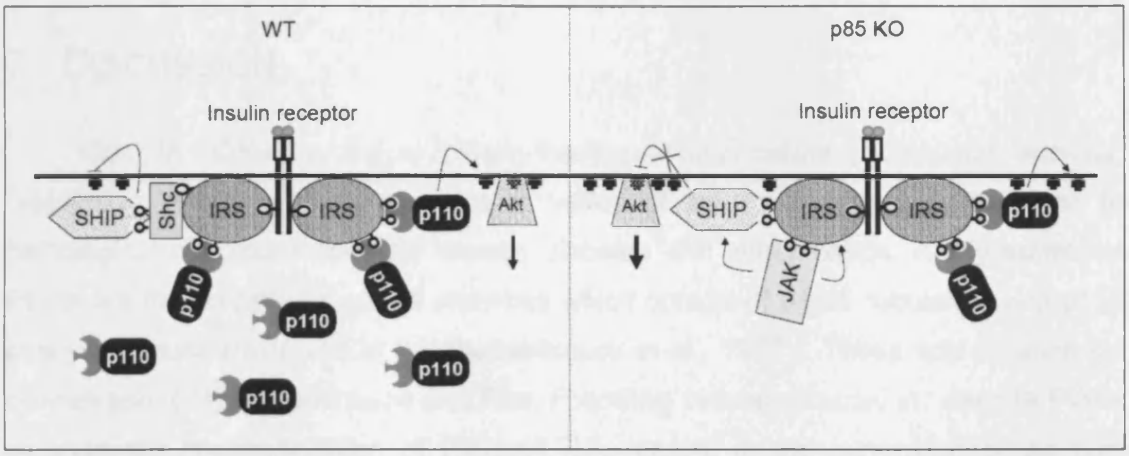

Figure 6.16. Hypothetical model explaining increased PI3K signalling in p85 KO cells
Following insulin receptor stimulation, IRS molecules are phosphorylated on Tyr residues. This allows for recruitment of p85-p110 to the plasma membrane in WT cells, but also of Shc, which can further recruit SHIP. While PI3Ks generate PIP_3 leading to Akt recruitment and activation, SHIP reduces PIP_3 levels. In p85 KO cells, less p85-p110 will bind to phosphorylated IRS molecules, leaving access for JAK and SHIP. JAK possibly phosphorylates SHIP, thereby inactivating its catalytic activity leading to an increase in PIP_3.

In summary, we have thoroughly investigated the molecular ratio between the regulatory and catalytic subunit of class IA PI3K using different biochemical approaches. Performing these analyses, we did not find any evidence for monomeric p85 therefore concluding that class IA PI3K activity is not regulated by free p85. However, we propose an alternative model in which the PI-phosphatase SHIP takes a central role.

7 DISCUSSION

Class IA PI3Ks play critical roles in the regulation of cellular proliferation, survival, metabolism and migration. Aberrant activation of the PI3K pathway contributes to pathological conditions such as cancer, diabetes and inflammation. A key subset of PI3Ks are the so-called class IA enzymes which consist of a p85 regulatory and p110 catalytic subunit (reviewed in (Vanhaesebroeck et al., 1997)). These lipid kinases act downstream of tyrosine kinases and Ras. Following cellular stimulation, class IA PI3Ks catalyse the phosphorylation of PtdIns(4,5)P_2 leading to the generation of the lipid second messenger PIP_3 (Hawkins et al., 1992). A variety of proteins can bind to PIP_3 and membrane association of these proteins often leads to changes in their catalytic activity (Musacchio et al., 1993). One important downstream effector of class IA PI3K is the protein kinase Akt (reviewed in (Brazil and Hemmings, 2001)).

The regulation of class IA PI3Ks is complex. In unstimulated cells, class IA PI3K heterodimers appear to reside in the cytosol. The regulatory subunit stabilises the thermally labile p110 protein, but also inhibits PI3K lipid kinase activity (Yu et al., 1998). The activity of class IA PI3Ks can be *enhanced* by

1) membrane recruitment of the catalytic subunit. Genetic modifications of p110 with membrane-targeting domains that induce constitutive membrane association leads to constitutively enhanced PIP_3 levels in transfected cells (Aoki et al., 2000; Auger et al., 2000; Didichenko et al., 1996; Reif et al., 1996).

2) interaction of the p85 SH2 domains with pTyr residues in YxxM-containing proteins such as receptor tyrosine kinases or adaptor molecules (Rordorf-Nikolic et al., 1995). Evidence has been presented that binding of the N-terminal SH2 domain of p85α to pYxxM-motifs, but not the binding of the C-terminal SH2 domain, is responsible for the rise in PI3K activity (Yu et al., 1998).

3) interaction of the catalytic subunit with Ras or nuclear protein PIKE, and interaction of p110β with Gβγ subunits of trimeric G proteins (Kurosu et al., 1997; Rodriguez-Viciana et al., 1994; Rodriguez-Viciana et al., 1996; Rong et al., 2003).

4) dissociation of the catalytic from the regulatory subunit. The lipid kinase activity of monomeric p110 purified from bovine thymi is increased compared to the activity of heterodimeric p85-p110 (Shibasaki et al., 1991). Similarly, the lipid kinase activity of recombinant p110α is decreased by *in vitro* reconstitution with recombinant p85α (Yu et al., 1998).

The enzymatic activity of class IA PI3K can be *decreased* by autophosphorylation of p110β or p110δ on Ser residues located in the C-terminus of the catalytic domain (Czupalla et al., 2003; Vanhaesebroeck et al., 1999). Furthermore,

transphosphorylation of Ser608 in p85α by p110α leads to the downregulation of p110α lipid kinase activity (Dhand et al., 1994; Foukas et al., 2004). Interaction of the regulatory subunit p85α with the adaptor protein Ruk also seems to reduce the intrinsic lipid kinase activity of PI3K (Gout et al., 2000). In addition, monomeric p85 has been implicated as a negative regulator in PI3K signalling (Luo and Cantley, 2005).

In this study, we focused on two aspects of PI3K regulation:

1) the role of known and novel post-translational modifications in the regulation of endogenous class IA PI3K activity, especially of the p110δ subunit. The established immature B cell line WEHI-231, which expresses all class IA PI3K isoforms, was used as a main model system. The aim was to separate extracts of these B cells by 2D-gel electrophoresis and to subsequently identify the modifications in class IA PI3K isoforms by MS. The biological relevance of the identified modifications would then be analysed using biochemical approaches. We used a cell-based assay, in-house Abs as well as a new class IA PI3K purification tool ('pTyr-matrix') to obtain sufficient amounts of PI3K for MS analysis.

2) the molar ratio between the regulatory and catalytic subunit. The ratio between class IA PI3K catalytic and regulatory subunit was analysed using affinity and ion exchange chromatography and absolute quantitation (AQUA) MS. The assessment of the molarity of class IA PI3K regulatory and catalytic subunit is relevant since an excess of p85 protein has been implicated in the negative regulation of PI3K activity (Luo and Cantley, 2005; Ueki et al., 2002).

Below, we first discuss the generation of the pTyr-matrix (§ 7.1), followed by an examination of post-translational modifications in the class IA PI3K p85 regulatory subunit (§ 7.2) and p110δ catalytic isoform (§ 7.3). Potential novel interaction partners of p85-p110δ detected in the course of these investigations are discussed in § 7.4. In § 7.5, we discuss our findings of equimolarity between class IA PI3K regulatory and catalytic subunit and finally in § 7.6, we provide conclusions and discuss potential future experiments.

7.1 Generation of a novel pTyr-matrix to enrich for class IA PI3K proteins

In order to identify proteins and post-translational modifications by peptide sequencing using MS, more than 100 ng target protein is required. This prerequisite not only necessitates cellular systems producing large amounts of proteins, but also efficient protein purification tools.

In our laboratory, a variety of home-made Abs to PI3K and synthetic PDGF-receptor peptides coupled to Actigel (Fry et al., 1992) were available for the enrichment

of class IA PI3K. While the use of some of these Abs was restricted by availability, others did not allow for high purity of immunocomplexes due to the association of the Ab with several proteins. Furthermore, preliminary results obtained by incubation of cell lysate with the synthetic PDGF-receptor matrix that is made of 6 amino acids (pYVPMLG, containing Y571) linked to Actigel did not reveal enrichment of pure or large quantities of class IA PI3K.

We therefore designed three PDGF-receptor peptides of different lengths, all containing Y751 with or without Y740. Residues Y751 and Y740 are both located in YxxM-motifs of the human PDGF-β-receptor (Klinghoffer et al., 1996). DNA constructs encoding these peptides were cloned into pGEX-4T-2 (AMERSHAM PHARMACIA BIOTECH), a plasmid containing the GST gene under the control of an inducible promoter (Figure 3.2). These plasmids were subsequently transformed into *E. coli* strain TKB1 that contains an inducible Tyr kinase gene (STRATAGENE). Following gene induction and phosphorylation of Tyr residues in the constructs by incubation of *E. coli* with the inducer IPTG, bacterial extracts were incubated with glutathione-bound sepharose in order to immobilise the GST-peptide complex. Class IA PI3Ks present in eukaryotic cell lysate was expected to be enriched by interaction of its SH2 domains with pY751 and/or pY740 of this so-called pTyr-matrix.

Successful cloning of the GST-PDGF-receptor peptide constructs and transformation into *E. coli* was confirmed by gel electrophoresis of PCR products (Figure 3.2), restriction digestion and DNA sequencing of purified plasmids. Expression of the GST-PDGF-receptor peptide constructs in TKB1 following promoter induction was assessed by SDS-PAGE and protein detection by colloidal Coomassie. This analysis revealed that expression of all 3 GST-PDGF-receptor peptides was highly induced (Figure 3.4). Immunoblotting of bacterial extract using pTyr Abs revealed a more than 5-fold increase in Tyr phosphorylation of the GST-PDGF-receptor peptides following gene induction (Figure 3.4). We further assessed the binding capacity of sepharose beads to the GST-PDGF-receptor peptides by titration experiments (Figure 3.5) and analysed the amount of pTyr-matrix required to bind p110δ (Figure 3.6). These analyses revealed that GST-PDGF-receptor peptides contained in 1 mg bacterial lysate was sufficient to saturate 500 µl glutathione sepharose matrix and that this amount of pTyr-matrix could bind the majority of p110δ present in 5 mg WEHI-231 cell extract.

Assessment of eukaryotic proteins pulled-down by the pTyr-matrix using SDS-PAGE and Coomassie staining revealed 4 major protein bands. Analysis of these bands by LC-MS/MS revealed enrichment of p110β, p110δ at M_r of 110 kDa, and p85α and p85β at M_r of 85 kDa (Figure 3.7). p110α, p55γ, p55α, and p50α could not be

detected by MS probably due to low protein expression levels in WEHI-231 cells (see also § 4.7.1). However, p110α could be detected by p110α-specific Abs in pull-downs using the pTyr-matrix (data not shown, Figure 6.5). Furthermore, Hsp70 and Elongation factor-1γ were identified by MS as the protein bands resolved at M_r of 70 and 45 kDa. The latter proteins were also detected in pull-downs with sepharose matrix only, indicating that these proteins bound non-specifically to the matrix.

In our hands, this pTyr-matrix proved to be more efficient than the synthetic PDGF-receptor peptide coupled to Actigel. This might be due to the different lengths of constructs or to the different characteristic of the linker region between PDGF-receptor peptide and glutathione sepharose (GST-protein) and synthetic PDGF-receptor peptide and Actigel (5-atom spacer). Furthermore, pTyr-matrix is cheaper than synthetic peptides plus Actigel. The advantage of this class IA PI3K purification tool over Abs lies in its potential capacity to interact with all regulatory subunits similarily and thus to enrich for all class IA PI3K isoforms simultanously.

In summary, the pTyr-matrix provided an enrichment method independent of IP and we successfully applied it for the enrichment of class IA PI3Ks in several projects of this thesis.

7.2 Class IA PI3K activity is not controlled by modifications of p85α following BCR stimulation of WEHI-231 cells

The five class IA PI3K regulatory subunits (p85α, p85β, p55γ, p55α, p50α) are generated by 3 independent genes (*PIK3R1*, *PIK3R2*, *PIK3R3*) and alternative splicing or differential promoter usage of *PIK3R1* (Abell et al., 2005). These proteins contain various protein-protein interaction domains, such as SH2, p110-binding and proline-rich domains and in case of p85α and p85β also a BH/Rac-binding and SH3 domain. The biological role of p85 likely lies in the modulation of PI3K activity by altering protein partner associations. Modifications of class IA PI3K regulatory subunit are therefore expected to impact on binding affinities between the regulatory subunit and protein partners and thus to impact on p110 catalytic activity.

Indeed, phosphorylation of Y508 of p85α in fibroblasts following PDGF receptor engagement leads to the dissociation of p85α from the receptor (Kavanaugh et al., 1994). Phosphorylation of Y688 by Lck or Abl does not induce changes in the *in vitro* lipid kinase activity of PI3K, but leads to alterations in the interaction of p85 with binding partners (von Willebrand et al., 1998). This likely enhances total PI3K lipid kinase activity as determined by an increase in Akt phosphorylation of Cos-7 cells transfected with p85α Y688D mutant compared to WT p85α (Cuevas et al., 2001). In

addition, nitration of Tyr residues in p85α following peroxynitrite treatment of macrophages seems to abrogate the interaction of p85 with the catalytic subunit (Hellberg et al., 1998). Treatment of endothelial cells with high doses of glucose and peroxynitrite has also been shown to induce Tyr nitration of p85, correlating with p85 dissociation from p110 (al-Shami et al., 1997).

As described in Chapter 4 and discussed below, the analysis of modifications in class IA PI3K regulatory subunits by 2D-gel electrophoresis and MS revealed that p85α is extensively modified in non-BCR stimulated, but proliferating WEHI-231 B cells. The observed modifications on 2D-gels might be due to protein phosphorylation, hydroxylation and amino acid substitutions as identified by MS. These modifications do not seem to be dynamic or of high stoichiometry since stimulation of WEHI-231 cells via BCR did not induce significant changes in these modifications.

7.2.1 Class IA PI3K regulatory subunit modifications in unstimulated immature B cells

Analysis of WEHI-231 cell extracts by 2D-gel electrophoresis revealed that the p85 regulatory subunit is extensively modified in unstimulated, but proliferating WEHI-231 cells, in agreement with investigations in murine fibroblasts (Cohen et al., 1990) (modifications identified by us using MS are shown in Figure 7.1). Evidence for modifications were primarily observed in p85α following immunoblotting using p85α isoform-specific Abs or following MS analysis (Figure 4.1, Figure 4.12, Figure 4.13). Due to a lack of good Abs to p85β, no conclusions on modifications in this regulatory subunit could be made.

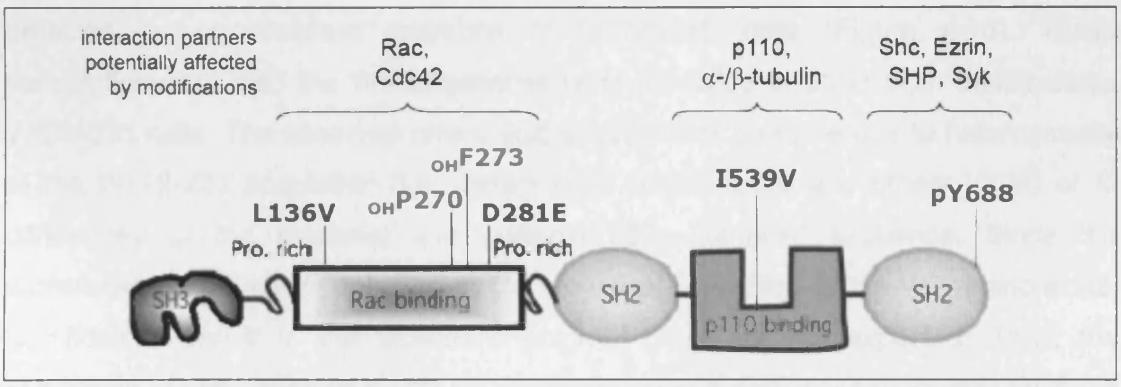

Figure 7.1: Summary of modifications identified by LC-MS/MS in p85α and their potential effect on protein-protein interactions

Immunoprecipitated p85α was analysed by LC-MS/MS for protein modifications. Identified modifications are depicted and potential effects on protein-protein interactions indicated.

The modifications detected following 2D-PAGE of WEHI-231 cells are partially due to phosphorylation. This was determined by immunoblotting analysis of *in vitro*

dephosphorylated (using alkaline phosphatase) p85 immunoprecipitates. Indeed, some basic p85 spots appeared following dephosphorylation (Figure 4.3). This finding is in agreement with indications of Thr phosphorylation of immunoprecipitated p85 by immunoblotting using phospho-specific Abs (Figure 4.2) and with the identification of the known p85α Tyr688 phosphorylation site by LC-MRM in unstimulated WEHI-231 B cells (Figure 4.12). Unfortunately, detailed MS analysis of peptides derived from the regulatory subunit only provided indications for novel potentially phosphorylated amino acid residues (Table 4.4, Table 4.5, Figure 4.13) without the capacity to confirm these by sequencing of the peptides of interest.

The remaining post-translational modifications of p85 identified by 2D-PAGE of unstimulated WEHI-231 cell extracts are likely due to modifications other than phosphorylation. Hydroxylation of P270 and F273 in p85α was identified by error-tolerant searches of LC-MS/MS data (Figure 4.13). Hydroxylation of Pro residues has been shown to occur in collagen and elastin, resulting in changes in their interaction with protein partners (Mazzorana et al., 1996; Perret et al., 2003; Urry et al., 1979) and in hypoxia-inducible factor (HIF) leading to HIF degradation (reviewed in (Safran and Kaelin, 2003)). Hydroxylation of Phe residues seems to be less abundant *in vivo*. Reducing agents are added to the sample in each step in order to prevent oxidation, but hydroxylation of proteins during sample preparation due to oxidative conditions cannot be excluded as the cause for the identified hydroxylated amino acids in p85α. Thus, it is possible that some of the p85 protein spots detected on 2D gels are due to protein hydroxylation, however, it is not known whether this hydroxylation might be an artefact.

In addition, amino acid substitutions in L136, D281 and I539 of p85α were detected by error-tolerant searches of LC-MS/MS data (Figure 4.13). These substitutions but also the WT sequences were identified in p85α from unstimulated WEHI-231 cells. The observed amino acid substitutions could be due to heterogeneity of the WEHI-231 population (i.e. certain cells contain L136 and others V136) or to differences in the maternal and paternal p85α genomic sequence. Since the substituted amino acids contained similar chemical properties as the WT amino acids, significant changes in the isoelectric point of p85α are not expected. Thus, the separation of p85α species by 2D-gel electrophoresis is probably not affected by these modifications. However, unless mutant protein was to be expressed and analysed by 2D-PAGE, these modifications can not be excluded as being part of the observed p85α spot pattern.

7.2.2 p85 does not undergo significant post-translational modifications upon cellular stimulation of WEHI-231 cells

In order to address whether physiologically relevant stimuli would impact on p85α post-translational modifications, WEHI-231 B cells were treated with α-IgM to induce BCR signalling. However, this treatment did not seem to alter p85 phosphorylation as assessed by immunoblotting of immunoprecipitated p85 using phospho-specific Abs following IP (Figure 4.2), even though the PI3K downstream effector Akt showed increased phosphorylation indicative for effective cellular stimulation. In addition, the p85 2D-gel spot pattern did only change marginally following cellular stimulation as assessed by immunoblotting using Abs to p85, suggesting that changes in the stoichiometry of p85 modifications, it they occurred, were very low. Only upon treatment with OA or pV, two potent inhibitors of protein phosphatases, could changes in p85 modifications be observed following 2D-PAGE of cell lysate (Figure 4.4).

Given that BCR engagement did not appear to induced p85 modifications, despite the increase in cellular PI3K lipid kinase activity, we speculate that PI3K activity is not modulated by p85α modifications in the chosen cell system. Alternatively, stoichiometry of modifications could be too low for detection.

7.2.3 Speculation on role of class IA PI3K regulatory subunit modifications

In order to gain insight into the potential biochemical role of the basal p85 modifications detected in unstimulated B cells, we compared the p85 2D-gel spot patterns of murine B cells to that of murine colon carcinoma, fibroblast and T cells. This analysis revealed only minor differences in the p85α spot pattern in these 4 different cell systems, suggesting that the observed modifications are not cell type-specific (Figure 4.5).

Since one of the amino acid substitutions (I539V) detected following LC-MS/MS is located in the p110-binding (iSH2) domain of p85α, we addressed whether the modifications detected by 2D-PAGE could have an impact on the interaction of p85 with the catalytic subunits. 2D-gel electrophoresis of p85 co-immunoprecipitated with Abs to p110α, p110β or p110δ revealed modest differences in the protein spot pattern of the regulatory subunit (Figure 4.6). This finding might indicate that the interaction of the regulatory and catalytic subunit could partially be dependent on the observed modifications, e.g. a certain p85 modification increases association with p110α. It is therefore possible that amino acid substitution of Ile539 might have an impact on the binding affinity of p85 to p110. Another possibility is that the observed changes in p85

pattern between p110 IPs are not consequences of modifications but their causes. Thus, the catalytic subunits might be responsible for phosphorylation of the regulatory subunit (Dhand et al., 1994) leading to the observed differences in the p85 2D gel spot pattern.

Furthermore, two potential amino acid substitutions and two protein hydroxylations (Leu136, P270, F273, D281; identified by error-tolerant searches of LC-MS/MS data) are located within the BH/Rac-binding domain of p85α. Since Rac and Cdc42 were shown to bind p85 via this domain (Zheng et al., 1994), it is possible that the modifications in this domain affect interaction of p85 with small GTPases. However, due to time constrictions, the analysis of p85α species associated with Rac or Cdc42 was not undertaken.

The p85α Y688 phosphorylation site identified by LC-MRM in WEHI-231 cells lies within the C-terminal SH2 domain. Y688 was previously identified in T cells where it seems to modulate the interaction with protein partners (von Willebrand et al., 1998) leading to enhanced PI3K lipid kinase activity (Cuevas et al., 2001). Since WEHI-231 cells proliferate independently of α-IgM stimulation, we speculate that Y688 might be phosphorylated at low stoichiometry in basal culture conditions leading to low level PI3K activity and contributing to cell proliferation.

7.3 Possible role of Tyr phosphorylation of p110δ in protein-protein interactions following BCR engagement of WEHI-231 cells

Activation of the BCR induces a complex signalling cascade also leading to an increase in PI3K activity and hence Akt phosphorylation (Figure 5.1; reviewed in (Dal Porto et al., 2004)). The rise in PI3K activity following BCR engagement of WEHI-231 cells is primarily mediated by an increase in p110δ activity as determined by α-IgM stimulation with or without p110δ isoform-specific inhibitors (Figure 5.2; (Bilancio et al., 2006)).

7.3.1 p110δ is phosphorylated on Tyr residue(s) following BCR engagement of WEHI-231 cells

In order to gain insight into the regulation of p110δ activity following BCR stimulation, post-translational modifications of p110δ were analysed. The analysis of *in vivo* labelling experiments using [γ-^{32}P]ATP (Figure 5.12) revealed that net phosphorylation of p110δ in WEHI-231 cells increased following BCR engagement. This increase was at least partially due to a rise in p110δ Tyr phosphorylation as determined by immunoblotting using pTyr-specific Abs (Figure 5.13). Since Tyr

phosphorylation of p110δ has not been reported, we further analysed the biological significance of this modification. A panel of p110δ-expressing cell lines were tested for p110δ Tyr phosphorylation following cellular stimulation with the Tyr phosphatase inhibitor pV. This analysis revealed that p110δ Tyr phosphorylation mainly occurred in B cells of murine and human origin, and could not be detected in mastocytoma, melanoma, gastrointestinal stromal sarcoma, breast cancer and T cells (Figure 5.15). Furthermore, IP of class IA PI3K catalytic subunits followed by immunoblotting with pTyr Abs revealed that primarily p110δ, and not p110α or p110β, was phosphorylated on Tyr residues (Figure 5.14). These data suggest that Tyr phosphorylation of p110δ might be implicated in the critical role that p110δ plays in B cells.

B cell-specific p110δ phosphorylation also indicates that the Tyr kinase catalysing this reaction might only exist in B cells. However, analysis of proteins co-immunoprecipitating with p110δ by MS (Table 5.1, Table 5.2) or by immunoblotting using a variety of Abs to Src-, Syk- and Tec-family kinases (data not shown) did not provide indications as to which Tyr kinase might phosphorylate p110δ. Studies performed in the chicken B cell line DT40 have revealed that Tyr phosphorylation of class IA PI3K catalytic subunit is dependent on Syk and Lyn following stimulation with either α-IgM or H_2O_2 (Craxton et al., 1999); (Qin and Chock, 2003). We therefore speculate that Syk or Lyn might constitute the p110δ Tyr kinase in B cells. This assumption is supported by our own observations that p110δ phosphorylation peaks within a very short time of stimulation (Figure 5.12), suggesting that its Tyr kinase is quickly activated upon BCR engagement.

7.3.2 Potential p110δ Tyr phosphorylation sites identified by MS

In order to identify the phosphorylated Tyr residue(s) in p110δ, 2D-gel electrophoresis was applied to enrich for the modified p110δ protein species. However, for reasons unknown to us, the class IA PI3K catalytic subunits did not enter the first dimension of 2D-PAGE (Figure 5.17). We therefore resolved immunoprecipitated p110δ by 1D-PAGE. Extensive mass spectrometric analysis was performed in order to determine phosphorylated Tyr residue(s) in p110δ peptides. However, these could not be identified by conventional LC-MS/MS, precursor-ion scanning (in collaboration with Dr. Morris of the MRC Phosphorylation Unit, University of Dundee), or multiple reaction monitoring of suspected phospho-peptides or error-tolerant searches of LC-MS/MS data. This might be due to low stoichiometry of p110δ phosphorylation or to incomplete p110δ sequence coverage. LC-MS/MS analysis usually generates incomplete sequence coverage because either the protease used to digest the protein produces

peptides of unsuitable length or hydrophobicity, which are lost during LC or MS, or because the peptide is not readily ionised at the ion source. Sequence coverage of immunoprecipitated p110δ was between 30-60%.

Analysis of p110δ peptides by MALDI mass fingerprinting allowed for the identification of m/z corresponding to peptides potentially containing non-phosphorylated (m=x) and phosphorylated (m=x+80) Tyr residues. A shift in 80 Da corresponds to the loss/addition of HPO_3. Thus, we found some evidence for 5 potentially phosphorylated Tyr residues in p110δ (Tyr239, Tyr395, Tyr670, Tyr812, Tyr963; Figure 5.18). Comparison of the p110δ amino acid sequence with the crystal structure of p110γ suggested that Tyr670 and Tyr963 are unlikely to be phospho-acceptors due to their shielded position within the molecule. Biocomputational analysis of the potentially phosphorylated Tyr in p110δ revealed that Tyr239, which is located in the Ras-binding domain, could be phosphorylated by Lyn (Figure 5.18), whereas Tyr 395 (within the C2-/lipid binding-domain) might be phosphorylated by the Tec-family kinase Itk. No potential Tyr kinase was identified for Tyr812 (located in the kinase domain).

7.3.3 Potential biological relevance of p110δ Tyr phosphorylation

In order to investigate the biological relevance of p110δ Tyr phosphorylation, we compared the intrinsic lipid kinase activity, membrane localisation and protein interaction partners of p110δ from unstimulated and α-IgM stimulated WEHI-231 cells. *In vitro* lipid kinase activity assays performed with immunoprecipitated p110δ did not show time- or substrate-dependent changes in p110δ lipid kinase activity following BCR stimulation (Figure 5.3). Thus, Tyr phosphorylation does not seem to have an impact on the intrinsic lipid kinase activity of p110δ. However, if only a small fraction of p110δ molecules became Tyr phosphorylated and activated following BCR engagement, the increase in PIP_3 due to these modified p110δ molecules compared to non-activated p110δ might not be detectable.

In contrast to its non-apparent role in the regulation of the intrinsic lipid kinase activity, p110δ Tyr phosphorylation might have a role in the subcellular localisation of p110δ and/or its interaction with protein partners. Enhanced interaction of p85-p110δ with membrane-bound BCAP and IRS-2 (Table 5.1, Table 5.2) could lead to an increase in p110δ membrane association following BCR engagement, i.e. when p110δ is Tyr-phosphorylated. Indeed, recruitment of p85 to the plasma membrane has been shown to be partially BCAP-dependent, since BCAP-deficient chicken DT40 cells have reduced PI3K membrane association following BCR engagement (Okada et al., 2000).

Also IRS can contribute to association of p110δ with the plasma membrane. Indeed, IRS-2 has been shown to accumulate at the plasma membrane following cellular stimulation, leading to a concomitant increase in recruitment of PI3K to the membrane (reviewed in (Whitehead et al., 2000)). Enhanced membrane association of p110δ could explain the observed increase in Akt phosphorylation upon cellular stimulation (Figure 5.1). Subcellular fractionation experiments did not indicate a shift of the predominantly cytosolic p110δ to the membrane post BCR engagement (Figure 5.6). However, the experimental conditions in the analysis of PI3K subcellular localisation might disrupt weak p110δ association with the membrane. It is also possible that the fraction of the p110δ protein translocated to the plasma membrane following B cell stimulation is too small to be detected by immunoblotting following cellular fractionation.

We also performed p110δ co-IP experiments and investigated potential p110δ interaction partners from unstimulated and α-IgM stimulated WEHI-231 cells by MS. This analysis revealed that p85-p110δ likely interacts with IRS-2, PARP-1 and caprin-1 following B cell stimulation, i.e. when p110δ is Tyr-phosphorylated (Table 5.1, Table 5.2). The biochemical aspects of these interactions are discussed in this paragraph, for the potential biological relevance of these interactions see § 7.4.

Interaction between p85-p110δ and **IRS-2** was increased more than 5-fold following BCR engagement, as assessed by qualitative MS (Figure 5.9). This interaction was confirmed by immunoblotting of co-immunoprecipitating partners following enrichment of p110δ or IRS-2 (Figure 5.11). Association of p85-p110δ with IRS-2 is likely due to Tyr phosphorylation of YxxM-motifs in IRS-2. However, IRS-2 also contains 2 phospho-Tyr-interacting domains that might mediate binding to phosphorylated Tyr residues in p110δ. One is an N-terminal PTB domain implicated in the interaction with NPxpY-containing proteins. p110δ possesses 2 NPxpY-homologous amino acid sequences. A second non-categorised domain in the central region of IRS-2 allows for interaction with pTyr residues, independent of NPxpY sequences (He et al., 1996).

Interaction of p85-p110δ with **PARP-1** was increased 3-times following BCR engagement (Figure 5.9). This association was reinforced by analysis of PARP-1 interaction partners, which revealed p110β and p110δ as binding partners of PARP-1 (T. Helleday, Institute for Cancer Studies, University of Sheffield; personal communication). PARP-1 contains a basic region leucine zipper (bZIP), which might dimerise with the bZIP of p110β/p110δ. Tyr395, one of the potentially phosphorylated amino acids in p110δ identified by MALDI-MS (Figure 5.18), is located next to the bZIP of p110δ and its phosphorylation might therefore enhance binding of p110δ to PARP-1.

In addition to dimerisation via bZIP, PARP-1 might also associate with p85-p110δ by complex formation via nucleolin (Borggrefe et al., 1998), a potential p85-p110δ interaction partner identified by us (Table 5.1, Figure 5.9) and others (Barel et al., 2001; Huddleson et al., 2006).

Interaction between p85-p110δ and **caprin-1** increased by more than 100-fold as assessed by qualitative MS (Figure 5.9). The potential association between p85-p110δ and caprin-1 remains to be confirmed by alternative techniques. This association might be mediated by SH3 domains of caprin-1 and the proline-rich domains of p85 or p110δ. It is also possible that p85-p110δ and caprin-1 interact via complex formation with G3BP, a novel potential interaction partner of p85-p110δ (Table 5.2, Figure 5.9). Interaction between G3BP and caprin-1 has been shown in HeLa cells transfected with Vaccinia virus intermediate transcription factor (Katsafanas and Moss, 2004).

Thus, while interaction between IRS-2 and PARP-1 with p85-p110δ might be mediated by Tyr phosphorylation of p110δ, it is not clear if such modification could have a role in the interaction between caprin-1 and PI3K.

7.4 Novel potential PI3K interaction partners identified in WEHI-231 cells

Signal transduction via the BCR is known to change during B cell development depending on the B cell maturation stage. In immature B cells, BCR engagement induces growth arrest or apoptosis, while BCR crosslinking in mature B cells leads to proliferation. In a primary phase of BCR signalling, PI3K activity is induced resulting in an increase in Akt phosphorylation (Bilancio et al., 2006). PI3K-dependent phospholipid levels drop within a short time following BCR engagement in B cells (Figure 7.2). While phosphoinositide concentrations return to the basal state in mature B cells following sustained BCR engagement, PIP_3 levels remain low in immature B cells. In the latter cells, a concomitant decrease is observed in the phosphorylation of S6K, upregulation of $p27^{KIP1}$ protein expression, and down-regulation of c-Myc expression (Carey and Scott, 2001; Donjerkovic and Scott, 2000). It has further been shown that downregulation of the PI3K pathway by LY294002 in B cells mimics the effects of BCR engagement in that these cells undergo growth arrest and apoptosis (Carey and Scott, 2001). Thus, downregulation of PI3K activity following BCR stimulation of immature B cells seems necessary for the induction of apoptosis. In addition, it is emerging that not only the level of PI3K activity at the plasma membrane might be critical for the switch between cell survival and apoptosis, but also the rate of PI3K activity at the nuclear membrane. Thus, the generation of nuclear PIP_3 by class IA PI3K has been shown to mediate anti-apoptotic effects in neuron-like cells following cellular stimulation (Ahn et

al., 2005). However, nuclear localisation of class IA PI3K is controversial due to experimental challenges in the fractionation of nucleus and cytosol.

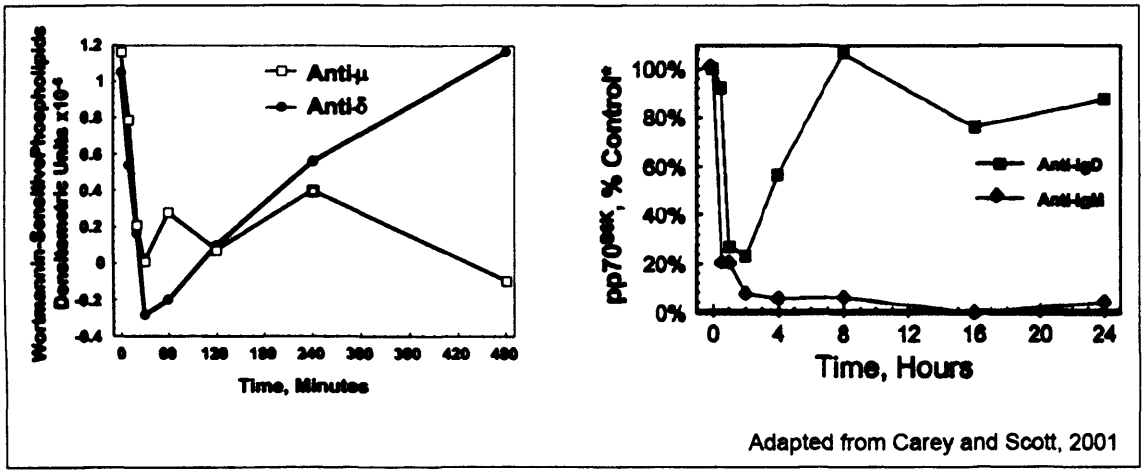

Figure 7.2: Differences in the regulation of the PI3K pathway between B cells stimulated with α-IgM or α-IgD

The B cell lymphoma cell line ECH408 was treated with either α-IgM (Anti-μ) leading to growth arrest and apoptosis or with α-IgD (Anti-δ). PI3K-dependent phospholipids dropped sharply following BCR engagement and returned to the basal state in α-IgD stimulated cells, but not in α-IgM stimulated cells. A concomitant increase in phosphorylation of S6K could be observed in α-IgD stimulated cells that is not noticeable in α-IgM treated cells. Figure adapted from (Carey and Scott, 2001).

How a decrease in PI3K activity following BCR engagement of immature B cells is achieved is unknown. Possibilities include PI3K degradation, changes in post-translational modifications, protein-protein interactions or subcellular localisation.

Our analysis of novel potential p85-p110δ interaction partners in the WEHI-231 cells by MS points at a possible sequestration of PI3K from the plasma and nuclear membrane to the cytosol following BCR engagement (Table 7.1, Figure 7.3). Proteins that co-immunoprecipitated in unstimulated and α-IgM stimulated cells were analysed by MS (Table 5.1, Table 5.2, § 5.13.5, § 5.13.6). While we are confident that the novel potential interaction partners do not result from aspecific binding to the matrix, we can not eliminate the possibility that these proteins cross-react with Ab. We therefore performed literature and database searches (such as PI3K yeast two-hybrid data available at Alliance for Cellular Signaling (http://www.signaling-gateway.org/data/Y2H/cgi-bin/y2h.cgi)) to independently confirm interaction of some of these binding partners with PI3K. However, none of the novel potential interaction p85-p110δ partners we identified by MS had previously been observed.

Below, we discuss the identified potential p85-p110δ interaction partners in WEHI-231 cells according to their potential role in the sequestration of PI3K from

membranes. We realise that this is speculative at this point in time but this provides a framework for discussion.

Table 7.1: Potential novel interaction partners of p85-p110δ in immature B cells

Binding partners of p85-p110δ were identified by LC-MS/MS following p110δ IP from unstimulated (-) or α-IgM stimulated (+) WEHI-231 cells. Analysis of integrated peak areas of LC-MS data allowed for refined assessment of interactions (in brackets). Biocomputational analysis and literature data of binding partners revealed potential interaction domains with PI3K and potential roles in the sequestration of p110δ from the plasma and nuclear membrane by these interaction partners. IB: immunoblotting, ?: not known.

Interaction partner	Impact of BCR stimulation	Interaction identified by	Potential interaction domain	Subcellular localisation of interaction partner	Potential role in p110δ sequestration
BCAP	- LC-MS (+)	MS, IB, (Okada et al., 2000)	PI3K regulatory subunit	cytosol, plasma membrane	plasma membrane to cytosol
caprin-1	+	MS	proline-rich domains/via G3BP	cytosol	?
DDB1	-	MS	?	nucleus	?
γ-tubulin	-	MS, (Kapeller et al., 1995)	PI3K regulatory subunit	microtubules	?
G3BP	-	MS	?	nucleus, cytosol	nuclear export
GPC2	-	MS	via γ-tubulin	microtubules	?
GPC3	-	MS	via γ-tubulin	microtubules	?
histone H4	-	MS	?	nucleus	?
IRS-2	+	MS, IB, (Backer et al., 1992)	PI3K regulatory subunit/pTyr of p110δ	cytosol	plasma membrane to cytosol
NEDD1	-	MS	via γ-tubulin	microtubules	?
nucleolin	- LC-MS (+)	MS, (Barel et al., 2001; Huddleson et al., 2006)	PI3K regulatory subunit	nucleus, cytosol	nuclear export
p200 Arf-GEF	-	MS	?	Golgi	?
PARP-1	+	MS, T. Helleday (personal communication)	bZIP/via nucleolin	nucleus	nuclear export

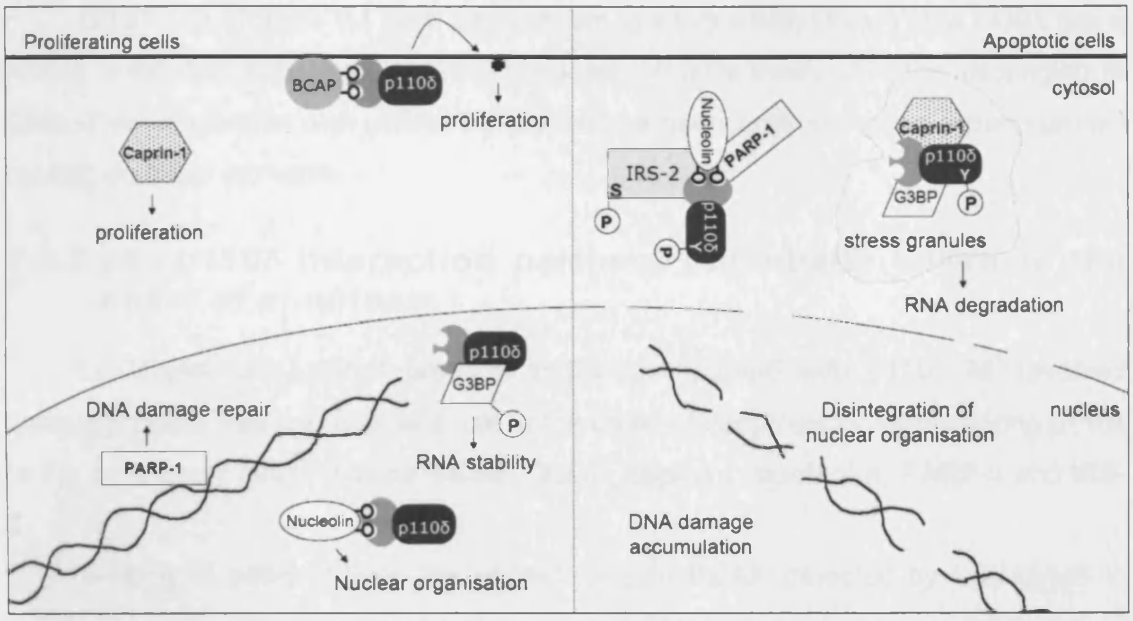

Figure 7.3: Potential role of p85-p110δ and interaction partners in the induction of apoptosis

In proliferating cells, p110δ is possibly found both at the plasma membrane and in the nucleus where its activity supports proliferation. In apoptotic cells, p110δ might be sequestered in the cytoplasm in complex with G3BP and caprin-1, or with nucleolin, IRS-2 and PARP-1 thereby possibly decreasing PI3K activity.

7.4.1 p85-p110δ interaction partners with diverse functions

Using p110δ co-IP and MS analysis, we identified the cytosolic proteins **γ-tubulin**, **GPC2**, **GPC3**, **NEDD1** and **p200 Arf-GEF** and the nuclear proteins **histone H4** and **DDB1** as potential p85-p110δ interaction partners by (Table 5.1, Table 5.2). These proteins have to the best of our knowledge not been implicated in apoptosis.

Interaction of p85-p110δ with **γ-tubulin** has been previously reported (Kapeller et al., 1995). γ-tubulin is part of microtubule-organising centres and stabilises the minus-end of microtubules. GPC2, GPC3 and NEDD1 have been shown to associate with γ-tubulin to form the so-called γ-tubulin ring complex (Murphy et al., 1998). Thus, their interaction with PI3K likely occurs via γ-tubulin. We speculate that interaction between PI3K and the γ-tubulin ring complex might be involved in the regulation of microtubule stability or vesicle transport along microtubules.

p200 Arf-GEF is a nucleotide exchange factor for small GTPases of the ADP ribosylation factor family (Mansour et al., 1999). The protein does not contain any known domain or motif which could explain its binding to PI3K. p200 Arf-GEF is localised at the Golgi and might therefore be involved in vesicle transport from the Golgi to the plasma membrane along microtubules in cooperation with γ-tubulin.

DDB1 and **histone H4** have been shown to interact with DNA. While DDB1 has a role in nucleotide excision repair, histones are proteins involved in the packaging of DNA. Their interaction with p85-p110δ can not be deduced from known protein-protein binding domains or motifs.

7.4.2 p85-p110δ interaction partners potentially linked to the onset of apoptosis

LC-MS/MS analysis of proteins immunoprecipitated with p110δ Ab revealed various proteins that might have a role in the onset of apoptosis by sequestering p110δ to the cytoplasm. These include **BCAP**, **G3BP**, **caprin-1**, **nucleolin**, **PARP-1** and **IRS-2**.

Binding of p85-p110δ to the adaptor protein **BCAP** detected by LC-MS/MS in WEHI-231 cells independent of cellular stimulation was confirmed by reciprocal IP experiments using Abs to BCAP and p110δ followed by immunoblotting (Figure 5.11). This interaction is likely due to binding of p85 SH2 domains to phosphorylated YxxM-motifs in BCAP (Okada et al., 2000). The interaction between PI3K and BCAP has been observed in unstimulated B cells, and seems to rapidly fluctuate following BCR engagement (Okada et al., 2000). BCAP has the potential to modulate PI3K subcellular localisation since it is a scaffolding protein for PI3K and BCR-associated kinases (Okada et al., 2000). It might therefore be involved in the sequestration of PI3K from the membrane to the cytoplasm at the onset of apoptosis.

G3BP is an endonuclease interacting with RasGAP and has a role in the regulation of mRNA stability. In growth factor-stimulated cells, G3BP is localised in the nucleus (Barnes et al., 2002) and translocates in response to cytotoxic stress to so-called cytosolic stress granules, where mRNA is stored in an abortive translation initiation complex (Tourriere et al., 2003; Tourriere et al., 2001). Even though G3BP association with PI3K can not easily be deduced from primary sequence analysis or literature data, on the basis of the described findings we speculate that G3BP might interact with PI3K in the nucleus of proliferating B cells and the complex might be exported to the cytoplasm at the onset of apoptosis. G3BP has also been shown to interact with caprin-1 (Katsafanas and Moss, 2004), a novel potential p85-p110δ interaction partner.

Caprin-1 is a cytosolic protein upregulated in proliferating B and T cells (Grill et al., 2004). DT40 cells deficient in caprin-1 show defects in proliferation (Wang et al., 2005). Due to its association with G3BP, we speculate that following BCR engagement caprin-1 forms a complex with PI3K and G3BP, possibly located in cytosolic stress-granules.

The association between **nucleolin** and p85-p110δ might be due to interaction of the p85 SH2 domains with Tyr phosphorylated residues in nucleolin (Barel et al., 2001) and has been shown to occur in endothelial cells subjected to fluid flow (Huddleson et al., 2006). Nucleolin is a multifunctional protein that plays a role in the nuclear organisation (reviewed in (Ginisty et al., 1999)). Although generally considered to be a nuclear protein, translocation of nucleolin from the nucleus to the cytosol has been observed in apoptotic B cells (Mi et al., 2003). We therefore hypothesise that the complex of p85-p110δ and nucleolin might be exported from the nucleus to the cytoplasm following apoptosis. Nucleolin has been observed in association with the p85-p110δ potential interaction partners IRS-2 and PARP-1.

PARP-1 is a novel potential interaction partner of p85-p110δ whose association with PI3K has been confirmed by reciprocal IP (see § 7.3.3). PARP-1 is activated following DNA damage and catalyses the reversible modification of proteins with ADP-ribose. This modification contributes to the survival of proliferating cells following DNA damage (reviewed in (Ame et al., 2004)). PARP-1 has been shown to interact with nucleolin (Borggrefe et al., 1998) and we therefore speculate that complex formation of PARP-1 with nucleolin and PI3K leads to the export of PI3K and PAPR-1 from the nucleus to the cytosol.

While interaction of PI3K with the adaptor molecule **IRS-2** has been reported in B cells downstream of cytokine receptors (Johnston et al., 1995), IRS-2 recruitment has not been implicated following BCR engagement. It is thus not clear how IRS-2 couples to the membrane and becomes Tyr phosphorylated upon BCR engagement. However, sequestration of PI3K from the plasma membrane could be achieved by interaction of PI3K with IRS-2 and nucleolin. Nucleolin has been shown to interact with the PH domain of IRS molecules, which was shown to interact with phosphoinositides (Burks et al., 1998). This interaction might lead to a decrease in membrane association of IRS-2. We therefore speculate that export of nucleolin from the nucleus to the cytoplasm following induction of apoptosis might lead to its association with IRS-2, to removal of IRS-2 complexed to PI3K from the plasma membrane and therefore to down-regulation of PI3K activity.

It is likely that not only the translocation of PI3K from the nuclear and plasma membrane to the cytosol has an impact on the induction of apoptosis but also the nuclear export of nucleolin, G3BP, and PARP-1. These molecules are involved in the regulation of nuclear organisation, RNA stability and DNA damage repair and disruption of their function most likely induces aberration of cellular proliferation.

7.5 Class IA PI3K activity is not regulated by monomeric p85

In the traditional model of class IA PI3K regulation, it is suggested that p110 and p85 form obligate heterodimers and that regulation of lipid kinase activity of the heterodimer is mainly steered by interaction with non-PI3K binding partners and membrane recruitment (Fry et al., 1992; Yu et al., 1998). Various reports have challenged this view. For example, purification of endogenous class IA PI3K from bovine thymi presented evidence for two catalytically active p110 subunits: p110 in complex with p85, and a p110 in what was considered to be a monomeric form (Shibasaki et al., 1991). Over the last couple of years, also a vast literature on the existence of free p85 has appeared, mainly in an attempt to explain the increase in PI3K signalling upon insulin stimulation in mice in which class IA regulatory subunits have been deleted. Thus, data gained from analysis of p85 KO mice compared to WT mice presented evidence for a greater than 30% molar excess of p85 over p110 in WT MEFs (Ueki et al., 2002) and WT murine liver cells (Mauvais-Jarvis et al., 2002) compared to p85-KO cells. Furthermore, evidence has been presented that this monomeric p85 can compete with heterodimeric p85-p110 for pTyr-binding motifs on IRS molecules since forced overexpression of p85α in muscle cells leads to a decrease in *in vitro* lipid kinase activity of PI3K following pTyr IP and to a decrease in Akt phosphorylation (Ueki et al., 2000). Based on this information, a model attributing a negative role of p85 to PI3K signalling was proposed: in WT cells, surplus, thus free p85 competes with heterodimeric p85-p110 for pTyr binding sites in receptor tyrosine kinases or adaptor molecules thereby dampening PI3K signalling. In p85 KO cells, expression of monomeric p85 is preferentially reduced leading to enhanced access of heterodimeric p85-p110 to pTyr binding sites and to increased PI3K signalling.

Arguments based on literature data that cast doubts on the existence of monomeric p85 in WT cells, and the role of p85 as a negative regulator are presented in § 6.6. Briefly, monomeric p85 seems to be unstable (Brachmann et al., 2005) and does not necessarily compete with p85-p110 for pTyr binding places (Ueki et al., 2002; Ueki et al., 2003; Ueki et al., 2002). In addition, several proteins other than the deleted p85 were found to be deregulated in p85 KO cells. This includes a decrease in p110 protein expression and increases in PTEN protein expression and IRS-2 phosphorylation have been observed (Fruman et al., 2000; Fruman et al., 1999; Suzuki et al., 1999; Terauchi et al., 1999).

7.5.1 Experimental evidence supporting the notion that class IA PI3Ks are obligate heterodimers

In Chapter 6, we present biochemical data demonstrating that class IA PI3Ks are obligate heterodimers. No excess of one subunit over the other was observed after affinity chromatography of fibroblast (data not shown) and leukocyte cell lysates using Abs to class IA PI3K regulatory and catalytic subunits or using pTyr-matrix (Figure 6.2). In addition, depletion of one class IA PI3K subunit from TCL by sequential IP using isoform-specific Abs led to the concomitant depletion of the other class IA PI3K subunit (Figure 6.7). Ion exchange chromatography of leukocyte cell lysate did also not reveal any evidence for the existence of free p85 *in vivo* (Figure 6.8). Thus, these data do not support a role of monomeric p85 in the regulation of PI3K activity.

We also employed a technique called AQUA (absolute quantitation) MS (Gerber et al., 2003) in order to determine the absolute amounts of class IA PI3K isoforms in WEHI-231 and NIH-3T3 cells. The AQUA method is based on the use of a synthetic internal standard (IS) peptide that is added to the cell sample at known concentrations before MS analysis. This IS mimicks an endogenous peptide produced during proteolysis of the target protein expect that it is enriched in stable isotopes. LC-MS or LC-MS/MS analysis of the cell sample spiked with the IS peptide results in the detection and quantitation of both the endogenous and AQUA peptide.

We used 11 IS peptides with equivalent sequences to stretches of class IA PI3K isoforms (Table 6.1). These IS peptides were added to regulatory and catalytic subunits following PI3K enrichment from cells. Absolute quantitation MS revealed similar protein amounts of class IA PI3K in NIH-3T3 and WEHI-231 cells, amounting to 25,000 molecules/cell (Table 6.2). Importantly, the total of all regulatory subunits matched the total of all catalytic subunits, indicating that class IA PI3K are obligate heterodimers. Furthermore, p110α protein expression was low in both cell lines compared to p110β, which seems highly expressed in NIH-3T3 cells, and p110δ, which is highly expressed in WEHI-231 cells. The amount of p85β was more than double that of p85α in both cell lines, while p55γ, p55α, p50α protein expression was low.

Thus, the use of this AQUA method did not only allow for the determination of the absolute amounts of regulatory and catalytic class IA PI3K subunits, but also for the determination of which class IA PI3K isoforms is the most prevalent, and thus probably most critical in different cell types.

7.5.2 Alternative model for the observed increase in PI3K signalling in p85 KO cells

Our findings that class IA PI3Ks are obligate heterodimers i.e. no monomeric p110 or p85 exists *in vivo*, necessitates an alternative model for the observed increase in PI3K activity in insulin-responsive cells of p85-KO mice. As discussed in more detail in § 6.6, changes in the protein concentrations of PI3K and PTEN/SHIP or in the intrinsic PI3K activity unlikely enhance the total lipid kinase activity of PI3K. Although p110, p85 and PTEN protein levels are affected in p85-KO cells, the observed variations in protein expression compared to WT cells are in fact expected to *decrease* PI3K signalling. Furthermore, the *in vitro* lipid kinase activity of p110 or pTyr immunoprecipitates is also *decreased* in p85-KO cells.

We therefore present a model that could explain an increase in PIP_3 levels independent of class IA PI3K (Figure 6.16). This model is based on the "interaction vacuum" of phosphorylated IRS molecules in cells with diminished levels of p85 molecules. Since phosphorylation of IRS is unchanged or slightly increased (Chen et al., 2004; Ueki et al., 2002), molecules usually not associated with IRS due to a stronger interaction between IRS and the p85 subunit of PI3K, might engage with IRS instead of p85. JAKs and SHIP are such molecules since they both possess SH2 domains (Al-Lazikani et al., 2001; Damen et al., 1996). Interaction of the Tyr kinase JAK with IRS might lead to the observed increase in IRS phosphorylation (Wang et al., 1997). JAK might also phosphorylate and inactivate the phosphoinositide phosphatase SHIP (Habib et al., 1998), which might be concomitantly associated with IRS. Inactivation of SHIP would subsequently lead to the observed increase in PIP_3 levels. In hematopoietic cells, JAK activation does not seem to be dependent on IRS molecules (Uddin et al., 1997), possibly explaining why p85 deletion in insulin-responsive cells leads to an *increase* in PI3K activation while p85-deficient B and T cells have *decreased* PI3K signalling.

7.6 Conclusions and future experiments

In this study, we used biochemical approaches to analyse the regulation of class IA PI3K activity in immature B cells. We thereby focused on the investigation of post-translational modifications of endogenous (i.e. non overexpressed) p85 and p110δ and of the molar ratio between the regulatory and catalytic subunits of PI3K.

A variety of modifications in the regulatory subunit were detected by 2D-PAGE, which might be due to protein phosphorylation, hydroxylation or amino acid substitutions, as identified by MS and *in vitro* dephosphorylation. These modifications do not seem to be dynamic, since BCR stimulation of WEHI-231 cells did not lead to

significant changes in the p85 spot pattern resolved by 2D-gel electrophoresis. Given that PI3K activity was found to be increased following BCR stimulation, the p85 modifications unlikely impact on the class IA PI3K activity. However, the stoichiometry of p85 modifications that affect PI3K activity might be too low to be detected by immunoblotting. If not involved in the regulation of intrinsic PI3K lipid kinase activity, the question arises therefore what role, if any, these modifications have. We presented some evidence to suggest that the interaction between p85 and p110 might be modestly affected by these modifications. Since the regulatory subunit contains various protein-protein interaction domains, it would be interesting to analyse whether these modifications impact on the association with other known protein partners. In order to address this question, these interaction partners (e.g. α-/β-tubulin, Rac/Cdc42, Shc/Ezrin/Syk) would have to be purified by IP using Abs to each of them and the modifications in the co-purified regulatory subunit analysed by 2D-PAGE (as performed for interactions between p110α/β/δ and p85; Figure 4.6). Furthermore, investigation of the biological relevance of p85α modifications identified by LC-MS/MS would be of interest. In order to do this, site-directed mutagenesis of p85α cDNA could be performed such that the amino acids identified by MS (Leu136, Pro270, Phe273, Asp281, Ile539, Tyr688) would be mutated to either the identified substitutions (Val136, Glu281, Val539), or to an amino acid residue mimicking the modification (Asp688). The p85α cDNA would subsequently be cloned to a tag. These mutant p85α proteins could then be analysed for association with interaction partners, including p110, by transfection of the mutated cDNA into cells and IP of the p85α protein using its tag. Co-immunoprecipitating proteins could be identified by LC-MS/MS.

Analysis of the p110δ catalytic subunit for post-translational modifications revealed dynamic changes following BCR engagement of WEHI-231 cells. We showed that p110δ becomes phosphorylated on Tyr residues upon B cell stimulation. Unfortunately, identification of phosphorylated Tyr residue(s) by MS was not successful. It was furthermore not feasible to determine the protein kinase or phosphatase involved in the modification. Based on literature data, we speculate that it might be Lyn or Syk. Further investigations into the biological relevance of p110δ Tyr phosphorylation revealed that this modification mainly occurs in B cells, in p110δ and not p110α or p110β and does not seem to impact on the intrinsic lipid kinase activity. The subcellular localisation of p110δ and its interaction with IRS-2, PARP-1 and caprin-1 might however be affected by Tyr phosphorylation of p110δ. In order to investigate whether interactions between p85-p110δ and PARP-1, caprin-1 or IRS-2 are mediated by p110δ Tyr phosphorylation, the phosphorylated Tyr residue would have to be determined. In order to do this, *in vitro* protein kinase assays using recombinant

Syk/Lyn or other Tyr kinases and p110δ could be performed to 1) determine the Tyr kinase which phosphorylates p110δ and 2) increase the stoichiometry of Tyr phosphorylation to enhance the probability of MS identification of phosphorylated residues. This Tyr residue could subsequently be mutated to a phospho-mimicking residue (Y→D/E) or a residue which can no longer be phosphorylated (Y→A). Following transfection, p110δ-WT and –mutant protein could be analysed for interaction with IRS-2, PARP-1 and caprin-1 by co-IP experiments and LC-MS/MS.

MS analysis of p110δ co-IP protein partners revealed novel potential p85-p110δ interaction partners in unstimulated and α-IgM stimulated WEHI-231 cells. The potential interaction with these proteins raises some interesting questions:

1) Does p110δ activity have a role in the onset of apoptosis? This question can be addressed by inhibiting PI3K activity in general and p110δ activity in particular by pharmacological inhibitors following BCR engagement of immature B cells and subsequently investigating the rate of apoptosis by MTS assays or PI staining. Pre-treatment of B cells with LY294002 followed by BCR crosslinking (α-IgM and α-IgD) has revealed increased $p27^{KIP}$ expression and decreased c-myc expression compared to non-inhibitor treated cells, indicating that a decrease in PI3K activity mimicks the effects of BCR stimulation in immature B cells (Banerji et al., 2001; Carey and Scott, 2001).

2) Do the associations between p85-p110δ and the indicated proteins exist *in vivo*? The interactions could be confirmed by IP of interaction partners with a different p110δ-specific Ab in order to eliminate the possibility that the association is due to Ab cross-reaction. Furthermore, we could perform reciprocal IP experiments with Abs to PI3K and the potential protein partners followed by immunoblotting as done in this study for confirmation of IRS-2 and BCAP as p85-p110δ binding partners. It would also be interesting to investigate interaction partners of p110β and p110α by IP and MS in order to identify PI3K isoform-specific binding partners.

3) Is p110δ translocated from the nucleus to the cytosol following BCR engagement? Preliminary fractionation experiments performed to analyse p85-p110δ subcellular localisation revealed that p110δ nuclear localisation indeed decreases following BCR engagement of immature B cells (data not shown). These fractionation experiments could be complemented by immunohistochemistry of WEHI-231 cells using Abs to p110δ and p85. It would furthermore be interesting to investigate whether the potential interaction partners change their subcellular localisation following α-IgM stimulation of B cells.

4) Which of the novel potential PI3K interaction partners is the most important one? We speculate that interaction of PI3K with caprin-1 will turn out to be crucial since

this association increased by more than 100-fold following BCR engagement. The important role of caprin-1 in the proliferation of leukocytes might link this protein to p110δ.

In order to investigate the potential role of monomeric regulatory subunit in the regulation of class IA PI3K activity, we analysed the molar ratio between p85 and p110. Extensive biochemical analysis of class IA PI3K protein levels by affinity and ion exchange chromatography did not reveal an excess of one subunit over the other. Furthermore, absolute quantitation MS allowed for the determination of precise protein amounts of each class IA PI3K isoform in cell lines, indicating that class IA PI3Ks are obligate heterodimers. Thus, our data do not support a role of monomeric p85 in the negative regulation of PI3K. We speculate that recruitment of JAK and SHIP to the plasma membrane by interaction with phosphorylated IRS might lead to the observed increase in PIP_3 generation following insulin stimulation in p85 KO cells.

The AQUA method could also be expanded to analyse molar ratios between PI3Ks and interaction partners, such as receptor molecules. Furthermore, it will be of interest to investigate how much class IA PI3K protein exists in more physiological material, such as murine tissues.

8 REFERENCES

Abell, K., Bilancio, A., Clarkson, R.W., Tiffen, P.G., Altaparmakov, A.I., Burdon, T.G., Asano, T., Vanhaesebroeck, B. and Watson, C.J. (2005) Stat3-induced apoptosis requires a molecular switch in PI(3)K subunit composition. *Nat Cell Biol*, **7**, 392-398.

Aebersold, R. and Goodlett, D.R. (2001) Mass spectrometry in proteomics. *Chem Rev*, **101**, 269-295.

Ahn, J.Y., Liu, X., Cheng, D., Peng, J., Chan, P.K., Wade, P.A. and Ye, K. (2005) Nucleophosmin/B23, a nuclear PI(3,4,5)P(3) receptor, mediates the antiapoptotic actions of NGF by inhibiting CAD. *Mol Cell*, **18**, 435-445.

Al-Lazikani, B., Sheinerman, F.B. and Honig, B. (2001) Combining multiple structure and sequence alignments to improve sequence detection and alignment: application to the SH2 domains of Janus kinases. *Proc Natl Acad Sci U S A*, **98**, 14796-14801.

al-Shami, A., Bourgoin, S.G. and Naccache, P.H. (1997) Granulocyte-macrophage colony-stimulating factor-activated signaling pathways in human neutrophils. I. Tyrosine phosphorylation-dependent stimulation of phosphatidylinositol 3-kinase and inhibition by phorbol esters. *Blood*, **89**, 1035-1044.

Alessi, D.R. and Cohen, P. (1998) Mechanism of activation and function of protein kinase B. *Curr Opin Genet Dev*, **8**, 55-62.

Alessi, D.R., James, S.R., Downes, C.P., Holmes, A.B., Gaffney, P.R., Reese, C.B. and Cohen, P. (1997) Characterization of a 3-phosphoinositide-dependent protein kinase which phosphorylates and activates protein kinase Balpha. *Curr Biol*, **7**, 261-269.

Algenstaedt, P., Hennigs, N., Telkamp, N., Schwarzloh, B., Kausch, C., Matthaei, S., Hansen-Algenstaedt, N. and Greten, H. (2004) Met326Ile aminoacid polymorphism in the human p85 alpha gene has no major impact on early insulin signaling in type 2 diabetes. *Horm Metab Res*, **36**, 686-692.

Ali, K., Bilancio, A., Thomas, M., Pearce, W., Gilfillan, A.M., Tkaczyk, C., Kuehn, N., Gray, A., Giddings, J., Peskett, E., Fox, R., Bruce, I., Walker, C., Sawyer, C., Okkenhaug, K., Finan, P. and Vanhaesebroeck, B. (2004) Essential role for the p110delta phosphoinositide 3-kinase in the allergic response. *Nature*, **431**, 1007-1011.

Aman, M.J., Lamkin, T.D., Okada, H., Kurosaki, T. and Ravichandran, K.S. (1998) The inositol phosphatase SHIP inhibits Akt/PKB activation in B cells. *J Biol Chem*, **273**, 33922-33928.

Ame, J.C., Spenlehauer, C. and de Murcia, G. (2004) The PARP superfamily. *Bioessays*, **26**, 882-893.

Amigorena, S., Bonnerot, C., Drake, J.R., Choquet, D., Hunziker, W., Guillet, J.G., Webster, P., Sautes, C., Mellman, I. and Fridman, W.H. (1992) Cytoplasmic domain heterogeneity and functions of IgG Fc receptors in B lymphocytes. *Science*, **256**, 1808-1812.

Andersson, L. and Porath, J. (1986) Isolation of phosphoproteins by immobilized metal (Fe3+) affinity chromatography. *Anal Biochem*, **154**, 250-254.

Andjelkovic, M., Alessi, D.R., Meier, R., Fernandez, A., Lamb, N.J., Frech, M., Cron, P., Cohen, P., Lucocq, J.M. and Hemmings, B.A. (1997) Role of translocation in the activation and function of protein kinase B. *J Biol Chem*, **272**, 31515-31524.

Antonetti, D.A., Algenstaedt, P. and Kahn, C.R. (1996) Insulin receptor substrate 1 binds two novel splice variants of the regulatory subunit of phosphatidylinositol 3-kinase in muscle and brain. *Mol Cell Biol*, **16**, 2195-2203.

Anzelon, A.N., Wu, H. and Rickert, R.C. (2003) Pten inactivation alters peripheral B lymphocyte fate and reconstitutes CD19 function. *Nat Immunol*, **4**, 287-294.

Aoki, M., Schetter, C., Himly, M., Batista, O., Chang, H.W. and Vogt, P.K. (2000) The catalytic subunit of phosphoinositide 3-kinase: requirements for oncogenicity. *J Biol Chem*, **275**, 6267-6275.

Arcaro, A., Volinia, S., Zvelebil, M.J., Stein, R., Watton, S.J., Layton, M.J., Gout, I., Ahmadi, K., Downward, J. and Waterfield, M.D. (1998) Human phosphoinositide 3-kinase C2beta, the role of calcium and the C2 domain in enzyme activity. *J Biol Chem*, **273**, 33082-33090.

Arcaro, A., Zvelebil, M.J., Wallasch, C., Ullrich, A., Waterfield, M.D. and Domin, J. (2000) Class II phosphoinositide 3-kinases are downstream targets of activated polypeptide growth factor receptors. *Mol Cell Biol*, **20**, 3817-3830.

Asano, T., Kanda, A., Katagiri, H., Nawano, M., Ogihara, T., Inukai, K., Anai, M., Fukushima, Y., Yazaki, Y., Kikuchi, M., Hooshmand-Rad, R., Heldin, C.H., Oka, Y. and Funaki, M. (2000) p110beta is up-regulated during differentiation of 3T3-L1 cells and contributes to the highly insulin-responsive glucose transport activity. *J Biol Chem*, **275**, 17671-17676.

Auger, K.R., Wang, J., Narsimhan, R.P., Holcombe, T. and Roberts, T.M. (2000) Constitutive cellular expression of PI 3-kinase is distinct from transient expression. *Biochem Biophys Res Commun*, **272**, 822-829.

Backer, J.M., Myers, M.G., Jr., Shoelson, S.E., Chin, D.J., Sun, X.J., Miralpeix, M., Hu, P., Margolis, B., Skolnik, E.Y., Schlessinger, J. and et al. (1992) Phosphatidylinositol 3'-kinase is activated by association with IRS-1 during insulin stimulation. *Embo J*, **11**, 3469-3479.

Bader, A.G., Kang, S. and Vogt, P.K. (2006) Cancer-specific mutations in PIK3CA are oncogenic in vivo. *Proc Natl Acad Sci U S A*, **103**, 1475-1479.

Baldwin, M.A. (2004) Protein identification by mass spectrometry: issues to be considered. *Mol Cell Proteomics*, **3**, 1-9.

Banerji, L., Glassford, J., Lea, N.C., Thomas, N.S., Klaus, G.G. and Lam, E.W. (2001) BCR signals target p27(Kip1) and cyclin D2 via the PI3-K signalling pathway to mediate cell cycle arrest and apoptosis of WEHI 231 B cells. *Oncogene*, **20**, 7352-7367.

Banin, S., Moyal, L., Shieh, S., Taya, Y., Anderson, C.W., Chessa, L., Smorodinsky, N.I., Prives, C., Reiss, Y., Shiloh, Y. and Ziv, Y. (1998) Enhanced phosphorylation of p53 by ATM in response to DNA damage. *Science*, **281**, 1674-1677.

Barbour, L.A., Mizanoor Rahman, S., Gurevich, I., Wayne Leitner, J., Fischer, S.J., Roper, M.D., Knotts, T.A., Vo, Y., McCurdy, C.E., Yakar, S., Leroith, D., Ronald Kahn, C., Cantley, L.C., Friedman, J.E. and Draznin, B. (2005) Increased P85alpha is a potent negative regulator of skeletal muscle insulin signaling and induces in vivo insulin resistance associated with growth hormone excess. *J Biol Chem*.

Barel, M., Le Romancer, M. and Frade, R. (2001) Activation of the EBV/C3d receptor (CR2, CD21) on human B lymphocyte surface triggers tyrosine phosphorylation of the 95-kDa nucleolin and its interaction with phosphatidylinositol 3 kinase. *J Immunol*, **166**, 3167-3173.

Barnes, C.J., Li, F., Mandal, M., Yang, Z., Sahin, A.A. and Kumar, R. (2002) Heregulin induces expression, ATPase activity, and nuclear localization of G3BP, a Ras signaling component, in human breast tumors. *Cancer Res*, **62**, 1251-1255.

Barnidge, D.R., Dratz, E.A., Martin, T., Bonilla, L.E., Moran, L.B. and Lindall, A. (2003) Absolute quantification of the G protein-coupled receptor rhodopsin by LC/MS/MS using proteolysis product peptides and synthetic peptide standards. *Anal Chem*, **75**, 445-451.

Barnouin, K.N., Hart, S.R., Thompson, A.J., Okuyama, M., Waterfield, M. and Cramer, R. (2005) Enhanced phosphopeptide isolation by Fe(III)-IMAC using 1,1,1,3,3,3-hexafluoroisopropanol. *Proteomics*, **5**, 4376-4388.

Barr, J.R., Maggio, V.L., Patterson, D.G., Jr., Cooper, G.R., Henderson, L.O., Turner, W.E., Smith, S.J., Hannon, W.H., Needham, L.L. and Sampson, E.J. (1996) Isotope dilution--mass spectrometric quantification of specific proteins: model application with apolipoprotein A-I. *Clin Chem*, **42**, 1676-1682.

Barroso, I., Luan, J., Middelberg, R.P., Harding, A.H., Franks, P.W., Jakes, R.W., Clayton, D., Schafer, A.J., O'Rahilly, S. and Wareham, N.J. (2003) Candidate gene association study in type 2 diabetes indicates a role for genes involved in beta-cell function as well as insulin action. *PLoS Biol*, **1**, E20.

Bavelloni, A., Santi, S., Sirri, A., Riccio, M., Faenza, I., Zini, N., Cecchi, S., Ferri, A., Auron, P., Maraldi, N.M. and Marmiroli, S. (1999) Phosphatidylinositol 3-kinase translocation to the nucleus is induced by interleukin 1 and prevented by mutation of interleukin 1 receptor in human osteosarcoma Saos-2 cells. *J Cell Sci*, **112 (Pt 5)**, 631-640.

Beckwith, M., Fenton, R.G., Katona, I.M. and Longo, D.L. (1996) Phosphatidylinositol-3-kinase activity is required for the anti-ig-mediated growth inhibition of a human B-lymphoma cell line. *Blood*, **87**, 202-210.

Beeton, C.A., Chance, E.M., Foukas, L.C. and Shepherd, P.R. (2000) Comparison of the kinetic properties of the lipid- and protein-kinase activities of the p110alpha and p110beta catalytic subunits of class-Ia phosphoinositide 3-kinases. *Biochem J*, **350 Pt 2**, 353-359.

Bellacosa, A., Chan, T.O., Ahmed, N.N., Datta, K., Malstrom, S., Stokoe, D., McCormick, F., Feng, J. and Tsichlis, P. (1998) Akt activation by growth factors is a multiple-step process: the role of the PH domain. *Oncogene*, **17**, 313-325.

Benes, C.H., Wu, N., Elia, A.E., Dharia, T., Cantley, L.C. and Soltoff, S.P. (2005) The C2 domain of PKCdelta is a phosphotyrosine binding domain. *Cell*, **121**, 271-280.

Benistant, C., Chapuis, H. and Roche, S. (2000) A specific function for phosphatidylinositol 3-kinase alpha (p85alpha-p110alpha) in cell survival and for phosphatidylinositol 3-kinase beta (p85alpha-p110beta) in de novo DNA synthesis of human colon carcinoma cells. *Oncogene*, **19**, 5083-5090.

Benvenuti, S., Cramer, R., Quinn, C.C., Bruce, J., Zvelebil, M., Corless, S., Bond, J., Yang, A., Hockfield, S., Burlingame, A.L., Waterfield, M.D. and Jat, P.S. (2002) Differential proteome analysis of replicative senescence in rat embryo fibroblasts. *Mol Cell Proteomics*, **1**, 280-292.

Beraud, C., Henzel, W.J. and Baeuerle, P.A. (1999) Involvement of regulatory and catalytic subunits of phosphoinositide 3-kinase in NF-kappaB activation. *Proc Natl Acad Sci U S A*, **96**, 429-434.

Bi, L., Okabe, I., Bernard, D.J. and Nussbaum, R.L. (2002) Early embryonic lethality in mice deficient in the p110beta catalytic subunit of PI 3-kinase. *Mamm Genome*, **13**, 169-172.

Bi, L., Okabe, I., Bernard, D.J., Wynshaw-Boris, A. and Nussbaum, R.L. (1999) Proliferative defect and embryonic lethality in mice homozygous for a deletion in the p110alpha subunit of phosphoinositide 3-kinase. *J Biol Chem*, **274**, 10963-10968.

Biemann, K. (1990) Sequencing of peptides by tandem mass spectrometry and high-energy collision-induced dissociation. *Methods Enzymol*, **193**, 455-479.

Bilancio, A., Okkenhaug, K., Camps, M., Emery, J.L., Ruckle, T., Rommel, C. and Vanhaesebroeck, B. (2006) Key role of the p110delta isoform of PI3K in B-cell antigen and IL-4 receptor signaling: comparative analysis of genetic and pharmacologic interference with p110delta function in B cells. *Blood*, **107**, 642-650.

Biondi, R.M., Kieloch, A., Currie, R.A., Deak, M. and Alessi, D.R. (2001) The PIF-binding pocket in PDK1 is essential for activation of S6K and SGK, but not PKB. *Embo J*, **20**, 4380-4390.

Bjellqvist, B., Ek, K., Righetti, P.G., Gianazza, E., Gorg, A., Westermeier, R. and Postel, W. (1982) Isoelectric focusing in immobilized pH gradients: principle, methodology and some applications. *J Biochem Biophys Methods*, **6**, 317-339.

Bokoch, G.M., Vlahos, C.J., Wang, Y., Knaus, U.G. and Traynor-Kaplan, A.E. (1996) Rac GTPase interacts specifically with phosphatidylinositol 3-kinase. *Biochem J*, **315 (Pt 3)**, 775-779.

Borer, R.A., Lehner, C.F., Eppenberger, H.M. and Nigg, E.A. (1989) Major nucleolar proteins shuttle between nucleus and cytoplasm. *Cell*, **56**, 379-390.

Borggrefe, T., Wabl, M., Akhmedov, A.T. and Jessberger, R. (1998) A B-cell-specific DNA recombination complex. *J Biol Chem*, **273**, 17025-17035.

Brachmann, S.M., Ueki, K., Engelman, J.A., Kahn, R.C. and Cantley, L.C. (2005) Phosphoinositide 3-kinase catalytic subunit deletion and regulatory subunit deletion have opposite effects on insulin sensitivity in mice. *Mol Cell Biol*, **25**, 1596-1607.

Brazil, D.P. and Hemmings, B.A. (2001) Ten years of protein kinase B signalling: a hard Akt to follow. *Trends Biochem Sci*, **26**, 657-664.

Brown, R.A., Domin, J., Arcaro, A., Waterfield, M.D. and Shepherd, P.R. (1999) Insulin activates the alpha isoform of class II phosphoinositide 3-kinase. *J Biol Chem*, **274**, 14529-14532.

Brown, W.J., DeWald, D.B., Emr, S.D., Plutner, H. and Balch, W.E. (1995) Role for phosphatidylinositol 3-kinase in the sorting and transport of newly synthesized lysosomal enzymes in mammalian cells. *J Cell Biol*, **130**, 781-796.

Brunet, A., Bonni, A., Zigmond, M.J., Lin, M.Z., Juo, P., Hu, L.S., Anderson, M.J., Arden, K.C., Blenis, J. and Greenberg, M.E. (1999) Akt promotes cell survival by phosphorylating and inhibiting a Forkhead transcription factor. *Cell*, **96**, 857-868.

Brunn, G.J., Williams, J., Sabers, C., Wiederrecht, G., Lawrence, J.C., Jr. and Abraham, R.T. (1996) Direct inhibition of the signaling functions of the mammalian target of rapamycin by the phosphoinositide 3-kinase inhibitors, wortmannin and LY294002. *Embo J*, **15**, 5256-5267.

Buhl, A.M. and Cambier, J.C. (1999) Phosphorylation of CD19 Y484 and Y515, and linked activation of phosphatidylinositol 3-kinase, are required for B cell antigen receptor-mediated activation of Bruton's tyrosine kinase. *J Immunol*, **162**, 4438-4446.

Buhl, A.M., Pleiman, C.M., Rickert, R.C. and Cambier, J.C. (1997) Qualitative regulation of B cell antigen receptor signaling by CD19: selective requirement for PI3-kinase activation, inositol-1,4,5-trisphosphate production and Ca2+ mobilization. *J Exp Med*, **186**, 1897-1910.

Burgering, B.M. and Coffer, P.J. (1995) Protein kinase B (c-Akt) in phosphatidylinositol-3-OH kinase signal transduction. *Nature*, **376**, 599-602.

Burgering, B.M. and Kops, G.J. (2002) Cell cycle and death control: long live Forkheads. *Trends Biochem Sci*, **27**, 352-360.

Burks, D.J., Wang, J., Towery, H., Ishibashi, O., Lowe, D., Riedel, H. and White, M.F. (1998) IRS pleckstrin homology domains bind to acidic motifs in proteins. *J Biol Chem*, **273**, 31061-31067.

Cambier, J.C., Pleiman, C.M. and Clark, M.R. (1994) Signal transduction by the B cell antigen receptor and its coreceptors. *Annu Rev Immunol*, **12**, 457-486.

Camps, M., Ruckle, T., Ji, H., Ardissone, V., Rintelen, F., Shaw, J., Ferrandi, C., Chabert, C., Gillieron, C., Francon, B., Martin, T., Gretener, D., Perrin, D., Leroy, D., Vitte, P.A., Hirsch, E., Wymann, M.P., Cirillo, R., Schwarz, M.K. and Rommel, C. (2005) Blockade of PI3Kgamma suppresses joint inflammation and damage in mouse models of rheumatoid arthritis. *Nat Med*, **11**, 936-943.

Cantley, L.C. and Neel, B.G. (1999) New insights into tumor suppression: PTEN suppresses tumor formation by restraining the phosphoinositide 3-kinase/AKT pathway. *Proc Natl Acad Sci U S A*, **96**, 4240-4245.

Cardone, M.H., Roy, N., Stennicke, H.R., Salvesen, G.S., Franke, T.F., Stanbridge, E., Frisch, S. and Reed, J.C. (1998) Regulation of cell death protease caspase-9 by phosphorylation. *Science*, **282**, 1318-1321.

Carey, G.B. and Scott, D.W. (2001) Role of phosphatidylinositol 3-kinase in anti-IgM- and anti-IgD-induced apoptosis in B cell lymphomas. *J Immunol*, **166**, 1618-1626.

Carpenter, C.L., Auger, K.R., Duckworth, B.C., Hou, W.M., Schaffhausen, B. and Cantley, L.C. (1993) A tightly associated serine/threonine protein kinase regulates phosphoinositide 3-kinase activity. *Mol Cell Biol*, **13**, 1657-1665.

Casamayor, A., Morrice, N.A. and Alessi, D.R. (1999) Phosphorylation of Ser-241 is essential for the activity of 3-phosphoinositide-dependent protein kinase-1: identification of five sites of phosphorylation in vivo. *Biochem J*, **342 (Pt 2)**, 287-292.

Cerione, R.A. and Zheng, Y. (1996) The Dbl family of oncogenes. *Curr Opin Cell Biol*, **8**, 216-222.

Chamberlain, M.D., Berry, T.R., Pastor, M.C. and Anderson, D.H. (2004) The p85alpha subunit of phosphatidylinositol 3'-kinase binds to and stimulates the GTPase activity of Rab proteins. *J Biol Chem*, **279**, 48607-48614.

Chan, T.O., Rodeck, U., Chan, A.M., Kimmelman, A.C., Rittenhouse, S.E., Panayotou, G. and Tsichlis, P.N. (2002) Small GTPases and tyrosine kinases coregulate a molecular switch in the phosphoinositide 3-kinase regulatory subunit. *Cancer Cell*, **1**, 181-191.

Chen, D., Mauvais-Jarvis, F., Bluher, M., Fisher, S.J., Jozsi, A., Goodyear, L.J., Ueki, K. and Kahn, C.R. (2004) p50alpha/p55alpha phosphoinositide 3-kinase knockout mice exhibit enhanced insulin sensitivity. *Mol Cell Biol*, **24**, 320-329.

Chen, D., Mauvais-Jarvis, F., Bluher, M., Fisher, S.J., Jozsi, A., Goodyear, L.J., Ueki, K., Kahn, C.R., Fruman, D.A., Hirshman, M.F., Sakamoto, K., Iannacone, M., Accili, D. and Cantley, L.C. (2004) p50alpha/p55alpha phosphoinositide 3-kinase knockout mice exhibit enhanced insulin sensitivity

Reduced expression of the murine p85alpha subunit of phosphoinositide 3-kinase improves insulin signaling and ameliorates diabetes. *Mol Cell Biol*, **24**, 320-329.

Cheng, X., Ma, Y., Moore, M., Hemmings, B.A. and Taylor, S.S. (1998) Phosphorylation and activation of cAMP-dependent protein kinase by phosphoinositide-dependent protein kinase. *Proc Natl Acad Sci U S A*, **95**, 9849-9854.

Chou, M.M., Hou, W., Johnson, J., Graham, L.K., Lee, M.H., Chen, C.S., Newton, A.C., Schaffhausen, B.S. and Toker, A. (1998) Regulation of protein kinase C zeta by PI 3-kinase and PDK-1. *Curr Biol*, **8**, 1069-1077.

Christoforidis, S., Miaczynska, M., Ashman, K., Wilm, M., Zhao, L., Yip, S.C., Waterfield, M.D., Backer, J.M. and Zerial, M. (1999) Phosphatidylinositol-3-OH kinases are Rab5 effectors. *Nat Cell Biol*, **1**, 249-252.

Clark, M.R., Campbell, K.S., Kazlauskas, A., Johnson, S.A., Hertz, M., Potter, T.A., Pleiman, C. and Cambier, J.C. (1992) The B cell antigen receptor complex: association of Ig-alpha and Ig-beta with distinct cytoplasmic effectors. *Science*, **258**, 123-126.

Clayton, E., Bardi, G., Bell, S.E., Chantry, D., Downes, C.P., Gray, A., Humphries, L.A., Rawlings, D., Reynolds, H., Vigorito, E. and Turner, M. (2002) A crucial role for the

p110delta subunit of phosphatidylinositol 3-kinase in B cell development and activation. *J Exp Med*, **196**, 753-763.

Clement, S., Krause, U., Desmedt, F., Tanti, J.F., Behrends, J., Pesesse, X., Sasaki, T., Penninger, J., Doherty, M., Malaisse, W., Dumont, J.E., Le Marchand-Brustel, Y., Erneux, C., Hue, L. and Schurmans, S. (2001) The lipid phosphatase SHIP2 controls insulin sensitivity. *Nature*, **409**, 92-97.

Cohen, B., Liu, Y.X., Druker, B., Roberts, T.M. and Schaffhausen, B.S. (1990) Characterization of pp85, a target of oncogenes and growth factor receptors. *Mol Cell Biol*, **10**, 2909-2915.

Cohen, B., Yoakim, M., Piwnica-Worms, H., Roberts, T.M. and Schaffhausen, B.S. (1990) Tyrosine phosphorylation is a signal for the trafficking of pp85, an 85-kDa phosphorylated polypeptide associated with phosphatidylinositol kinase activity. *Proc Natl Acad Sci U S A*, **87**, 4458-4462.

Cohen, P. (1989) The structure and regulation of protein phosphatases. *Annu Rev Biochem*, **58**, 453-508.

Condliffe, A.M., Davidson, K., Anderson, K.E., Ellson, C.D., Crabbe, T., Okkenhaug, K., Vanhaesebroeck, B., Turner, M., Webb, L., Wymann, M.P., Hirsch, E., Ruckle, T., Camps, M., Rommel, C., Jackson, S.P., Chilvers, E.R., Stephens, L.R. and Hawkins, P.T. (2005) Sequential activation of class IB and class IA PI3K is important for the primed respiratory burst of human but not murine neutrophils. *Blood*, **106**, 1432-1440.

Conus, N.M., Hannan, K.M., Cristiano, B.E., Hemmings, B.A. and Pearson, R.B. (2002) Direct identification of tyrosine 474 as a regulatory phosphorylation site for the Akt protein kinase. *J Biol Chem*, **277**, 38021-38028.

Cornillet-Lefebvre, P., Cuccuini, W., Bardet, V., Tamburini, J., Gillot, L., Ifrah, N., Nguyen, P., Dreyfus, F., Mayeux, P., Lacombe, C. and Bouscary, D. (2006) Constitutive phosphoinositide 3-kinase activation in acute myeloid leukemia is not due to p110delta mutations. *Leukemia*, **20**, 374-376.

Cotter, R.J. (1989) Time-of-flight mass spectrometry: an increasing role in the life sciences. *Biomed Environ Mass Spectrom*, **18**, 513-532.

Crackower, M.A., Oudit, G.Y., Kozieradzki, I., Sarao, R., Sun, H., Sasaki, T., Hirsch, E., Suzuki, A., Shioi, T., Irie-Sasaki, J., Sah, R., Cheng, H.Y., Rybin, V.O., Lembo, G., Fratta, L., Oliveira-dos-Santos, A.J., Benovic, J.L., Kahn, C.R., Izumo, S., Steinberg, S.F., Wymann, M.P., Backx, P.H. and Penninger, J.M. (2002) Regulation of myocardial contractility and cell size by distinct PI3K-PTEN signaling pathways. *Cell*, **110**, 737-749.

Craxton, A., Jiang, A., Kurosaki, T. and Clark, E.A. (1999) Syk and Bruton's tyrosine kinase are required for B cell antigen receptor-mediated activation of the kinase Akt. *J Biol Chem*, **274**, 30644-30650.

Cuevas, B., Lu, Y., Watt, S., Kumar, R., Zhang, J., Siminovitch, K.A. and Mills, G.B. (1999) SHP-1 regulates Lck-induced phosphatidylinositol 3-kinase phosphorylation and activity. *J Biol Chem*, **274**, 27583-27589.

Cuevas, B.D., Lu, Y., Mao, M., Zhang, J., LaPushin, R., Siminovitch, K. and Mills, G.B. (2001) Tyrosine phosphorylation of p85 relieves its inhibitory activity on phosphatidylinositol 3-kinase. *J Biol Chem*, **276**, 27455-27461.

Cutillas, P.R., Geering, B., Waterfield, M.D. and Vanhaesebroeck, B. (2005) Quantification of gel-separated proteins and their phosphorylation sites by LC-MS using unlabeled internal standards: analysis of phosphoprotein dynamics in a B cell lymphoma cell line. *Mol Cell Proteomics*, **4**, 1038-1051.

Czupalla, C., Culo, M., Muller, E.C., Brock, C., Reusch, H.P., Spicher, K., Krause, E. and Nurnberg, B. (2003) Identification and characterization of the autophosphorylation sites of phosphoinositide 3-kinase isoforms beta and gamma. *J Biol Chem*, **278**, 11536-11545.

Czupalla, C., Nurnberg, B. and Krause, E. (2003) Analysis of class I phosphoinositide 3-kinase autophosphorylation sites by mass spectrometry. *Rapid Commun Mass Spectrom*, **17**, 690-696.

D'Souza-Schorey, C., Boshans, R.L., McDonough, M., Stahl, P.D. and Van Aelst, L. (1997) A role for POR1, a Rac1-interacting protein, in ARF6-mediated cytoskeletal rearrangements. *Embo J*, **16**, 5445-5454.

Dal Porto, J.M., Gauld, S.B., Merrell, K.T., Mills, D., Pugh-Bernard, A.E. and Cambier, J. (2004) B cell antigen receptor signaling 101. *Mol Immunol*, **41**, 599-613.

Damen, J.E., Liu, L., Rosten, P., Humphries, R.K., Jefferson, A.B., Majerus, P.W. and Krystal, G. (1996) The 145-kDa protein induced to associate with Shc by multiple cytokines is an

inositol tetraphosphate and phosphatidylinositol 3,4,5-triphosphate 5-phosphatase. *Proc Natl Acad Sci U S A*, **93**, 1689-1693.

Datta, K., Bellacosa, A., Chan, T.O. and Tsichlis, P.N. (1996) Akt is a direct target of the phosphatidylinositol 3-kinase. Activation by growth factors, v-src and v-Ha-ras, in Sf9 and mammalian cells. *J Biol Chem*, **271**, 30835-30839.

Deane, J.A. and Fruman, D.A. (2004) Phosphoinositide 3-kinase: diverse roles in immune cell activation. *Annu Rev Immunol*, **22**, 563-598.

Deane, J.A., Trifilo, M.J., Yballe, C.M., Choi, S., Lane, T.E. and Fruman, D.A. (2004) Enhanced T cell proliferation in mice lacking the p85beta subunit of phosphoinositide 3-kinase. *J Immunol*, **172**, 6615-6625.

Dennehy, K.M., Broszeit, R., Garnett, D., Durrheim, G.A., Spruyt, L.L. and Beyers, A.D. (1997) Thymocyte activation induces the association of phosphatidylinositol 3-kinase and pp120 with CD5. *Eur J Immunol*, **27**, 679-686.

Deprez, J., Vertommen, D., Alessi, D.R., Hue, L. and Rider, M.H. (1997) Phosphorylation and activation of heart 6-phosphofructo-2-kinase by protein kinase B and other protein kinases of the insulin signaling cascades. *J Biol Chem*, **272**, 17269-17275.

Dhand, R., Hara, K., Hiles, I., Bax, B., Gout, I., Panayotou, G., Fry, M.J., Yonezawa, K., Kasuga, M. and Waterfield, M.D. (1994) PI 3-kinase: structural and functional analysis of intersubunit interactions. *Embo J*, **13**, 511-521.

Dhand, R., Hiles, I., Panayotou, G., Roche, S., Fry, M.J., Gout, I., Totty, N.F., Truong, O., Vicendo, P., Yonezawa, K. and et al. (1994) PI 3-kinase is a dual specificity enzyme: autoregulation by an intrinsic protein-serine kinase activity. *Embo J*, **13**, 522-533.

Di Cristofano, A., Pesce, B., Cordon-Cardo, C. and Pandolfi, P.P. (1998) Pten is essential for embryonic development and tumour suppression. *Nat Genet*, **19**, 348-355.

Didichenko, S.A., Tilton, B., Hemmings, B.A., Ballmer-Hofer, K. and Thelen, M. (1996) Constitutive activation of protein kinase B and phosphorylation of p47phox by a membrane-targeted phosphoinositide 3-kinase. *Curr Biol*, **6**, 1271-1278.

Dijkers, P.F., Medema, R.H., Pals, C., Banerji, L., Thomas, N.S., Lam, E.W., Burgering, B.M., Raaijmakers, J.A., Lammers, J.W., Koenderman, L. and Coffer, P.J. (2000) Forkhead transcription factor FKHR-L1 modulates cytokine-dependent transcriptional regulation of p27(KIP1). *Mol Cell Biol*, **20**, 9138-9148.

Domin, J., Pages, F., Volinia, S., Rittenhouse, S.E., Zvelebil, M.J., Stein, R.C. and Waterfield, M.D. (1997) Cloning of a human phosphoinositide 3-kinase with a C2 domain that displays reduced sensitivity to the inhibitor wortmannin. *Biochem J*, **326 (Pt 1)**, 139-147.

Donjerkovic, D. and Scott, D.W. (2000) Activation-induced cell death in B lymphocytes. *Cell Res*, **10**, 179-192.

Downward, J. (1999) How BAD phosphorylation is good for survival. *Nat Cell Biol*, **1**, E33-35.

Du, K. and Montminy, M. (1998) CREB is a regulatory target for the protein kinase Akt/PKB. *J Biol Chem*, **273**, 32377-32379.

Durocher, D., Henckel, J., Fersht, A.R. and Jackson, S.P. (1999) The FHA domain is a modular phosphopeptide recognition motif. *Mol Cell*, **4**, 387-394.

Dutil, E.M., Toker, A. and Newton, A.C. (1998) Regulation of conventional protein kinase C isozymes by phosphoinositide-dependent kinase 1 (PDK-1). *Curr Biol*, **8**, 1366-1375.

el-Remessy, A.B., Bartoli, M., Platt, D.H., Fulton, D. and Caldwell, R.B. (2005) Oxidative stress inactivates VEGF survival signaling in retinal endothelial cells via PI 3-kinase tyrosine nitration. *J Cell Sci*, **118**, 243-252.

End, P., Gout, I., Fry, M.J., Panayotou, G., Dhand, R., Yonezawa, K., Kasuga, M. and Waterfield, M.D. (1993) A biosensor approach to probe the structure and function of the p85 alpha subunit of the phosphatidylinositol 3-kinase complex. *J Biol Chem*, **268**, 10066-10075.

Escobedo, J.A., Kaplan, D.R., Kavanaugh, W.M., Turck, C.W. and Williams, L.T. (1991) A phosphatidylinositol-3 kinase binds to platelet-derived growth factor receptors through a specific receptor sequence containing phosphotyrosine. *Mol Cell Biol*, **11**, 1125-1132.

Escobedo, J.A., Navankasattusas, S., Kavanaugh, W.M., Milfay, D., Fried, V.A. and Williams, L.T. (1991) cDNA cloning of a novel 85 kd protein that has SH2 domains and regulates binding of PI3-kinase to the PDGF beta-receptor. *Cell*, **65**, 75-82.

Fang, D. and Liu, Y.C. (2001) Proteolysis-independent regulation of PI3K by Cbl-b-mediated ubiquitination in T cells. *Nat Immunol*, **2**, 870-875.

Fang, D., Wang, H.Y., Fang, N., Altman, Y., Elly, C. and Liu, Y.C. (2001) Cbl-b, a RING-type E3 ubiquitin ligase, targets phosphatidylinositol 3-kinase for ubiquitination in T cells. *J Biol Chem*, **276**, 4872-4878.

Fantus, I.G., Kadota, S., Deragon, G., Foster, B. and Posner, B.I. (1989) Pervanadate [peroxide(s) of vanadate] mimics insulin action in rat adipocytes via activation of the insulin receptor tyrosine kinase. *Biochemistry*, **28**, 8864-8871.

Farias, E.F., Marzan, C. and Mira-y-Lopez, R. (2005) Cellular retinol-binding protein-I inhibits PI3K/Akt signaling through a retinoic acid receptor-dependent mechanism that regulates p85-p110 heterodimerization. *Oncogene*, **24**, 1598-1606.

Fenn, J.B., Mann, M., Meng, C.K., Wong, S.F. and Whitehouse, C.M. (1989) Electrospray ionization for mass spectrometry of large biomolecules. *Science*, **246**, 64-71.

Ficarro, S.B., McCleland, M.L., Stukenberg, P.T., Burke, D.J., Ross, M.M., Shabanowitz, J., Hunt, D.F. and White, F.M. (2002) Phosphoproteome analysis by mass spectrometry and its application to Saccharomyces cerevisiae. *Nat Biotechnol*, **20**, 301-305.

Fluckiger, A.C., Li, Z., Kato, R.M., Wahl, M.I., Ochs, H.D., Longnecker, R., Kinet, J.P., Witte, O.N., Scharenberg, A.M. and Rawlings, D.J. (1998) Btk/Tec kinases regulate sustained increases in intracellular Ca2+ following B-cell receptor activation. *Embo J*, **17**, 1973-1985.

Forssell, J., Nilsson, A. and Sideras, P. (1999) Bruton's tyrosine-kinase-deficient murine B lymphocytes fail to enter S phase when stimulated with anti-immunoglobulin plus interleukin-4. *Scand J Immunol*, **49**, 155-161.

Foukas, L.C., Beeton, C.A., Jensen, J., Phillips, W.A. and Shepherd, P.R. (2004) Regulation of phosphoinositide 3-kinase by its intrinsic serine kinase activity in vivo. *Mol Cell Biol*, **24**, 966-975.

Foukas, L.C., Claret, M., Pearce, W., Okkenhaug, K., Meek, S., Peskett, E., Sancho, S., Smith, A.J., Withers, D.J. and Vanhaesebroeck, B. (2006) Critical role for the p110alpha phosphoinositide-3-OH kinase in growth and metabolic regulation. *Nature*.

Foukas, L.C. and Shepherd, P.R. (2004) eIF4E binding protein 1 and H-Ras are novel substrates for the protein kinase activity of class-I phosphoinositide 3-kinase. *Biochem Biophys Res Commun*, **319**, 541-549.

Foukas, L.C. and Shepherd, P.R. (2004) Phosphoinositide 3-kinase: the protein kinase that time forgot. *Biochem Soc Trans*, **32**, 330-331.

Frevert, E.U. and Kahn, B.B. (1997) Differential effects of constitutively active phosphatidylinositol 3-kinase on glucose transport, glycogen synthase activity, and DNA synthesis in 3T3-L1 adipocytes. *Mol Cell Biol*, **17**, 190-198.

Fruman, D.A., Cantley, L.C. and Carpenter, C.L. (1996) Structural organization and alternative splicing of the murine phosphoinositide 3-kinase p85 alpha gene. *Genomics*, **37**, 113-121.

Fruman, D.A., Mauvais-Jarvis, F., Pollard, D.A., Yballe, C.M., Brazil, D., Bronson, R.T., Kahn, C.R. and Cantley, L.C. (2000) Hypoglycaemia, liver necrosis and perinatal death in mice lacking all isoforms of phosphoinositide 3-kinase p85 alpha. *Nat Genet*, **26**, 379-382.

Fruman, D.A., Snapper, S.B., Yballe, C.M., Alt, F.W. and Cantley, L.C. (1999) Phosphoinositide 3-kinase knockout mice: role of p85alpha in B cell development and proliferation. *Biochem Soc Trans*, **27**, 624-629.

Fruman, D.A., Snapper, S.B., Yballe, C.M., Davidson, L., Yu, J.Y., Alt, F.W. and Cantley, L.C. (1999) Impaired B cell development and proliferation in absence of phosphoinositide 3-kinase p85alpha. *Science*, **283**, 393-397.

Fry, M.J., Panayotou, G., Dhand, R., Ruiz-Larrea, F., Gout, I., Nguyen, O., Courtneidge, S.A. and Waterfield, M.D. (1992) Purification and characterization of a phosphatidylinositol 3-kinase complex from bovine brain by using phosphopeptide affinity columns. *Biochem J*, **288 (Pt 2)**, 383-393.

Fu, C., Turck, C.W., Kurosaki, T. and Chan, A.C. (1998) BLNK: a central linker protein in B cell activation. *Immunity*, **9**, 93-103.

Fu, Z., Aronoff-Spencer, E., Wu, H., Gerfen, G.J. and Backer, J.M. (2004) The iSH2 domain of PI 3-kinase is a rigid tether for p110 and not a conformational switch. *Arch Biochem Biophys*, **432**, 244-251.

Fukui, Y. and Hanafusa, H. (1989) Phosphatidylinositol kinase activity associates with viral p60src protein. *Mol Cell Biol*, **9**, 1651-1658.

Funaki, M., Katagiri, H., Inukai, K., Kikuchi, M. and Asano, T. (2000) Structure and function of phosphatidylinositol-3,4 kinase. *Cell Signal*, **12**, 135-142.

Gautreau, A., Poullet, P., Louvard, D. and Arpin, M. (1999) Ezrin, a plasma membrane-microfilament linker, signals cell survival through the phosphatidylinositol 3-kinase/Akt pathway. *Proc Natl Acad Sci U S A*, **96**, 7300-7305.

Geltz, N.R. and Augustine, J.A. (1998) The p85 and p110 subunits of phosphatidylinositol 3-kinase-alpha are substrates, in vitro, for a constitutively associated protein tyrosine kinase in platelets. *Blood*, **91**, 930-939.

Gerber, S.A., Rush, J., Stemman, O., Kirschner, M.W. and Gygi, S.P. (2003) Absolute quantification of proteins and phosphoproteins from cell lysates by tandem MS. *Proc Natl Acad Sci U S A*, **100**, 6940-6945.

Giallourakis, C., Kashiwada, M., Pan, P.Y., Danial, N., Jiang, H., Cambier, J., Coggeshall, K.M. and Rothman, P. (2000) Positive regulation of interleukin-4-mediated proliferation by the SH2-containing inositol-5'-phosphatase. *J Biol Chem*, **275**, 29275-29282.

Ginisty, H., Sicard, H., Roger, B. and Bouvet, P. (1999) Structure and functions of nucleolin. *J Cell Sci*, **112 (Pt 6)**, 761-772.

Giorgino, F., Pedrini, M.T., Matera, L. and Smith, R.J. (1997) Specific increase in p85alpha expression in response to dexamethasone is associated with inhibition of insulin-like growth factor-I stimulated phosphatidylinositol 3-kinase activity in cultured muscle cells. *J Biol Chem*, **272**, 7455-7463.

Gold, M.R., Scheid, M.P., Santos, L., Dang-Lawson, M., Roth, R.A., Matsuuchi, L., Duronio, V. and Krebs, D.L. (1999) The B Cell Antigen Receptor Activates the Akt (Protein Kinase B)/Glycogen Synthase Kinase-3 Signaling Pathway Via Phosphatidylinositol 3-Kinase. *J Immunol*, **163**, 1894-1905.

Gorg, A., Obermaier, C., Boguth, G., Harder, A., Scheibe, B., Wildgruber, R. and Weiss, W. (2000) The current state of two-dimensional electrophoresis with immobilized pH gradients. *Electrophoresis*, **21**, 1037-1053.

Gorg, A., Postel, W. and Johann, P. (1985) pH, urea and substrate gradients for the optimization of ultrathin polyacrylamide gel zymograms. *J Biochem Biophys Methods*, **10**, 341-350.

Gotoh, A., Miyazawa, K., Ohyashiki, K. and Toyama, K. (1994) Potential molecules implicated in downstream signaling pathways of p185BCR-ABL in Ph+ ALL involve GTPase-activating protein, phospholipase C-gamma 1, and phosphatidylinositol 3'-kinase. *Leukemia*, **8**, 115-120.

Gout, I., Dhand, R., Hiles, I.D., Fry, M.J., Panayotou, G., Das, P., Truong, O., Totty, N.F., Hsuan, J., Booker, G.W. and et al. (1993) The GTPase dynamin binds to and is activated by a subset of SH3 domains. *Cell*, **75**, 25-36.

Gout, I., Middleton, G., Adu, J., Ninkina, N.N., Drobot, L.B., Filonenko, V., Matsuka, G., Davies, A.M., Waterfield, M. and Buchman, V.L. (2000) Negative regulation of PI 3-kinase by Ruk, a novel adaptor protein. *Embo J*, **19**, 4015-4025.

Grill, B., Wilson, G.M., Zhang, K.X., Wang, B., Doyonnas, R., Quadroni, M. and Schrader, J.W. (2004) Activation/division of lymphocytes results in increased levels of cytoplasmic activation/proliferation-associated protein-1: prototype of a new family of proteins. *J Immunol*, **172**, 2389-2400.

Groisman, R., Polanowska, J., Kuraoka, I., Sawada, J., Saijo, M., Drapkin, R., Kisselev, A.F., Tanaka, K. and Nakatani, Y. (2003) The ubiquitin ligase activity in the DDB2 and CSA complexes is differentially regulated by the COP9 signalosome in response to DNA damage. *Cell*, **113**, 357-367.

Gronborg, M., Kristiansen, T.Z., Stensballe, A., Andersen, J.S., Ohara, O., Mann, M., Jensen, O.N. and Pandey, A. (2002) A mass spectrometry-based proteomic approach for identification of serine/threonine-phosphorylated proteins by enrichment with phospho-specific antibodies: identification of a novel protein, Frigg, as a protein kinase A substrate. *Mol Cell Proteomics*, **1**, 517-527.

Gu, H., Maeda, H., Moon, J.J., Lord, J.D., Yoakim, M., Nelson, B.H. and Neel, B.G. (2000) New role for Shc in activation of the phosphatidylinositol 3-kinase/Akt pathway. *Mol Cell Biol*, **20**, 7109-7120.

Guo, S., Rena, G., Cichy, S., He, X., Cohen, P. and Unterman, T. (1999) Phosphorylation of serine 256 by protein kinase B disrupts transactivation by FKHR and mediates effects of insulin on insulin-like growth factor-binding protein-1 promoter activity through a conserved insulin response sequence. *J Biol Chem*, **274**, 17184-17192.

Gupta, N., Scharenberg, A.M., Fruman, D.A., Cantley, L.C., Kinet, J.P. and Long, E.O. (1999) The SH2 domain-containing inositol 5'-phosphatase (SHIP) recruits the p85 subunit of phosphoinositide 3-kinase during FcgammaRIIb1-mediated inhibition of B cell receptor signaling. *J Biol Chem*, **274**, 7489-7494.

Gygi, S.P., Rist, B., Gerber, S.A., Turecek, F., Gelb, M.H. and Aebersold, R. (1999) Quantitative analysis of complex protein mixtures using isotope-coded affinity tags. *Nat Biotechnol*, **17**, 994-999.

Habib, T., Hejna, J.A., Moses, R.E. and Decker, S.J. (1998) Growth factors and insulin stimulate tyrosine phosphorylation of the 51C/SHIP2 protein. *J Biol Chem*, **273**, 18605-18609.

Han, J., Luby-Phelps, K., Das, B., Shu, X., Xia, Y., Mosteller, R.D., Krishna, U.M., Falck, J.R., White, M.A. and Broek, D. (1998) Role of substrates and products of PI 3-kinase in regulating activation of Rac-related guanosine triphosphatases by Vav. *Science*, **279**, 558-560.

Hansen, T., Andersen, C.B., Echwald, S.M., Urhammer, S.A., Clausen, J.O., Vestergaard, H., Owens, D., Hansen, L. and Pedersen, O. (1997) Identification of a common amino acid polymorphism in the p85alpha regulatory subunit of phosphatidylinositol 3-kinase: effects on glucose disappearance constant, glucose effectiveness, and the insulin sensitivity index. *Diabetes*, **46**, 494-501.

Haren, L., Remy, M.H., Bazin, I., Callebaut, I., Wright, M. and Merdes, A. (2006) NEDD1-dependent recruitment of the gamma-tubulin ring complex to the centrosome is necessary for centriole duplication and spindle assembly. *J Cell Biol*, **172**, 505-515.

Harpur, A.G., Layton, M.J., Das, P., Bottomley, M.J., Panayotou, G., Driscoll, P.C. and Waterfield, M.D. (1999) Intermolecular interactions of the p85alpha regulatory subunit of phosphatidylinositol 3-kinase. *J Biol Chem*, **274**, 12323-12332.

Harrison-Findik, D., Susa, M. and Varticovski, L. (1995) Association of phosphatidylinositol 3-kinase with SHC in chronic myelogeneous leukemia cells. *Oncogene*, **10**, 1385-1391.

Hartley, D., Meisner, H. and Corvera, S. (1995) Specific association of the beta isoform of the p85 subunit of phosphatidylinositol-3 kinase with the proto-oncogene c-cbl. *J Biol Chem*, **270**, 18260-18263.

Hartley, K.O., Gell, D., Smith, G.C., Zhang, H., Divecha, N., Connelly, M.A., Admon, A., Lees-Miller, S.P., Anderson, C.W. and Jackson, S.P. (1995) DNA-dependent protein kinase catalytic subunit: a relative of phosphatidylinositol 3-kinase and the ataxia telangiectasia gene product. *Cell*, **82**, 849-856.

Hawkins, P.T., Jackson, T.R. and Stephens, L.R. (1992) Platelet-derived growth factor stimulates synthesis of PtdIns(3,4,5)P3 by activating a PtdIns(4,5)P2 3-OH kinase. *Nature*, **358**, 157-159.

Hayashi, H., Kamohara, S., Nishioka, Y., Kanai, F., Miyake, N., Fukui, Y., Shibasaki, F., Takenawa, T. and Ebina, Y. (1992) Insulin treatment stimulates the tyrosine phosphorylation of the alpha-type 85-kDa subunit of phosphatidylinositol 3-kinase in vivo. *J Biol Chem*, **267**, 22575-22580.

Hayashi, H., Miyake, N., Kanai, F., Shibasaki, F., Takenawa, T. and Ebina, Y. (1991) Phosphorylation in vitro of the 85 kDa subunit of phosphatidylinositol 3-kinase and its possible activation by insulin receptor tyrosine kinase. *Biochem J*, **280 (Pt 3)**, 769-775.

Hayashi, H., Nishioka, Y., Kamohara, S., Kanai, F., Ishii, K., Fukui, Y., Shibasaki, F., Takenawa, T., Kido, H., Katsunuma, N. and et al. (1993) The alpha-type 85-kDa subunit of phosphatidylinositol 3-kinase is phosphorylated at tyrosines 368, 580, and 607 by the insulin receptor. *J Biol Chem*, **268**, 7107-7117.

He, W., Craparo, A., Zhu, Y., O'Neill, T.J., Wang, L.M., Pierce, J.H. and Gustafson, T.A. (1996) Interaction of insulin receptor substrate-2 (IRS-2) with the insulin and insulin-like growth factor I receptors. Evidence for two distinct phosphotyrosine-dependent interaction domains within IRS-2. *J Biol Chem*, **271**, 11641-11645.

He, Z., Ismail, A., Kriazhev, L., Sadvakassova, G. and Bateman, A. (2002) Progranulin (PC-cell-derived growth factor/acrogranin) regulates invasion and cell survival. *Cancer Res*, **62**, 5590-5596.

Hellberg, C.B., Boggs, S.E. and Lapetina, E.G. (1998) Phosphatidylinositol 3-kinase is a target for protein tyrosine nitration. *Biochem Biophys Res Commun*, **252**, 313-317.

Herman, P.K. and Emr, S.D. (1990) Characterization of VPS34, a gene required for vacuolar protein sorting and vacuole segregation in Saccharomyces cerevisiae. *Mol Cell Biol*, **10**, 6742-6754.

Herman, P.K., Stack, J.H. and Emr, S.D. (1992) An essential role for a protein and lipid kinase complex in secretory protein sorting. *Trends Cell Biol*, **2**, 363-368.

Hiles, I.D., Otsu, M., Volinia, S., Fry, M.J., Gout, I., Dhand, R., Panayotou, G., Ruiz-Larrea, F., Thompson, A., Totty, N.F. and et al. (1992) Phosphatidylinositol 3-kinase: structure and expression of the 110 kd catalytic subunit. *Cell*, **70**, 419-429.

Hirsch, E., Katanaev, V.L., Garlanda, C., Azzolino, O., Pirola, L., Silengo, L., Sozzani, S., Mantovani, A., Altruda, F. and Wymann, M.P. (2000) Central role for G protein-coupled phosphoinositide 3-kinase gamma in inflammation. *Science*, **287**, 1049-1053.

Holt, K.H., Olson, L., Moye-Rowley, W.S. and Pessin, J.E. (1994) Phosphatidylinositol 3-kinase activation is mediated by high-affinity interactions between distinct domains within the p110 and p85 subunits. *Mol Cell Biol*, **14**, 42-49.

Hooshmand-Rad, R., Hajkova, L., Klint, P., Karlsson, R., Vanhaesebroeck, B., Claesson-Welsh, L. and Heldin, C.H. (2000) The PI 3-kinase isoforms p110(alpha) and p110(beta) have differential roles in PDGF- and insulin-mediated signaling. *J Cell Sci*, **113 Pt 2**, 207-214.

Hu, P., Margolis, B., Skolnik, E.Y., Lammers, R., Ullrich, A. and Schlessinger, J. (1992) Interaction of phosphatidylinositol 3-kinase-associated p85 with epidermal growth factor and platelet-derived growth factor receptors. *Mol Cell Biol*, **12**, 981-990.

Hu, P., Mondino, A., Skolnik, E.Y. and Schlessinger, J. (1993) Cloning of a novel, ubiquitously expressed human phosphatidylinositol 3-kinase and identification of its binding site on p85. *Mol Cell Biol*, **13**, 7677-7688.

Hubbard, M.J. and Cohen, P. (1993) On target with a new mechanism for the regulation of protein phosphorylation. *Trends Biochem Sci*, **18**, 172-177.

Huddleson, J.P., Ahmad, N. and Lingrel, J.B. (2006) Upregulation of the KLF2 transcription factor by fluid shear stress requires nucleolin. *J Biol Chem*.

Hunter, T. (1995) Protein kinases and phosphatases: the yin and yang of protein phosphorylation and signaling. *Cell*, **80**, 225-236.

Huyer, G., Liu, S., Kelly, J., Moffat, J., Payette, P., Kennedy, B., Tsaprailis, G., Gresser, M.J. and Ramachandran, C. (1997) Mechanism of inhibition of protein-tyrosine phosphatases by vanadate and pervanadate. *J Biol Chem*, **272**, 843-851.

Inabe, K. and Kurosaki, T. (2002) Tyrosine phosphorylation of B-cell adaptor for phosphoinositide 3-kinase is required for Akt activation in response to CD19 engagement. *Blood*, **99**, 584-589.

Inukai, K., Anai, M., Van Breda, E., Hosaka, T., Katagiri, H., Funaki, M., Fukushima, Y., Ogihara, T., Yazaki, Y., Kikuchi, Oka, Y. and Asano, T. (1996) A novel 55-kDa regulatory subunit for phosphatidylinositol 3-kinase structurally similar to p55PIK Is generated by alternative splicing of the p85alpha gene. *J Biol Chem*, **271**, 5317-5320.

Inukai, K., Funaki, M., Nawano, M., Katagiri, H., Ogihara, T., Anai, M., Onishi, Y., Sakoda, H., Ono, H., Fukushima, Y., Kikuchi, M., Oka, Y. and Asano, T. (2000) The N-terminal 34 residues of the 55 kDa regulatory subunits of phosphoinositide 3-kinase interact with tubulin. *Biochem J*, **346 Pt 2**, 483-489.

Inukai, K., Funaki, M., Ogihara, T., Katagiri, H., Kanda, A., Anai, M., Fukushima, Y., Hosaka, T., Suzuki, M., Shin, B.C., Takata, K., Yazaki, Y., Kikuchi, M., Oka, Y. and Asano, T. (1997) p85alpha gene generates three isoforms of regulatory subunit for phosphatidylinositol 3-kinase (PI 3-Kinase), p50alpha, p55alpha, and p85alpha, with different PI 3-kinase activity elevating responses to insulin. *J Biol Chem*, **272**, 7873-7882.

Izzard, R.A., Jackson, S.P. and Smith, G.C. (1999) Competitive and noncompetitive inhibition of the DNA-dependent protein kinase. *Cancer Res*, **59**, 2581-2586.

Jackson, S.P., Schoenwaelder, S.M., Goncalves, I., Nesbitt, W.S., Yap, C.L., Wright, C.E., Kenche, V., Anderson, K.E., Dopheide, S.M., Yuan, Y., Sturgeon, S.A., Prabaharan, H., Thompson, P.E., Smith, G.D., Shepherd, P.R., Daniele, N., Kulkarni, S., Abbott, B., Saylik, D., Jones, C., Lu, L., Giuliano, S., Hughan, S.C., Angus, J.A., Robertson, A.D. and Salem, H.H. (2005) PI 3-kinase p110beta: a new target for antithrombotic therapy. *Nat Med*, **11**, 507-514.

Jimenez, C., Hernandez, C., Pimentel, B. and Carrera, A.C. (2002) The p85 regulatory subunit controls sequential activation of phosphoinositide 3-kinase by Tyr kinases and Ras. *J Biol Chem*, **277**, 41556-41562.

Johnston, J.A., Wang, L.M., Hanson, E.P., Sun, X.J., White, M.F., Oakes, S.A., Pierce, J.H. and O'Shea, J.J. (1995) Interleukins 2, 4, 7, and 15 stimulate tyrosine phosphorylation of insulin

receptor substrates 1 and 2 in T cells. Potential role of JAK kinases. *J Biol Chem*, **270**, 28527-28530.

Jou, S.T., Carpino, N., Takahashi, Y., Piekorz, R., Chao, J.R., Wang, D. and Ihle, J.N. (2002) Essential, nonredundant role for the phosphoinositide 3-kinase p110delta in signaling by the B-cell receptor complex. *Mol Cell Biol*, **22**, 8580-8591.

Jumaa, H., Wollscheid, B., Mitterer, M., Wienands, J., Reth, M. and Nielsen, P.J. (1999) Abnormal development and function of B lymphocytes in mice deficient for the signaling adaptor protein SLP-65. *Immunity*, **11**, 547-554.

Jung, O.J., Lee, E.J., Kim, J.W., Chung, Y.R. and Lee, C.W. (1997) Identification of putative phosphoinositide-specific phospholipase C genes in filamentous fungi. *Mol Cells*, **7**, 192-199.

Kam, J.L., Miura, K., Jackson, T.R., Gruschus, J., Roller, P., Stauffer, S., Clark, J., Aneja, R. and Randazzo, P.A. (2000) Phosphoinositide-dependent activation of the ADP-ribosylation factor GTPase-activating protein ASAP1. Evidence for the pleckstrin homology domain functioning as an allosteric site. *J Biol Chem*, **275**, 9653-9663.

Kanai, F., Ito, K., Todaka, M., Hayashi, H., Kamohara, S., Ishii, K., Okada, T., Hazeki, O., Ui, M. and Ebina, Y. (1993) Insulin-stimulated GLUT4 translocation is relevant to the phosphorylation of IRS-1 and the activity of PI3-kinase. *Biochem Biophys Res Commun*, **195**, 762-768.

Kang, S., Bader, A.G., Zhao, L. and Vogt, P.K. (2005) Mutated PI 3-kinases: cancer targets on a silver platter. *Cell Cycle*, **4**, 578-581.

Kapeller, R. and Cantley, L.C. (1994) Phosphatidylinositol 3-kinase. *Bioessays*, **16**, 565-576.

Kapeller, R., Toker, A., Cantley, L.C. and Carpenter, C.L. (1995) Phosphoinositide 3-kinase binds constitutively to alpha/beta-tubulin and binds to gamma-tubulin in response to insulin. *J Biol Chem*, **270**, 25985-25991.

Kaplan, D.R., Whitman, M., Schaffhausen, B., Pallas, D.C., White, M., Cantley, L. and Roberts, T.M. (1987) Common elements in growth factor stimulation and oncogenic transformation: 85 kd phosphoprotein and phosphatidylinositol kinase activity. *Cell*, **50**, 1021-1029.

Karas, M. and Hillenkamp, F. (1988) Laser desorption ionization of proteins with molecular masses exceeding 10,000 daltons. *Anal Chem*, **60**, 2299-2301.

Karnitz, L.M., Sutor, S.L. and Abraham, R.T. (1994) The Src-family kinase, Fyn, regulates the activation of phosphatidylinositol 3-kinase in an interleukin 2-responsive T cell line. *J Exp Med*, **179**, 1799-1808.

Katsafanas, G.C. and Moss, B. (2004) Vaccinia virus intermediate stage transcription is complemented by Ras-GTPase-activating protein SH3 domain-binding protein (G3BP) and cytoplasmic activation/proliferation-associated protein (p137) individually or as a heterodimer. *J Biol Chem*, **279**, 52210-52217.

Kaufmann, S.H., Desnoyers, S., Ottaviano, Y., Davidson, N.E. and Poirier, G.G. (1993) Specific proteolytic cleavage of poly(ADP-ribose) polymerase: an early marker of chemotherapy-induced apoptosis. *Cancer Res*, **53**, 3976-3985.

Kavanaugh, W.M., Klippel, A., Escobedo, J.A. and Williams, L.T. (1992) Modification of the 85-kilodalton subunit of phosphatidylinositol-3 kinase in platelet-derived growth factor-stimulated cells. *Mol Cell Biol*, **12**, 3415-3424.

Kavanaugh, W.M., Turck, C.W., Klippel, A. and Williams, L.T. (1994) Tyrosine 508 of the 85-kilodalton subunit of phosphatidylinositol 3-kinase is phosphorylated by the platelet-derived growth factor receptor. *Biochemistry*, **33**, 11046-11050.

Kavanaugh, W.M. and Williams, L.T. (1994) An alternative to SH2 domains for binding tyrosine-phosphorylated proteins. *Science*, **266**, 1862-1865.

Kazlauskas, A. and Cooper, J.A. (1990) Phosphorylation of the PDGF receptor beta subunit creates a tight binding site for phosphatidylinositol 3 kinase. *Embo J*, **9**, 3279-3286.

Kellerer, M., Koch, M., Metzinger, E., Mushack, J., Capp, E. and Haring, H.U. (1997) Leptin activates PI-3 kinase in C2C12 myotubes via janus kinase-2 (JAK-2) and insulin receptor substrate-2 (IRS-2) dependent pathways. *Diabetologia*, **40**, 1358-1362.

Kim, S.J. (1998) Insulin rapidly induces nuclear translocation of PI3-kinase in HepG2 cells. *Biochem Mol Biol Int*, **46**, 187-196.

Kirkpatrick, D.S., Gerber, S.A. and Gygi, S.P. (2005) The absolute quantification strategy: a general procedure for the quantification of proteins and post-translational modifications. *Methods*, **35**, 265-273.

Klinghoffer, R.A., Duckworth, B., Valius, M., Cantley, L. and Kazlauskas, A. (1996) Platelet-derived growth factor-dependent activation of phosphatidylinositol 3-kinase is regulated by

receptor binding of SH2-domain-containing proteins which influence Ras activity. *Mol Cell Biol*, **16**, 5905-5914.

Klippel, A., Escobedo, J.A., Hu, Q. and Williams, L.T. (1993) A region of the 85-kilodalton (kDa) subunit of phosphatidylinositol 3-kinase binds the 110-kDa catalytic subunit in vivo. *Mol Cell Biol*, **13**, 5560-5566.

Klose, J. (1975) Protein mapping by combined isoelectric focusing and electrophoresis of mouse tissues. A novel approach to testing for induced point mutations in mammals. *Humangenetik*, **26**, 231-243.

Knight, Z.A., Chiang, G.G., Alaimo, P.J., Kenski, D.M., Ho, C.B., Coan, K., Abraham, R.T. and Shokat, K.M. (2004) Isoform-specific phosphoinositide 3-kinase inhibitors from an arylmorpholine scaffold. *Bioorganic & Medicinal Chemistry*, **12**, 4749-4759.

Knobbe, C.B. and Reifenberger, G. (2003) Genetic alterations and aberrant expression of genes related to the phosphatidyl-inositol-3'-kinase/protein kinase B (Akt) signal transduction pathway in glioblastomas. *Brain Pathol*, **13**, 507-518.

Kobayashi, T., Deak, M., Morrice, N. and Cohen, P. (1999) Characterization of the structure and regulation of two novel isoforms of serum- and glucocorticoid-induced protein kinase. *Biochem J*, **344 Pt 1**, 189-197.

Kodaki, T., Woscholski, R., Hallberg, B., Rodriguez-Viciana, P., Downward, J. and Parker, P.J. (1994) The activation of phosphatidylinositol 3-kinase by Ras. *Curr Biol*, **4**, 798-806.

Kohn, A.D., Summers, S.A., Birnbaum, M.J. and Roth, R.A. (1996) Expression of a constitutively active Akt Ser/Thr kinase in 3T3-L1 adipocytes stimulates glucose uptake and glucose transporter 4 translocation. *J Biol Chem*, **271**, 31372-31378.

Krishna, R.G. and Wold, F. (1993) Post-translational modification of proteins. *Adv Enzymol Relat Areas Mol Biol*, **67**, 265-298.

Krugmann, S., Cooper, M.A., Williams, D.H., Hawkins, P.T. and Stephens, L.R. (2002) Mechanism of the regulation of type IB phosphoinositide 3OH-kinase byG-protein betagamma subunits. *Biochem J*, **362**, 725-731.

Krugmann, S., Williams, R., Stephens, L. and Hawkins, P.T. (2004) ARAP3 is a PI3K- and rap-regulated GAP for RhoA. *Curr Biol*, **14**, 1380-1384.

Kurosaki, T., Johnson, S.A., Pao, L., Sada, K., Yamamura, H. and Cambier, J.C. (1995) Role of the Syk autophosphorylation site and SH2 domains in B cell antigen receptor signaling. *J Exp Med*, **182**, 1815-1823.

Kurosu, H. and Katada, T. (2001) Association of phosphatidylinositol 3-kinase composed of p110beta-catalytic and p85-regulatory subunits with the small GTPase Rab5. *J Biochem (Tokyo)*, **130**, 73-78.

Kurosu, H., Maehama, T., Okada, T., Yamamoto, T., Hoshino, S., Fukui, Y., Ui, M., Hazeki, O. and Katada, T. (1997) Heterodimeric phosphoinositide 3-kinase consisting of p85 and p110beta is synergistically activated by the betagamma subunits of G proteins and phosphotyrosyl peptide. *J Biol Chem*, **272**, 24252-24256.

Kwon, M., Ling, Y., Maile, L.A., Badley-Clark, J. and Clemmons, D.R. (2005) Recruitment of the Tyrosine Phosphatase SHP-2 to the p85 Subunit of Phosphatidylinositol-3 (PI-3) Kinase is Required for Insulin-like Growth Factor I Dependent PI-3 Kinase Activation in Smooth Muscle Cells. *Endocrinology*.

Laffargue, M., Calvez, R., Finan, P., Trifilieff, A., Barbier, M., Altruda, F., Hirsch, E. and Wymann, M.P. (2002) Phosphoinositide 3-kinase gamma is an essential amplifier of mast cell function. *Immunity*, **16**, 441-451.

Lam, K., Carpenter, C.L., Ruderman, N.B., Friel, J.C. and Kelly, K.L. (1994) The phosphatidylinositol 3-kinase serine kinase phosphorylates IRS-1. Stimulation by insulin and inhibition by Wortmannin. *J Biol Chem*, **269**, 20648-20652.

Lee, J.O., Yang, H., Georgescu, M.M., Di Cristofano, A., Maehama, T., Shi, Y., Dixon, J.E., Pandolfi, P. and Pavletich, N.P. (1999) Crystal structure of the PTEN tumor suppressor: implications for its phosphoinositide phosphatase activity and membrane association. *Cell*, **99**, 323-334.

Leevers, S.J., Weinkove, D., MacDougall, L.K., Hafen, E. and Waterfield, M.D. (1996) The Drosophila phosphoinositide 3-kinase Dp110 promotes cell growth. *Embo J*, **15**, 6584-6594.

Lefebvre, V., Mechin, M.C., Louckx, M.P., Rider, M.H. and Hue, L. (1996) Signaling pathway involved in the activation of heart 6-phosphofructo-2-kinase by insulin. *J Biol Chem*, **271**, 22289-22292.

Lemmon, M.A. and Ferguson, K.M. (2000) Signal-dependent membrane targeting by pleckstrin homology (PH) domains. *Biochem J*, **350 Pt 1**, 1-18.

Leslie, N.R. and Downes, C.P. (2004) PTEN function: how normal cells control it and tumour cells lose it. *Biochem J*, **382**, 1-11.

Lev, S., Givol, D. and Yarden, Y. (1992) Interkinase domain of kit contains the binding site for phosphatidylinositol 3' kinase. *Proc Natl Acad Sci U S A*, **89**, 678-682.

Li, G., Robinson, G.W., Lesche, R., Martinez-Diaz, H., Jiang, Z., Rozengurt, N., Wagner, K.U., Wu, D.C., Lane, T.F., Liu, X., Hennighausen, L. and Wu, H. (2002) Conditional loss of PTEN leads to precocious development and neoplasia in the mammary gland. *Development*, **129**, 4159-4170.

Li, H.L., Davis, W.W., Whiteman, E.L., Birnbaum, M.J. and Pure, E. (1999) The tyrosine kinases Syk and Lyn exert opposing effects on the activation of protein kinase Akt/PKB in B lymphocytes. *Proc Natl Acad Sci U S A*, **96**, 6890-6895.

Li, L., Ernsting, B.R., Wishart, M.J., Lohse, D.L. and Dixon, J.E. (1997) A family of putative tumor suppressors is structurally and functionally conserved in humans and yeast. *J Biol Chem*, **272**, 29403-29406.

Li, T., Tsukada, S., Satterthwaite, A., Havlik, M.H., Park, H., Takatsu, K. and Witte, O.N. (1995) Activation of Bruton's tyrosine kinase (BTK) by a point mutation in its pleckstrin homology (PH) domain. *Immunity*, **2**, 451-460.

Li, X., Sandoval, D., Freeberg, L. and Carter, R.H. (1997) Role of CD19 tyrosine 391 in synergistic activation of B lymphocytes by coligation of CD19 and membrane Ig. *J Immunol*, **158**, 5649-5657.

Li, Z., Jiang, H., Xie, W., Zhang, Z., Smrcka, A.V. and Wu, D. (2000) Roles of PLC-beta2 and -beta3 and PI3Kgamma in chemoattractant-mediated signal transduction. *Science*, **287**, 1046-1049.

Linassier, C., MacDougall, L.K., Domin, J. and Waterfield, M.D. (1997) Molecular cloning and biochemical characterization of a Drosophila phosphatidylinositol-specific phosphoinositide 3-kinase. *Biochem J*, **321 (Pt 3)**, 849-856.

Lioubin, M.N., Algate, P.A., Tsai, S., Carlberg, K., Aebersold, A. and Rohrschneider, L.R. (1996) p150Ship, a signal transduction molecule with inositol polyphosphate-5-phosphatase activity. *Genes Dev*, **10**, 1084-1095.

Liu, Q., Oliveira-Dos-Santos, A.J., Mariathasan, S., Bouchard, D., Jones, J., Sarao, R., Kozieradzki, I., Ohashi, P.S., Penninger, J.M. and Dumont, D.J. (1998) The inositol polyphosphate 5-phosphatase ship is a crucial negative regulator of B cell antigen receptor signaling. *J Exp Med*, **188**, 1333-1342.

Liu, X., Marengere, L.E., Koch, C.A. and Pawson, T. (1993) The v-Src SH3 domain binds phosphatidylinositol 3'-kinase. *Mol Cell Biol*, **13**, 5225-5232.

Liu, Y., Casey, L. and Pike, L.J. (1998) Compartmentalization of phosphatidylinositol 4,5-bisphosphate in low-density membrane domains in the absence of caveolin. *Biochem Biophys Res Commun*, **245**, 684-690.

Luo, J. and Cantley, L.C. (2005) The negative regulation of phosphoinositide 3-kinase signaling by p85 and it's implication in cancer. *Cell Cycle*, **4**, 1309-1312.

Macara, I.G., Marinetti, G.V. and Balduzzi, P.C. (1984) Transforming protein of avian sarcoma virus UR2 is associated with phosphatidylinositol kinase activity: possible role in tumorigenesis. *Proc Natl Acad Sci U S A*, **81**, 2728-2732.

MacDougall, L.K., Domin, J. and Waterfield, M.D. (1995) A family of phosphoinositide 3-kinases in Drosophila identifies a new mediator of signal transduction. *Curr Biol*, **5**, 1404-1415.

Maehama, T. and Dixon, J.E. (1998) The tumor suppressor, PTEN/MMAC1, dephosphorylates the lipid second messenger, phosphatidylinositol 3,4,5-trisphosphate. *J Biol Chem*, **273**, 13375-13378.

Maehama, T., Taylor, G.S. and Dixon, J.E. (2001) PTEN and myotubularin: novel phosphoinositide phosphatases. *Annu Rev Biochem*, **70**, 247-279.

Maier, U., Babich, A., Macrez, N., Leopoldt, D., Gierschik, P., Illenberger, D. and Nurnberg, B. (2000) Gbeta 5gamma 2 is a highly selective activator of phospholipid-dependent enzymes. *J Biol Chem*, **275**, 13746-13754.

Mak, P., He, Z. and Kurosaki, T. (1996) Identification of amino acid residues required for a specific interaction between Src-tyrosine kinase and proline-rich region of phosphatidylinositol-3' kinase. *FEBS Lett*, **397**, 183-185.

Manke, I.A., Lowery, D.M., Nguyen, A. and Yaffe, M.B. (2003) BRCT repeats as phosphopeptide-binding modules involved in protein targeting. *Science*, **302**, 636-639.

Mann, M., Ong, S.E., Gronborg, M., Steen, H., Jensen, O.N. and Pandey, A. (2002) Analysis of protein phosphorylation using mass spectrometry: deciphering the phosphoproteome. *Trends Biotechnol*, **20**, 261-268.

Mansour, S.J., Skaug, J., Zhao, X.H., Giordano, J., Scherer, S.W. and Melancon, P. (1999) p200 ARF-GEP1: a Golgi-localized guanine nucleotide exchange protein whose Sec7 domain is targeted by the drug brefeldin A. *Proc Natl Acad Sci U S A*, **96**, 7968-7973.

Marchisio, M., Bertagnolo, V., Colamussi, M.L., Capitani, S. and Neri, L.M. (1998) Phosphatidylinositol 3-kinase in HL-60 nuclei is bound to the nuclear matrix and increases during granulocytic differentiation. *Biochem Biophys Res Commun*, **253**, 346-351.

Matsumura, N., Mandai, M., Miyanishi, M., Fukuhara, K., Baba, T., Higuchi, T., Kariya, M., Takakura, K. and Fujii, S. (2006) Oncogenic Property of Acrogranin in Human Uterine Leiomyosarcoma: Direct Evidence of Genetic Contribution in In vivo Tumorigenesis. *Clin Cancer Res*, **12**, 1402-1411.

Mauvais-Jarvis, F., Ueki, K., Fruman, D.A., Hirshman, M.F., Sakamoto, K., Goodyear, L.J., Iannacone, M., Accili, D., Cantley, L.C. and Kahn, C.R. (2002) Reduced expression of the murine p85alpha subunit of phosphoinositide 3-kinase improves insulin signaling and ameliorates diabetes. *J Clin Invest*, **109**, 141-149.

Mazerolles, F. and Fischer, A. (1998) Binding of CD4 ligands induces tyrosine phosphorylation of phosphatidylinositol-3 kinase p110 subunit. *Int Immunol*, **10**, 1897-1905.

Mazzorana, M., Snellman, A., Kivirikko, K.I., van der Rest, M. and Pihlajaniemi, T. (1996) Involvement of prolyl 4-hydroxylase in the assembly of trimeric minicollagen XII. Study in a baculovirus expression system. *J Biol Chem*, **271**, 29003-29008.

Meier, R., Alessi, D.R., Cron, P., Andjelkovic, M. and Hemmings, B.A. (1997) Mitogenic activation, phosphorylation, and nuclear translocation of protein kinase Bbeta. *J Biol Chem*, **272**, 30491-30497.

Mi, Y., Thomas, S.D., Xu, X., Casson, L.K., Miller, D.M. and Bates, P.J. (2003) Apoptosis in leukemia cells is accompanied by alterations in the levels and localization of nucleolin. *J Biol Chem*, **278**, 8572-8579.

Misawa, H., Ohtsubo, M., Copeland, N.G., Gilbert, D.J., Jenkins, N.A. and Yoshimura, A. (1998) Cloning and characterization of a novel class II phosphoinositide 3-kinase containing C2 domain. *Biochem Biophys Res Commun*, **244**, 531-539.

Moon, K.D., Post, C.B., Durden, D.L., Zhou, Q., De, P., Harrison, M.L. and Geahlen, R.L. (2005) Molecular basis for a direct interaction between the Syk protein-tyrosine kinase and phosphoinositide 3-kinase. *J Biol Chem*, **280**, 1543-1551.

Morris, H.R., Paxton, T., Dell, A., Langhorne, J., Berg, M., Bordoli, R.S., Hoyes, J. and Bateman, R.H. (1996) High sensitivity collisionally-activated decomposition tandem mass spectrometry on a novel quadrupole/orthogonal-acceleration time-of-flight mass spectrometer. *Rapid Commun Mass Spectrom*, **10**, 889-896.

Morris, H.R., Paxton, T., Panico, M., McDowell, R. and Dell, A. (1997) A novel geometry mass spectrometer, the Q-TOF, for low-femtomole/attomole-range biopolymer sequencing. *J Protein Chem*, **16**, 469-479.

Morris, J.Z., Tissenbaum, H.A. and Ruvkun, G. (1996) A phosphatidylinositol-3-OH kinase family member regulating longevity and diapause in Caenorhabditis elegans. *Nature*, **382**, 536-539.

Murphy, S.M., Urbani, L. and Stearns, T. (1998) The mammalian gamma-tubulin complex contains homologues of the yeast spindle pole body components spc97p and spc98p. *J Cell Biol*, **141**, 663-674.

Musacchio, A., Cantley, L.C. and Harrison, S.C. (1996) Crystal structure of the breakpoint cluster region-homology domain from phosphoinositide 3-kinase p85 alpha subunit. *Proc Natl Acad Sci U S A*, **93**, 14373-14378.

Musacchio, A., Gibson, T., Rice, P., Thompson, J. and Saraste, M. (1993) The PH domain: a common piece in the structural patchwork of signalling proteins. *Trends Biochem Sci*, **18**, 343-348.

Muta, T., Kurosaki, T., Misulovin, Z., Sanchez, M., Nussenzweig, M.C. and Ravetch, J.V. (1994) A 13-amino-acid motif in the cytoplasmic domain of Fc gamma RIIB modulates B-cell receptor signalling. *Nature*, **369**, 340.

Myers, M.P. and Tonks, N.K. (1997) PTEN: sometimes taking it off can be better than putting it on. *Am J Hum Genet*, **61**, 1234-1238.

Neri, L.M., Milani, D., Bertolaso, L., Stroscio, M., Bertagnolo, V. and Capitani, S. (1994) Nuclear translocation of phosphatidylinositol 3-kinase in rat pheochromocytoma PC 12 cells after treatment with nerve growth factor. *Cell Mol Biol (Noisy-le-grand)*, **40**, 619-626.

Nicholson, K.M. and Anderson, N.G. (2002) The protein kinase B/Akt signalling pathway in human malignancy. *Cell Signal*, **14**, 381-395.

Nisitani, S., Kato, R.M., Rawlings, D.J., Witte, O.N. and Wahl, M.I. (1999) In situ detection of activated Bruton's tyrosine kinase in the Ig signaling complex by phosphopeptide-specific monoclonal antibodies. *Proc Natl Acad Sci U S A*, **96**, 2221-2226.

Nooren, I.M. and Thornton, J.M. (2003) Diversity of protein-protein interactions. *Embo J*, **22**, 3486-3492.

O'Farrell, P.H. (1975) High resolution two-dimensional electrophoresis of proteins. *J Biol Chem*, **250**, 4007-4021.

Okada, T., Maeda, A., Iwamatsu, A., Gotoh, K. and Kurosaki, T. (2000) BCAP: the tyrosine kinase substrate that connects B cell receptor to phosphoinositide 3-kinase activation. *Immunity*, **13**, 817-827.

Okkenhaug, K., Bilancio, A., Farjot, G., Priddle, H., Sancho, S., Peskett, E., Pearce, W., Meek, S.E., Salpekar, A., Waterfield, M.D., Smith, A.J. and Vanhaesebroeck, B. (2002) Impaired B and T cell antigen receptor signaling in p110delta PI 3-kinase mutant mice. *Science*, **297**, 1031-1034.

Okkenhaug, K. and Vanhaesebroeck, B. (2001) New responsibilities for the PI3K regulatory subunit p85 alpha. *Sci STKE*, **2001**, PE1.

Ong, C.H. and Bateman, A. (2003) Progranulin (granulin-epithelin precursor, PC-cell derived growth factor, acrogranin) in proliferation and tumorigenesis. *Histol Histopathol*, **18**, 1275-1288.

Ong, S.E., Blagoev, B., Kratchmarova, I., Kristensen, D.B., Steen, H., Pandey, A. and Mann, M. (2002) Stable isotope labeling by amino acids in cell culture, SILAC, as a simple and accurate approach to expression proteomics. *Mol Cell Proteomics*, **1**, 376-386.

Ono, M., Bolland, S., Tempst, P. and Ravetch, J.V. (1996) Role of the inositol phosphatase SHIP in negative regulation of the immune system by the receptor Fc(gamma)RIIB. *Nature*, **383**, 263-266.

Ono, M., Okada, H., Bolland, S., Yanagi, S., Kurosaki, T. and Ravetch, J.V. (1997) Deletion of SHIP or SHP-1 reveals two distinct pathways for inhibitory signaling. *Cell*, **90**, 293-301.

Otsu, M., Hiles, I., Gout, I., Fry, M.J., Ruiz-Larrea, F., Panayotou, G., Thompson, A., Dhand, R., Hsuan, J., Totty, N. and et al. (1991) Characterization of two 85 kd proteins that associate with receptor tyrosine kinases, middle-T/pp60c-src complexes, and PI3-kinase. *Cell*, **65**, 91-104.

Pacold, M.E., Suire, S., Perisic, O., Lara-Gonzalez, S., Davis, C.T., Walker, E.H., Hawkins, P.T., Stephens, L., Eccleston, J.F. and Williams, R.L. (2000) Crystal structure and functional analysis of Ras binding to its effector phosphoinositide 3-kinase gamma. *Cell*, **103**, 931-943.

Pages, F., Ragueneau, M., Rottapel, R., Truneh, A., Nunes, J., Imbert, J. and Olive, D. (1994) Binding of phosphatidylinositol-3-OH kinase to CD28 is required for T-cell signalling. *Nature*, **369**, 327-329.

Panayotou, G., Gish, G., End, P., Truong, O., Gout, I., Dhand, R., Fry, M.J., Hiles, I., Pawson, T. and Waterfield, M.D. (1993) Interactions between SH2 domains and tyrosine-phosphorylated platelet-derived growth factor beta-receptor sequences: analysis of kinetic parameters by a novel biosensor-based approach. *Mol Cell Biol*, **13**, 3567-3576.

Pappin, D.J., Hojrup, P. and Bleasby, A.J. (1993) Rapid identification of proteins by peptide-mass fingerprinting. *Curr Biol*, **3**, 327-332.

Pappu, R., Cheng, A.M., Li, B., Gong, Q., Chiu, C., Griffin, N., White, M., Sleckman, B.P. and Chan, A.C. (1999) Requirement for B cell linker protein (BLNK) in B cell development. *Science*, **286**, 1949-1954.

Park, J., Leong, M.L., Buse, P., Maiyar, A.C., Firestone, G.L. and Hemmings, B.A. (1999) Serum and glucocorticoid-inducible kinase (SGK) is a target of the PI 3-kinase-stimulated signaling pathway. *Embo J*, **18**, 3024-3033.

Patrucco, E., Notte, A., Barberis, L., Selvetella, G., Maffei, A., Brancaccio, M., Marengo, S., Russo, G., Azzolino, O., Rybalkin, S.D., Silengo, L., Altruda, F., Wetzker, R., Wymann, M.P., Lembo, G. and Hirsch, E. (2004) PI3Kgamma modulates the cardiac response to chronic

pressure overload by distinct kinase-dependent and -independent effects. *Cell*, **118**, 375-387.

Paz, K., Liu, Y.F., Shorer, H., Hemi, R., LeRoith, D., Quan, M., Kanety, H., Seger, R. and Zick, Y. (1999) Phosphorylation of insulin receptor substrate-1 (IRS-1) by protein kinase B positively regulates IRS-1 function. *J Biol Chem*, **274**, 28816-28822.

Pederson, T.M., Kramer, D.L. and Rondinone, C.M. (2001) Serine/threonine phosphorylation of IRS-1 triggers its degradation: possible regulation by tyrosine phosphorylation. *Diabetes*, **50**, 24-31.

Perret, S., Eble, J.A., Siljander, P.R., Merle, C., Farndale, R.W., Theisen, M. and Ruggiero, F. (2003) Prolyl hydroxylation of collagen type I is required for efficient binding to integrin alpha 1 beta 1 and platelet glycoprotein VI but not to alpha 2 beta 1. *J Biol Chem*, **278**, 29873-29879.

Pleiman, C.M., Hertz, W.M. and Cambier, J.C. (1994) Activation of phosphatidylinositol-3' kinase by Src-family kinase SH3 binding to the p85 subunit. *Science*, **263**, 1609-1612.

Podsypanina, K., Ellenson, L.H., Nemes, A., Gu, J., Tamura, M., Yamada, K.M., Cordon-Cardo, C., Catoretti, G., Fisher, P.E. and Parsons, R. (1999) Mutation of Pten/Mmac1 in mice causes neoplasia in multiple organ systems. *Proc Natl Acad Sci U S A*, **96**, 1563-1568.

Pons, S., Asano, T., Glasheen, E., Miralpeix, M., Zhang, Y., Fisher, T.L., Myers, M.G., Jr., Sun, X.J. and White, M.F. (1995) The structure and function of p55PIK reveal a new regulatory subunit for phosphatidylinositol 3-kinase. *Mol Cell Biol*, **15**, 4453-4465.

Posada, J. and Cooper, J.A. (1992) Molecular signal integration. Interplay between serine, threonine, and tyrosine phosphorylation. *Mol Biol Cell*, **3**, 583-592.

Powis, G., Bonjouklian, R., Berggren, M.M., Gallegos, A., Abraham, R., Ashendel, C., Zalkow, L., Matter, W.F., Dodge, J., Grindey, G. and et al. (1994) Wortmannin, a potent and selective inhibitor of phosphatidylinositol-3-kinase. *Cancer Res*, **54**, 2419-2423.

Prasad, K.V., Janssen, O., Kapeller, R., Raab, M., Cantley, L.C. and Rudd, C.E. (1993) Src-homology 3 domain of protein kinase p59fyn mediates binding to phosphatidylinositol 3-kinase in T cells. *Proc Natl Acad Sci U S A*, **90**, 7366-7370.

Prior, I.A. and Clague, M.J. (1999) Localization of a class II phosphatidylinositol 3-kinase, PI3KC2alpha, to clathrin-coated vesicles. *Mol Cell Biol Res Commun*, **1**, 162-166.

Ptasznik, A., Prossnitz, E.R., Yoshikawa, D., Smrcka, A., Traynor-Kaplan, A.E. and Bokoch, G.M. (1996) A tyrosine kinase signaling pathway accounts for the majority of phosphatidylinositol 3,4,5-trisphosphate formation in chemoattractant-stimulated human neutrophils. *J Biol Chem*, **271**, 25204-25207.

Pullen, N., Dennis, P.B., Andjelkovic, M., Dufner, A., Kozma, S.C., Hemmings, B.A. and Thomas, G. (1998) Phosphorylation and activation of p70s6k by PDK1. *Science*, **279**, 707-710.

Qin, S. and Chock, P.B. (2003) Implication of phosphatidylinositol 3-kinase membrane recruitment in hydrogen peroxide-induced activation of PI3K and Akt. *Biochemistry*, **42**, 2995-3003.

Rabilloud, T. (1998) Use of thiourea to increase the solubility of membrane proteins in two-dimensional electrophoresis. *Electrophoresis*, **19**, 758-760.

Rabilloud, T. (1999) Solubilization of proteins in 2-D electrophoresis. An outline. *Methods Mol Biol*, **112**, 9-19.

Rameh, L.E., Arvidsson, A., Carraway, K.L., 3rd, Couvillon, A.D., Rathbun, G., Crompton, A., VanRenterghem, B., Czech, M.P., Ravichandran, K.S., Burakoff, S.J., Wang, D.S., Chen, C.S. and Cantley, L.C. (1997) A comparative analysis of the phosphoinositide binding specificity of pleckstrin homology domains. *J Biol Chem*, **272**, 22059-22066.

Ravetch, J.V. (1997) Fc receptors. *Curr Opin Immunol*, **9**, 121-125.

Rawlings, D.J., Scharenberg, A.M., Park, H., Wahl, M.I., Lin, S., Kato, R.M., Fluckiger, A.C., Witte, O.N. and Kinet, J.P. (1996) Activation of BTK by a phosphorylation mechanism initiated by SRC family kinases. *Science*, **271**, 822-825.

Razzini, G., Ingrosso, A., Brancaccio, A., Sciacchitano, S., Esposito, D.L. and Falasca, M. (2000) Different subcellular localization and phosphoinositides binding of insulin receptor substrate protein pleckstrin homology domains. *Mol Endocrinol*, **14**, 823-836.

Reif, K., Gout, I., Waterfield, M.D. and Cantrell, D.A. (1993) Divergent regulation of phosphatidylinositol 3-kinase P85 alpha and P85 beta isoforms upon T cell activation. *J Biol Chem*, **268**, 10780-10788.

Reif, K., Nobes, C.D., Thomas, G., Hall, A. and Cantrell, D.A. (1996) Phosphatidylinositol 3-kinase signals activate a selective subset of Rac/Rho-dependent effector pathways. *Curr Biol*, **6**, 1445-1455.

Rhee, S.G. and Bae, Y.S. (1997) Regulation of phosphoinositide-specific phospholipase C isozymes. *J Biol Chem*, **272**, 15045-15048.

Roche, S., Dhand, R., Waterfield, M.D. and Courtneidge, S.A. (1994) The catalytic subunit of phosphatidylinositol 3-kinase is a substrate for the activated platelet-derived growth factor receptor, but not for middle-T antigen-pp60c-src complexes. *Biochem J*, **301 (Pt 3)**, 703-711.

Roche, S., Downward, J., Raynal, P. and Courtneidge, S.A. (1998) A function for phosphatidylinositol 3-kinase beta (p85alpha-p110beta) in fibroblasts during mitogenesis: requirement for insulin- and lysophosphatidic acid-mediated signal transduction. *Mol Cell Biol*, **18**, 7119-7129.

Rodriguez-Borlado, L., Barber, D.F., Hernandez, C., Rodriguez-Marcos, M.A., Sanchez, A., Hirsch, E., Wymann, M., Martinez, A.C. and Carrera, A.C. (2003) Phosphatidylinositol 3-kinase regulates the CD4/CD8 T cell differentiation ratio. *J Immunol*, **170**, 4475-4482.

Rodriguez-Viciana, P., Warne, P.H., Dhand, R., Vanhaesebroeck, B., Gout, I., Fry, M.J., Waterfield, M.D. and Downward, J. (1994) Phosphatidylinositol-3-OH kinase as a direct target of Ras. *Nature*, **370**, 527-532.

Rodriguez-Viciana, P., Warne, P.H., Vanhaesebroeck, B., Waterfield, M.D. and Downward, J. (1996) Activation of phosphoinositide 3-kinase by interaction with Ras and by point mutation. *Embo J*, **15**, 2442-2451.

Roepstorff, P. (2000) MALDI-TOF mass spectrometry in protein chemistry. *Exs*, **88**, 81-97.

Roepstorff, P. and Fohlman, J. (1984) Proposal for a common nomenclature for sequence ions in mass spectra of peptides. *Biomed Mass Spectrom*, **11**, 601.

Rohrschneider, L.R., Fuller, J.F., Wolf, I., Liu, Y. and Lucas, D.M. (2000) Structure, function, and biology of SHIP proteins. *Genes Dev*, **14**, 505-520.

Rong, R., Ahn, J.Y., Huang, H., Nagata, E., Kalman, D., Kapp, J.A., Tu, J., Worley, P.F., Snyder, S.H. and Ye, K. (2003) PI3 kinase enhancer-Homer complex couples mGluRI to PI3 kinase, preventing neuronal apoptosis. *Nat Neurosci*, **6**, 1153-1161.

Rordorf-Nikolic, T., Van Horn, D.J., Chen, D., White, M.F. and Backer, J.M. (1995) Regulation of phosphatidylinositol 3'-kinase by tyrosyl phosphoproteins. Full activation requires occupancy of both SH2 domains in the 85-kDa regulatory subunit. *J Biol Chem*, **270**, 3662-3666.

Rush, J., Moritz, A., Lee, K.A., Guo, A., Goss, V.L., Spek, E.J., Zhang, H., Zha, X.M., Polakiewicz, R.D. and Comb, M.J. (2005) Immunoaffinity profiling of tyrosine phosphorylation in cancer cells. *Nat Biotechnol*, **23**, 94-101.

Sadhu, C., Dick, K., Tino, W.T. and Staunton, D.E. (2003) Selective role of PI3Kdelta in neutrophil inflammatory responses. *Biochem Biophys Res Commun*, **308**, 764-769.

Sadhu, C., Masinovsky, B., Dick, K., Sowell, C.G. and Staunton, D.E. (2003) Essential role of phosphoinositide 3-kinase delta in neutrophil directional movement. *J Immunol*, **170**, 2647-2654.

Sadowski, I., Stone, J.C. and Pawson, T. (1986) A noncatalytic domain conserved among cytoplasmic protein-tyrosine kinases modifies the kinase function and transforming activity of Fujinami sarcoma virus P130gag-fps. *Mol Cell Biol*, **6**, 4396-4408.

Safran, M. and Kaelin, W.G., Jr. (2003) HIF hydroxylation and the mammalian oxygen-sensing pathway. *J Clin Invest*, **111**, 779-783.

Samuels, Y. and Velculescu, V.E. (2004) Oncogenic mutations of PIK3CA in human cancers. *Cell Cycle*, **3**, 1221-1224.

Samuels, Y., Wang, Z., Bardelli, A., Silliman, N., Ptak, J., Szabo, S., Yan, H., Gazdar, A., Powell, S.M., Riggins, G.J., Willson, J.K., Markowitz, S., Kinzler, K.W., Vogelstein, B. and Velculescu, V.E. (2004) High frequency of mutations of the PIK3CA gene in human cancers. *Science*, **304**, 554.

Sarkaria, J.N., Tibbetts, R.S., Busby, E.C., Kennedy, A.P., Hill, D.E. and Abraham, R.T. (1998) Inhibition of phosphoinositide 3-kinase related kinases by the radiosensitizing agent wortmannin. *Cancer Res*, **58**, 4375-4382.

Sasaki, T., Irie-Sasaki, J., Jones, R.G., Oliveira-dos-Santos, A.J., Stanford, W.L., Bolon, B., Wakeham, A., Itie, A., Bouchard, D., Kozieradzki, I., Joza, N., Mak, T.W., Ohashi, P.S., Suzuki, A. and Penninger, J.M. (2000) Function of PI3Kgamma in thymocyte development, T cell activation, and neutrophil migration. *Science*, **287**, 1040-1046.

Sawyer, C., Sturge, J., Bennett, D.C., O'Hare, M.J., Allen, W.E., Bain, J., Jones, G.E. and Vanhaesebroeck, B. (2003) Regulation of breast cancer cell chemotaxis by the phosphoinositide 3-kinase p110delta. *Cancer Res*, **63**, 1667-1675.

Schaeffer, E.M. and Schwartzberg, P.L. (2000) Tec family kinases in lymphocyte signaling and function. *Curr Opin Immunol*, **12**, 282-288.

Scharenberg, A.M., El-Hillal, O., Fruman, D.A., Beitz, L.O., Li, Z., Lin, S., Gout, I., Cantley, L.C., Rawlings, D.J. and Kinet, J.P. (1998) Phosphatidylinositol-3,4,5-trisphosphate (PtdIns-3,4,5-P3)/Tec kinase-dependent calcium signaling pathway: a target for SHIP-mediated inhibitory signals. *Embo J*, **17**, 1961-1972.

Schlosser, A., Bodem, J., Bossemeyer, D., Grummt, I. and Lehmann, W.D. (2002) Identification of protein phosphorylation sites by combination of elastase digestion, immobilized metal affinity chromatography, and quadrupole-time of flight tandem mass spectrometry. *Proteomics*, **2**, 911-918.

Serve, H., Hsu, Y.C. and Besmer, P. (1994) Tyrosine residue 719 of the c-kit receptor is essential for binding of the P85 subunit of phosphatidylinositol (PI) 3-kinase and for c-kit-associated PI 3-kinase activity in COS-1 cells. *J Biol Chem*, **269**, 6026-6030.

Shan, X., Czar, M.J., Bunnell, S.C., Liu, P., Liu, Y., Schwartzberg, P.L. and Wange, R.L. (2000) Deficiency of PTEN in Jurkat T cells causes constitutive localization of Itk to the plasma membrane and hyperresponsiveness to CD3 stimulation. *Mol Cell Biol*, **20**, 6945-6957.

Shepherd, P.R., Nave, B.T., Rincon, J., Nolte, L.A., Bevan, A.P., Siddle, K., Zierath, J.R. and Wallberg-Henriksson, H. (1997) Differential regulation of phosphoinositide 3-kinase adapter subunit variants by insulin in human skeletal muscle. *J Biol Chem*, **272**, 19000-19007.

Shibasaki, F., Fukami, K., Fukui, Y. and Takenawa, T. (1994) Phosphatidylinositol 3-kinase binds to alpha-actinin through the p85 subunit. *Biochem J*, **302 (Pt 2)**, 551-557.

Shibasaki, F., Homma, Y. and Takenawa, T. (1991) Two types of phosphatidylinositol 3-kinase from bovine thymus. Monomer and heterodimer form. *J Biol Chem*, **266**, 8108-8114.

Shim, E.K., Moon, C.S., Lee, G.Y., Ha, Y.J., Chae, S.K. and Lee, J.R. (2004) Association of the Src homology 2 domain-containing leukocyte phosphoprotein of 76 kD (SLP-76) with the p85 subunit of phosphoinositide 3-kinase. *FEBS Lett*, **575**, 35-40.

Shioi, T., Kang, P.M., Douglas, P.S., Hampe, J., Yballe, C.M., Lawitts, J., Cantley, L.C. and Izumo, S. (2000) The conserved phosphoinositide 3-kinase pathway determines heart size in mice. *Embo J*, **19**, 2537-2548.

Simoncini, T., Hafezi-Moghadam, A., Brazil, D.P., Ley, K., Chin, W.W. and Liao, J.K. (2000) Interaction of oestrogen receptor with the regulatory subunit of phosphatidylinositol-3-OH kinase. *Nature*, **407**, 538-541.

Sipeki, S., Bander, E., Parker, P.J. and Farago, A. (2006) PKCalpha reduces the lipid kinase activity of the p110alpha/p85alpha PI3K through the phosphorylation of the catalytic subunit. *Biochem Biophys Res Commun*, **339**, 122-125.

Skolnik, E.Y., Margolis, B., Mohammadi, M., Lowenstein, E., Fischer, R., Drepps, A., Ullrich, A. and Schlessinger, J. (1991) Cloning of PI3 kinase-associated p85 utilizing a novel method for expression/cloning of target proteins for receptor tyrosine kinases. *Cell*, **65**, 83-90.

Sleeman, M.W., Wortley, K.E., Lai, K.M., Gowen, L.C., Kintner, J., Kline, W.O., Garcia, K., Stitt, T.N., Yancopoulos, G.D., Wiegand, S.J. and Glass, D.J. (2005) Absence of the lipid phosphatase SHIP2 confers resistance to dietary obesity. *Nat Med*, **11**, 199-205.

Smith, D.B. and Johnson, K.S. (1988) Single-step purification of polypeptides expressed in Escherichia coli as fusions with glutathione S-transferase. *Gene*, **67**, 31-40.

Snyder, L.R. (1997) Changing reversed-phase high performance liquid chromatography selectivity. Which variables should be tried first? *J Chromatogr B Biomed Sci Appl*, **689**, 105-115.

Soltoff, S.P. and Cantley, L.C. (1996) p120cbl is a cytosolic adapter protein that associates with phosphoinositide 3-kinase in response to epidermal growth factor in PC12 and other cells. *J Biol Chem*, **271**, 563-567.

Songyang, Z., Shoelson, S.E., Chaudhuri, M., Gish, G., Pawson, T., Haser, W.G., King, F., Roberts, T., Ratnofsky, S., Lechleider, R.J. and et al. (1993) SH2 domains recognize specific phosphopeptide sequences. *Cell*, **72**, 767-778.

Stack, J.H. and Emr, S.D. (1994) Vps34p required for yeast vacuolar protein sorting is a multiple specificity kinase that exhibits both protein kinase and phosphatidylinositol-specific PI 3-kinase activities. *J Biol Chem*, **269**, 31552-31562.

Stack, J.H., Herman, P.K., Schu, P.V. and Emr, S.D. (1993) A membrane-associated complex containing the Vps15 protein kinase and the Vps34 PI 3-kinase is essential for protein sorting to the yeast lysosome-like vacuole. *Embo J*, **12**, 2195-2204.

Stambolic, V., Suzuki, A., de la Pompa, J.L., Brothers, G.M., Mirtsos, C., Sasaki, T., Ruland, J., Penninger, J.M., Siderovski, D.P. and Mak, T.W. (1998) Negative regulation of PKB/Akt-dependent cell survival by the tumor suppressor PTEN. *Cell*, **95**, 29-39.

Steck, P.A., Pershouse, M.A., Jasser, S.A., Yung, W.K., Lin, H., Ligon, A.H., Langford, L.A., Baumgard, M.L., Hattier, T., Davis, T., Frye, C., Hu, R., Swedlund, B., Teng, D.H. and Tavtigian, S.V. (1997) Identification of a candidate tumour suppressor gene, MMAC1, at chromosome 10q23.3 that is mutated in multiple advanced cancers. *Nat Genet*, **15**, 356-362.

Stein, R.C. and Waterfield, M.D. (2000) PI3-kinase inhibition: a target for drug development? *Mol Med Today*, **6**, 347-357.

Stephens, L., Anderson, K., Stokoe, D., Erdjument-Bromage, H., Painter, G.F., Holmes, A.B., Gaffney, P.R., Reese, C.B., McCormick, F., Tempst, P., Coadwell, J. and Hawkins, P.T. (1998) Protein kinase B kinases that mediate phosphatidylinositol 3,4,5-trisphosphate-dependent activation of protein kinase B. *Science*, **279**, 710-714.

Stephens, L., Smrcka, A., Cooke, F.T., Jackson, T.R., Sternweis, P.C. and Hawkins, P.T. (1994) A novel phosphoinositide 3 kinase activity in myeloid-derived cells is activated by G protein beta gamma subunits. *Cell*, **77**, 83-93.

Stephens, L.R., Eguinoa, A., Erdjument-Bromage, H., Lui, M., Cooke, F., Coadwell, J., Smrcka, A.S., Thelen, M., Cadwallader, K., Tempst, P. and Hawkins, P.T. (1997) The G beta gamma sensitivity of a PI3K is dependent upon a tightly associated adaptor, p101. *Cell*, **89**, 105-114.

Stoddart, A., Dykstra, M.L., Brown, B.K., Song, W., Pierce, S.K. and Brodsky, F.M. (2002) Lipid rafts unite signaling cascades with clathrin to regulate BCR internalization. *Immunity*, **17**, 451-462.

Stoyanov, B., Volinia, S., Hanck, T., Rubio, I., Loubtchenkov, M., Malek, D., Stoyanova, S., Vanhaesebroeck, B., Dhand, R., Nurnberg, B. and et al. (1995) Cloning and characterization of a G protein-activated human phosphoinositide-3 kinase. *Science*, **269**, 690-693.

Sugimoto, Y., Whitman, M., Cantley, L.C. and Erikson, R.L. (1984) Evidence that the Rous sarcoma virus transforming gene product phosphorylates phosphatidylinositol and diacylglycerol. *Proc Natl Acad Sci U S A*, **81**, 2117-2121.

Suire, S., Coadwell, J., Ferguson, G.J., Davidson, K., Hawkins, P. and Stephens, L. (2005) p84, a new Gbetagamma-activated regulatory subunit of the type IB phosphoinositide 3-kinase p110gamma. *Curr Biol*, **15**, 566-570.

Sun, M., Yang, L., Feldman, R.I., Sun, X.M., Bhalla, K.N., Jove, R., Nicosia, S.V. and Cheng, J.Q. (2003) Activation of phosphatidylinositol 3-kinase/Akt pathway by androgen through interaction of p85alpha, androgen receptor, and Src. *J Biol Chem*, **278**, 42992-43000.

Suzuki, A., de la Pompa, J.L., Stambolic, V., Elia, A.J., Sasaki, T., del Barco Barrantes, I., Ho, A., Wakeham, A., Itie, A., Khoo, W., Fukumoto, M. and Mak, T.W. (1998) High cancer susceptibility and embryonic lethality associated with mutation of the PTEN tumor suppressor gene in mice. *Curr Biol*, **8**, 1169-1178.

Suzuki, A., Ji, G., Numabe, Y., Ishii, K., Muramatsu, M. and Kamoi, K. (2004) Large-scale investigation of genomic markers for severe periodontitis. *Odontology*, **92**, 43-47.

Suzuki, A., Yamaguchi, M.T., Ohteki, T., Sasaki, T., Kaisho, T., Kimura, Y., Yoshida, R., Wakeham, A., Higuchi, T., Fukumoto, M., Tsubata, T., Ohashi, P.S., Koyasu, S., Penninger, J.M., Nakano, T. and Mak, T.W. (2001) T cell-specific loss of Pten leads to defects in central and peripheral tolerance. *Immunity*, **14**, 523-534.

Suzuki, H., Matsuda, S., Terauchi, Y., Fujiwara, M., Ohteki, T., Asano, T., Behrens, T.W., Kouro, T., Takatsu, K., Kadowaki, T. and Koyasu, S. (2003) PI3K and Btk differentially regulate B cell antigen receptor-mediated signal transduction. *Nat Immunol*, **4**, 280-286.

Suzuki, H., Terauchi, Y., Fujiwara, M., Aizawa, S., Yazaki, Y., Kadowaki, T. and Koyasu, S. (1999) Xid-like immunodeficiency in mice with disruption of the p85alpha subunit of phosphoinositide 3-kinase. *Science*, **283**, 390-392.

Tanti, J.F., Gremeaux, T., Grillo, S., Calleja, V., Klippel, A., Williams, L.T., Van Obberghen, E. and Le Marchand-Brustel, Y. (1996) Overexpression of a constitutively active form of phosphatidylinositol 3-kinase is sufficient to promote Glut 4 translocation in adipocytes. *J Biol Chem*, **271**, 25227-25232.

Tanti, J.F., Gremeaux, T., Van Obberghen, E. and Le Marchand-Brustel, Y. (1994) Insulin receptor substrate 1 is phosphorylated by the serine kinase activity of phosphatidylinositol 3-kinase. *Biochem J*, **304 (Pt 1)**, 17-21.

Tanti, J.F., Gremeaux, T., van Obberghen, E. and Le Marchand-Brustel, Y. (1994) Serine/threonine phosphorylation of insulin receptor substrate 1 modulates insulin receptor signaling. *J Biol Chem*, **269**, 6051-6057.

Teaching-Resources. (2005) *STKE Science*.

Terauchi, Y., Tsuji, Y., Satoh, S., Minoura, H., Murakami, K., Okuno, A., Inukai, K., Asano, T., Kaburagi, Y., Ueki, K., Nakajima, H., Hanafusa, T., Matsuzawa, Y., Sekihara, H., Yin, Y., Barrett, J.C., Oda, H., Ishikawa, T., Akanuma, Y., Komuro, I., Suzuki, M., Yamamura, K., Kodama, T., Suzuki, H. and Kadowaki, T. (1999) Increased insulin sensitivity and hypoglycaemia in mice lacking the p85 alpha subunit of phosphoinositide 3-kinase. *Nat Genet*, **21**, 230-235.

Toker, A. and Newton, A.C. (2000) Cellular signaling: pivoting around PDK-1. *Cell*, **103**, 185-188.

Tolias, K.F., Cantley, L.C. and Carpenter, C.L. (1995) Rho family GTPases bind to phosphoinositide kinases. *J Biol Chem*, **270**, 17656-17659.

Tourriere, H., Chebli, K., Zekri, L., Courselaud, B., Blanchard, J.M., Bertrand, E. and Tazi, J. (2003) The RasGAP-associated endoribonuclease G3BP assembles stress granules. *J Cell Biol*, **160**, 823-831.

Tourriere, H., Gallouzi, I.E., Chebli, K., Capony, J.P., Mouaikel, J., van der Geer, P. and Tazi, J. (2001) RasGAP-associated endoribonuclease G3Bp: selective RNA degradation and phosphorylation-dependent localization. *Mol Cell Biol*, **21**, 7747-7760.

Traynor-Kaplan, A.E., Harris, A.L., Thompson, B.L., Taylor, P. and Sklar, L.A. (1988) An inositol tetrakisphosphate-containing phospholipid in activated neutrophils. *Nature*, **334**, 353-356.

Turner, S.J., Domin, J., Waterfield, M.D., Ward, S.G. and Westwick, J. (1998) The CC chemokine monocyte chemotactic peptide-1 activates both the class I p85/p110 phosphatidylinositol 3-kinase and the class II PI3K-C2alpha. *J Biol Chem*, **273**, 25987-25995.

Tuveson, D.A., Carter, R.H., Soltoff, S.P. and Fearon, D.T. (1993) CD19 of B cells as a surrogate kinase insert region to bind phosphatidylinositol 3-kinase. *Science*, **260**, 986-989.

Uddin, S., Fish, E.N., Sher, D., Gardziola, C., Colamonici, O.R., Kellum, M., Pitha, P.M., White, M.F. and Platanias, L.C. (1997) The IRS-pathway operates distinctively from the Stat-pathway in hematopoietic cells and transduces common and distinct signals during engagement of the insulin or interferon-alpha receptors. *Blood*, **90**, 2574-2582.

Ueki, K., Algenstaedt, P., Mauvais-Jarvis, F. and Kahn, C.R. (2000) Positive and negative regulation of phosphoinositide 3-kinase-dependent signaling pathways by three different gene products of the p85alpha regulatory subunit. *Mol Cell Biol*, **20**, 8035-8046.

Ueki, K., Fruman, D.A., Brachmann, S.M., Tseng, Y.H., Cantley, L.C. and Kahn, C.R. (2002) Molecular balance between the regulatory and catalytic subunits of phosphoinositide 3-kinase regulates cell signaling and survival. *Mol Cell Biol*, **22**, 965-977.

Ueki, K., Fruman, D.A., Yballe, C.M., Fasshauer, M., Klein, J., Asano, T., Cantley, L.C. and Kahn, C.R. (2003) Positive and negative roles of p85 alpha and p85 beta regulatory subunits of phosphoinositide 3-kinase in insulin signaling. *J Biol Chem*, **278**, 48453-48466.

Ueki, K., Yballe, C.M., Brachmann, S.M., Vicent, D., Watt, J.M., Kahn, C.R. and Cantley, L.C. (2002) Increased insulin sensitivity in mice lacking p85beta subunit of phosphoinositide 3-kinase. *Proc Natl Acad Sci U S A*, **99**, 419-424.

Urry, D.W., Sugano, H., Prasad, K.U., Long, M.M. and Bhatnagar, R.S. (1979) Prolyl hydroxylation of the polypentapeptide model of elastin impairs fiber formation. *Biochem Biophys Res Commun*, **90**, 194-198.

Vanhaesebroeck, B. and Alessi, D.R. (2000) The PI3K-PDK1 connection: more than just a road to PKB. *Biochem J*, **346 Pt 3**, 561-576.

Vanhaesebroeck, B., Ali, K., Bilancio, A., Geering, B. and Foukas, L.C. (2005) Signalling by PI3K isoforms: insights from gene-targeted mice. *Trends Biochem Sci*, **30**, 194-204.

Vanhaesebroeck, B., Higashi, K., Raven, C., Welham, M., Anderson, S., Brennan, P., Ward, S.G. and Waterfield, M.D. (1999) Autophosphorylation of p110delta phosphoinositide 3-kinase: a new paradigm for the regulation of lipid kinases in vitro and in vivo. *Embo J*, **18**, 1292-1302.

Vanhaesebroeck, B., Jones, G.E., Allen, W.E., Zicha, D., Hooshmand-Rad, R., Sawyer, C., Wells, C., Waterfield, M.D. and Ridley, A.J. (1999) Distinct PI(3)Ks mediate mitogenic signalling and cell migration in macrophages. *Nat Cell Biol*, **1**, 69-71.

Vanhaesebroeck, B., Leevers, S.J., Ahmadi, K., Timms, J., Katso, R., Driscoll, P.C., Woscholski, R., Parker, P.J. and Waterfield, M.D. (2001) Synthesis and function of 3-phosphorylated inositol lipids. *Annu Rev Biochem*, **70**, 535-602.

Vanhaesebroeck, B., Leevers, S.J., Panayotou, G. and Waterfield, M.D. (1997) Phosphoinositide 3-kinases: a conserved family of signal transducers. *Trends Biochem Sci*, **22**, 267-272.

Vanhaesebroeck, B., Rohn, J.L. and Waterfield, M.D. (2004) Gene targeting: attention to detail. *Cell*, **118**, 274-276.

Vanhaesebroeck, B. and Waterfield, M.D. (1999) Signaling by distinct classes of phosphoinositide 3-kinases. *Exp Cell Res*, **253**, 239-254.

Vanhaesebroeck, B., Welham, M.J., Kotani, K., Stein, R., Warne, P.H., Zvelebil, M.J., Higashi, K., Volinia, S., Downward, J. and Waterfield, M.D. (1997) P110delta, a novel phosphoinositide 3-kinase in leukocytes. *Proc Natl Acad Sci U S A*, **94**, 4330-4335.

Varnai, P., Rother, K.I. and Balla, T. (1999) Phosphatidylinositol 3-kinase-dependent membrane association of the Bruton's tyrosine kinase pleckstrin homology domain visualized in single living cells. *J Biol Chem*, **274**, 10983-10989.

Varticovski, L., Daley, G.Q., Jackson, P., Baltimore, D. and Cantley, L.C. (1991) Activation of phosphatidylinositol 3-kinase in cells expressing abl oncogene variants. *Mol Cell Biol*, **11**, 1107-1113.

Venkateswarlu, K., Oatey, P.B., Tavare, J.M., Jackson, T.R. and Cullen, P.J. (1999) Identification of centaurin-alpha1 as a potential in vivo phosphatidylinositol 3,4,5-trisphosphate-binding protein that is functionally homologous to the yeast ADP-ribosylation factor (ARF) GTPase-activating protein, Gcs1. *Biochem J*, **340 (Pt 2)**, 359-363.

Vigorito, E., Bardi, G., Glassford, J., Lam, E.W., Clayton, E. and Turner, M. (2004) Vav-dependent and vav-independent phosphatidylinositol 3-kinase activation in murine B cells determined by the nature of the stimulus. *J Immunol*, **173**, 3209-3214.

Virbasius, J.V., Guilherme, A. and Czech, M.P. (1996) Mouse p170 is a novel phosphatidylinositol 3-kinase containing a C2 domain. *J Biol Chem*, **271**, 13304-13307.

Vlahos, C.J., Matter, W.F., Hui, K.Y. and Brown, R.F. (1994) A specific inhibitor of phosphatidylinositol 3-kinase, 2-(4-morpholinyl)-8-phenyl-4H-1-benzopyran-4-one (LY294002). *J Biol Chem*, **269**, 5241-5248.

Voigt, P., Dorner, M.B. and Schaefer, M. (2006) Characterization of p87PIKAP, a novel regulatory subunit of phosphoinositide 3-kinase gamma that is highly expressed in heart and interacts with PDE3B. *J Biol Chem*, **281**, 9977-9986.

Volinia, S., Dhand, R., Vanhaesebroeck, B., MacDougall, L.K., Stein, R., Zvelebil, M.J., Domin, J., Panaretou, C. and Waterfield, M.D. (1995) A human phosphatidylinositol 3-kinase complex related to the yeast Vps34p-Vps15p protein sorting system. *Embo J*, **14**, 3339-3348.

von Willebrand, M., Williams, S., Saxena, M., Gilman, J., Tailor, P., Jascur, T., Amarante-Mendes, G.P., Green, D.R. and Mustelin, T. (1998) Modification of phosphatidylinositol 3-kinase SH2 domain binding properties by Abl- or Lck-mediated tyrosine phosphorylation at Tyr-688. *J Biol Chem*, **273**, 3994-4000.

Walker, E.H., Pacold, M.E., Perisic, O., Stephens, L., Hawkins, P.T., Wymann, M.P. and Williams, R.L. (2000) Structural determinants of phosphoinositide 3-kinase inhibition by wortmannin, LY294002, quercetin, myricetin, and staurosporine. *Mol Cell*, **6**, 909-919.

Walker, E.H., Perisic, O., Ried, C., Stephens, L. and Williams, R.L. (1999) Structural insights into phosphoinositide 3-kinase catalysis and signalling. *Nature*, **402**, 313-320.

Wang, B., David, M.D. and Schrader, J.W. (2005) Absence of caprin-1 results in defects in cellular proliferation. *J Immunol*, **175**, 4274-4282.

Wang, H.Y., Zamorano, J., Yoerkie, J.L., Paul, W.E. and Keegan, A.D. (1997) The IL-4-induced tyrosine phosphorylation of the insulin receptor substrate is dependent on JAK1 expression in human fibrosarcoma cells. *J Immunol*, **158**, 1037-1040.

Wang, J., Auger, K.R., Jarvis, L., Shi, Y. and Roberts, T.M. (1995) Direct association of Grb2 with the p85 subunit of phosphatidylinositol 3-kinase. *J Biol Chem*, **270**, 12774-12780.

Wang, Y., Brooks, S.R., Li, X., Anzelon, A.N., Rickert, R.C. and Carter, R.H. (2002) The physiologic role of CD19 cytoplasmic tyrosines. *Immunity*, **17**, 501-514.

Welch, H.C., Coadwell, W.J., Stephens, L.R. and Hawkins, P.T. (2003) Phosphoinositide 3-kinase-dependent activation of Rac. *FEBS Lett*, **546**, 93-97.

Whitehead, J.P., Clark, S.F., Urso, B. and James, D.E. (2000) Signalling through the insulin receptor. *Curr Opin Cell Biol*, **12**, 222-228.

Whitman, M., Downes, C.P., Keeler, M., Keller, T. and Cantley, L. (1988) Type I phosphatidylinositol kinase makes a novel inositol phospholipid, phosphatidylinositol-3-phosphate. *Nature*, **332**, 644-646.

Whitman, M., Kaplan, D.R., Schaffhausen, B., Cantley, L. and Roberts, T.M. (1985) Association of phosphatidylinositol kinase activity with polyoma middle-T competent for transformation. *Nature*, **315**, 239-242.

Wijkander, J., Landstrom, T.R., Manganiello, V., Belfrage, P. and Degerman, E. (1998) Insulin-induced phosphorylation and activation of phosphodiesterase 3B in rat adipocytes: possible role for protein kinase B but not mitogen-activated protein kinase or p70 S6 kinase. *Endocrinology*, **139**, 219-227.

Williams, M.R., Arthur, J.S., Balendran, A., van der Kaay, J., Poli, V., Cohen, P. and Alessi, D.R. (2000) The role of 3-phosphoinositide-dependent protein kinase 1 in activating AGC kinases defined in embryonic stem cells. *Curr Biol*, **10**, 439-448.

Withers, D.J., Ouwens, D.M., Nave, B.T., van der Zon, G.C., Alarcon, C.M., Cardenas, M.E., Heitman, J., Maassen, J.A. and Shepherd, P.R. (1997) Expression, enzyme activity, and subcellular localization of mammalian target of rapamycin in insulin-responsive cells. *Biochem Biophys Res Commun*, **241**, 704-709.

Woscholski, R., Kodaki, T., McKinnon, M., Waterfield, M.D. and Parker, P.J. (1994) A comparison of demethoxyviridin and wortmannin as inhibitors of phosphatidylinositol 3-kinase. *FEBS Lett*, **342**, 109-114.

Wymann, M.P. and Pirola, L. (1998) Structure and function of phosphoinositide 3-kinases. *Biochim Biophys Acta*, **1436**, 127-150.

Yamamoto, K., Altschuler, D., Wood, E., Horlick, K., Jacobs, S. and Lapetina, E.G. (1992) Association of phosphorylated insulin-like growth factor-I receptor with the SH2 domains of phosphatidylinositol 3-kinase p85. *J Biol Chem*, **267**, 11337-11343.

Yamanashi, Y., Fukui, Y., Wongsasant, B., Kinoshita, Y., Ichimori, Y., Toyoshima, K. and Yamamoto, T. (1992) Activation of Src-like protein-tyrosine kinase Lyn and its association with phosphatidylinositol 3-kinase upon B-cell antigen receptor-mediated signaling. *Proc Natl Acad Sci U S A*, **89**, 1118-1122.

Yamanashi, Y., Kakiuchi, T., Mizuguchi, J., Yamamoto, T. and Toyoshima, K. (1991) Association of B cell antigen receptor with protein tyrosine kinase Lyn. *Science*, **251**, 192-194.

Yip, S.C., El-Sibai, M., Hill, K.M., Wu, H., Fu, Z., Condeelis, J.S. and Backer, J.M. (2004) Over-expression of the p110beta but not p110alpha isoform of PI 3-kinase inhibits motility in breast cancer cells. *Cell Motil Cytoskeleton*, **59**, 180-188.

Yu, J., Wjasow, C. and Backer, J.M. (1998) Regulation of the p85/p110alpha phosphatidylinositol 3'-kinase. Distinct roles for the n-terminal and c-terminal SH2 domains. *J Biol Chem*, **273**, 30199-30203.

Yu, J., Zhang, Y., McIlroy, J., Rordorf-Nikolic, T., Orr, G.A. and Backer, J.M. (1998) Regulation of the p85/p110 phosphatidylinositol 3'-kinase: stabilization and inhibition of the p110alpha catalytic subunit by the p85 regulatory subunit. *Mol Cell Biol*, **18**, 1379-1387.

Yu, Z., Su, L., Hoglinger, O., Jaramillo, M.L., Banville, D. and Shen, S.H. (1998) SHP-1 associates with both platelet-derived growth factor receptor and the p85 subunit of phosphatidylinositol 3-kinase. *J Biol Chem*, **273**, 3687-3694.

Yuan, Z.M., Utsugisawa, T., Huang, Y., Ishiko, T., Nakada, S., Kharbanda, S., Weichselbaum, R. and Kufe, D. (1997) Inhibition of phosphatidylinositol 3-kinase by c-Abl in the genotoxic stress response. *J Biol Chem*, **272**, 23485-23488.

Zekri, L., Chebli, K., Tourriere, H., Nielsen, F.C., Hansen, T.V., Rami, A. and Tazi, J. (2005) Control of fetal growth and neonatal survival by the RasGAP-associated endoribonuclease G3BP. *Mol Cell Biol*, **25**, 8703-8716.

Zhang, J., Banfic, H., Straforini, F., Tosi, L., Volinia, S. and Rittenhouse, S.E. (1998) A type II phosphoinositide 3-kinase is stimulated via activated integrin in platelets. A source of phosphatidylinositol 3-phosphate. *J Biol Chem*, **273**, 14081-14084.

Zhang, Y. and Xiong, Y. (1999) Mutations in human ARF exon 2 disrupt its nucleolar localization and impair its ability to block nuclear export of MDM2 and p53. *Mol Cell*, **3**, 579-591.

Zheng, Y., Bagrodia, S. and Cerione, R.A. (1994) Activation of phosphoinositide 3-kinase activity by Cdc42Hs binding to p85. *J Biol Chem*, **269**, 18727-18730.

Zhou, K., Takegawa, K., Emr, S.D. and Firtel, R.A. (1995) A phosphatidylinositol (PI) kinase gene family in Dictyostelium discoideum: biological roles of putative mammalian p110 and yeast Vps34p PI 3-kinase homologs during growth and development. *Mol Cell Biol*, **15**, 5645-5656.

Zvelebil, M.J., MacDougall, L., Leevers, S., Volinia, S., Vanhaesebroeck, B., Gout, I., Panayotou, G., Domin, J., Stein, R., Pages, F. and et al. (1996) Structural and functional diversity of phosphoinositide 3-kinases. *Philos Trans R Soc Lond B Biol Sci*, **351**, 217-223.